

AD-752 897

DESIGN DATA FOR THE DEVELOPMENT OF
PORTABLE, INFRARED RADIANT HEATERS

Adi R. Guzdar, et al

Foster-Miller Associates, Incorporated

Prepared for:

Army Natick Laboratories

September 1972

DISTRIBUTED BY:

NTIS

National Technical Information Service
U. S. DEPARTMENT OF COMMERCE
5285 Port Royal Road, Springfield Va. 22151

AD752897

AD

TECHNICAL REPORT

73-14-GP

**DESIGN DATA FOR THE DEVELOPMENT OF PORTABLE,
INFRARED, RADIANT HEATERS**

by

A. R. Guzdar

S. S. Rhee,

and

A. C. Harvey

Foster-Miller Associates, Inc.

Waltham, Massachusetts

Contract No. DAAG 17-70-C-0046

September 1972

Approved for public release;
distribution unlimited.



UNITED STATES ARMY
NATICK LABORATORIES
Natick, Massachusetts 01760



GENERAL EQUIPMENT & PACKAGING LABORATORY

334

R

UNCLASSIFIED

Security Classification

DOCUMENT CONTROL DATA - R & D

(Security classification of title, body of abstract and indexing annotation must be entered when the overall report is classified)

1. ORIGINATING ACTIVITY (Corporate author) Foster-Miller Associates, Inc. 135 Second Avenue Waltham, Massachusetts 02154		2a. REPORT SECURITY CLASSIFICATION UNCLASSIFIED	
3. REPORT TITLE DESIGN DATA FOR THE DEVELOPMENT OF PORTABLE, INFRARED RADIANT HEATERS		2b. GROUP	
4. DESCRIPTIVE NOTES (Type of report and inclusive dates) Final Report			
5. AUTHOR(S) (First name, middle initial, last name) Adi R. Guzdar Sang Soon Rhee Andrew C. Harvey			
6. REPORT DATE September 1972	7a. TOTAL NO. OF PAGES 333	7b. NO. OF REFS 13	
8a. CONTRACT OR GRANT NO. DAAG17-76-C-0046	9a. ORIGINATOR'S REPORT NUMBER(S) QM-6933		
b. PROJECT NO. c. d.	9b. OTHER REPORT NO(S) (Any other numbers that may be assigned this report) 73-14-GP		
10. DISTRIBUTION STATEMENT Approved for public release; distribution unlimited.			
11. SUPPLEMENTARY NOTES		12. SPONSORING MILITARY ACTIVITY U. S. Army Natick Laboratories General Equipment and Packaging Labs. Natick, Massachusetts	
13. ABSTRACT The purpose of this study was to develop the necessary design information for the development of a portable, gasoline-fired, radiant heater to keep personnel and equipment warm in the Arctic environment. The heater is required to adequately heat a space 8 feet in diameter located from 4 to 10 feet from the heater, at an ambient temperature in the range of 0 to -50° F and winds up to 20 mph. Focusing of the radiation emanating from the heater is considered essential to maintain high heating rates at these distances. To accomplish these objectives a combined approach of analysis and experimentation was utilized. The heat loss from equipment and personnel in the specified thermal environment was calculated from which the heating rate necessary to maintain comfort and adequate manual dexterity was established. The heat transfer from various source geometries and reflector combinations was analyzed to predict the spatial flux density distribution at the target area. The range of commercially available radiant heaters was surveyed and evaluated to select the more promising configurations for experimental evaluation. A test apparatus was designed and instrumentation selected to measure the radiant output of the heater and the flux density at the target surface. Special reflectors were designed to improve the focusing of radiation from these heaters. Performance tests were conducted on these heaters in a stationary ambient and with a 20 mph wind. The results obtained were utilized to refine the theoretical analysis. Based on these results it was concluded that a hemispherical source in a paraboloidal or hyperboloidal reflector represents the optimum configuration for the specified requirements. Since no such			

DD FORM 1473

REPLACES DD FORM 1473, 1 JAN 54, WHICH IS OBSOLETE FOR ARMY USE.

UNCLASSIFIED
Security Classification

UNCLASSIFIED
Security Classification

14. KEY WORDS	LINK A		LINK B		LINK C	
	ROLE	WT	ROLE	WT	ROLE	WT
Design	8					
Development	8					
Heaters	9		9			
Heating Equipment	9		9			
Mobile Equipment	9		9			
Portable Equipment	9		9			
Gasoline-Fired	0		0			
Thermal Radiation	4				4	
Heat Radiation	4				4	
Military Personnel	4				4	
Equipment	4				4	
Arctic Regions	4				4	
Tests			8			
Performance Tests			8			
Analysis			8			
Experimentation			8			
Infrared Heating			10			
Radiant Heating			10			
Test Apparatus					9	
Reflectors					9	

CONTENTS (Cont.)

	<u>Page No.</u>
5.2.1 Area Sources	88
5.2.2 Line Sources	94
5.2.3 Point Sources	99
5.2.4 Other Heaters	104
5.2.5 Commercial Heaters Selected for Experimental Evaluation	104
6. Test Program	109
6.1 Scope of Test Program	109
6.2 Instrumentation for Measuring the Performance of the Radiant Heater	110
6.2.1 Eppley Thermopile Radiometer	111
6.2.2 Ircon 300 Series Infrared Radiation Thermometer	116
6.2.3 Keithley Model 155 Microvoltmeter	116
6.3 Design of Test Apparatus	116
6.3.1 Radiant Flux Measurement	118
6.3.2 Temperature Measurement	121
6.3.3 Fuel Flow Rate	121
6.3.4 Wind Test	121
6.4 Experimental Results	121
6.4.1 Government Furnished Gasoline Heater	122
6.4.2 Pyrocore Propane Heater	141

Approved for public release;
distribution unlimited.

AD _____

TECHNICAL REPORT

73-14-GP

DESIGN DATA

FOR THE DEVELOPMENT OF
PORTABLE, INFRARED, RADIANT HEATERS

by

A. R. Guzdar, S. S. Rhee, and A. C. Harvey

FOSTER-MILLER ASSOCIATES, INC.

Waltham, Massachusetts

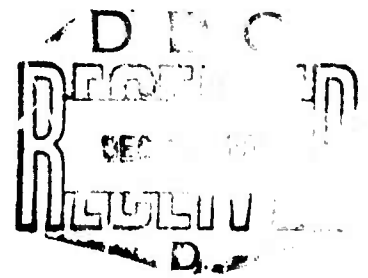
Prepared under Contract No. DAAG17-70-C-0046

Project Reference:
1J662708D503

September 1972

General Equipment & Packaging Laboratory
U. S. ARMY NATICK LABORATORIES
Natick, Massachusetts 01760

- 1d -



FOREWORD

This report was prepared by Foster-Miller Associates, Inc., Waltham, Massachusetts, under U.S. Army Natick Laboratories Contract No. DAAG17-70-C-0046. This is the final technical report for the contract.

The contract was initiated under Army Project No. 16-0081-X159. The work was administered under the direction of the General Equipment and Packaging Laboratory of the U.S. Army Natick Laboratories, Natick, Massachusetts, Dr. Roger M. Stinchfield and Mr. Alton J. Rohr were the Project Officers.

This report covers work performed from 20 October 1969 to 20 April 1971. The investigation was performed by the Engineering Studies Division of Foster-Miller Associates, Inc. Mr. Adi R. Guzdar was the Program Manager. Mr. Sang S. Rhee, Mr. Andrew C. Harvey and Mr. Philip Ayers were responsible for the technical analysis and experimental test work.

The authors wish to acknowledge and express their appreciation for the assistance provided by Dr. Roger M. Stinchfield and Mr. Alton J. Rohr of the U.S. Army Natick Laboratories.

TABLE OF CONTENTS

	<u>Page No.</u>
FOREWORD	ii
LIST OF ILLUSTRATIONS	vii
LIST OF TABLES	xvii
ABSTRACT	xviii
1. Introduction	1
1.1 Objectives	1
1.2 Background	3
1.3 Scope of Studies	4
2. Summary and Conclusions	7
2.1 Radiant Flux Density Required	8
2.2 Analysis of Radiant Heating Performance of Various Source-Reflector Configurations	9
2.3 Survey and Evaluation of Commercial Infrared Heaters	10
2.4 Experimental Program	11
2.5 Parametric Design Analysis of a Radiant Heater	17
2.6 Materials for Emitter Construction	18
2.7 Special Design Requirements for a Liquid-Fuel Fired Radiant Heater	18
2.8 Conclusions	18
2.9 Recommendations	23

CONTENTS (Cont.)

	<u>Page No.</u>
3. Heating Rate Requirements	25
3.1 Radiant Flux Inputs Required for Personnel Comfort	26
3.2 Radiant Flux Inputs Required to Warm Metal Tools	32
3.3 Radiant Flux Inputs Required to Warm Equipment Under Repair	34
3.4 Design Recommendation for Heating Rate Requirement	34
4. Analysis of Radiant Energy Transfer from Various Source-Reflector Combinations	36
4.1 Analytical Objectives and Method	36
4.2 Radiant Heat Transfer Performance of Various Source-Reflector Geometries	38
4.3 Spatial Distribution of Flux Density at the Target	44
4.4 Charts for Heater Design	50
4.5 Sample Use of Design Charts	63
4.6 Evaluation of Optimum Source-Reflector Configuration	69
5. Survey and Evaluation of Commercial Radiant Heaters	72
5.1 General Discussion of Radiant Heaters	72
5.1.1 Spectral Content of Infrared Energy	72
5.1.2 Types of Infrared Energy Generators	78
5.2 Survey and Preliminary Evaluation of Commercial Radiant Heaters	86

CONTENTS (Cont.)

	<u>Page No.</u>
5. 2. 1 Area Sources	88
5. 2. 2 Line Sources	94
5. 2. 3 Point Sources	99
5. 2. 4 Other Heaters	104
5. 2. 5 Commercial Heaters Selected for Experimental Evaluation	104
6. Test Program	109
6. 1 Scope of Test Program	109
6. 2 Instrumentation for Measuring the Performance of the Radiant Heater	110
6. 2. 1 Eppley Thermopile Radiometer	111
6. 2. 2 Ircon 300 Series Infrared Radiation Thermometer	116
6. 2. 3 Keithley Model 155 Microvoltmeter	116
6. 3 Design of Test Apparatus	116
6. 3. 1 Radiant Flux Measurement	118
6. 3. 2 Temperature Measurement	121
6. 3. 3 Fuel Flow Rate	121
6. 3. 4 Wind Test	121
6. 4 Experimental Results	121
6. 4. 1 Government Furnished Gasoline Heater	122
6. 4. 2 Pyrocore Propane Heater	141

CONTENTS (Cont.)

	<u>Page No.</u>
6.4.3 Hupp Propane Heater	151
6.4.4 Hupp Hot-Tot Heater	162
6.4.5 Foster-Miller Radiant Heater (FMA)	168
6.4.6 Selas Burner	183
6.4.7 Hi-Shear Electric Heater	186
6.5 Summary of Test Results	186
7. Emitter Materials for Radiant Heater Construction	193
8. Special Design Requirements for a Liquid-Fuel Fired Radiant Heater	195
8.1 Burner Design for Liquid Fuel Operation	195
8.2 Safety Controls for Liquid-Fuel Operation	196
9. Conclusions and Recommendations	198
9.1 Conclusions	198
9.2 Recommendations	202
LITERATURE CITED	204
APPENDIX A - Theoretical Analysis of the Axial Distribution of the Radiant Heat Flux Density From Various Emitter and Reflector Combinations	206
APPENDIX B - Spatial Distribution of Radiant Flux Density Over The Receiver Area - Theoretical Analysis and Comparison with Experimental Data	250
APPENDIX C - Design Synthesis of a Radiant Burner	283

LIST OF ILLUSTRATIONS

<u>Figure No.</u>		<u>Page No.</u>
1	Heat Balance in a Human Body	27
2	Disc Source with Conical Reflector	39
3	Circular Cylinder (Line Source)	39
4	Circular Cylinder with Parabolic Reflector	40
5	Circular Cylinder with Hyperbolic Reflector	40
6	Spherical Source with Paraboloid Reflector	41
7	Spherical Source with Hyperboloid Reflector	41
8	Comparison of Theoretical and Experimentally Measured Values of the Radiant Flux Density Distribution at the Target from the GFP Gasoline Heater	45
9	Comparison of Experimental and Theoretical Values of the Radiant Flux Density Distribution at the Target from the GFP Gasoline Heater with the Long Conical Reflector	47
10	Comparison of Experimental and Theoretical Values of the Radiant Flux Density Distribution at the Target from the Pyrocore Heater	48
11	Comparison of Experimental and Theoretical Values of the Radiant Flux Density Distribution at the Target from the Foster-Miller Hemispherical Source Radiant Heater	49
12	Geometry of Various Source-Reflector Configurations	52
13	Design Chart for a Disc-Source-Conical Reflector Heater-Target Distance 4 Feet	53
14	Design Chart for Disc-Source-Conical Reflector Heater-Target Distance 6 Feet	54

LIST OF ILLUSTRATIONS (Cont.)

<u>Figure No.</u>		<u>Page No.</u>
15	Design Chart for Disc-Source-Conical-Reflector Heater-Target Distance 8 Feet	55
16	Design Chart for Disc-Source-Conical-Reflector Heater-Target Distance 10 Feet	56
17	Configuration Chart for Design of Optimum Conical Reflector	58
18	Design Chart for a Cylindrical-Source-Paraboloidal Reflector Heater - Target Distance 4 Feet	59
19	Design Chart for a Cylindrical-Source-Paraboloidal-Reflector Heater - Target Distance 6 Feet	60
20	Design Chart for a Cylindrical-Source-Paraboloidal-Reflector Heater - Target Distance 8 Feet	61
21	Design Chart for a Cylindrical-Source-Paraboloidal-Reflector Heater - Target Distance 10 Feet	62
22	Design Chart for a Hemispherical-Source-Paraboloidal-Reflector Heater - Target Distance 4 Feet	64
23	Design Chart for a Hemispherical-Source-Paraboloidal-Reflector Heater - Target Distance 6 Feet	65
24	Design Chart for a Hemispherical-Source-Paraboloidal-Reflector Heater - Target Distance 8 Feet	66
25	Design Chart for a Hemispherical-Source-Paraboloidal-Reflector Heater - Target Distance 10 Feet	67

LIST OF ILLUSTRATIONS (Cont.)

<u>Figure No.</u>		<u>Page No.</u>
26	Optimum Source-Reflector Configurations	70
27	Comparison of Relative Heating Performance of Different Source-Reflector Configurations	71
28	Absorption Curve for H ₂ O Film and Radiant Energy Curves for 4,050°F and 700°F Sources	74
29	Spectral Radiation Curve for (1) Gas-Fired Infrared Burner, (2) Flue Gases, and (3) Hot Surface	75
30	Absorption Characteristics of Film of Linseed Oil and Emission Curve of Two Infrared Sources	77
31	Four Different Types of Gas-Fired I-R Burners	80
32	Surface Combustion Burner	89
33	Schematic of Hunter Manufacturing Company's Radiant Heater	92
34	Sketch of Hi-Shear Corporation's Quartz Lamp Infrared Heaters	95
35	Radiation vs. Air Velocity Curves for Electrical Radiant Heaters	98
36	Schematic Drawing of the Roberts-Gordon Radiant Tube Heater	100
37	Radiant Systems Pyrocore Heater	102
38	Drawing of the Selas Duradiant Burner	102
39	Schematic of Hupp Hot-Tot Heater	105
40	Schematic Arrangement of a Duradiant Burner to Approximate a Point Source	108

LIST OF ILLUSTRATIONS (Cont.)

<u>Figure No.</u>		<u>Page No.</u>
41	Eppley Thermopile Radiometer	114
42	Spectral Response Characteristics of Several Infrared Detectors	115
43	Schematic of the Ircon Model 300 Radiation Pyrometer	117
44	Test Instrumentation for Measuring Radiant Heater Performance	119
45	Radiometer Support Assembly	120
46	GFP Gasoline Heater	123
47	Black Body Temperature Map, °F, of the Gasoline Heater	125
48	Radiant Flux Density Distribution, BTU/hr-ft^2 , - GFP Gasoline Heater - Target Distance, 4 feet	127
49	Radiant Flux Density Distribution, BTU/hr-ft^2 , - GFP Gasoline Heater - Target Distance, 6 feet	128
50	Radiant Flux Density Distribution, BTU/hr-ft^2 , - GFP Gasoline Heater - Target Distance, 8 feet	129
51	Radiant Flux Density Distribution, BTU/hr-ft^2 , - GFP Gasoline Heater - Target Distance, 10 feet	130
52	Schematic Drawings of Conical Reflectors	132
53	Reflectors for Gasoline Heater	133
54	Radiant Flux Density Distribution, BTU/hr-ft^2 , - GFP Gasoline Heater with Small Conical Reflector	134
55	Radiant Flux Density Distribution, BTU/hr-ft^2 , - GFP Gasoline Heater with Large Conical Reflector	135

LIST OF ILLUSTRATIONS (Cont.)

<u>Figure No.</u>		<u>Page No.</u>
56	Variation in Flux Distribution Caused by the Addition of Reflectors to the Gasoline Heater - Target Distance, 4 feet	136
57	Variation in Flux Distribution Caused by the Addition of Reflectors to the Gasoline Heater - Target Distance, 8 feet	137
58	Multicellular Conical Reflector	138
59	Gasoline Heater with Wind Blowing Parallel to the Heater Face	140
60	Pyrocore Propane Heater Under Normal Operating Conditions	142
61	Radiant Flux Density Distribution, BTU/hr-ft^2 , - Pyrocore Propane Heater - Target Distance, 4 feet	144
62	Radiant Flux Density Distribution, BTU/hr-ft^2 , - Pyrocore Propane Heater - Target Distance, 6 feet	145
63	Radiant Flux Density Distribution, BTU/hr-ft^2 , - Pyrocore Propane Heater - Target Distance, 8 feet	146
64	Radiant Flux Density Distribution, BTU/hr-ft^2 , - Pyrocore Propane Heater - Target Distance, 10 feet	147
65	Reflector Combinations for Pyrocore Heater	148
66	Comparison of the Effect of Additional Reflectors on the Performance of the Pyrocore Propane Heaters - Target Distance, 4 feet	149
67	Comparison of the Effect of Additional Reflectors on the Performance of the Pyrocore Propane Heaters - Target Distance, 8 feet	150

LIST OF ILLUSTRATIONS (Cont.)

<u>Figure No.</u>		<u>Page No.</u>
68	Pyrocore Propane Heater with a 15 mph Wind Blowing Directly at the Heater	152
69	Temperature Map of the Emitter Surface of the Pyrocore Heater in a Wind	152
70	Comparison of the Effects of the Wind on the Performance of the Pyrocore Heater - Target Distance, 4 feet	153
71	Comparison of the Effects of the Wind on the Performance on the Pyrocore Heater - Target Distance, 8 feet	154
72	Hupp Propane Heater	155
73	Hupp Propane Heater Temperature Map - °F	157
74	Radiant Flux Density Distribution, BTU/hr-ft^2 , - Hupp Propane Heater - Target Distance, 4 feet	158
75	Radiant Flux Density Distribution, BTU/hr-ft^2 , - Hupp Propane Heater - Target Distance, 6 feet	159
76	Radiant Flux Density Distribution, BTU/hr-ft^2 , - Hupp Propane Heater - Target Distance, 8 feet	160
77	Radiant Flux Density Distribution, BTU/hr-ft^2 , - Hupp Propane Heater - Target Distance, 10 feet	161
78	Hot-Tot Heater with Conical Reflectors	163
79	Radiant Flux Density Distribution, BTU/hr-ft^2 , - Hupp Hot-Tot Heater with Long Reflector - Target Distance, 4 feet	164
80	Radiant Flux Density Distribution, BTU/hr-ft^2 , - Hupp Hot-Tot Heater with Long Reflector - Target Distance, 6 feet	165

LIST OF ILLUSTRATIONS (Cont.)

<u>Figure No.</u>		<u>Page No.</u>
81	Radiant Flux Density Distribution, BTU/hr-ft^2 , - Hupp Hot-Tot Heater with Long Reflector - Target Distance, 8 feet	166
82	Radiant Flux Density Distribution, BTU/hr-ft^2 , - Hupp Hot-Tot Heater with Long Reflector - Target Distance, 10 feet	167
83	Performance of Hot-Tot Heater with Conical Reflector in a 15 mph Cross-Wind	169
84	Schematic of Foster-Miller Radiant Heater	171
85	Photograph of the Foster-Miller Radiant Hemispherical Source and Wingaersheek Turbo Torch Burner	173
86	Schematic of Wingaersheek Turbo Torch Burner	175
87	Schematic Section of Experimental Hemispherical Heat Exchanger	176
88	Foster-Miller Radiant Heater	179
89	Black Body Temperature Distribution of the Foster- Miller Hemispherical Radiant Source, $^{\circ}\text{F}$	181
90	Radiant Flux Density Distribution, BTU/hr-ft^2 , - Foster-Miller Radiant Heater	182
91	Effect of Wind on the Radiant Flux Density Distribution - Foster-Miller Radiant Heater	184
92	Schematic Diagram of Gas-Air Mixer for Selas Burner	185

LIST OF ILLUSTRATIONS (Cont.)

<u>Figure No.</u>		<u>Page No.</u>
A-1	Radiation Heat Transfer between Source and Receiver	208
A-2	View Factor F_{rs} , for Direct Radiation between an Element and a Circular Disc	212
A-3	View Factor for Direct Radiation between an Element and a Rectangular Source	214
A-4	Coordinate System for the Analysis of a Line Source	216
A-5	Coordinate System for the Analysis of a Spherical Point Source	217
A-6	Definition of Nomenclature for Conical Reflector	222
A-7	Image Rings Produced by Source Ring Elements	226
A-8	Partial Image Cone Due to Finite Reflector Length	228
A-9	Selection Chart for Optimum Dimensions for Conical Reflector	230
A-10	Effect of Cone Angle, α on Reflector Performance	232
A-11	Effect of Reflector Length on Reflector Performance	233
A-12	Flux Density Distribution for Various Reflectors	234
A-13	Geometry of Ellipsoidal Reflector	238
A-14	Geometry of Ellipsoid for Various Focal Distances, \bar{H}_f	241
A-15	Image of Source as Seen from Various Target Distances	242
A-16	Nomenclature Definition for Partial Image Conditions	245

LIST OF ILLUSTRATIONS (Cont.)

<u>Figure No.</u>		<u>Page No.</u>
A-17	Axial Flux Density Distribution for Ellipsoidal Reflector with Circular Disc Source	248
A-18	Magnification Factor for Ellipsoidal Reflector for Disc Source	249
A-19	Geometry of Line Source-Parabolic Reflector	250
A-20	Distribution of View Factor for a Tubular Source Parabolic Reflector Geometry	255
A-21	Dispersion Due to Finite Source Area	256
A-22	Coordinate System for the Hyperboloidal Reflector	259
B-1	Schematic of Source-Reflector Configuration	268
B-2	Reduction in Image Area due to Shading of Reflector	271
B-3	Comparison of Experimental and Theoretical Values of the Radiant Flux Density Distribution at the Target from the GFP Gasoline Heater with the Long Conical Reflector	274
B-4	Comparison of Experimental and Theoretical Values of the Radiant Flux Density Distribution at the Target from the Pyrocore Heater	276
B-5	Comparison of Experimental and Theoretical Values of the Radiant Flux Density Distribution of the Hupp Hot-Tot Heater	277
B-6	Comparison of Experimental and Theoretical Values of the Radiant Flux Density Distribution at the Target from the Foster-Miller Hemispherical Source Radiant Heater	279

LIST OF ILLUSTRATIONS (Cont.)

<u>Figure No.</u>		<u>Page No.</u>
B-7	Optimum Source-Reflector Configurations	281
B-8	Comparison of Relative Heating Performance	282
C-1	Schematic of a Radiant Burner Showing Possible Systems Options	285
C-2	Schematic of the Usual Simple Radiant Burner System	286
C-3	Schematic of Jet Pump	291
C-4	Basic Schemes for Convective to Radiant Heat Exchange	296
C-5	Nomenclature for the Convective Heat Exchange for a Radiant Burner	299
C-6	Typical Variation of Radiant Burner Parameters	304
C-7	Schematic Comparison of Different Heat Exchange Matrices versus Matrix Size	305
C-8	Schematic of Wingaersheek Turbo Torch Burner	307
C-9	Schematic Section of Experimental Hemispherical Heat Exchanger	312

LIST OF TABLES

<u>Table No.</u>		<u>Page No.</u>
I	Summary of Experimental Results for Performance of Various Heaters	12
II	Radiant Energy Transfer Performance of Various Source and Reflector Geometries	43
III	Preliminary Sizing of Heater Configurations to Supply A Mean Flux Density of 200 BTU/hr-ft ² at a 10 feet Target Distance	68
IV	Absorption Characteristics of Some Typical	76
V	Absorption of Infrared Radiation from Various Gas and Electrical Sources by Three Representative Loads	78
VI	Radiation Data for Gas Fired Infrared Burners	82
VII	Radiation Data for Electric Infrared Generators	84
VIII	Characteristics of Radiant Heaters	87
IX	Comparison of Pyrometers for Temperature Measurement	112
X	Summary of Experimental Results for Performance of Various Heaters	187
A-I	Comparison of Performance of Various Source Geometries	220
A-II	Optimum Cone Angle for Conical Reflector	231
A-III	Comparison of Theoretically Predicted and Experimentally Measured Values of the Magnification Factor	236

DESIGN DATA FOR THE DEVELOPMENT OF PORTABLE, INFRARED, RADIANT HEATERS

1. Introduction

This report summarizes the results of a technical program conducted to determine the necessary design information and make recommendations for a liquid-fuel-fired radiant heater to effectively warm personnel and disabled equipment in the Arctic so that repair work can be performed.

1.1 Objectives

The ultimate objective of this program is to develop an efficient, portable radiant heater to keep personnel and disabled equipment warm in an Arctic environment, in order to permit repairs to equipment without necessitating its removal to a heated repair area. The present program is restricted to demonstrating the feasibility of such a liquid-fuel-fired burner and the securing of necessary analytical and experimental information for the design of such a unit.

The specific objectives of this program are as follows:

- (a) Determine the heating rate required to adequately warm equipment and personnel working outdoors in temperatures of 0 to -50°F and with winds up to 20 mph.
- (b) Investigate various measuring techniques for determining the spatial distribution of the radiant heat flux falling on the target area and of the radiant intensity over the surface of the radiating element of the heater.

- (c) Study the effectiveness of various models of radiant energy heaters to determine the most feasible type for personnel heating. These are to include state-of-the-art commercially available examples of electric, natural gas, and propane gas heaters as well as a liquid fuel fired heater to be supplied by the Government. The spatial radiant heat flux distribution will be studied for a target 8 ft in diameter and located at distances up to 10 ft from the heater.
- (d) Investigate various methods to focus infrared heat to obtain the desired spatial heat flux distribution from heat sources having various geometries such as points, lines, and convex, concave or flat surfaces. Particular emphasis will be placed on developing a practical method of collimating or focusing the energy from the round flat disc used as the emitter surface in the existing liquid-fueled heater which will prevent excessive diffusion or spreading of the heat flux at distances of 4 to 8 ft from the heater.
- (e) Evaluate various materials for construction of the radiant burner face and emitter for the liquid-fuel-fired heaters.
- (f) Provide design recommendations for a liquid-fuel-fired radiant heater with adequate safety controls.

1.2 Background

Personnel exposure to the intense Arctic cold and high winds makes the repair of disabled equipment in the field without removal to heated repair areas extremely difficult. A requirement exists for a radiant heater to adequately warm personnel and disabled equipment so that such work can be conducted. A radiant heater was selected as the most direct means of heating the object with a minimum of dependence on the intervening space. Because of Army fuel policy and logistics, leaded gasoline was selected as the fuel.

Under contract to the Army, a radiant heater was developed using gasoline as the fuel with a "Cercor"* radiant burner. The heating rate of the burner was 25,000 BTU/hr based on the fuel input rate. This was sufficient to warm a person close (less than 4 ft) to the heater surface. However, due to excessive heat dispersion, the radiant heat flux at a distance of 8 to 10 ft from the emitter was inadequate to provide sufficient heating.

The final heater design weighed 12 lbs, whereas the desirable weight was 10 lbs or less. It lacked a safety control to shut off fuel in case of flame failure or rupture of the fuel lines. In addition, its performance deteriorated significantly in windy environments.

These results suggested that a more general program was necessary to review the necessary personnel heating requirements

* Corning Glass Works, New York

and the capability of various commercially available radiant type heaters. Such a program has been outlined in the previous section. A more detailed exposition of the technical aspects of radiant heaters and the approach followed is presented in the following sections.

1.3 Scope of Studies

The scope of this study includes the analysis and experimental evaluation of the radiant heating performance of various radiant source-reflector configurations from which an optimum configuration has been selected.

Specific studies conducted during this program cover the following major areas:

(a) Estimation of Radiant Heat Rate Requirement

This task was devoted to an analysis of the radiant heat input required to keep equipment and personnel reasonably warm under the specified environmental conditions. The results of this analysis are presented in Section 3.

(b) Radiant Energy Transfer from Various Source-Reflector Combinations

This study was aimed at analyzing the effectiveness of radiant heat transfer and the spatial flux density distribution at the target from various source-reflector combinations. The analysis covered area, line, and point source and conical, parabolic, and hyperbolic reflectors. The results of this analysis are summarized in Section 4 while the detailed analytical development is presented in Appendices A and B.

(c) Survey and Evaluation of Commercially Available Radiant Heater

This study was devoted to a general survey of the performance characteristics of infrared heaters as well as a detailed survey of commercial units. In order to compare the performance of these heaters with theoretical predictions, they have been classified according to source type such as, area, line, or point. This evaluation was used as a basis for the selection of certain heaters for further experimental evaluation. The results of this study are described in Section 5.

(d) Experimental Program

An experimental program was designed to measure heater performance and the spatial flux density distribution at the target. Test instrumentation was selected based on a survey of commercial units. Measurements were made on the heaters, with and without additional reflectors, both in a stationary ambient and in the specified wind. Measured values were compared with theoretical predictions. The results of this experimental program are discussed in Section 6.

(e) Materials of Construction of the Emitter Surface

This task was devoted to a study of different construction materials for the emitter surface and a summary discussion presented in Section 7.

(f) Special Design Requirements for a Liquid-Fuel-Fired Radiant Heater

Special design features for liquid fuel operation and safety under the operating environments are discussed in Section 8.

(g) Parametric Design Analysis of a Radiant Heater

A radiant heater was analyzed as a system consisting of a burner, heat exchanger and a emitter. Parametric analyses have been developed for these heater subsystems from which a novel radiant heater system has been synthesized. The results of this analysis are presented in Appendix C.

(h) Conclusions and Recommendations

The salient conclusions of this study and recommendations for further development work are summarized in Section 9.

2. Summary and Conclusions

This program, conducted for the U. S. Army Natick Laboratories, Natick, Massachusetts, was aimed at developing the necessary design information for the development of a portable, gasoline-fired, radiant heater to keep personnel and equipment warm in the Arctic environment. Such a heater would permit equipment to be repaired on site without necessitating removal to a heated repair area. The environmental conditions specified are temperatures in the range of 0 to -50°F and winds up to 20 mph. The heater is required to adequately heat a space 8 ft in diameter and located from 4 to 10 feet from the heater. Focusing of the radiation emanating from the heater is essential to maintain high heating rates at these distances.

To accomplish these objectives a combined approach of analysis and experimentation was utilized. The heat loss from equipment and personnel in the specified thermal environment was calculated, from which the heating rate necessary to maintain comfort and adequate manual dexterity was established. The heat transfer from various source geometries and reflector combinations was analyzed to predict the spatial flux density distribution at the target area. The range of commercially available radiant heaters was surveyed and evaluated to select the more promising configurations for experimental evaluation. A test apparatus was designed and instrumentation selected to measure the radiant output of the heater and the flux density at the target surface. Special reflectors were designed to improve the focusing of radiation from these heaters. Performance tests were conducted on these heaters in a stationary ambient and with a 15 mph wind. The results obtained were utilized to refine the theoretical analysis and to develop design charts for the preliminary

sizing of radiant heaters to meet a specified flux density requirement at the target. From this it was concluded that a heater consisting of a hemispherical source in a paraboloidal or hyperboloidal reflector represents the optimum configuration for the specified requirements.

No commercially available heater was found which is capable of operating in the specified Arctic environment of -50°F and 20 mph winds and providing the necessary heating rate to keep personnel and equipment warm. The Government furnished (GFP) gasoline heater was found to be totally unsuitable for this application.

With a limited amount of design effort, a novel radiant heater design has been developed, called the FMA radiant heater, which has the best performance of all the heaters tested and offers the potential of being designed for Arctic operation. The radiant flux density at the target from this heater was found to approach the minimum considered necessary for personnel and equipment heating. A further program for the development of a liquid-fuel-fired Foster-Miller radiant heater has been recommended.

The scope of the specific studies conducted during this program and the resulting principal conclusions are summarized in the following paragraphs.

2.1 Radiant Flux Density Required

From a survey of the literature on personnel comfort and minimum temperature for adequate manual dexterity, such as the handling of tools while repairing equipment, a minimum allowable hand temperature of 55°F is indicated. From an analysis of heat

loss from personnel and tools, to an ambient of -50°F , a minimum radiant flux density of 200 Btu/hr-ft^2 to the clothed body and 400 Btu/hr-ft^2 to the hand-work area was considered necessary to maintain a 55°F hand temperature. The higher value of 400 Btu/hr-ft^2 is to help maintain the tools and hands adequately warm and has been used as one of the design criteria for this program. It is realized that an impractically high heating rate may be required to heat and maintain large pieces of disabled equipment at 50°F . Rather, effort must be made to minimize contact of the hands with cold equipment and tools and to replace heat which is lost from the hands. Also, since infrared radiation is directional, several units, suitably placed will be needed to provide uniform heating over the maintenance personnel and the work site. This is the recommended mode of operation.

2.2 Analysis of Radiant Heating Performance of Various Source-Reflector Configurations

The spatial flux density distribution over the 8-foot diameter target area located from 4 to 10 feet away from the heater was analyzed. Sources were categorized into area, line and point sources; within these, circular disc, rectangular, cylindrical and spherical geometries were analyzed. Reflectors analyzed included conical, parabolic, and hyperbolic configurations.

These source geometries correspond to the actual units tested as part of the experimental program. Theoretically predicted values of the spatial flux distribution were compared with actual measured values. The correlation was found to be extremely good. Based on this analysis, design charts were developed for the preliminary sizing of heaters to provide a specified flux density at the target.

The analysis was utilized to compare on an equal basis, the heating performance of three source-reflector configurations, namely, circular disc source - conical reflector, cylindrical source - parabolic reflector, hemispherical source - parabolic reflector. The results showed the hemispherical source - parabolic reflector system to be the optimum, having a flux density which is 50 percent greater than that of the disc source - conical reflector system.

For the Government furnished (GFP) gasoline-heater, consisting of a circular disc source, a conical reflector was found to be the optimum configuration with a possible increase in the flux density by a factor of 3.

2.3 Survey and Evaluation of Commercial Infrared Heaters

The range of commercially available infrared radiant heaters was surveyed. This included liquid fuel and gas-fired and electric. No commercial, liquid fuel-fired, portable, infrared heater could be found. A variety of electric heaters are commercially available. They are generally high temperature, high intensity sources which radiate energy at shorter wavelengths, considered non-optimum for absorption by the receiver. In addition, the complexity, inconvenience, and inefficiency of generating electricity at site, added to the overall unattractiveness of electric heating for this application. Thus, though one electric heater was selected for testing, general consideration of electric heating was deemphasized.

Of the fifteen commercial heaters surveyed, five were selected for testing. The principal selection criterion was source geometry of the heater. They include:

1. Radiant System's Pyrocure - cylindrical source.
2. Hupp Propane Heater - rectangular source.
3. Hot-Tot Heater - cylindrical source.
4. Selas Radiant Burner - hemispherical source.
5. Hi-Shear Electric Heater - circular disc source.

In addition two other heaters tested are:

1. Government furnished gasoline heater - circular disc source.
2. Foster-Miller Radiant Heater - hemispherical source.

2.4 Experimental Program

A test apparatus was designed to measure the fuel input, the radiant intensity of the emitter, and the spatial flux density distribution at the target area. An Ircon Model 300 Radiation Pyrometer was used to measure the black body temperature distribution of the source and hence its radiant intensity. An Eppley Thermopile Radiometer was used to measure the radiant flux density distribution over the target area.

Test measurements were made on these heaters in a stationary ambient and with a 15 mph wind. The Hi-Shear Electric Heater and Selas Radiant Burner were found to be unsatisfactory and were not tested extensively. Tests results for the other heaters are summarized in the following Table I. This table includes a comparison of the heater source temperature, the total radiant

TABLE I

SUMMARY OF EXPERIMENTAL RESULTS FOR PERFORMANCE OF VARIOUS HEATERS

Heater Specifications							No Wind Target Distance					
Type of Heater	Mean Source Temp. (° F)	Area of Source (in ²)	Total Fuel Input (BTU/hr)	Total Heat Radiated (BTU/hr)	Burner Efficiency (Percent)	Description of Reflector	4 feet		8 feet		Mean Value	
							R= 1 ft	R= 4 ft	R= 1 ft	R= 4 ft	Value	
Government Furnished Gasoline Heater	1200	90	20,000	8,060	40	As received	186	65	135	43	35	40
						Small conical reflector	270	78	190	75	50	67
						Large conical reflector	372	20	205	115	45	85
Pyrocore Propane Heater	1540	43	12,500	8,210	65.7	As received	166	25	116	55	30	45
						Added inner cone	155	20	93	48	25	40
						Added outer cone	240	60	142	90	30	60
						Added both inner and outer cones	240	30	143	120	25	70
Hupp Propane	1360	76	20,000	9,980	50	As received	375	38	235	83	58	77
Hupp Hot-Tot Propane Heater	1500	334	86,000	59,200	69	Long conical	710	120	497	200	114	162
FMA Heater	1400	113	20,000	14,900	74.5	Three stage conical reflector (Parabolic equivalent)	560	50	313	195	58	145

Notes: R = Radial Distance at the Target

energy output, the fuel efficiency and the radiant flux density at target distances of 4 and 8 feet when operating in both stationary and windy environments. The salient results of this experimental program are summarized here.

a. Source Temperature and Fuel Efficiency

The mean source temperature and fuel efficiency are direct measures of the effectiveness of the burner and emitter design of the radiant heater. In general it is desirable to have a high mean source temperature together with a high fuel efficiency.

The surface combustion heater designs, such as the GFP gasoline heater and the Hupp propane heater, where the flame holder is both the heat exchanger and the emitter, have a poor heat exchange effectiveness. This results in a high exhaust gas temperature, low emitter temperature and poor fuel efficiency. The measured fuel efficiency of the GFP gasoline heater is only 40 percent at a mean source temperature of 1200°F. Similar values for the Hupp propane heater are 50 percent and 1360°F.

The FMA heater and the Hupp Hot-Tot heater designs have separate burner and heat exchange surfaces thus resulting in higher fuel efficiencies and emitter temperatures. The FMA heater has the highest measured efficiency of 74.5 percent at a mean source temperature of 1400°F. The Hupp Hot-Tot is equally efficient at 69 percent at a source temperature of 1500°F.

The Pyrocore heater is a good design of a surface combustion type burner operating at a fuel efficiency of

65.7 percent at a source temperature of 1540°F. It has the highest source temperature of all the heaters tested.

The FMA heater design has not been optimized. An improved heat exchanger design for the source is likely to result in a source having a mean black body temperature of 1600°F with a small reduction in fuel efficiency but a 50 percent increase in the total heat flux radiated.

b. Heat Flux Density at the Target Surface -
Effect of Reflectors

The measured flux density distribution at the target surface from the various heater source and reflector configurations is seen to confirm the theoretical predictions of their relative performance. For comparable fuel inputs, the highest flux density is obtained with the hemispherical-source, paraboloidal-reflector FMA heater and the lowest with the area-source, conical-reflector GFP gasoline heater. The cylindrical or line source with a paraboloidal reflector, such as the Pyrocore heater, is intermediate in value.

The flux density distribution over the target was generally non-uniform for all heaters, with a peak along the axis and a minimum at the outer radius of the target. This ratio of maximum to minimum flux density was largest at target distances close to the heater, such as 4 feet. At the larger target distances, such as 8 feet, the flux density distribution would tend to be more uniform. The addition of reflectors to direct the radiation at the target would generally result in an increase in both the mean flux

density and the nonuniformity as measured by the ratio of maximum to minimum flux density. Thus suitable trade-offs must necessarily be made to optimally match source and reflector designs in order to achieve both maximum uniformity and mean value of the flux density distribution at the target.

The target heating performance of the GFP gasoline heater was found to be extremely poor. At a target distance of 4 feet a peak heat flux density of 186 BTU/hr-ft^2 was measured at a target radius of 1 foot which dropped off to a value of 65 BTU/hr-ft^2 at a target radius of 4 feet and a mean value of 135 BTU/hr-ft^2 . As the original heater came with no reflector for focusing of the radiation, the flux density at a target distance of 8 feet dropped off to 45 and 35 BTU/hr-ft^2 at target radii of 1 and 4 feet and a mean value of 40 BTU/hr-ft^2 . This heating performance was increased substantially when the GFP heater was fitted with conical reflectors designed to optimize the radiant heat flux density at the target. With the large conical reflector, having a maximum diameter of 24 inches and a length of 12 inches, the flux density at the target was almost twice that of the original heater. The flux density at a target distance of 8 feet is still quite low, having a mean of 85 BTU/hr-ft^2 as compared with the 200 BTU/hr-ft^2 desired from each heater unit. It is unlikely that further substantial increases could be made with improved reflector designs. The source temperature is also limited, and cannot be increased with the present Cercor flame holder design due to the danger of flash-backs.

The FMA radiant heater, with the exception of the much larger Hot-Tot heater, gave the highest flux density at the target area. At a target distance of 4 feet this varied from 560

to 50 BTU/hr-ft² over target radii of 1 to 4 feet with a mean value of 313 BTU/hr-ft², and at a target distance of 8 feet this similarly varied from 195 to 58 BTU/hr-ft² with a mean value of 145 BTU/hr-ft². These results show that the heater performance is approaching the desired value of 200 BTU/hr-ft². The radial flux density distribution as obtained from this source-reflector combination is highly concentrated along the axis and is seen to fall off very rapidly at the larger target radii. We feel that the radial flux density distribution could be made more uniform by using a hyperboloidal reflector instead of the paraboloidal one. As discussed earlier, it is likely that with an improved source design, the source temperature could be increased to 1600°F resulting in a 50 percent increase in the flux density at the target. With both these modifications incorporated into the FMA heater, a mean flux density of 200 BTU/hr-ft² at a target distance of 8 feet appears to be achievable.

The Pyrocore propane heater had the best performance of all the commercial heaters tested. At 60 percent of the fuel input of the GFP gasoline heater, it provided a flux density on the target which was comparable to that of the gasoline heater. The performance of the original Pyrocore heater was substantially improved with the addition of the large conical reflector so as to increase the overall diameter of the paraboloidal reflector and a small inner cone to control the radiation from the front end of the cylindrical source. Thus, mean flux densities of 143 and 70 BTU/hr-ft² at target distances of 4 and 8 feet respectively were obtained.

c. Heater Performance in a 15 MPH Wind

The GFP gasoline heater and the Hupp propane

heater would not operate with a 15 mph head on wind due to flame-outs. This is a characteristic of all surface combustion burners. The Pyrocore, though a surface combustion burner, has good wind resistance, due possibly to its high operating gas pressure. It remained operational at approximately 30 percent of its original flux density.

The FMA radiant heater has extremely good wind resistance. There was no danger of a flame out with this heater design. The heater was extremely easy to light. The flux density obtained from this heater when operating in a 15 mph head wind was about 70 percent of its value in a stationary ambient.

To summarize, the test program has shown that the Foster-Miller Radiant heater has by far the best performance of all the heaters tested. It has extremely good wind resistance. It offers the potential for the development of a compact, rugged radiant heater to meet the needs of personnel working in an Arctic environment.

2.5 Parametric Design Analysis of a Radiant Heater

A parametric design analysis of a generalized fuel fired radiant heater was conducted to determine the interrelationships between fuel flow, combustor design, convective heat transfer from the hot gases to the emitter and finally radiation from the emitter to the environment. The design of the Foster-Miller hemispherical source was based on this analysis.

2.6 Materials for Emitter Construction

Inconel and a ceramic-glass, such as Cercor, are the two most commonly used materials for emitter construction. The emissivities of both these materials at the operating temperatures of the heaters (1400 to 1600°F) are practically the same and reasonably high, 0.65 to 0.78. Thus there is very little to be gained in increased performance from a high emittance material or coating.

2.7 Special Design Requirements for a Liquid-Fuel Fired Radiant Heater

Design features specific to the development of a liquid fuel fired radiant heater were analyzed. These included design modifications to the burner for operation on liquid fuel and special control features for safety.

2.8 Conclusions

The major conclusion from the studies reported in the preceding sections is that there is no commercially available heater capable of operating in the specified Arctic environment of -50°F and 20 mph winds and supplying the necessary heating rate to keep personnel and equipment warm. The GFP gasoline heater is totally unsuitable for this application.

With a limited amount of design effort, a novel radiant heater design has been developed, called the FMA radiant heater, which has the best performance of all the heaters tested. The radiant flux density at the target from this heater configuration

was found to approach the minimum considered necessary for personnel and equipment heating. This design offers the potential of being developed into a portable, rugged, compact, high intensity, high efficiency radiant heater for Arctic operations.

The specific major conclusions derived from this study are presented as follows:

(1) Calculations indicate that a flux density from a heater on the order of 200 Btu/hr-ft^2 to the clothed maintenance personnel will be required to prevent a drop in body temperature when working at -50°F even when exposure to wind is prevented by use of suitable windbreaks. Estimates indicated that even higher flux densities will be required on the hands and tools to maintain hand temperature at 55°F or greater.

(2) This heat input can best be achieved by use of several radiant heaters. For example, two large units might be used as large area heaters to cover the maintenance personnel and help maintain body temperature. Each should provide about 200 Btu/hr-ft^2 at the target area from about 8 feet away and should be suitably placed to equalize coverage of the target. Additional smaller heaters might operate from 2-4 feet distance from the target to help maintain higher flux levels in the immediate working area of the hands.

(3) The theoretical radiant heat transfer analysis developed during this program is capable of predicting the radiant flux density distribution at the target from various heater configurations, consisting of area, cylindrical and hemispherical sources

and conical, paraboloidal, and hyperboloidal reflectors. The correlation between theoretical predictions and experimental measurements of flux density distribution at the target is extremely good.

(4) A hemispherical source with a paraboloidal or hyperboloidal reflector is considered to be the most effective configuration for meeting the design requirements. It is capable of providing a 50 percent higher flux density at the target surface than possible with an optimum disc source, conical reflector configuration of the same source area, source temperature and overall reflector size. A cylindrical source with a paraboloidal reflector is intermediate in performance between the above two configurations.

(5) The design charts developed can be used for the preliminary design of a heater configuration to provide any specified flux density requirement at the target. Though the charts have been developed for a source temperature of 1500°F, designs for other source temperatures can easily be obtained by suitable scaling of the radiated emissive power (i.e. scaling by the fourth power of the absolute temperature).

(6) A source temperature in the range of 1400°F to 1800°F is considered desirable to optimize the radiant energy absorption at the target.

(7) The GFP gasoline heater is considered unsuitable for operation in the specified Arctic environment. It is extremely difficult to light and will not operate with a head wind blowing on it. In a stationary ambient it operates at a mean black body emitter temperature of 1200°F. Its source temperature could

not be increased due to the danger of a flash back. The heating performance of the original gasoline heater was extremely poor with a mean flux density of 40 BTU/hr-ft^2 at a target distance of 8 feet. This can be improved by the use of a conical reflector having a maximum diameter of 24 inches and a length of 12 inches, to 85 BTU/hr-ft^2 . This is still substantially less than 200 BTU/hr-ft^2 required. Substantial increases above this value with improved reflector designs do not appear to be possible.

(8) The Foster-Miller radiant heater consisting of a high intensity Wingaersheek Turbo Torch burner, a hemispherical shaped heat-exchanger and emitter, and a paraboloidal reflector showed the best performance of all the heaters tested. It is easy to light and operates extremely well in a windy environment. The heater-source configuration design is one where a high mean source temperature can be achieved with a relatively high fuel efficiency. The heater operated at a mean black body temperature of the emitter of 1400°F and a fuel efficiency of 74.5 percent. The mean flux density at a target distance of 8 feet was 145 BTU/hr-ft^2 which is 72 percent of the 200 BTU/hr-ft^2 required.

(9) The Foster-Miller radiant heater continued to operate in a 15 mph head-on wind with a mean flux density at 8 feet estimated to be 100 BTU/hr-ft^2 . This represents a 30 percent reduction in its radiant power output. This performance was found to be superior to any of the other heaters tested and is attributable to the special design features of the hemispherical source.

(10) The source configuration and the reflector design of the Foster-Miller heater have not been optimized. Improved heat

exchanger design of the source could result in an increase in the mean temperature to 1600°F resulting in a 50 percent increase in the radiant flux radiated. Thus, a value of 210 BTU/hr-ft² for the mean flux density at an 8 feet target distance could be obtained. An improved reflector, such as a hyperboloidal design, could result in a more uniform flux distribution at the target and possibly a higher flux density.

(11) The burner design used with the Foster-Miller heater can be modified to liquid fuel design with the addition of a prevaporization section. It is inherently safe. The chance of a flash-back upstream of the flame holder leading to an explosion is negligible.

(12) The most commonly used materials for emitter construction are inconel and a ceramic, such as, Cercor. Their emissivities at the high temperatures of 1400 to 1600°F are comparable. Cercor, being fragile and brittle is likely to be damaged by mechanical shock due to rough handling. It is therefore, not recommended for this application. Inconel is the better choice. The FMA radiant heater design lends itself to fabrication with inconel,

(13) Radiant System's Pyrocore heater was the best of all the commercially available heaters tested. It has a cylindrical source of inconel in a paraboloidal reflector. The mean flux density at a target distance of 8 feet was 45 BTU/hr-ft² at a source temperature of 1540°F and a fuel input which is 60 percent of the input value to the GFP and FMA heaters. The mean flux density at the target was increased to 70 BTU/hr-ft² with the

addition of the 24 inch (large) conical reflector used for the GFP heater and an inner conical reflector. The heater was easy to light and has good wind resistance.

2.9 Recommendations

The preliminary prototype model of the Foster-Miller radiant heater has clearly demonstrated its superiority over all other commercially available designs for the specified application of heating personnel and equipment in an Arctic environment. It is therefore recommended that a development program be undertaken to optimize the design and to modify it for liquid fuel operation. Such a development program would have as its specific objectives;

(a) Optimization of the burner and heat exchanger to increase the mean source temperature to 1600°F from the presently achieved 1400°F. This would result in an increase in the radiant intensity of the source by 50 percent and result in a mean radiant flux density of 210 BTU/hr-ft² at a target distance of 8 feet.

(b) Optimization of the reflector design to achieve a more uniform radial distribution over the target area, such as, with a hyperboloidal reflector.

(c) Detailed design of the heat exchanger configuration, including selection of material of construction, mode of construction and fabrication to minimize weight and cost.

(d) Modification of the burner design for liquid-fuel operation by incorporating a prevaporization section for the liquid fuel.

(e) Optimization of the configuration design for portability, reliability of operation, resistance to shock and rough handling and finally good wind resistance.

(f) Design for safety and controls to optimize operation in the specified Arctic environment.

3. Heating Rate Requirements

The purpose of this program is to develop design recommendations for a radiant heater to provide the necessary heat input which will enable personnel to work with reasonable comfort in the specified environment. The specific heat rate required to achieve this comfort is extremely difficult to theoretically estimate, especially with radiant heat which is highly directional. It is tacitly assumed that the worker is protected thermally with Arctic clothing and the primary function of the radiant heater is to heat the exposed surfaces of his hands and his working tools such that normal manual dexterity can be maintained.

Experiments conducted by Gaydos, Adams and others have demonstrated that as the finger skin temperature falls below 50 to 55°F, hand tactile function and mobility are most seriously impaired.^{1,2*} Stinchfield and Rohr confirmed that this temperature limit agreed well with observations made at the U.S. Army Natick Laboratories of men working in a cold environment.³ It has also been shown that with adequate heating of the body hand temperatures can be maintained.² In fact, face warming is capable of increasing blood flow to the hands. Thus both general heating of the body, as well as local heating of the exposed hand surfaces, is likely to aid in increased manual dexterity.

Since no data could be found for the direct heating rate for the hands, heat density requirements for maintaining personnel comfort and a temperature of 50°F for the metal tools were estimated. These data are used as a basis for radiant heater design requirements.

* Raised numbers refer to literature cited.

3.1 Radiant Flux Inputs Required for Personnel Comfort

The theoretical radiant heating requirements for personnel comfort can best be estimated from a consideration of an overall body heat balance and the heat loss relationships from the skin to the ambient surroundings.

A schematic diagram for body heat balance in a clothed human body is shown in Figure 1a and the heat loss relationships are diagrammed in Figure 1b. These heat terms and relationships are discussed and used in the following sections:

(a) Heat Produced by Metabolism, M

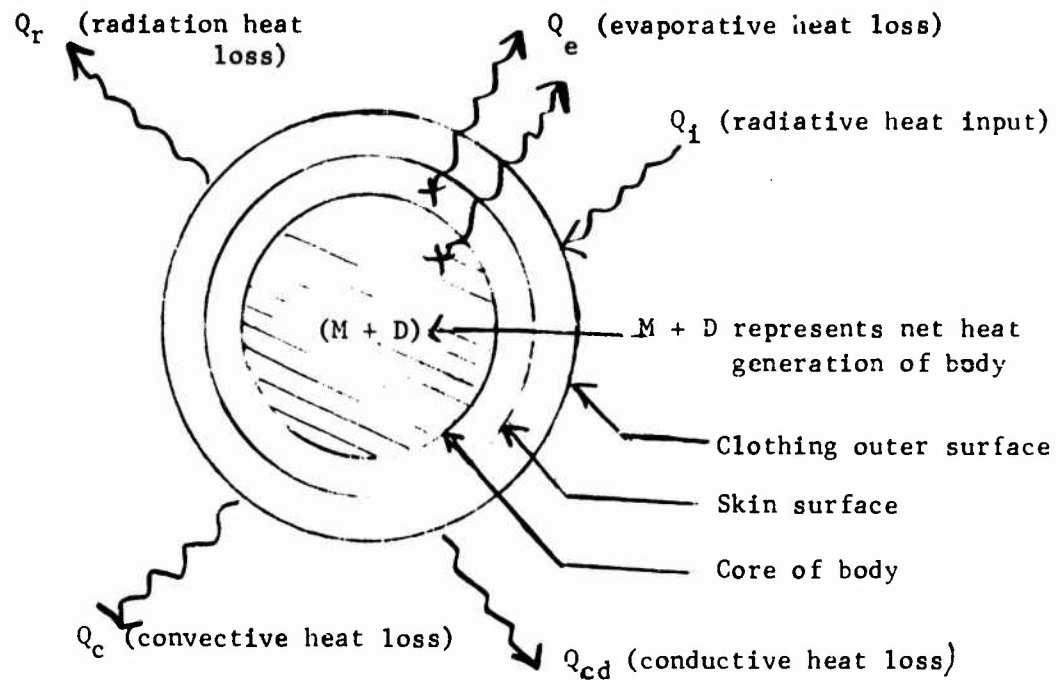
The production of heat due to internal metabolism of the body is very strongly dependent on its state of activity. Values for M reported in the literature fall in the range of 0.7 Met to 17.2 Met (where 1 Met = 18.5 Btu/hr-ft²), depending upon the level of activity.^{4,5} As a conservative approximation for design, a metabolism level of 1 Met is assumed, which essentially corresponds to a condition of rest.

(b) Heat Content of the Body, D

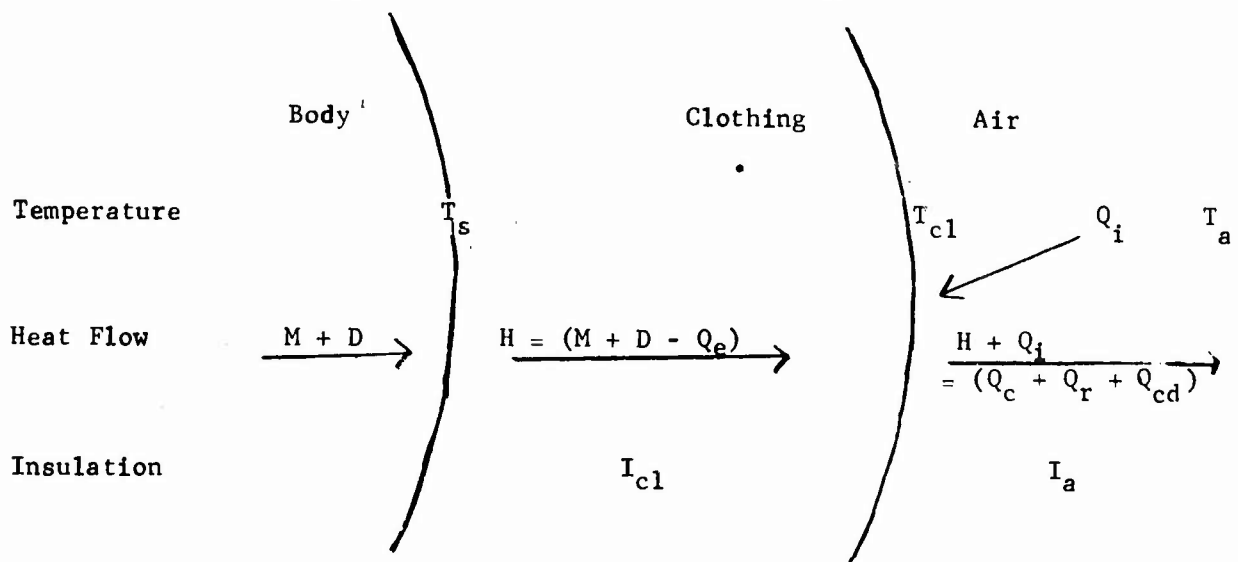
For personal comfort the net loss of heat content of the body has to be zero. Therefore the value of $D = 0$ will be used in our calculations.

(c) Evaporation Heat Loss, Q_e

Loss of heat due to breathing and perspiration evaporation are two factors which contribute to the total evaporation heat loss from the body. The parameters which affect evaporation heat loss are the ambient



(a) Heat Balance with Surroundings



(b) Heat Loss Relationship

Figure 1 Heat Relationships for a Clothed human Body

temperature, relative humidity, clothing, and level of activity.

Empirical relationships for the evaporation heat loss in terms of these various parameters are discussed in detail in References 4, 5, 6 and 7. For design, a good estimate of evaporation heat loss is 25 percent of the metabolic heat production.

(d) Convection, Radiation and Conduction
Heat Loss, $(Q_c + Q_r + Q_{cd})$

Heat losses from the outer surface of the clothing are completely accounted for by conduction, radiation, and convection and the heat losses are known to be proportional to the temperature gradient between the clothing surface and the ambient, $T_{cl} - T_a$, and inversely proportional to a quantity representing the insulating value of the air, I_a . Because air movement due to thermal gradients or wind is always present, convection and radiation are the primary heat transfer mechanisms. With variation in ambient temperature the relative proportion of heat loss by radiation and convection changes. While in colder environments the loss by radiation decreases, the loss by convection, for the same velocity of air movement, increases because of the increase in air density and decrease in air viscosity with decreasing temperature which contribute to an overall increase in the convective heat transfer coefficient. The increase in convective loss tends to compensate, very nearly, the decrease in radiative loss, and this is so over practically the whole range of values of air movement. Thus the insulation value of air, I_a , is essentially independent of the ambient temperature. The quantity I_a is, however, strongly dependent on the wind velocity and varies from about 1 clo unit in still ambient air to 0.15 clo unit in a 20-mph wind. One clo unit is equivalent to $0.88^\circ\text{F}/\text{Btu}\cdot\text{hr}\cdot\text{ft}^2$. The thermal insulation value of clothing, I_{cl} , is about 4 clo/inch of clothing thickness and for cold weather situations normally ranges from 2-5.6 clo, depending on the clothing selected.

(e) Calculation of Radiant Heat Input to a Fully Clothed Body

It may be seen from Figure 1b that under steady state conditions the two relationships for heat transfer from the skin to the outer surface of the clothing and from this clothing surface to the ambient surroundings must be satisfied by the same values of H and T_{cl} . These relationships are:

$$H = M + D - Q_e = \frac{T_s - T_{cl}}{I_{cl}} \quad (1)$$

$$H + Q_i = Q_c + Q_r + Q_{cd} = \frac{T_{cl} - T_a}{I_a} \quad (2)$$

If these equations are added and rearranged we obtain:

$$H + Q_i \frac{I_a}{I_{cl} + I_a} = \frac{T_s - T_a}{I_{cl} + I_a} \quad (3)$$

It may be noted from this equation that the effectiveness of the radiant flux, Q_i , in reducing the heat flow, H , from the body and across the clothing is dependent on the ratio of the insulation outside the point of absorption of the radiant flux, I_a , to the total insulation, $I_a + I_{cl}$. Thus one can see that the radiant flux would be most effective if the clothing was transparent to the radiant flux and it was absorbed at the skin surface.

Alternatively, equation (3) may be rearranged in the form:

$$H = \frac{T_s - (T_a + Q_i I_a)}{I_{cl} + I_a} \quad (3a)$$

This arrangement shows that the effect of the radiant energy can be considered

as a moderation of the ambient temperature in which the effective radiation increment is the product of the radiant flux and the thermal insulation outside the point of radiant flux absorption.

The radiant flux input required to maintain body temperature with a 1-Met metabolism level, corresponding to a rest situation, may be calculated from equation (3) for the following assumed conditions:

$$\begin{aligned} D &= 0 \\ T_s &= 90^{\circ}\text{F} \\ T_a &= -50^{\circ}\text{F} \\ I_{cl} &= 4 \text{ clo} \\ I_a &= 0.75 \text{ clo assuming use of windbreak} \\ Q_e &= 0.25M \end{aligned}$$

A value of $Q_1 = 124 \text{ Btu/hr-ft}^2$ is obtained. Recognize that, as calculated, this represents a quantity absorbed uniformly over all surfaces of the clothed body. Note also that for khaki clothing only about 60% of the radiant flux will be absorbed and that energy from a single radiant source will be incident on only about 1/3 of the body surface; thus it becomes evident that much higher flux levels should be necessary in a field situation utilizing radiant heaters to maintain body temperature.

If this calculation was made assuming a 20-mph wind corresponding to $I_a = 0.15 \text{ clo}$, then the quantity Q_1 required is on the order of 600 Btu/hr-ft^2 . The need for use of a windbreak is evident.

(f) Calculation of Radiant Heat Input to Bare Hands

Recalling that hand skin temperatures must be 50°F

or greater to maintain manual dexterity one can calculate the rate of heat loss from bare hands and thus the maximum radiant energy input required at the skin surface, assuming no input from the body. For the relationship

$$H + Q_1 = \frac{T_s - T_a}{I_a} \quad (4)$$

assume

$$\begin{aligned} H &= 0 \\ T_s &= 50^\circ\text{F} \\ T_a &= -50^\circ\text{F} \\ I_a &= 0.75 \text{ clo for a windbreak resulting in very} \\ &\quad \text{little air movement} \end{aligned}$$

Then the Q_1 requirement is 150 Btu/ft²/hr. Recognize that this is a maximum requirement assuming no input from the body and that it represents a value for the flux absorbed uniformly over the hand surfaces. Since the flux from a single radiant source would only be partially absorbed and would reach only about 1/3 the area of the hand, it is evident that the flux level requirement could be much higher to compensate for heat loss by convection and radiation from bare hands.

If we assume that no windbreak is used and that the hands are exposed to a 20-mph wind corresponding to a thermal insulation value of air, I_a , equal to 0.15 clo, then the Q_1 requirement calculated is 750 Btu/ft²/hr.

Even higher rates of heat loss could occur if hand contact was made with cold tools or other high thermal conductivity material.

3.2 Radiant Flux Inputs Required to Warm Metal Tools

A working temperature of the tools in the range of 50 to 55°F is desirable. The radiant heat input to achieve this condition is calculated by equating the heat input to the heat loss to the ambient. The total heat loss Q_L , BTU/hr can be expressed by

$$Q_L = Q_r + Q_c \quad (5)$$

where

Q_r = radiation heat loss, BTU/hr

Q_c = convection heat loss, BTU/hr

In general, the predominant heat loss is due to convection; radiation cooling is relatively small and has been neglected. Therefore, the required heat input, Q_i can be approximated by

$$Q_i = h_c A_s (T_s - T_a) \quad (6)$$

where

h_c = convection heat transfer coefficient

A_s = surface area

T_s = surface temperature of tool

T_a = ambient temperature

Though the radiant heat input is directional and would heat only the tool surface directly exposed to the radiation, the thermal conductivity is sufficiently high so that the tool is assumed to be at a uniform temperature. Then A_s represents the total surface area of the tool.

The convection heat transfer coefficient is determined from the following correlations,

$$\frac{h_c L}{k} = 0.664 P_r^{0.33} R_e^{0.5} \text{ for laminar flow} \quad (7a)$$

$$\frac{h_c L}{k} = 0.037 P_r^{0.33} R_e^{0.8} \text{ for turbulent flow} \quad (7b)$$

where

L = length of the plate

k = thermal conductivity of air

P_r = Prandtl number = $\frac{c_p \mu}{k}$

R_e = Reynolds number = $\frac{\rho V L}{\mu}$

c_p = specific heat capacity of air

ρ = density of air

μ = viscosity of air

For air at 0°F and 14.7 psia, with a wind of 20 mph blowing past a metal tool approximately 1 foot in length, the heat transfer coefficient is estimated to be $4 \text{ Btu/hr-ft}^2\text{-}^{\circ}\text{F}$. For a design tool temperature of 50°F and an ambient of -50°F , a radiant flux input of 400 Btu/hr-ft^2 is calculated.

3.3 Radiant Flux Inputs Required to Warm Equipment Under Repair

Similar estimates of the radiant heating rate required to warm disabled equipment are difficult to obtain because of the variety of sizes, shapes and materials of construction possible. The heating rate required to warm an automobile tire may vary significantly from that required to heat the carburetor of an engine due to their significantly different thermal diffusivity and thermal capacity. These parameters affect the time required to achieve a thermal steady state.

It is likely that the convective heat transfer coefficient for most equipment would be of the same magnitude as that calculated for tools (in the form of a flat plate) as given by Equation (6) and hence 400 Btu/hr-ft^2 would be sufficient to keep the equipment warm in the steady state. However, the time required to achieve this steady state will often be too large to be considered acceptable, and consequently a much higher heating rate may be required. Furthermore, radiant heat, being directional will only reach a fraction, about one-third, of the surface of a three-dimensional body exposed to it.

The selection of an actual design heating rate for equipment would have to be based on a detailed analysis of the initial time available for warm-up and the transient thermal behavior of the equipment being heated. In the absence of such an analysis the steady state heating rate of 400 Btu/hr-ft^2 is recommended as a minimum flux level over the total surface of the equipment. Higher heating rates, achievable by irradiating the same surface with more than one heater unit or with the heater placed close (less than 4 feet) to the target would be required to reduce the initial warm-up period.

3.4 Design Recommendation for Heating Rate Requirement

The basic problem, if personnel are to efficiently perform

routine maintenance and emergency repair of equipment under extreme cold conditions, appears to be to maintain their hand skin temperature above 55°F without inhibiting their performance by the presence of bulky hand protection/insulation. It is obvious that the nature of the specific job to be done, together with the weather situation at the time, will determine the magnitude of the problem. Present knowledge is too incomplete to define the optimum approach but the calculations of the previous sections can offer some guidance.

Since circulatory input to the body extremities is reduced as body temperature is reduced, it appears desirable to supply area heating to help maintain body temperature. The calculations of Section 3.1 stress the need for minimizing exposure to wind in order to keep the required flux level within reason and indicate that from an area heater flux levels on the order of 200 Btu/hr-ft² at the target are required.

The problem of heating equipment under repair to 50°F is considered in Section 3.3. The discussions indicate that for many jobs it will be completely impractical to attempt to heat the equipment to 50°F to prevent loss of heat from the hands. Rather, the approach to the problem must be one of minimizing heat loss from the hands by minimizing direct contact with the equipment and of rapidly replacing heat which is lost. The use of tools made of low conductivity material and with insulated handles, of suitable insulated clamps to minimize hand contact with massive equipment parts, of lightweight gloves to reduce the rate of heat loss to cold metal and tools, and of radiant heat at the working site to rapidly rewarm the hands is called for in this situation. The calculations of Sections 3.1 and 3.2 indicate that the flux level from a heater directly on the hands and tools should probably be at a minimum of 400 Btu/hr-ft² and much higher levels may be required.

Because of the directional nature of the output from radiant heaters it will often be necessary to use arrangements of several heaters, for example, two area heaters set back about 8 feet from the job and providing heat from different angles together with one smaller heater set 2 to 4 feet from the working site and heating a smaller target area where the hand-work is concentrated.

4. Analysis of Radiant Energy Transfer from Various Source-Reflector Combinations

4.1 Analytical Objectives and Method

Personnel heating, with the gasoline fueled radiant heater developed for the U. S. Army, under a previous contract, was adequate up to distances of 4 feet from the heater but totally inadequate at distances of 8 to 10 feet from the heater. Better control or focusing of the radiant energy was considered necessary. Consequently, one of the principal objectives of this program is to analyze the radiant heating performance of various source configurations; such as area, line and point sources, with and without reflectors designed to direct the radiation on the target area specified. Adequate heating is considered necessary over a target area 8 ft in diameter, located 4 to 10 ft from the heater. A theoretical analysis was conducted to predict such performance.

The specific objectives of this analysis are:

1. To analyze the radiant heat transfer to the target from various sources, such as, discs, cylinders, spheres.
2. To design various reflector configurations for these sources and to analyze the radiant heat transfer to the target with these source-reflector combinations.
3. To calculate the spatial distribution of radiant flux density on the 8 ft diameter target located 4 to 10 ft from the heater.

4. To develop optimum reflector configurations for the Government furnished gasoline heater.
5. To develop design curves for the preliminary design of source and reflector combinations to meet a specified flux density at the target.
6. To develop and recommend an optimum source-reflector combination for personnel heating.

The theoretical analysis conducted to satisfy these objectives is presented in Appendices A and B. Analytical predictions were supported by experimental data obtained during the test program which was used to establish the value of certain constants or the validity of certain approximations. This semi-empirical approach has resulted in a model which satisfactorily predicts the performance of the different source-reflector configurations. Based on these results, charts for the preliminary design of heater configurations have been developed and an optimum configuration of a hemispherical source with a paraboloidal or hyperboloidal reflector has been selected.

The analyses was conducted in two parts:

- (1) The axial distribution of the radiant heat flux density at the center of the target and target locations from 4 to 10 ft from the heater was analyzed, as described in Appendix A. These results were utilized to approximately predict the performance of the various heater configurations in heating the target area.

- (2) The radial distribution of flux density over the target area was approximated, using the analysis of Appendix A and the test results reported in Section 6. A discussion of this analysis is presented in Appendix B.

The major results obtained from these analyses are presented in the following sections.

4.2 Radiant Heat Transfer Performance of Various Source Reflector Geometries

The radiant heat transfer performance of the various source-reflector configurations is expressed in the following terms:

- (a) Heat Transfer efficiency, η_T , defined as

$$\eta_T = \frac{\text{Total heat flux received by the target}}{\text{Total heat flux emitted by the source}}$$

- (b) A Flux Density ratio, R_{FD} , defined as

$$R_{FD} = \frac{\text{Heat flux received per unit area of target}}{\text{Heat flux emitted per unit area of source}}$$

- (c) i_T = Radiant flux density at the target
generated by a source of unit area,
BTU/hr-ft⁴

Figures 2 through 7 show schematic diagrams of the different source and reflector geometries analyzed in Appendix A. Performance values were calculated for each of these geometries based on the following assumptions:

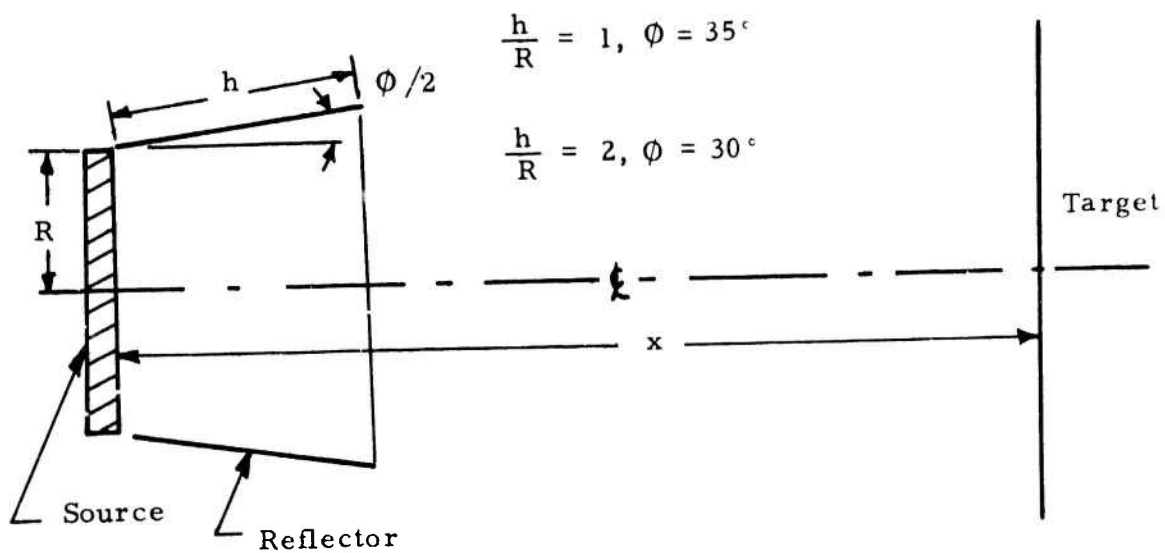


Figure 2 Disc Source with Conical Reflector

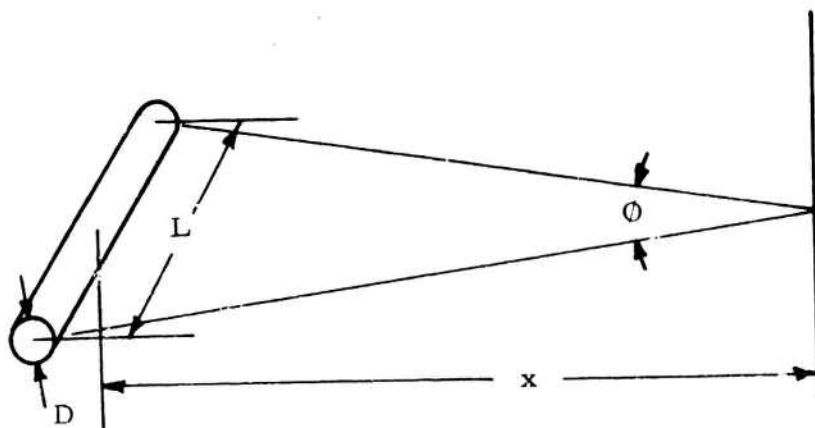


Figure 3 Circular Cylinder (Line Source)

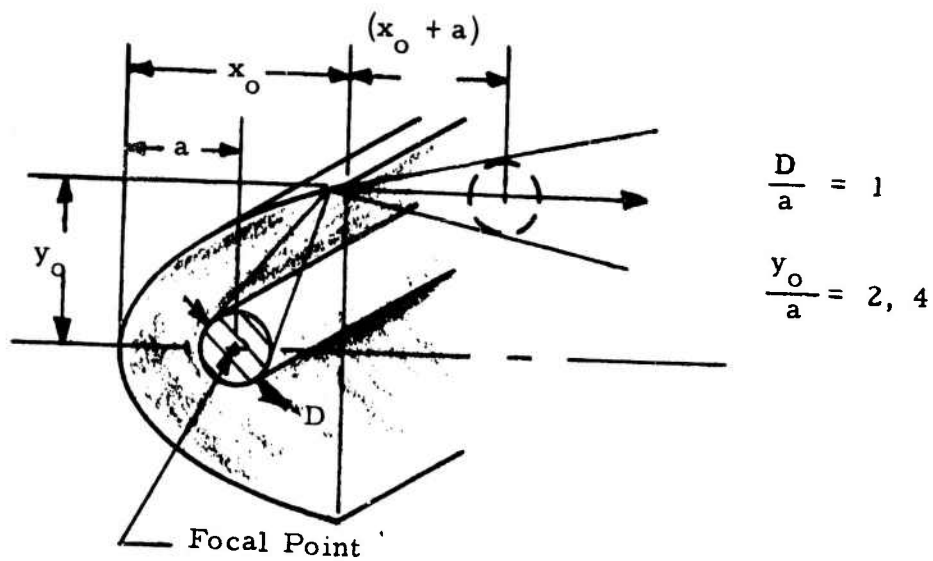


Figure 4 Circular Cylinder with Parabolic Reflector

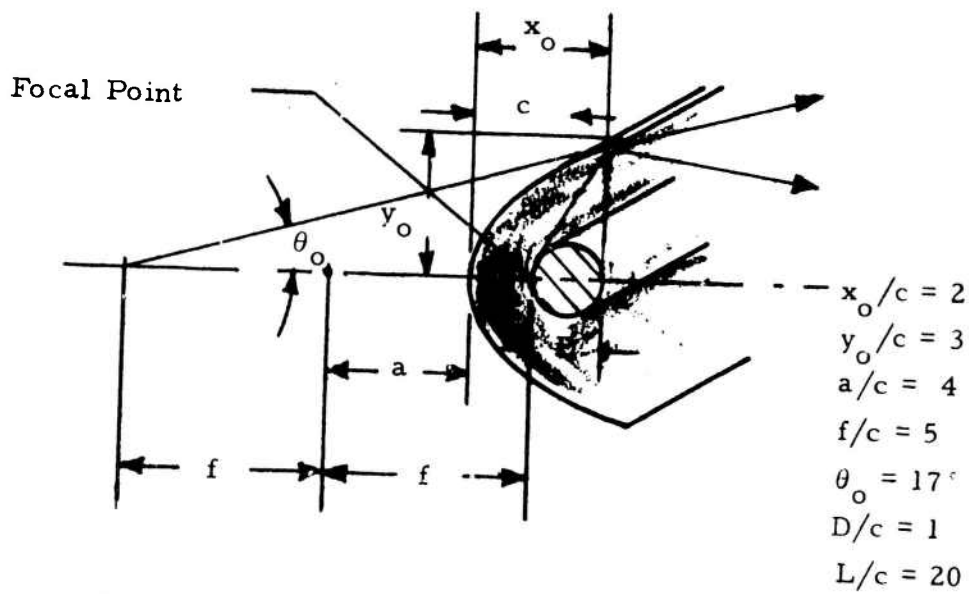


Figure 5 Circular Cylinder with Hyperbolic Reflector

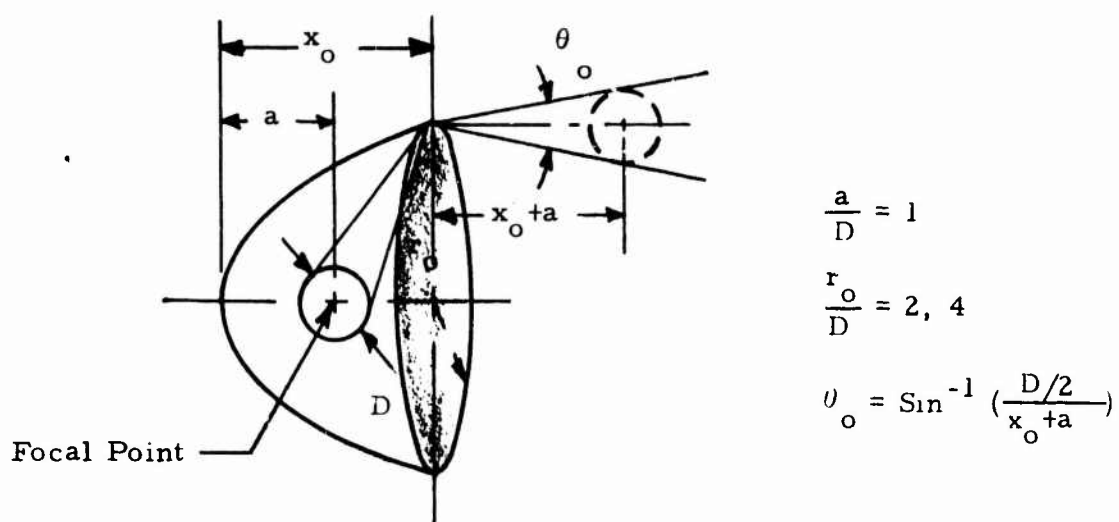


Figure 6 Spherical Source with Paraboloid Reflector

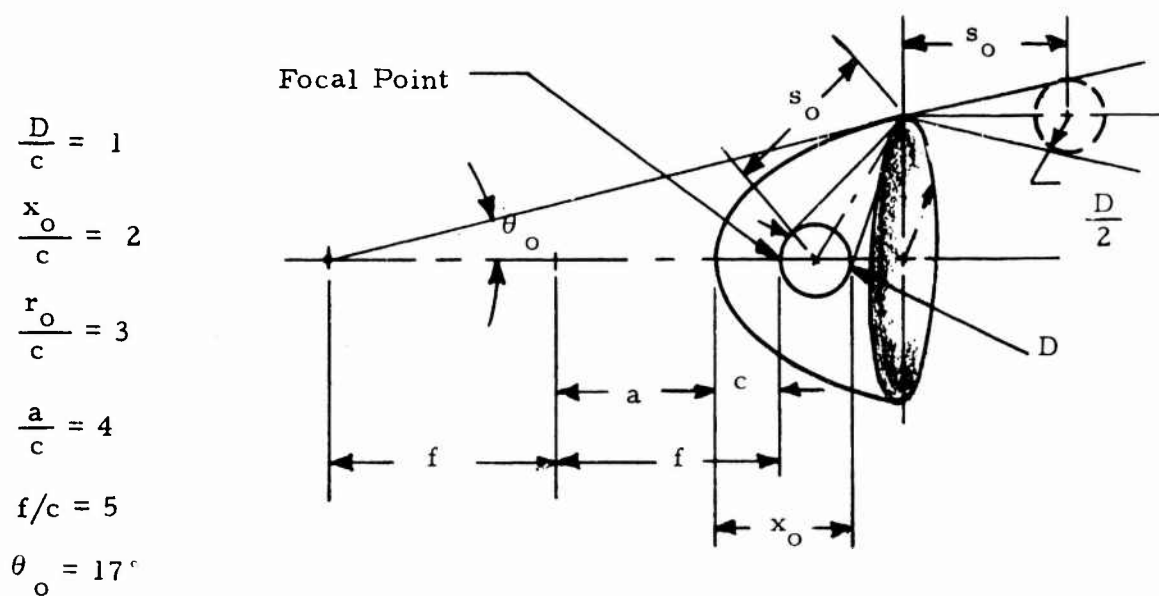


Figure 7 Spherical Source with Hyperboloid Reflector

- (1) The source temperature is constant and uniform over the total source area as well as for all different source types. An assumed temperature of 1500°F and an emissivity of 1 results in an emissive power of 25,000 BTU/hr-ft².
- (2) The target is 6 ft in diameter and 10 ft away from the source. It has an absorptivity of 1.
- (3) The radiant flux densities calculated represent a mean over the target area.

The calculated performance is summarized in Table II. The ideal configuration is one where all the radiant energy output of the source is received by the target area. It represents a maximum in possible performance.

The results of this simplified analysis are useful in obtaining a comparison of the relative heating performance of the various source geometries and reflector configurations. The principal conclusions from this analysis are:

1. The heat transfer efficiency, η_T is a strong function of source geometry and reflector design. In general a higher efficiency is obtained with a smaller size source and the largest possible reflector. For example the efficiency obtainable with the small diameter spherical source is greater than 50 percent as compared with only 20 percent with the large diameter disc source.

TABLE II
RADIANT ENERGY TRANSFER PERFORMANCE OF VARIOUS
SOURCE AND REFLECTOR GEOMETRIES

Source	Reflector	Reference Figure No.	η_T Percent	$R_{FD} \times 100$	\bar{i}_T BTU/hr-ft ⁴
Ideal	Ideal	-	100	3.52	892
Disc (Area) R = 6"	None	2	9.45	0.259	84
	Conical, $\frac{h}{R} = 1$, $\phi = 35^\circ (0)$	2	13.8	0.384	116
	Conical, $\frac{h}{R} = 2$, $\phi = 30^\circ$	2	19.7	0.55	166
Circular Cylinder (Line) l = 0.1', L = 2'	None	3	2.83	0.063	25.3
	Parabola, $\frac{y_o}{a} = 2$	4	17	0.392	158
	Parabola, $\frac{y_o}{a} = 4$	4	20.8	0.465	185
	Hyperbola, $\frac{y_o}{c} = 3$	5	15.8	0.35	141
Sphere (Point) D = 0.1'	Paraboloid, $\frac{r_o}{a} = 2$	6	67	0.074	596
	Paraboloid, $\frac{r_o}{a} = 4$	6	80	0.089	712
	Hyperboloid, $\frac{r_o}{a} = 3$	7	72	0.08	646

2. The major factor in reflector design which affects overall performance is the degree of directional control. One direction control, such as with a parabolic reflector and a line source, is less efficient than two direction control as obtained with a paraboloidal reflector and a spherical source.
3. A spherical source with a paraboloid reflector is estimated to yield the best performance amongst the various geometries considered. A heat transfer efficiency approaching 80 percent has been calculated. This value could possibly be increased further by controlling the emission from the front surface of the source with a suitable reflector.

4.3 Spatial Distribution of Flux Density at the Target

The flux density distribution at the target from a source without a reflector can be calculated from Figures A-2 and A-3 of Appendix A, which show the spatial distribution of view factor for disc and rectangular sources. The GFP gasoline heater is essentially equivalent to a 1 ft diameter disc source with no reflector. The heater has a preheater which shades about 30 percent of the source area. Theoretically predicted values of the flux density distribution for this configuration at target distances of 4 and 8 ft are shown in Figure 8. Also shown for comparison are the experimentally measured values, presented in Section 6.4.1 of this report. The results show good agreement between theoretical predictions and actual measurements.

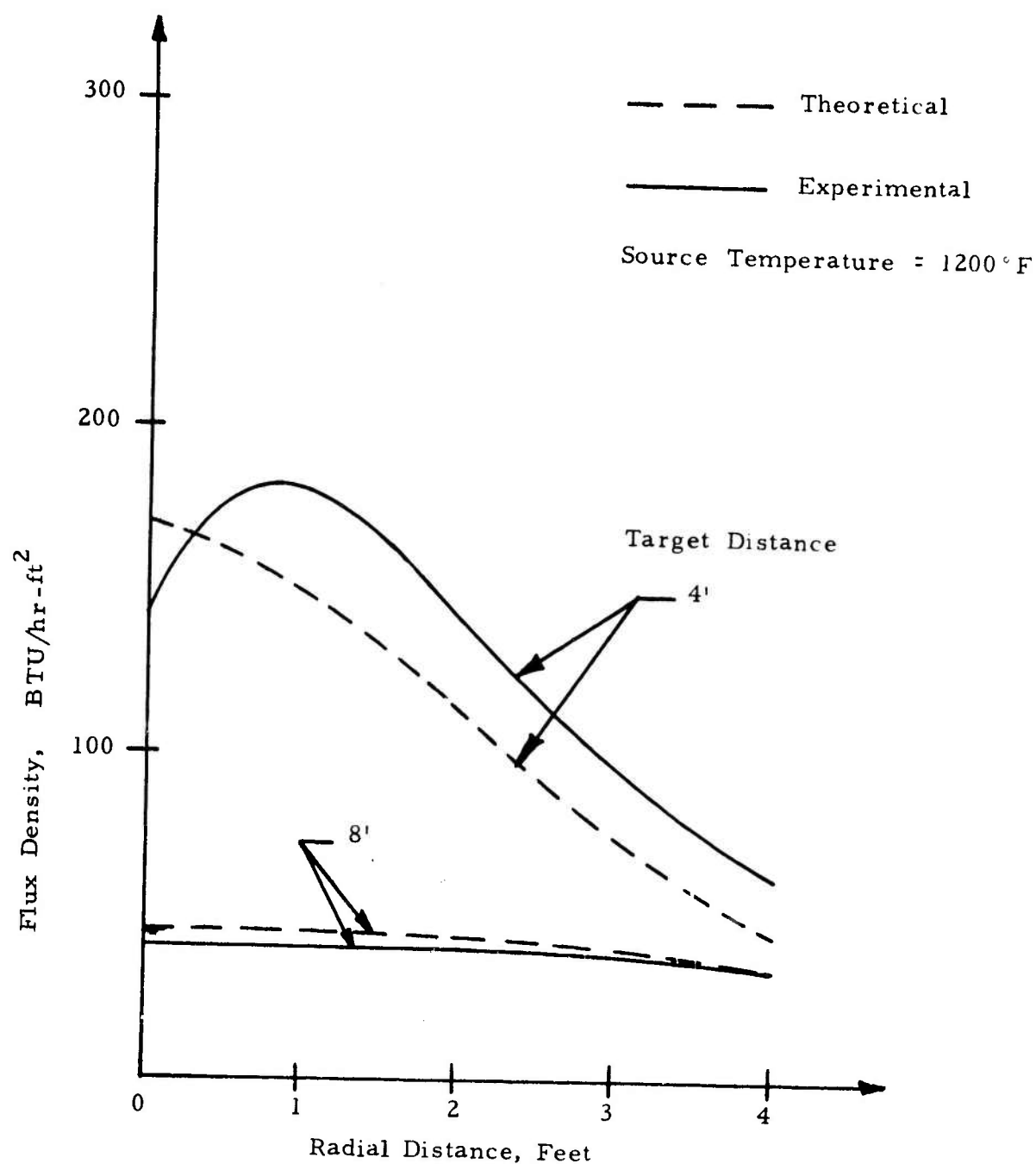


Figure 8 Comparison of Theoretical and Experimentally Measured Values of the Radiant Flux Density Distribution at the Target from the GFP Gasoline Heater

The small increase in measured values over theoretical predictions at the target distance of 4 ft, is probably due to the very short cylindrical reflector integral to the heater.

The analysis to predict the spatial flux density distribution for heaters with reflectors is presented in Appendix B. Theoretically predicted values of the flux density distribution at target distances of 4 and 8 feet and for three different source types are shown in Figures 9, 10 and 11. Each figure also shows, for comparison, experimental measurements of the flux density as obtained in the experimental program with heaters having similarly configured sources.

Figure 9 is for a disc source with a conical reflector and, for comparison, test results of the GFP gasoline heater with a large conical reflector as given in Section 6.4.1 of this report.

Figure 10 shows the distribution from a cylindrical source in a parabolic reflector and the results are compared with the measured performance of the Pyrocore heater as given in Section 6.4.2 of this report.

Figure 11 shows the distribution from a hemispherical source in a paraboloidal reflector and the results are compared with the measured performance of the Foster-Miller Radiant Heater as given in Section 6.4.5 of this report.

All these figures show good correlation between theory and practice, thus verifying the theoretical basis used in Appendices A and B for deriving the spatial flux density distribution.

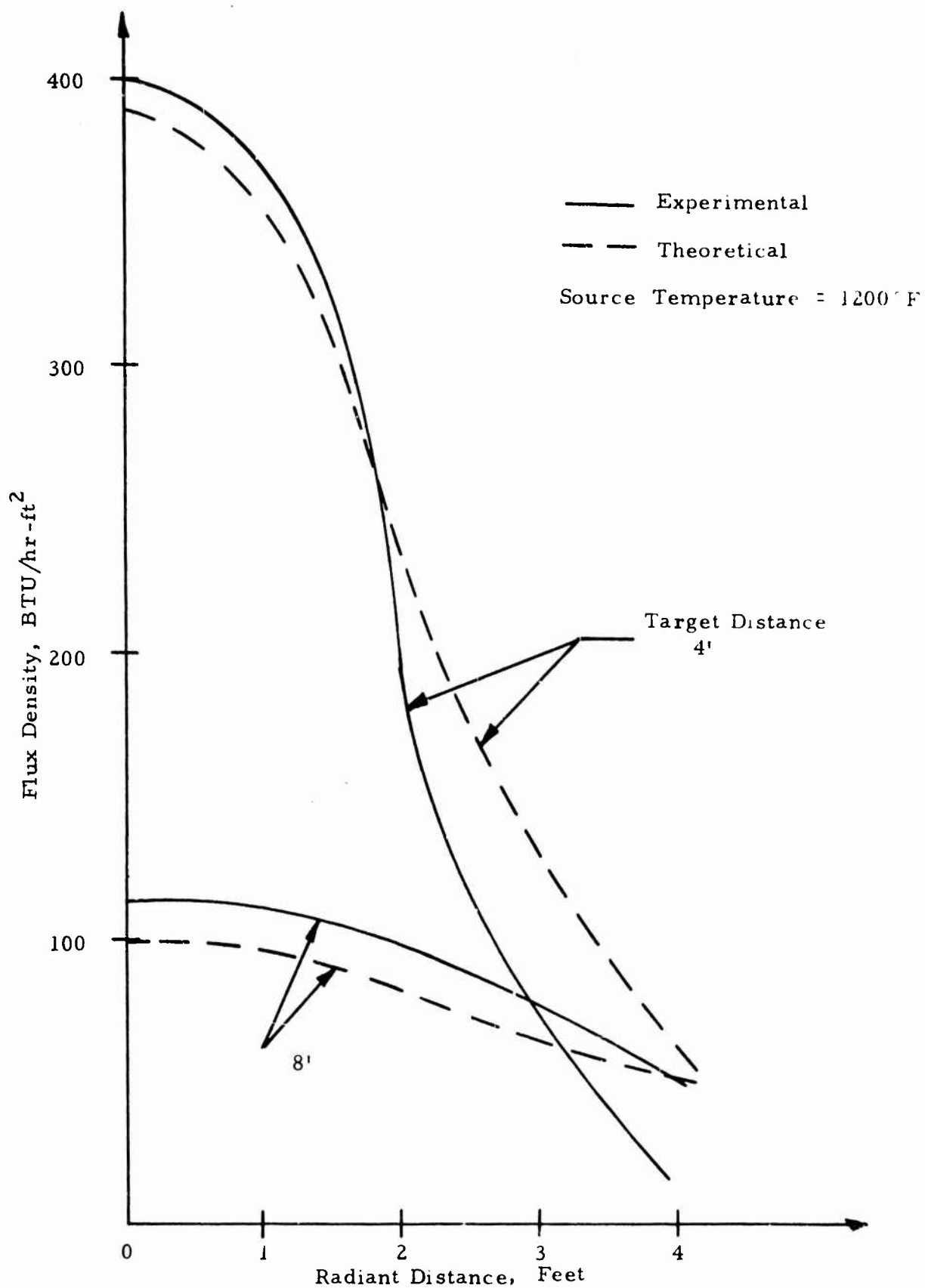


Figure 9 Comparison of Experimental and Theoretical Values of the Radiant Flux Density Distribution at the Target from the GFP Gasoline Heater with the Long Conical Reflector

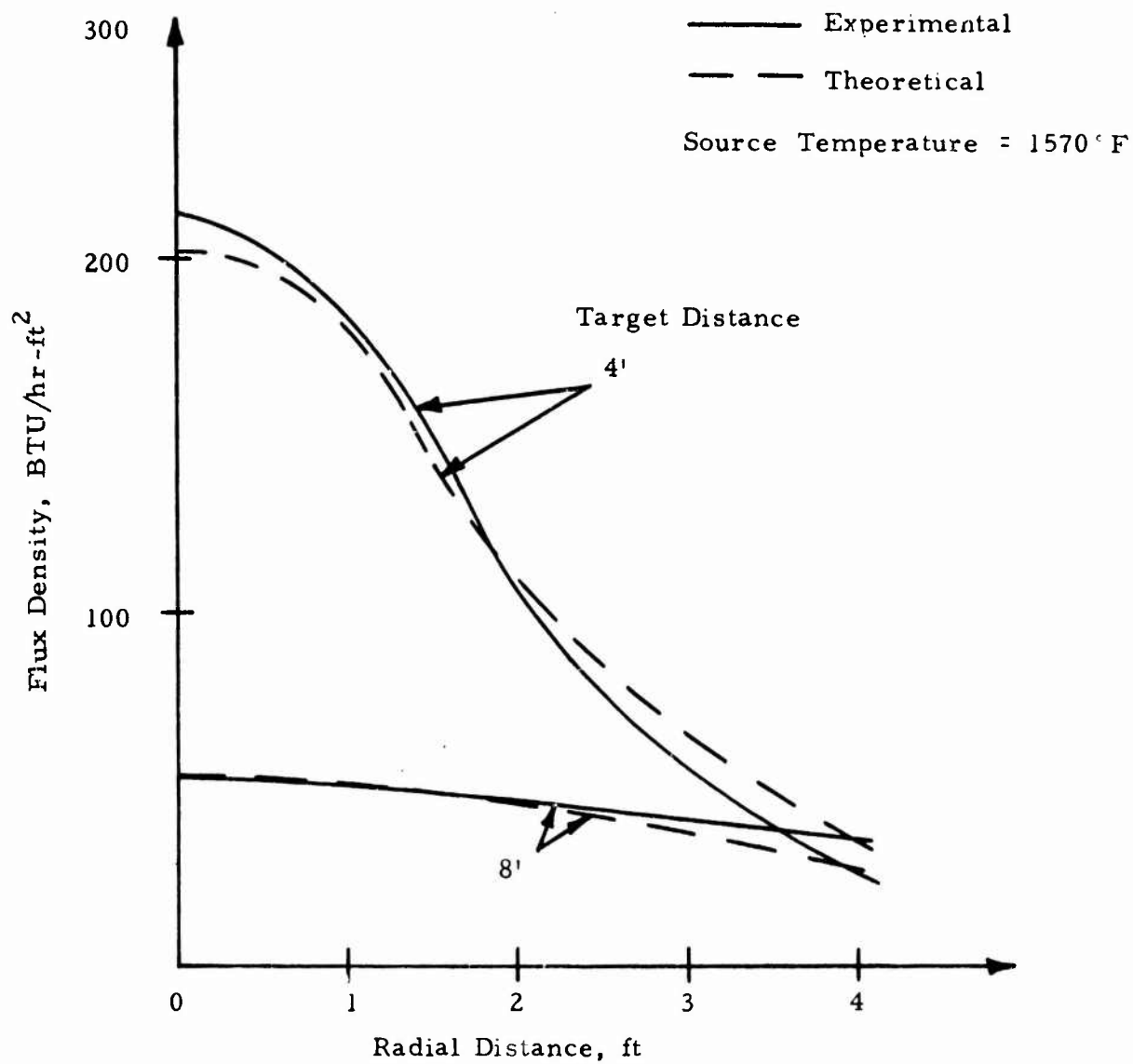


Figure 10 Comparison of Experimental and Theoretical Values of the Radiant Flux Density Distribution at the Target from the Pyrocore Heater

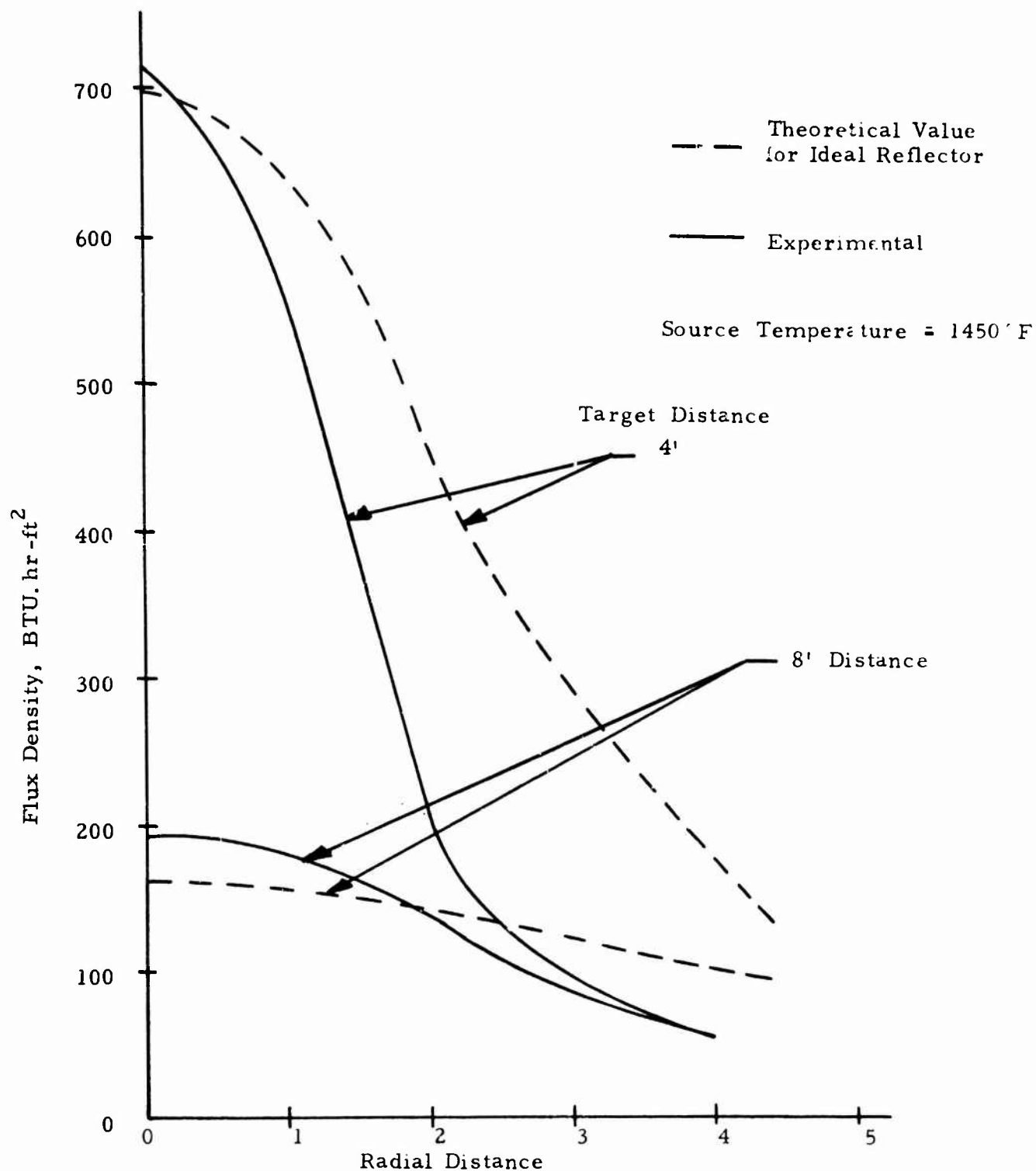


Figure 11: Comparison of Experimental and Theoretical Values of the Radiant Flux Density Distribution at the Target from the Foster-Miller Hemispherical Source Radiant Heater

The analysis has been further utilized to develop design charts for the preliminary sizing of source-reflector configurations to achieve a specified flux density at a given target distance. The actual flux density over the target diameter of 8 feet is seen to be quite nonuniform, specially at the close target distance of 4 feet, and approaches uniformity at the larger target distances of 8 feet. To simplify the presentation of the design curves, a mean value of the flux density has been used. In addition, the performance of these source-reflector configurations has been theoretically compared to select the optimum. These results are described in the following two sections.

4.4 Charts for Heater Design

Figures 13 through 25 present charts for the preliminary design of three different heater configurations consisting of,

- (a) Disc Source - Conical Reflector (Figures 13 to 17)
- (b) Cylindrical Source - Paraboloidal Reflector (Figures 18 to 21)
- (c) Hemispherical Source - Paraboloidal Reflector (Figures 22 to 25)

These charts permit the selection of a source and reflector size to meet any specified value of mean flux density over a target 8 feet in diameter and located at distances of 4, 6, 8 and 10 feet from the heater. There are four sets of charts for each heater configuration corresponding to the four target distances. An

additional chart for the geometrical design of the conical reflector, as developed in Appendix A, is included here for completeness.

These design charts are based on a source temperature of 1500°F and an emissive power of 25,000 BTU/hr-ft². They can be used equally well for any other source temperature by multiplying the abscissa (i. e. flux density) of these curves by the following source temperature correction factor, f_T ,

$$f_T = \left(\frac{T_s}{1960} \right)^4$$

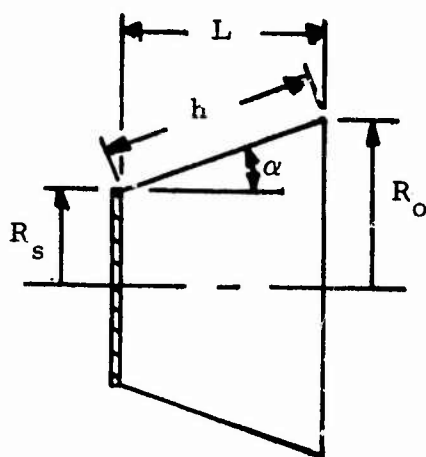
where

T_s is the absolute temperature of the source, °R

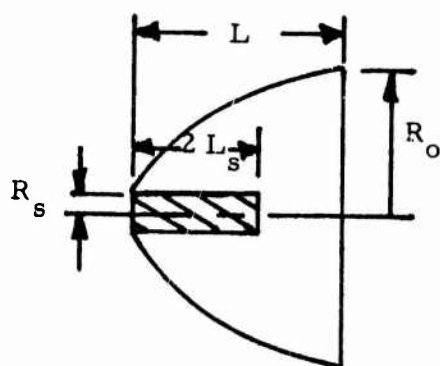
Figure 12 identifies the geometrical configuration of the three sources used in the development of these charts. The principal design parameters are the source diameter, the reflector diameter and reflector length. The charts are plotted with the mean flux density at the target as the abscissa and the radius of the source as the ordinate. The charts can be used for heater design and for estimating the mean flux density at the target from a specific design configuration.

(a) Design of Disc-Source-Conical Reflector Heater

Figures 13 through 17 are the design charts to be used for the preliminary design of a disc-source-conical-reflector heater. Figures 13 through 16 show the variation of flux density at the target with source radius as a function of constant reflector length



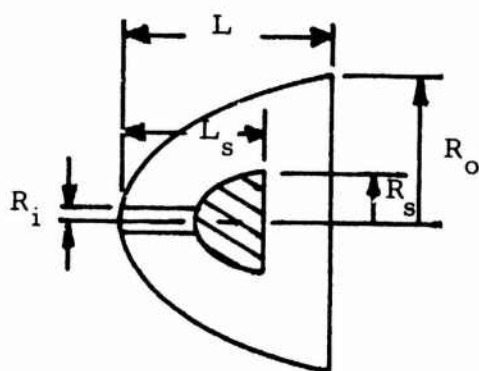
(a) Disc Source



(b) Cylindrical Source

$$L_s = 2 R_s$$

$$L = \frac{R_o^2}{8 R_s}$$



(c) Hemispherical Source

$$R_i = \frac{R_s}{2}$$

$$L_s = 2 R_s$$

$$L = \frac{R_o^2}{8 R_s}$$

Figure 12 Geometry of Various Source-Reflector Configurations

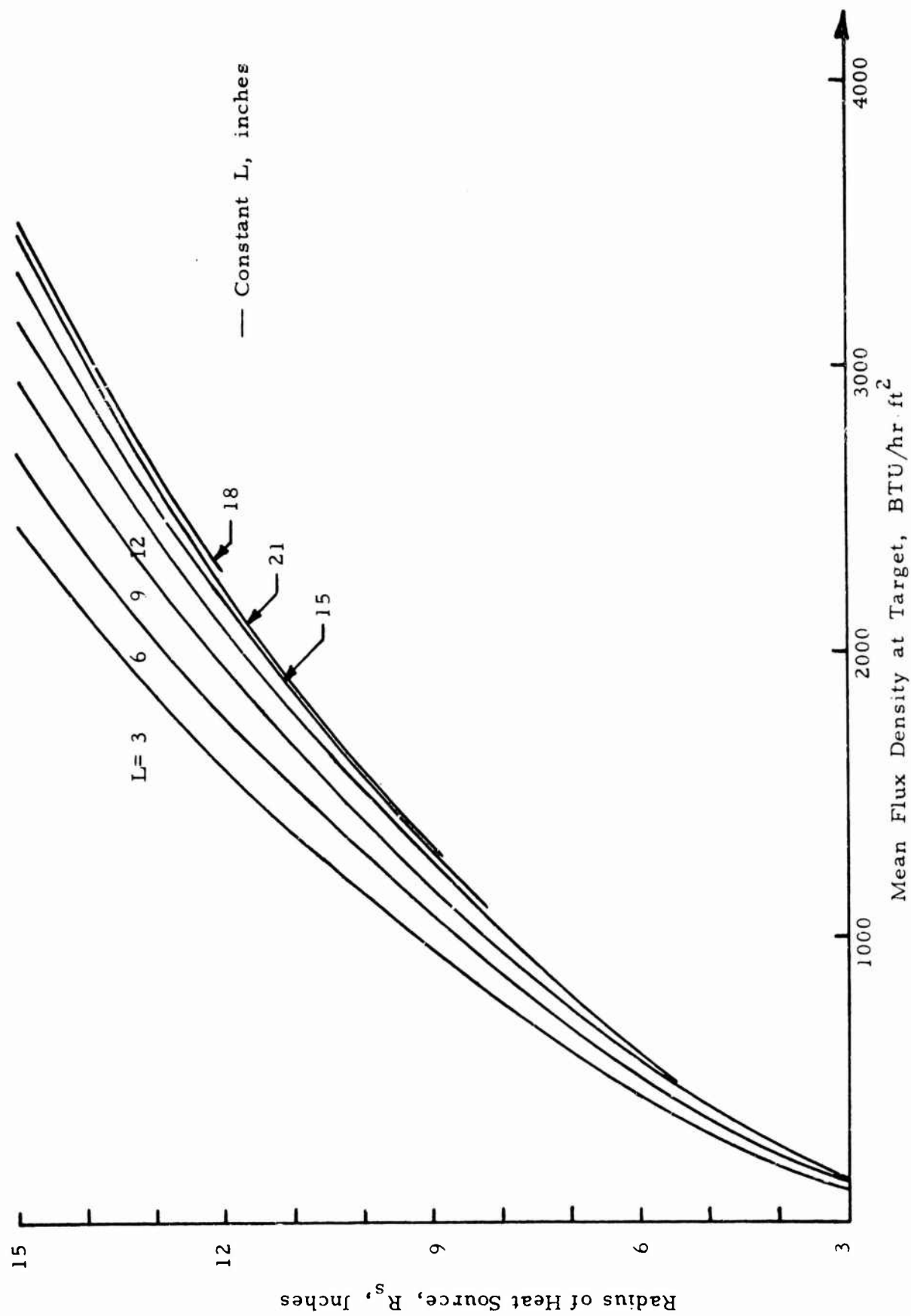


Figure 13 Design Chart for a Disc-Source-Conical Reflector: Heater-Target Distance 4 Feet

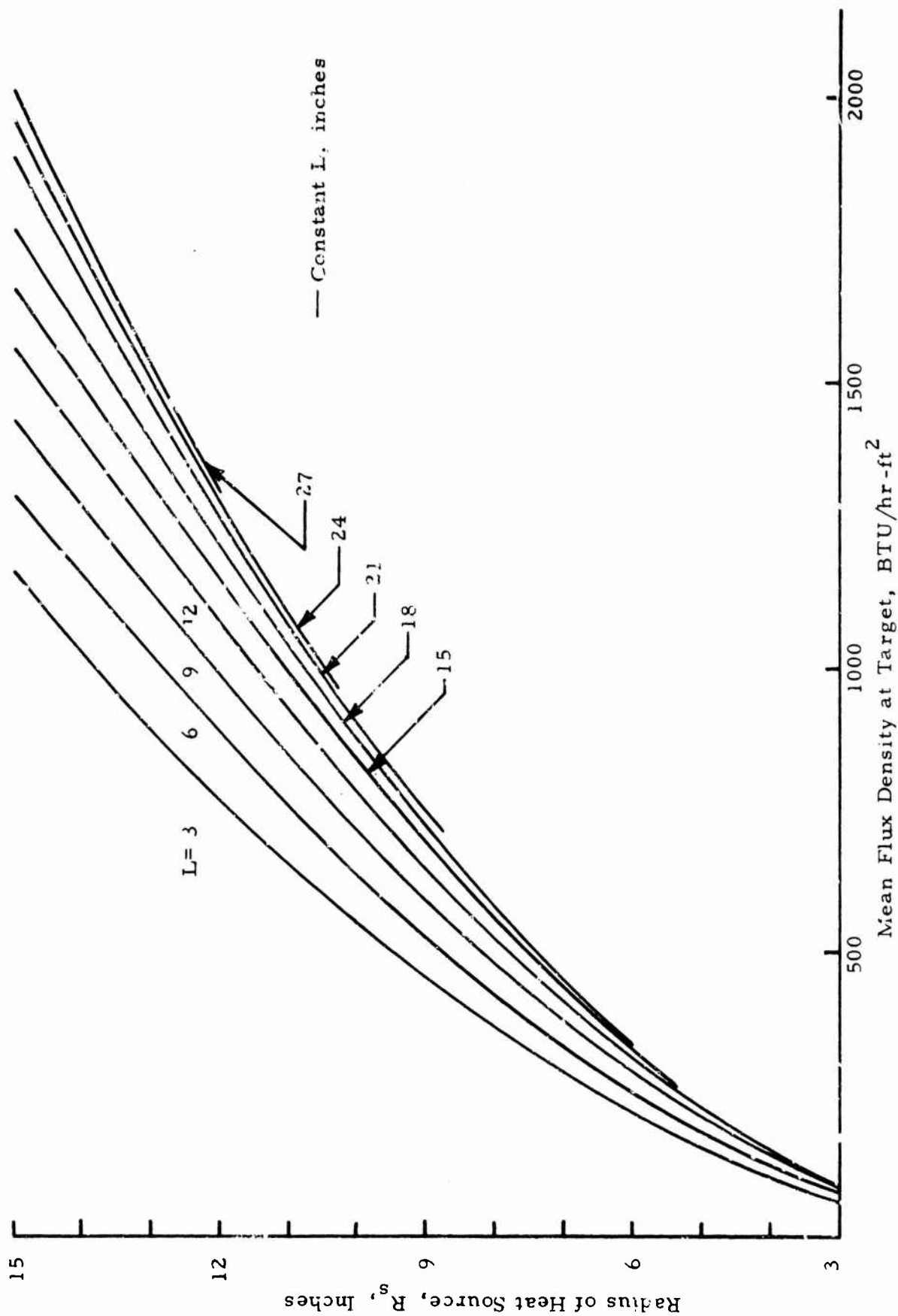


Figure 14 Design Chart for Disc-Source-Conical-Reflector Heater - Target Distance 6 Feet

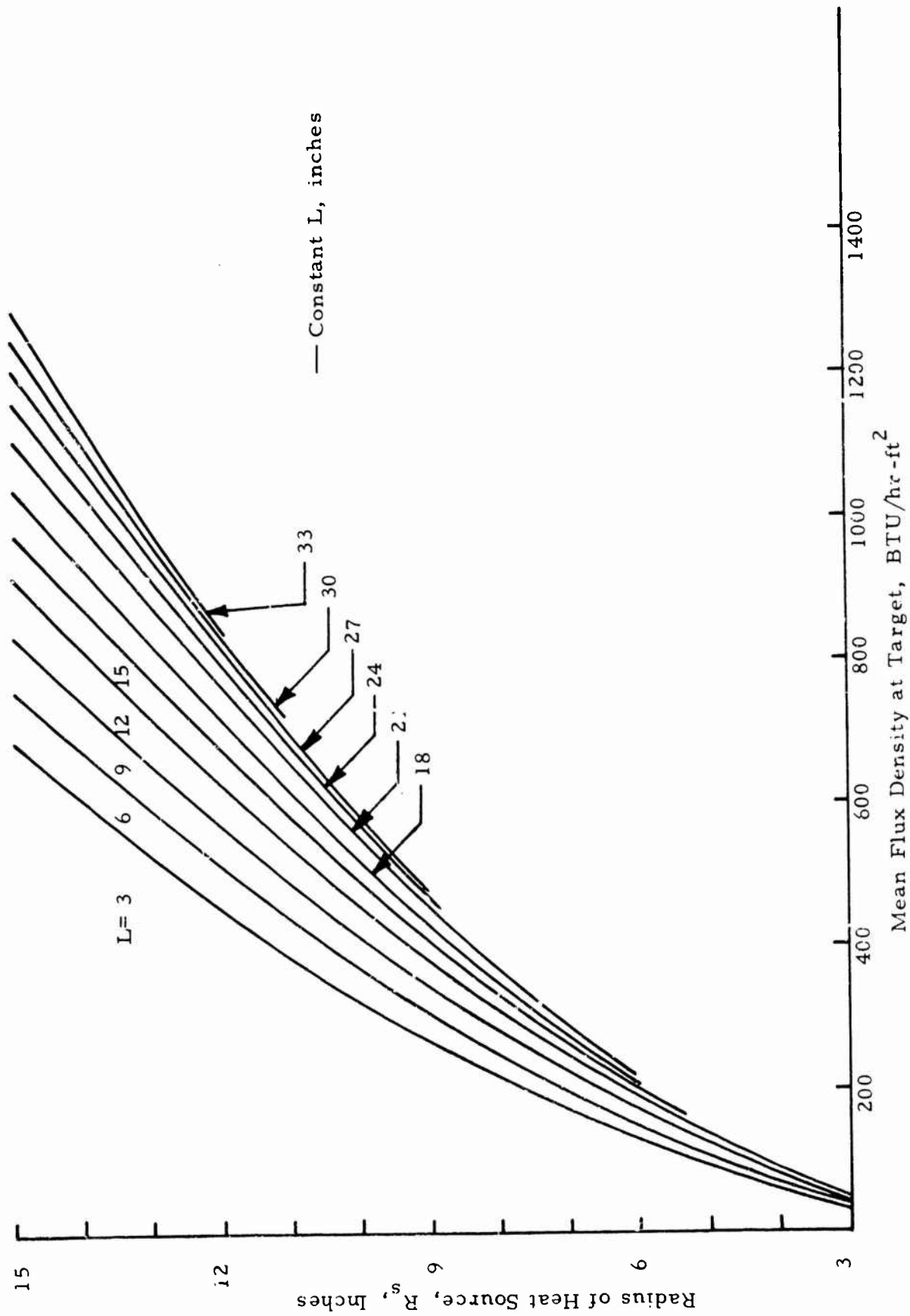


Figure 15 Design Chart for Disc-Source-Conical-Reflector Heater - Target Distance 8 Feet

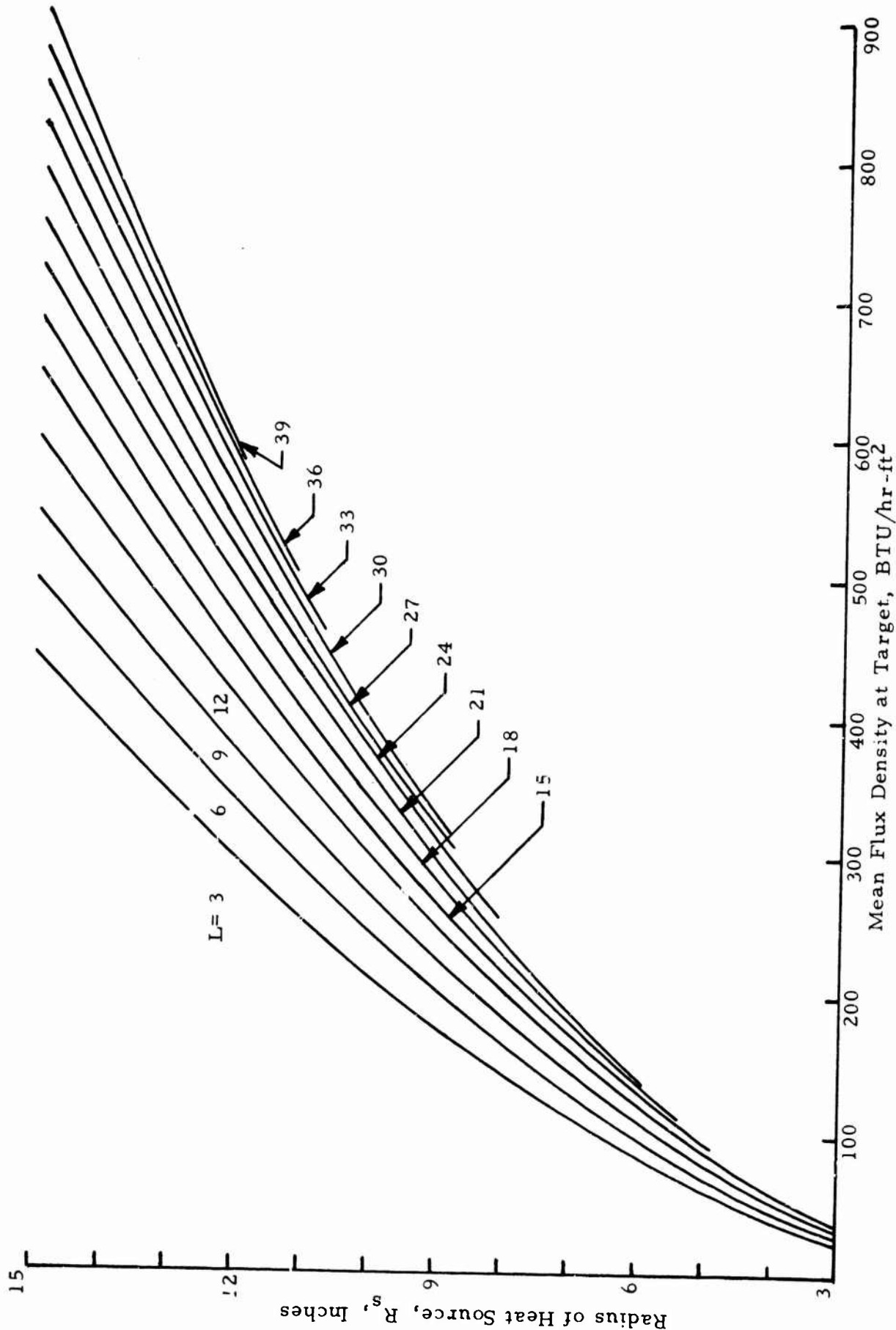


Figure 16 Design Chart for Disc-Source-Conical-Reflector Heater-Target Distance 10 Feet

for target distances of 4, 6, 8 and 10 feet respectively. Figure 17 shows the geometrical relationships for an optimum conical reflector design. It shows the variation of R_o/R_s as a function of L/R_s for various target distances \bar{H} (i.e. H/R_s). Thus for any R_s , L/R_s and \bar{H} the reflector radius R_o can be determined. The cone angle of the reflector can also be determined from Figure 17. In general, for high heat transfer efficiency, it is preferable to use the smallest diameter source and largest diameter reflector consistent with the flux density required at the target.

(b) Design of Cylindrical-Source-Paraboloidal Reflector Heater

Figures 18 through 21 are the design charts to be used for the preliminary design of a cylindrical-source-paraboloidal-reflector heater. These figures show the variation of source radius with mean flux density at the target. The charts show lines of constant reflector radius R_o and constant R_o/R_s , i.e. the ratio of reflector radius to source radius. These charts can be used in the following two ways:

(1) When the design for a certain application has specified size constraints, such as, maximum reflector radius, the source size can be directly obtained from these charts by drawing a vertical line from the required flux density on the abscissa to intersect the specified constant reflector radius curve. The ordinate of this intersection point then represents the source size.

(2) When there are no such constraints on reflector size, the design can best be achieved by selecting a

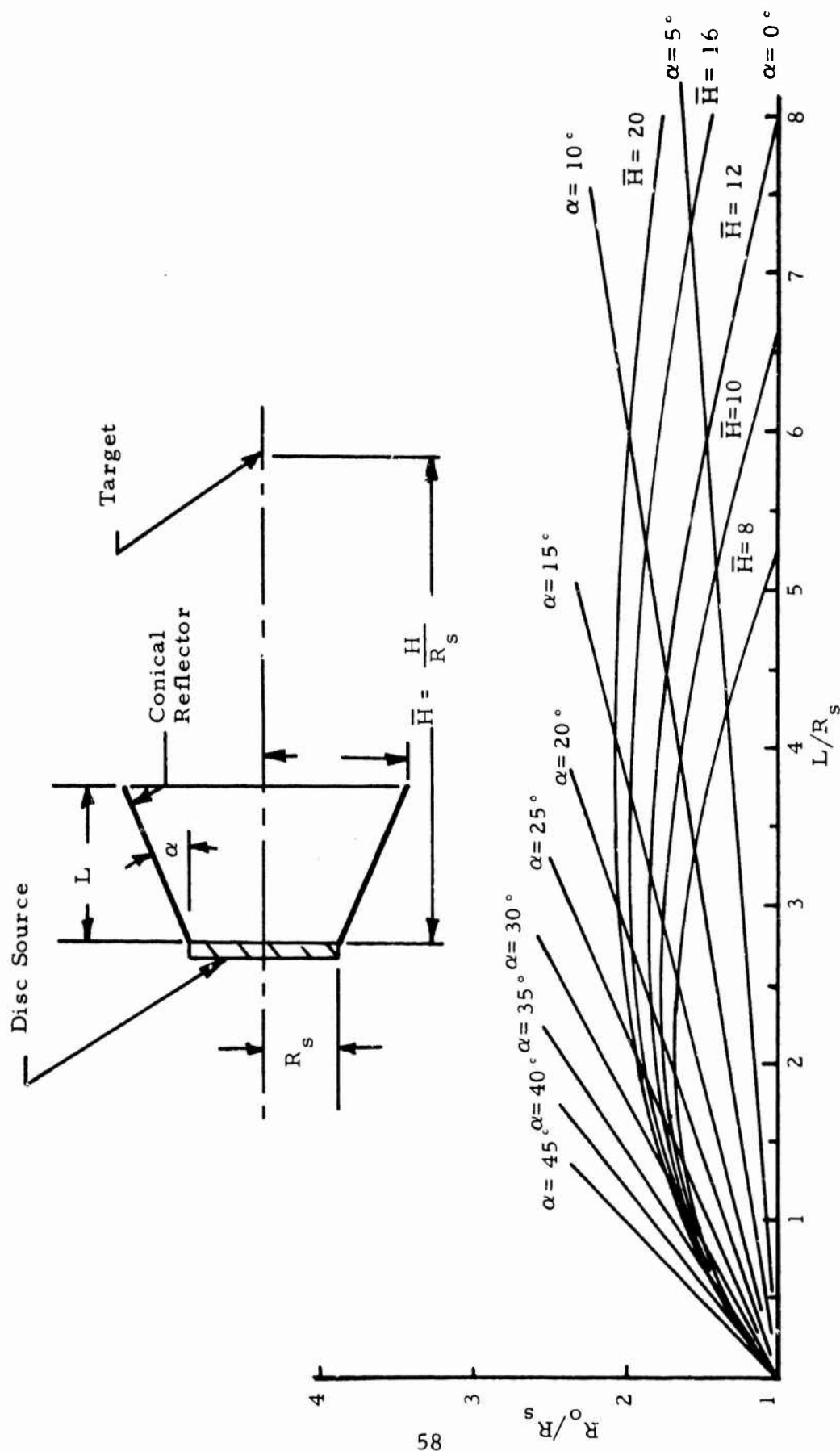


Figure 17 Configuration Chart for Design of Optimum Conical Reflector

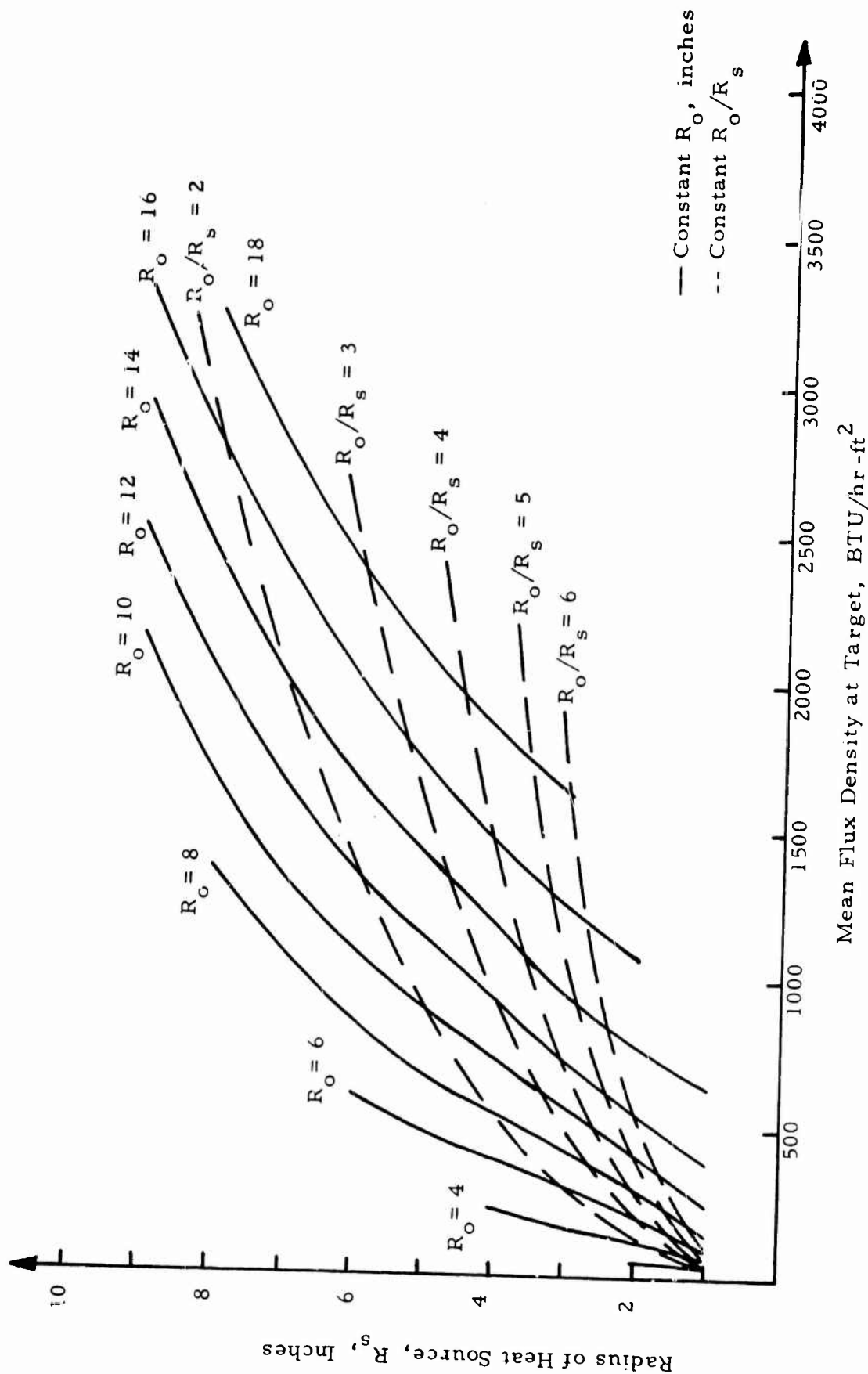


Figure 18 Design Chart for a Cylindrical-Source-Paraboloidal Reflector Heater - Target

Distance 4 Feet

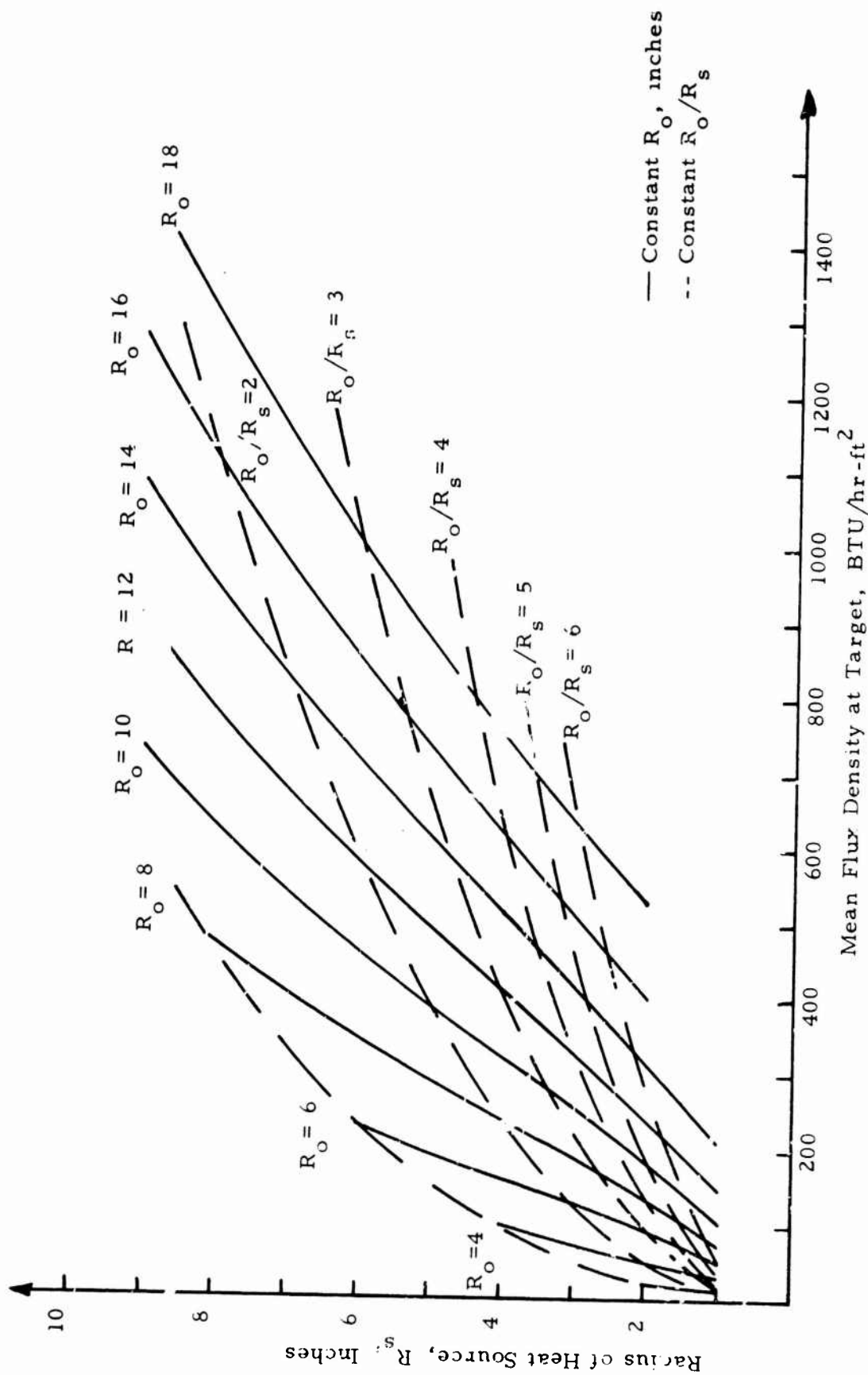


Figure 19 Design Chart for a Cylindrical-Source-Paraboloidal-Reflector Heater: - Target

Distance 6 Feet

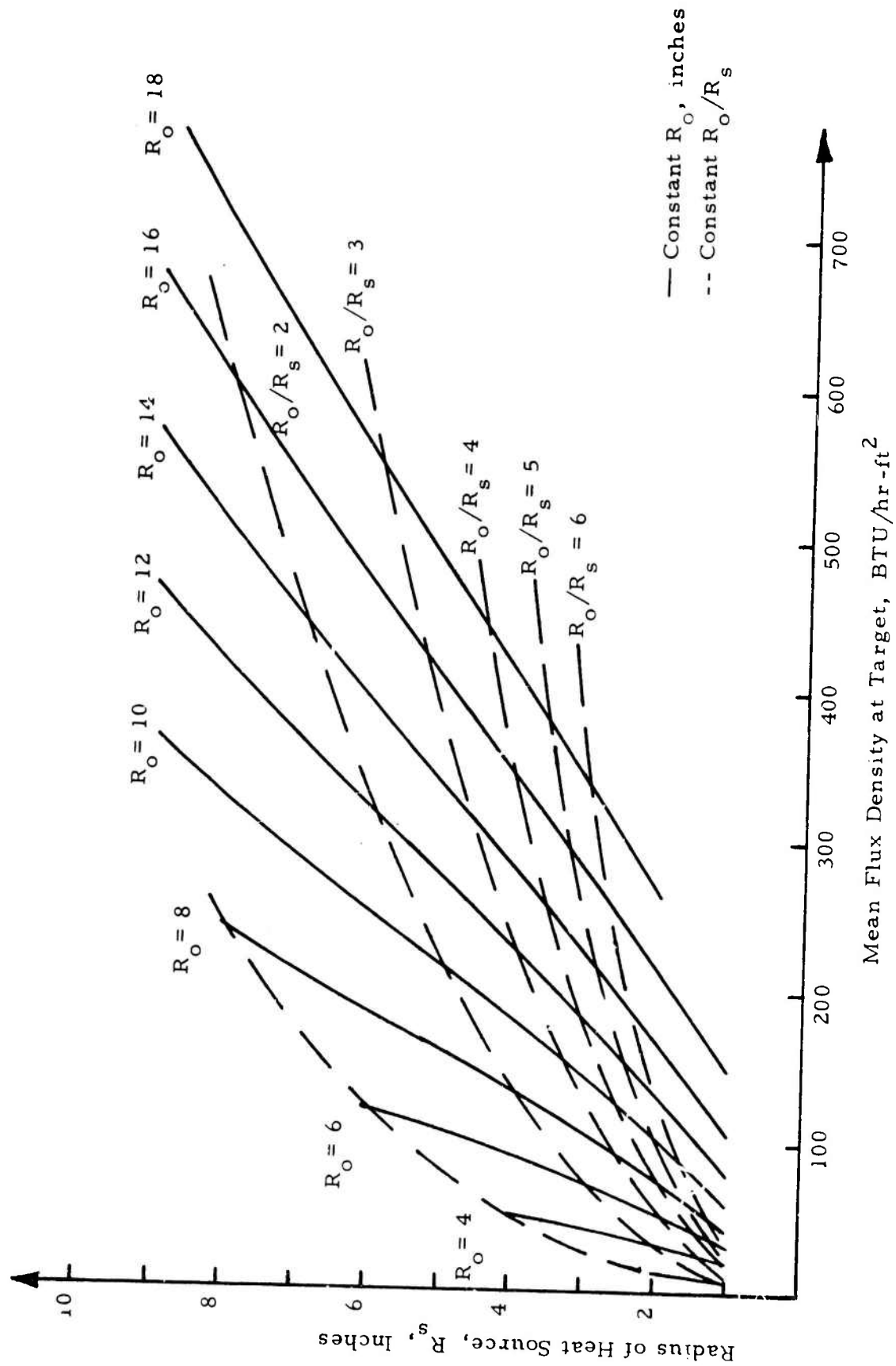


Figure 20 Design Chart for a Cylindrical-Source-Paraboloidal-Reflector Heater - Target
Distance 8 Feet

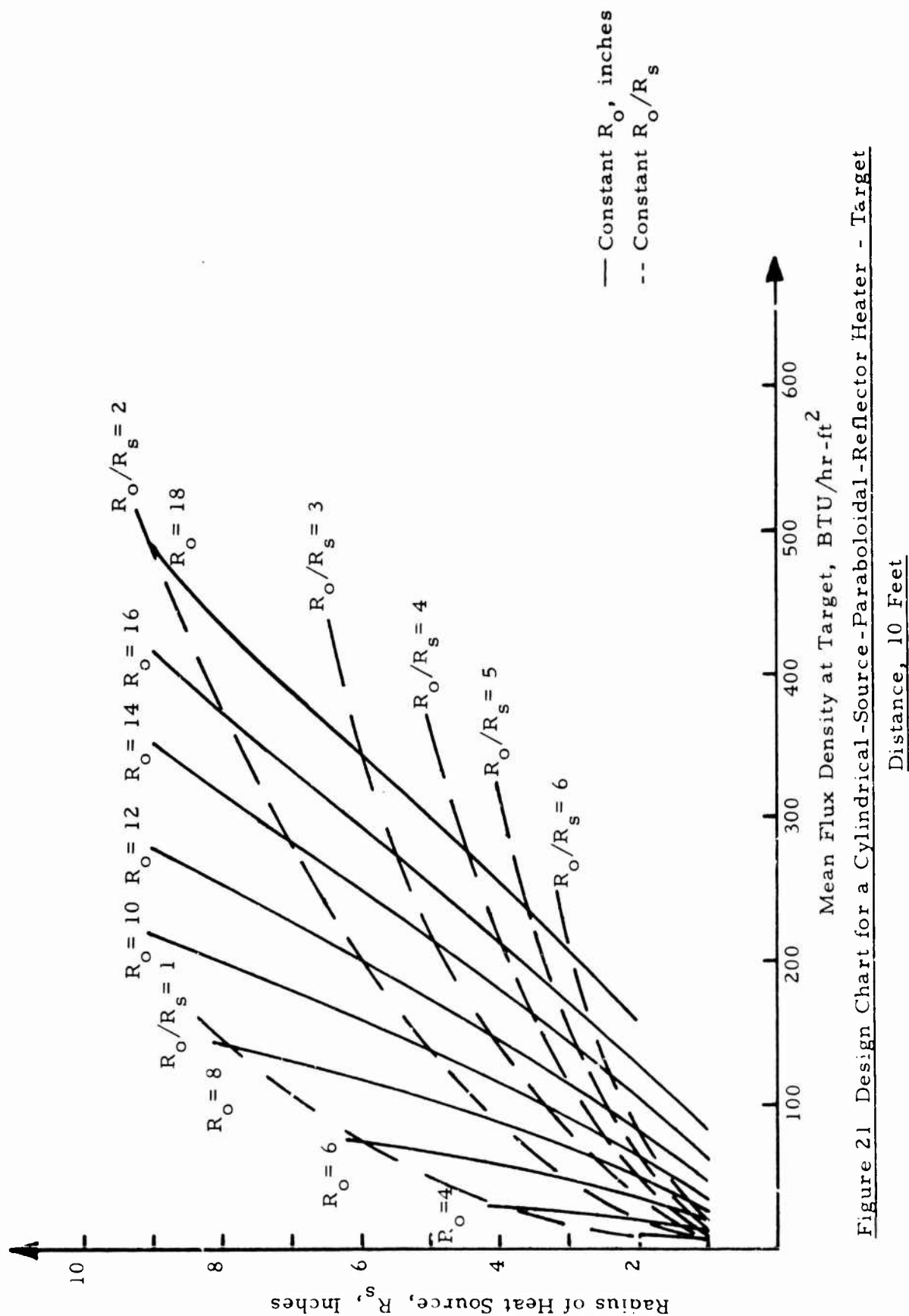


Figure 21 Design Chart for a Cylindrical-Source-Paraboloidal-Reflector Heater - Target

small source size on the ordinate of the chart and drawing a horizontal line on the chart till it intersects a constant R_o/R_s curve which gives the necessary mean flux density at the target. From this, the reflector radius can be obtained.

(c) Design of Hemispherical-Source-Paraboloidal-Reflector-Heater

Figures 22 through 25 are the design charts to be used for the preliminary design of a hemispherical-source-paraboloidal-reflector heater. These charts are identical to those developed for the cylindrical source design described in (b) and are to be used similarly.

4.5 Sample Use of Design Charts

To demonstrate the use of these charts heater configurations have been sized as per the following design requirements:

- (1) Mean flux density of 200 BTU/hr-ft² at target distance of 10 feet.
- (2) Maximum reflector radius = 12 inches
- (3) Maximum reflector length = 12 inches.

The calculated source size for the three different configurations is presented in Table III. This table also shows the mean flux density at 4, 6 and 8 feet target distances for these design configurations.

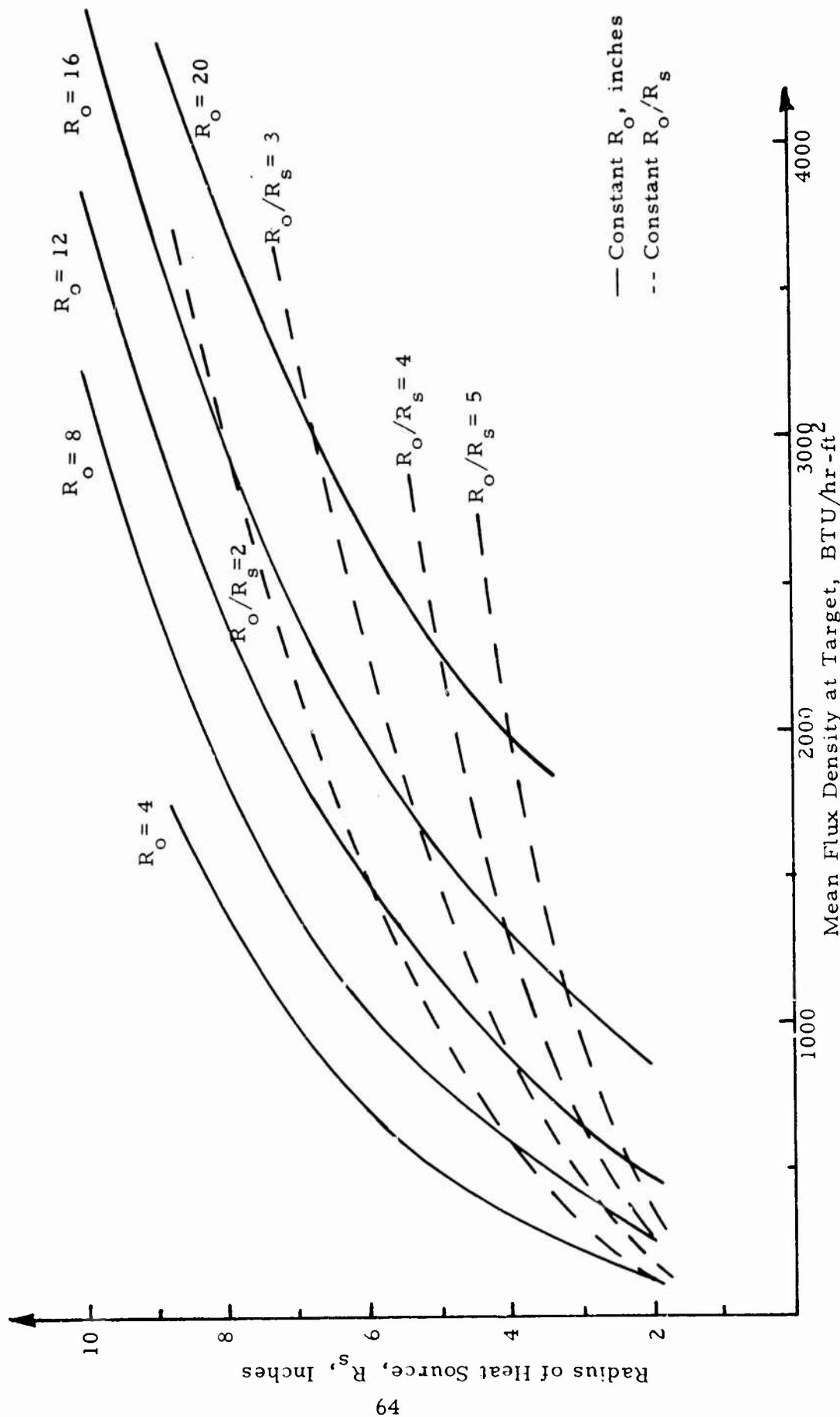


Figure 22 Design Chart for a Hemispherical-Source-Paraboloidal-Reflector Heater

- Target Distance 4 Feet

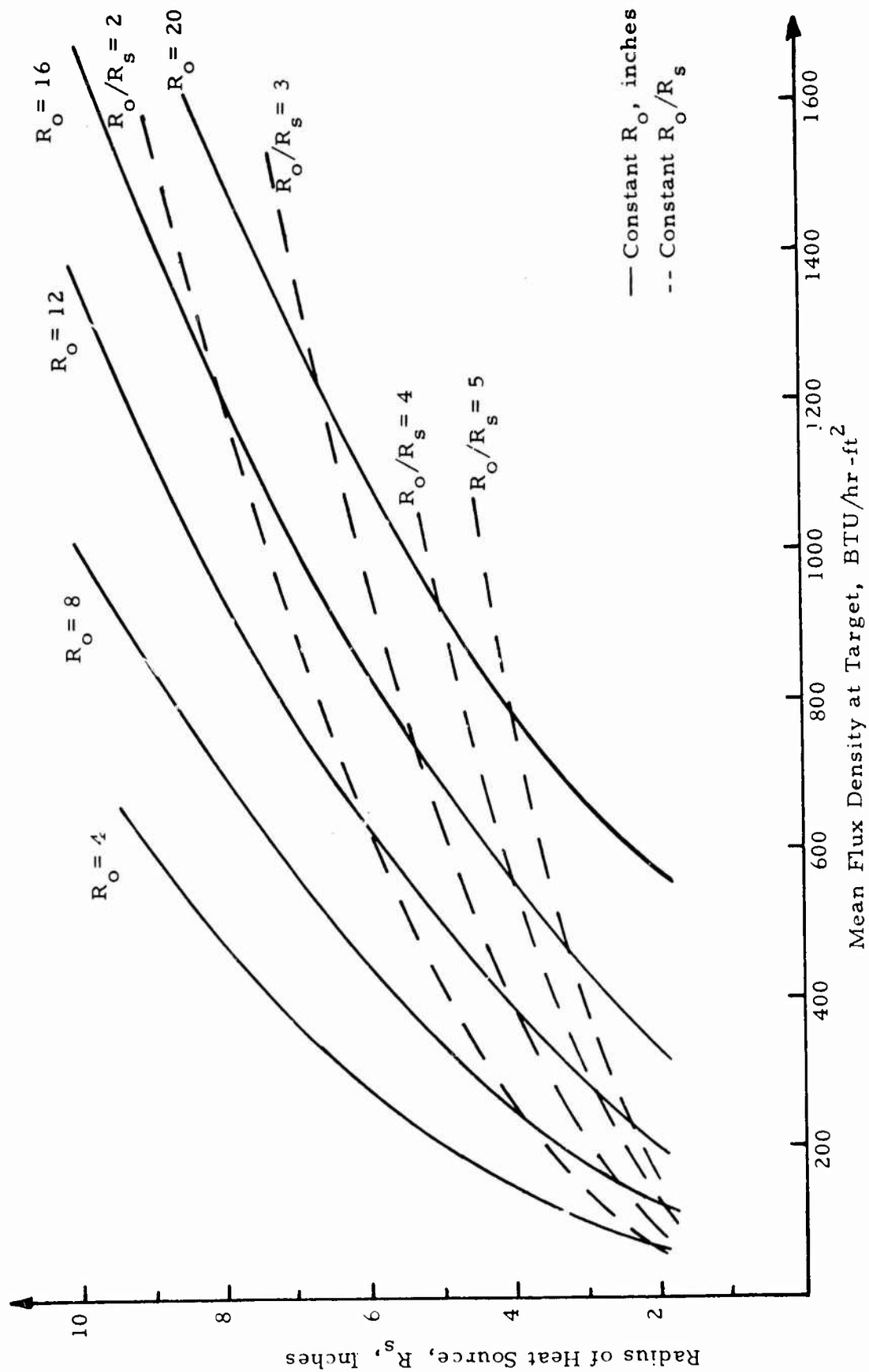


Figure 23 Design Chart for a Hemispherical-Source-Paraboloidal-Reflector Heater-Target

Distance 6 Feet

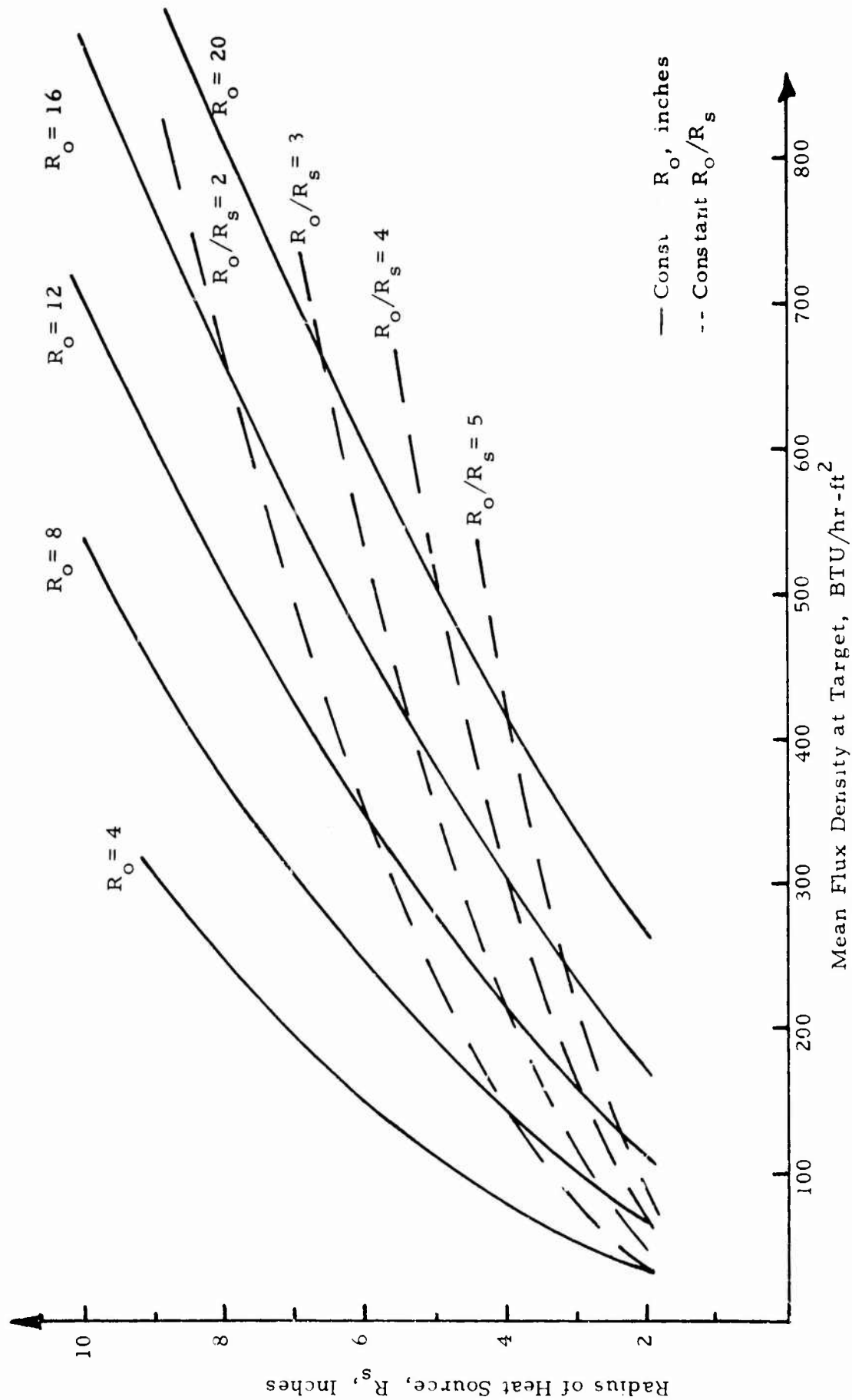


Figure 24 Design Chart for a Hemispherical-Source-Paraboloidal-Reflector Heater - Target

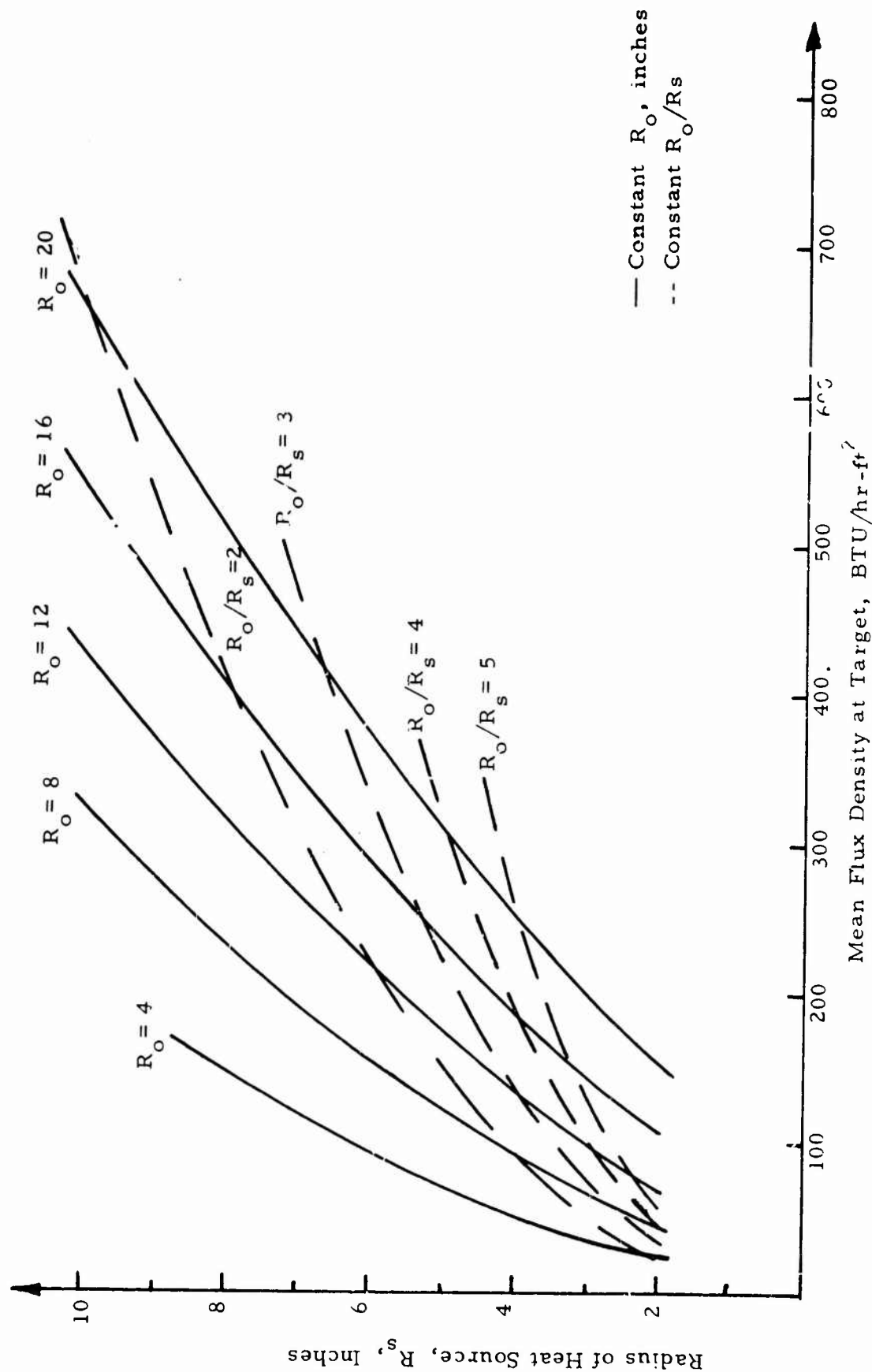


Figure 25 Design Chart for a Hemispherical-Source-Paraboloidal-Reflector Heater-Target

TABLE III

PRELIMINARY SIZING OF HEATER CONFIGURATIONS TO SUPPLY

A MEAN FLUX DENSITY OF 200 BTU/hr-ft²

AT A 10 FEET TARGET DISTANCE

	Heater Design - Source Type		
	Disc	Cylindrical	Hemispherical
Source Radius, inches -Source Temperature, 1500 °F	8	6	5.5
Source Radius, inches -Source Temperature, 1600 °F	7	4.5	4.5
* Mean Flux Density at 8 feet, BTU/hr-ft ²	300	290	325
* Mean Flux Density at 6 feet, BTU/hr-ft ²	500	525	550
* Mean Flux Density at 4 feet, BTU/hr-ft ²	1000	1250	1350

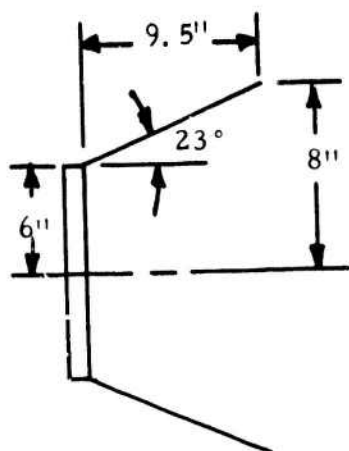
* Source Temperature = 1500 °F

These heater designs have different source areas and consequently different values of the total heat flux radiated and net fuel input. For example, the hemispherical source has the smallest area and hence the highest fuel efficiency. In the next section we compare the relative performance of the three different heater configurations on the basis of constant fuel input and constant total heat flux radiated.

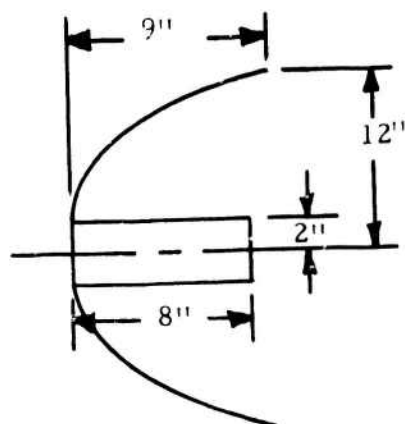
4.6 Evaluation of Optimum Source-Reflector Configuration

Three source geometries, disc, cylindrical, and hemispherical were theoretically compared, using the analysis of Appendix B, under identical conditions of total heat flux radiated, that is source area and temperature. Each source is assumed to have an optimum reflector design to fit within the same overall envelope. The comparison was based on a source area of 113 sq. in and an envelope size of 96 sq. in (i. e., length x radius). Figure 26 shows schematically the relative size and configuration of the heaters. Figure 27 shows the flux density distribution at target distances of 4 and 8 feet for a source black body temperature of 1500°F and an emissive power of 25,000 BTU/hr-ft².

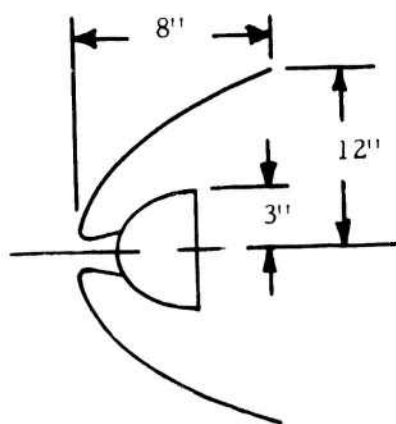
The results show that the flux density from the hemispherical source heater is at least 50 percent greater than the flux density available from the disc source. This shows the superiority of the hemispherical-source-paraboloidal reflector design.



(a) Disc Source with Conical Reflector



(b) Cylindrical Source with Paraboloidal Reflector



(c) Hemispherical Source with Paraboloidal Reflector

Figure 26 Optimum Source-Reflector Configurations

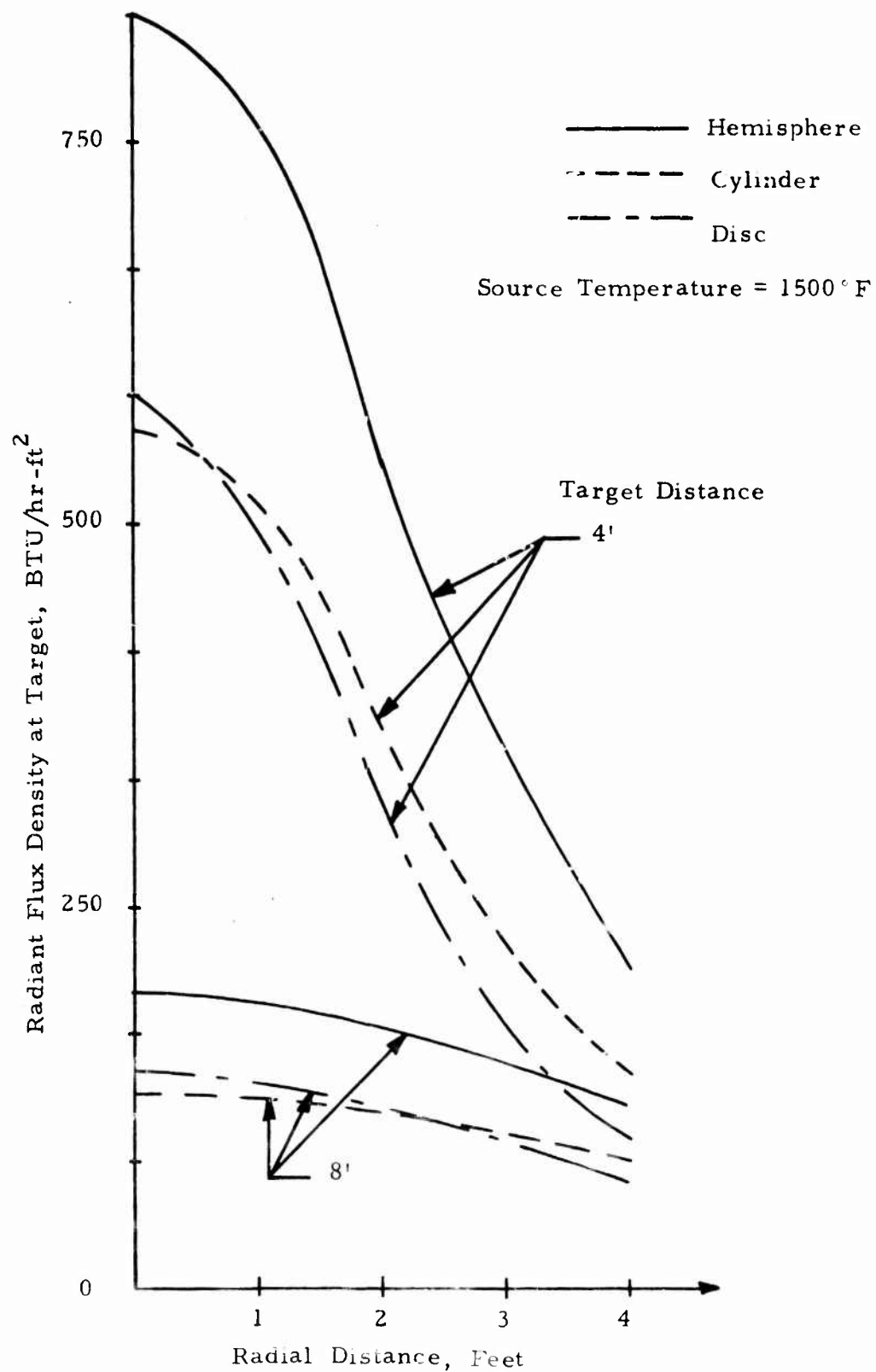


Figure 27 Comparison of Relative Heating Performance of Different Source-Reflector Configurations

5. Survey and Evaluation of Commercial Radiant Heaters

The effectiveness of this survey of commercially available radiant heaters was substantially increased by virtue of the information available in two research bulletins published by the American Gas Association Laboratories on infrared energy generated by radiant gas burners.^{9,10} The reader is referred to these publications for further information on the spectral energy distribution of radiation, the spectral emissivity and absorptivity of various materials, and the radiant heating effectiveness due to matching of the spectral energy content of radiation with the spectral absorptivity of the load.

A short discussion of some general considerations affecting radiant heater design, as abstracted from these reports, is presented in the following section. (A quantitative parametric analysis of a radiant heater is presented in Appendix C.) This is followed by a detailed evaluation of the commercial heaters surveyed and identification of the heater designs selected for further experimental evaluation.

5.1 General Discussion of Radiant Heaters

5.1.1 Spectral Content of Infrared Energy

A radiant or infrared heater is commonly used in industry for the direct heating of objects placed in its path. As a personnel heater, it holds the highest potential among the various types of heaters for approaching the benefits of solar heating. With proper design, it can provide a uniform radiant flux intensity on the object.

For the present application, radiant heaters can be classified into three categories, based on the type of energy utilized for heating, namely: electric, gas, and liquid-fuel-fired burners. In general, all these heaters consist of an infrared energy emitter which is heated to a temperature high enough to radiate in the infrared band of the electromagnetic spectrum. This wavelength span extends from the limit of visible red to the ultra short Hertzian range, namely, 0.75 to 400 microns. The most useful range of wavelengths of infrared energy for these types of burners lies in the range of 1.4 to 16 microns. For a high effectiveness, it is necessary that the spectral emissivity or absorptivity of the source and the receiver be properly matched. For example, Figure 28 shows the effect of mismatch between source and load, where a large portion of the emitted energy is wasted when using a high temperature 4,030°F radiation source.⁹ A much higher efficiency would be obtained using the 700°F source.

The gas and liquid-fuel-fired burners differ from the electric infrared heaters in that they utilize the combustion of fuel to raise the temperature of the emitter surface. The hot gases produced as a result of combustion can contribute to the total energy radiated. Tests on gas burners indicated that this could be as much as 15 percent of the total energy radiated.¹⁰ In addition, the total spectral radiation curve is modified by radiation from gases resulting in certain peaks, as shown in Figure 29, which in some cases can be utilized advantageously to match corresponding peaks in absorptivity of the load. For example, Table IV shows the absorption characteristics of some typical load materials found in industrial practice.

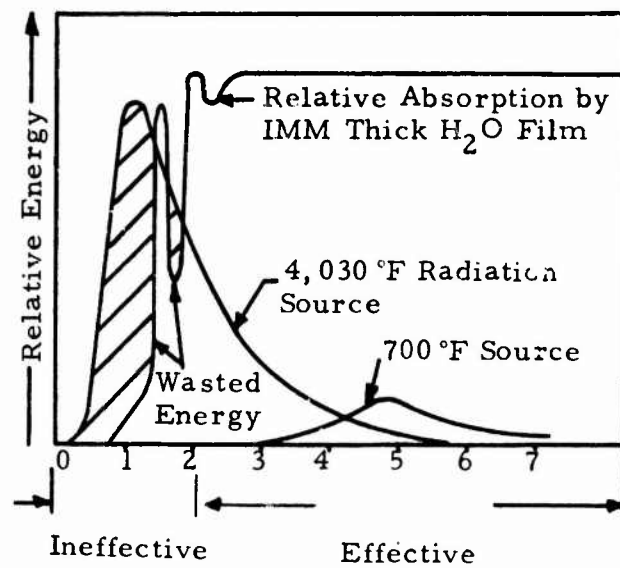


Figure 28 Absorption Curve for H₂O Film and Radiant
Energy Curves for 4,030 °F and 700 °F Sources⁹

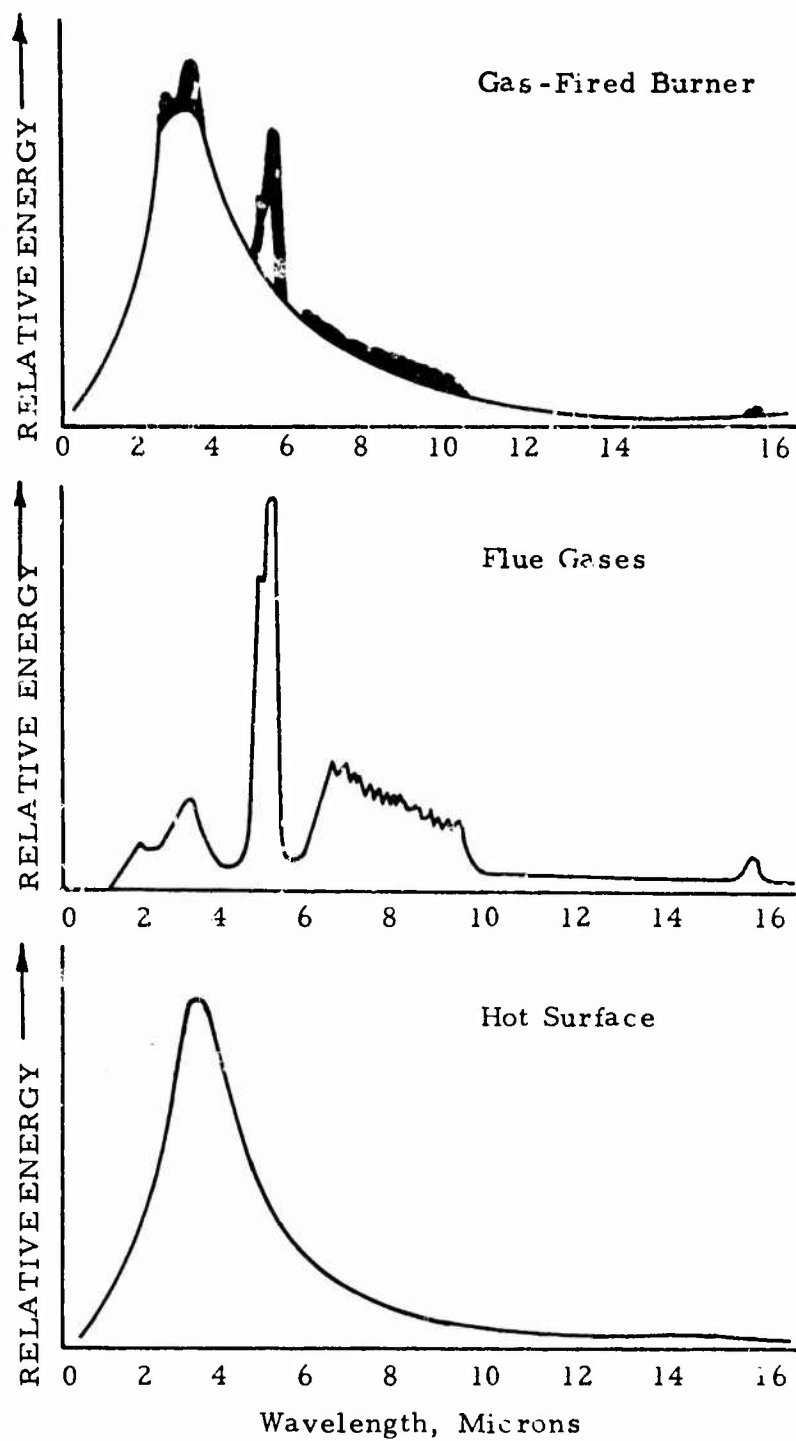


Figure 29 Spectral Radiation Curve for (1) Gas-Fired Infrared Burner, (2) Flue Gases, and (3) Hot Surface⁹

TABLE IV
ABSORPTION CHARACTERISTICS OF SOME
TYPICAL MATERIALS ⁹

Product	Major Absorption Wavelengths, Microns
Paints	2.8 to 3.5, 5.7 to 6.2, 7.5, 10.0
Printing Inks	3.5, 5.8, 6.8 to 10.0, 13.75
Oils	3.5, 5.75, 8.0 to 9.0, 13.80

An evaluation of various gas-fired generators showed these to emit energy at longer wavelengths than most electrical generators.¹⁰ Further, it has been shown that longer wavelength energy was more readily absorbed by most common load materials than shorter wavelength energy. Figure 30 shows the differences in behavior of two infrared sources on heating a film of linseed oil. Table V summarizes the effectiveness of various gas and electrical sources for heating three representative loads.

Though specific, quantitative data on the spectral absorptivities of clothing and human skin was not available, it is concluded, based on the organic content of the receiving material, that the longer wave length energy would be more effective for personnel heating. Therefore a source temperature in the range of 1400°F to 2000°F is recommended.

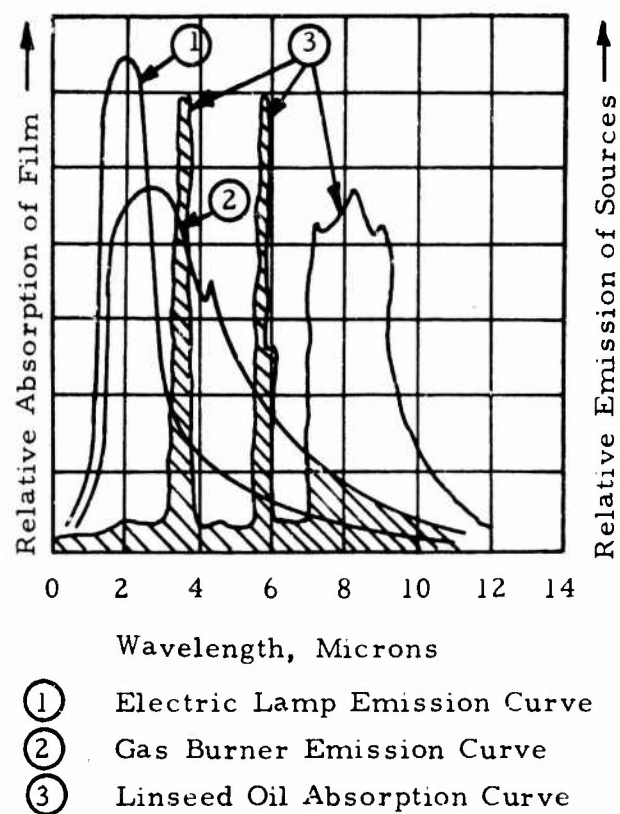


Figure 30 Absorption Characteristics of Film of Linseed Oil
and Emission Curve of Two Infrared Sources⁹

TABLE V
ABSORPTION OF INFRARED RADIATION FROM VARIOUS
GAS AND ELECTRICAL SOURCES BY THREE REPRESENTATIVE
LOADS⁹

Radiant Source	Percent of Total Radiated Energy Absorbed		
	(a) 1-mm-Thick H ₂ O Film	by (b) Linseed Oil Film	(c) Concrete
Infrared Gas Burner	95.50	27.50	41.40
250-W Industrial I-R Lamp	59.00	8.56	9.28
500-W Translucent Quartz Lamp	62.00	10.70	16.28
750-W Translucent Quartz Tube	94.00	25.50	44.80
(a) Major absorption wavelengths, 1.5 to 16.0 μ			
(b) Major absorption wavelengths, 3.3 to 3.7 μ , 5.6 to 5.9 μ , 6.8 to 9.5 μ			
(c) Major absorption wavelengths, 2.7 to 6.0 μ			

5.1.2 Types of Infrared Energy Generators

5.1.2.1 Liquid and Gas-Fuel-Fired I-R Generators

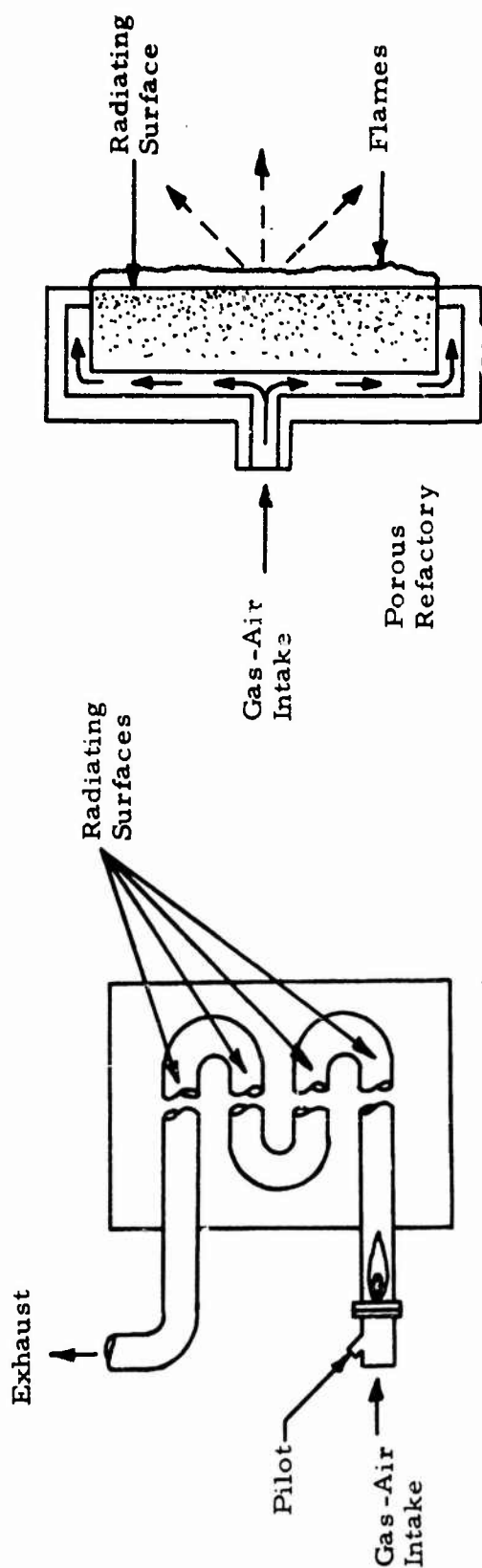
Liquid- and gas-fueled infrared energy

generators utilize the combustion of the fuel to raise the temperature of a solid emitter. As discussed in the previous section, only a small fraction of the total radiated energy is supplied directly by the luminous flame. Solids are better radiators than gases as they offer the potential of controlling the radiated wavelength span by a control of the temperature, while flame radiation is limited to well defined bands due to the characteristic radiation wavelengths of the CO_2 and H_2O molecules. Four classes of the common types of I-R burners are shown in Figure 31.

An internally fired radiant tube type of burner is shown in Figure 31(a). This may also be of the panel type. These are indirect units where the radiant surface is between the flame and the load and are used particularly where contamination of the atmosphere by gases is not permitted. Surface temperatures between 900° to 2500°F can be achieved.

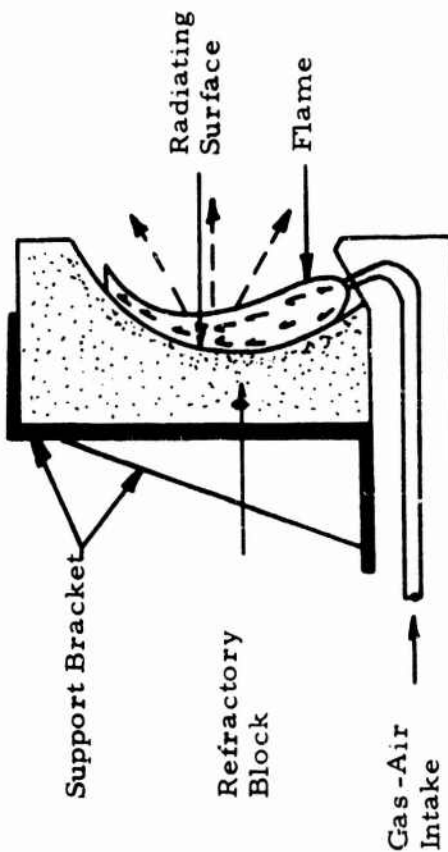
A surface combustion I-R burner which uses a porous refractory as its radiating surface is shown in Figure 31(b). The fuel-air mixture flows through the ceramic material and burns on its outer surface. The refractory is heated and becomes the radiating surface. Typical atmospheric burners of this type can achieve temperatures up to 1650°F . Higher density refractories used with power burners can achieve somewhat higher temperatures up to 1800°F . This type of burner is extensively used in space heating applications.

A directly fired refractory burner where the radiating surface is heated directly by a flame on its surface is shown in Figure 31(c). These are generally used with power burners resulting in operating temperatures up to 2800°F .

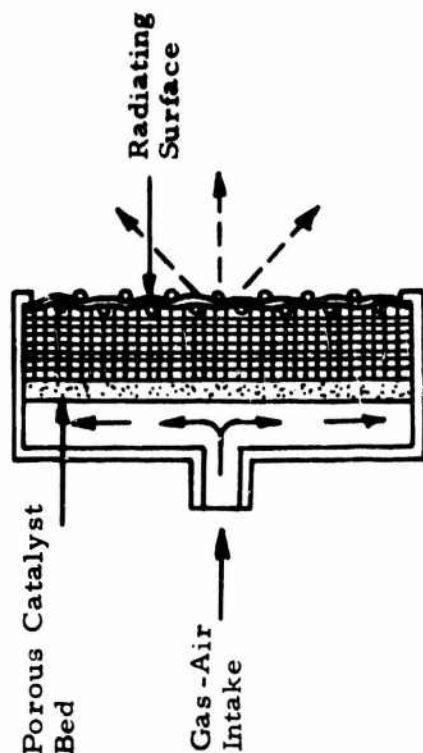


(a) I-R Radiant Tube

(b) Porous Refractory I-R Burners



(c) Direct-Fired Refractory I-R Burner



(d) Catalytic Oxidation I-R Burner

Figure 31 Four Different Types of Gas-Fired I-R Burners

Figure 31(d) shows a low temperature catalytic type atmospheric burner with typical operating temperatures up to 650°F.

Table VI shows pertinent radiation data for gas-fired infrared burners as given in Reference 10.

5.1.2.2 Electric Infrared Generators

Three types of electric I-R lamps commonly exist:

(a) Conventional I-R Lamps

These lamps are emitters of principally shortwave energy with a filament temperature of approximately 4000°F. They require a reflector which may be in the form of a coating inside the lamp to direct the I-R energy.

(b) Radiant Rods

These consist of sheathed metal tubes heated by the resistance principle to about 1500°F. High operating cost is quoted as a principal limitation.

(c) Quartz Lamp

Such a lamp consist of small diameter

Figure 31(d) shows a low temperature catalytic type atmospheric burner with typical operating temperatures up to 650°F.

Table VI shows pertinent radiation data for gas-fired infrared burners as given in Reference 10.

5.1.2.2 Electric Infrared Generators

Three types of electric I-R lamps commonly exist:

(a) Conventional I-R Lamps

These lamps are emitters of principally shortwave energy with a filament temperature of approximately 4000°F. They require a reflector which may be in the form of a coating inside the lamp to direct the I-R energy.

(b) Radiant Rods

These consist of sheathed metal tubes heated by the resistance principle to about 1500°F. High operating cost is quoted as a principal limitation.

(c) Quartz Lamp

Such a lamp consist of small diameter

TABLE VI
RADIATION DATA FOR GAS FIRED INFRARED BURNERS¹⁰

Burner	Type	Emitting Face Material of Construction	Red Brightness Temperature, F	Total Normal Radiation, W, BTU/hr, Square Foot	GIR* Factor	Spectral Distribution of Energy at Maximum Temperature in Selected Wavelength Spans (Microns), Percent				
						0.75-2	2-3	3-4	4-5	5-6
A	Atmospheric	Ceramic Tile	1420 1500 1675	18,400 22,420 29,920	0.85 0.87 0.84	14.6	25.3	20.0	14.7	6.7
A ₁	Atmospheric	Ceramic Tile	1400 1490	14,000 17,820	0.76 0.71	8.2	20.8	14.6	23.0	10.4
B	Atmospheric	Inconel	1400 1540 1595	18,720 28,200 32,600	0.90 1.02 1.06	14.1	28.2	21.2	14.0	8.5
C	Catalytic	Glass Wool	600 700 850	800 1,120 3,300	0.37 0.36 0.65	1.2	4.3	13.7	17.5	15.3
D	Powered	Cordurite	1500 1800 2000	22,250 32,700 44,400	0.87 0.73 0.69	17.4	19.0	14.3	19.0	8.6
E	Powered	Low Density Refractory	1500 1665 1720	17,700 23,500 29,100	0.79 0.66 0.74	14.9	23.9	21.1	14.1	8.4
F	Powered	Refractory Brick	1800 2000 2300	38,800 51,500 62,800	0.86 0.81 0.63	26.0	24.5	15.3	12.9	7.1
G	Powered	Refractory Brick	1600 1800 2000	21,650 34,600 58,000	0.69 0.77 0.91	20.2	26.0	14.2	13.0	7.8
H	Powered	Inconel	1660 1790 1900	25,650 36,700 46,600	0.73 0.83 0.85	17.8	29.4	20.3	12.8	6.8
I	Atmospheric	Ceramic Tile	1420 1500 1590	17,800 21,450 27,650	0.83 0.84 0.94	10.6	23.3	19.9	17.1	9.2
J	Atmospheric	Inconel	1480 1550	19,000 24,000	1.06 0.85	12.7	26.7	20.7	16.7	7.0
K	Powered	Silicon Carbide	1450 1525 1610	24,550 30,900 37,150	1.06 1.16 1.17	11.5	25.4	21.6	14.9	9.5
L	Atmospheric	"Cercor" Glass	1550 1710	14,380 23,200	0.51 0.60	8.2	20.9	15.8	21.0	10.8
										22.3

* GIR Factor is the effective emissivity for this type of burner and includes direct radiation from the hot gases.

translucent tubes heated by a high temperature tungsten filament. It requires a reflector to direct its energy. Extremely high intensities are possible with this type of lamp; particularly useful where instantaneous response is required.

(d)

Quartz Tubes

These are similar in construction to quartz lamps but use a lower temperature nichrome wire filament with an operating temperature near 1500° F. Thus, this type of lamp emits energy at a longer wavelength than the other electric I-R sources. The tubes require reflectors and are not capable of high intensity operation. It produces I-R energy that is quite similar to that produced by the fuel fired burners.

Table VII shows some pertinent radiation data for electric I-R generators as abstracted from Reference 10.

5.1.2.3 Application to Personnel Heating in the Arctic

The thermal efficiency of the fuel fired burner depends on the efficiency of combustion and energy transfer to the solid emitter. The heat carried away by the hot combustion gases

TABLE VII

RADIATION DATA FOR ELECTRIC INFRARED GENERATORS¹⁰

	Rating, Watts	Red Brightness Temperature, °F	Total Normal Radiation BTU/hr, Square Foot	Percentage Distribution of Energy Into Selected Wavelength Intervals, in Microns Percent					
				0.75-2	2-3	3-4	4-5	5-6	6-16
A Clear Quartz	500	3500	63,087	64.96	19.50	4.07	4.07	2.53	4.87
Translucent Quartz	500	3000	40,560	52.50	22.90	6.55	6.55	3.28	8.22
B Translucent Quartz - Tube (22 inches)	500	1400	10,580	16.00	16.00	16.00	20.00	12.00	26.00
Translucent Quartz - Tube (22 inches)	750	1600	23,640	12.60	21.20	17.40	16.00	11.40	21.40
C Chromolox Resistance Heater	800	1570	23,150	10.50	26.80	21.60	13.45	8.65	18.00
D Industrial Lamp with Integral Reflector	250	3160	24,280	59.23	26.90	4.63	2.78	1.85	4.61
Industrial Lamp with Integral Reflector	125	2950	12,900	48.00	17.30	24.70	3.70	2.40	4.90
E Red End Lamp	250	3100	22,840	63.26	23.00	3.80	1.97	1.25	4.76

is wasted if these gases are directly exhausted to the atmosphere. Thermal efficiency can be improved by:

- a. Utilizing a high temperature burner with air-fuel ratios close to stoichiometric.
- b. Utilizing the waste heat in the exhaust gases for preheating the incoming air and fuel. A simple analysis shows that approximately 50 percent of the heat is wasted in the high temperature exhaust gases.

An electric I-R heater for this application will require its own portable generator with a capacity of 5 to 10 Kw including a gasoline engine and electric generator. Such a unit would add considerable weight to the overall heater. A thermal efficiency of electric power generation of 30 percent or less can be expected.

5.1.2.4 Effect of Special Burner Coatings

Radiation from a solid body is inherently a surface phenomenon dependent on the temperature and the emissivity. It is possible to change the emissivity by mechanical working of the surface such as polishing and sandblasting or by coating the surface with metallic oxides, salts, or sintered metal. This will vary the surface radiation at the same temperature.

A study of the effect of metallic oxide coatings on gas-fired I-R burners revealed that a change of -12 to +15 percent of the total normal radiation could be effected.¹⁰ However, this is not a significantly large effect to merit a detailed investigation.

5.2 Survey and Preliminary Evaluation of Commercial Radiant Heaters

A large number of commercial radiant heaters were surveyed. The more applicable ones have been catalogued in Table VIII. Almost all use electricity or gas as their energy source. One commercially available, oil-fired radiant heater was found; however, it is designed for permanent installation for the heating of buildings, and is very large and heavy. It was excluded from further evaluation in this study.

No commercial gasoline-fired infrared heaters were found. One possible producer of such a heater, the Hunter Manufacturing Company, was contacted. They did make a few heaters under contract to the Army nearly 10 years ago. However these heaters were probably found to be unsatisfactory since they were never produced in quantity.

For the purpose of comparison and evaluation in terms of radiant heat transfer efficiency, the heaters have been classified in Table VIII as area, line, or point sources based on the geometry of their emitting surfaces. A summary discussion of these heaters is presented in the following sections.

TABLE V.11
CHARACTERISTICS OF RADIANT HEATERS

TYPE	MANUFACTURER	DESCRIPTION	FUEL	SURFACE TEMP.	MECH. SHOCK RESISTANCE	THERMAL SHOCK RESISTANCE	WIND RESISTANCE	ADVANTAGES	DISADVANTAGES
AREA	Bettcher Manufacturing	Inconel Burner and Reverberator - Thermo-couple Flame Sensor	L.P. Gas	1550°F	Good	Good	Poor	Gas shut off if flame is extinguished.	L.P. Gas will not vaporize at low temp. Unit is easily blown out.
	Van Dorn	Burner designed similar to above	L.P. Gas	1550°F to 1650°F	Good	Good	Good	Pilot will not go out when exposed to wind.	Very Heavy - 40#
	Infralux	Ceramic Grid with Reverberator Rods. Stainless Steel Reflector	Natural or Propane Gas	1500°F	Fair	Good	Fair	Not Designed for Outdoors.	Very Heavy
	Solaronics	Nickel Chromium Grid over a Ceramic Combustion Surface	Propane	1400°F	Fair	Good	Needs a Canopy	Very wind resistant with a canopy.	
	Corning Glass Panel Heater	Tempered Glass Panel with a Resistance Film that heats the Glass when Electricity is applied.	Electricity	600°F	Poor	Good	Good		Low Temperature Glass would lose heat through convection.
	Hi Shear Corp. Hastra LTH 500	Quartz tube in a circular geometry backed by a reflector	Electricity	4000°F	Poor	Good	Good	Only area source using a quartz lamp.	
	Cargo Safe Camp Heater	Low temperature catalytic heaters	Propane	270°F to 750°F	Good	Good	Good	Very safe. Gasoline will not ignite if spilled on burner.	Low temperature source with low output.
	Hupp Inc. Marqu Heater	Ceramic Heater in a weather-proof housing	Natural Gas	1650°F	Fair	Good	Good	Weather-proof housing not affected by wind.	Very heavy - 45#
	General Electric Quartz Lamp	Tungsten Filament in an Evacuated Quartz tube	Electricity	4000°F	Fair	Good	Good	Very high temperature source not affected by wind.	
	General Electric Quartz Tube	Nichrome Filament in an Open Quartz Tube	Electricity	1600°F	Fair	Good	Good	Moderately high temperature source not affected by wind.	
POINT	General Electric Metal Sheath	Resistance Element Surrounded by Magnesium Oxide in a Metal Sheath	Electricity	1200°F	Good	Good	Good		Loses much more energy thru connection than other electric heaters.
	Roberts Gordon Co-Ray-Vac	Combustion Gases flow through a Steel Pipe causing it to Radiate	Natural Gas	1000°F	Good	Good	Good		Very Heavy
	Radiant Systems Pyrocure	Cylindrical shaped sensor in a parabolic reflector	Propane	2000°F Max.	Good	Good	Good	Lightweight. Can be made in a variety of shapes.	
	Selas Inc. Duradant Burner	Ceramic Refractory with cup-shaped combustion surface	Propane	2000°F	Fair	Good	Poor	Wide variety of shapes.	Open burners will be greatly affected by the wind.
	General Electric R-49 Bulbs	Tungsten Filament sealed in a Glass Bulb	Electricity	4000°F	Fair	Fair	Good	Very high temperature source	

* Heaters chosen for testing.

5.2.1 Area Sources

5.2.1.1 Surface Combustion Burners

Many of the area-type heaters use propane or natural gas for fuel, and most can be further classified as Surface Combustion Burners. Surface Combustion Burners, in general, consist of a plenum, a burner grid, and a reverberator screen as shown in Figure 32.

The plenum performs two functions: it allows the mixing of gas and air in the proper ratio, and then distributes it along the back of the burner grid. The gas-air mixture flows through the burner grid and burns on the grid surface. The reverberator screen is mounted about 1/2 inch beyond the burner face. The screen is generally coarse and acts as a re-radiator, reflecting and radiating energy back to the burner face. In addition, the screen itself radiates energy directly to the object and adds to the heater output. Experiments have shown that the temperature and total normal radiation is higher for the screened burner than the unscreened one, at the same fuel input and air adjustment.

The unit made by Bettcher Manufacturing Corporation and listed in Table VIII consists of a portable heater mounted on a two-wheeled cart. The heater has an inconel burner and reverberator screen which is surrounded by an aluminum reflector to better direct the radiation.

The heater operates on liquid propane gas that is carried in a tank on the two-wheeled cart. One interesting feature of this heater is a thermocouple flame sensor that shuts off

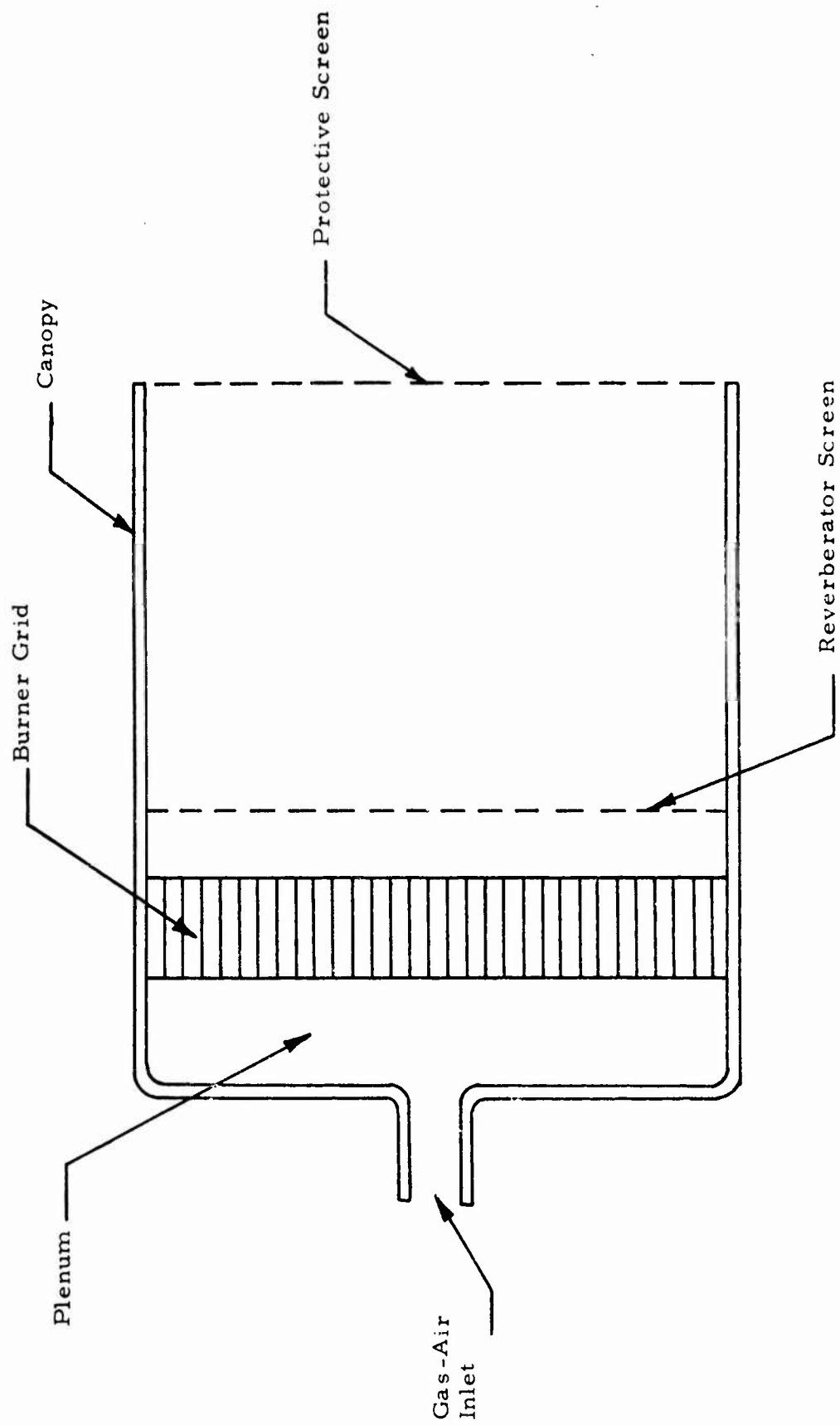


Figure 32 Surface Combustion Burner

all gas if the flame is extinguished. This heater has been designed for outdoor operation but has no provisions to prevent flame-out caused by the wind; therefore, it must be used in a sheltered area.

The Van Dorn All-Weather heater is basically very similar to the previous heater. It has a 3-layer woven inconel 600 burner and an inconel reverberator screen. By adding an enclosure and a control system, the heater has been made wind-proof. The manufacturer claims that the pilot will not blow out even under an air hose blast. The heater does not require an electrical hook-up.

The Solaronics and Hupp Heaters have a ceramic burner instead of the inconel burner used by the two previous manufacturers. They both use a nickel-chromium reverberator screen. The Hupp ceramic is perforated with 200 holes per inch² and is heated to about 1650 °F under normal conditions.

The last surface combustion burner listed in Table VIII is made by Infralux. It consists of a ceramic grid covered by reverberator rods instead of a reverberator screen. The rods are thin and serve the same purpose as a screen.

All these heaters are basically very similar in principle and design with the only differences being in the materials used for construction of the emitter and the screen. This can have some effect on operation. The inconel burner is likely to be more rugged and less susceptible to breakage by mishandling. The emissivity of inconel is a little, but not significantly higher than ceramic as detailed in Table VI. This would result in a higher emitted power for the same surface temperature.

These surface combustion heaters seem to have inherently poor wind-resistance in their basic forms. The flame is exposed and can be blown out or blown off the burner face. Some protection can be afforded by enclosing the heater in a canopy with a screen across the front opening (Figure 32). However, for complete wind protection, a control system is necessary with pilot reignition which greatly increases the heaters' complexity.

The heater supplied by the Army to Foster-Miller Associates consists of a surface combustion burner made of ceramic and covered by a metal reverberator screen. It uses gasoline as a fuel. The gasoline is fed under pressure to the heater where it passes through a preheater, is vaporized and burned. This heater is likely to be as adversely affected by the wind as the gas-fired burners previously discussed. In addition the unit is difficult to light in still air and would probably be extremely difficult to light in a wind.

The other gasoline-fired radiant heater developed for the Army by Hunter Manufacturing Company, is very different in principle from the heaters previously discussed. As shown in Figure 33, a Hunter Model SPX-2 torch head is supplied gasoline and air from 2 tanks. The flames from the torch are directed against a perforated nickel-steel surface in the shape of a frustum of a cone. The radiating surface is backed by a sheet-metal reflector. Performance data for this heater is unavailable. Hence a proper evaluation could not be made. However, it is likely that this heater did not fulfill the Army's requirements for only a limited number were built and tested.

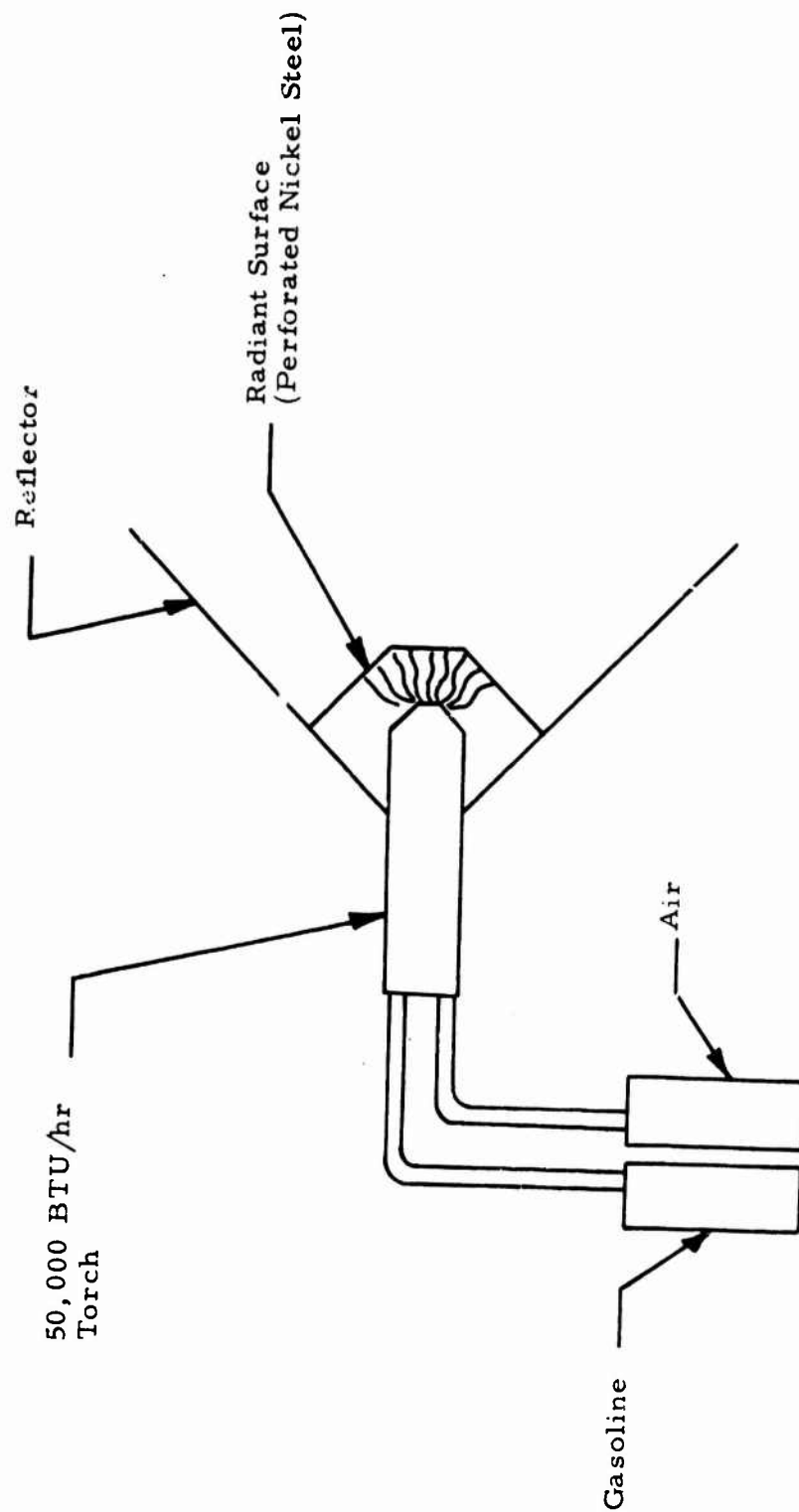


Figure 33 Schematic of Hunter Manufacturing Company's Radiant Heater

5.2.1.2 Catalytic Heaters

The catalytic heater made by Cargo Safe, Inc. is another type of area source. In this heater, catalytic oxidation, a chemical reaction in which the hydrocarbons in the propane combine with oxygen while exposed to a platinum catalyst, heats the emitter surface. The heater is flameless and operates in a temperature range of 250° to 750°F.

Since the heater is flameless, it can not be blown out by the wind and gasoline or lighter fluid will not ignite if thrown on the radiating surface. However, a major drawback of this type of heater is its low temperature and low energy output per unit area. To obtain an output of 25,000 BTU/hr, a very large emitter surface would be required. The convection losses from this large surface area would be high and would increase with increasing wind velocity causing a substantial reduction in the surface temperature and the radiant energy output of the heater.

5.2.1.3 Electric Panel Heater

Another type of low temperature area source is made by Corning Glass Works. The Pyrex Panel Heater is a tempered borosilicate glass panel with an electroconductive film on one surface. When an electric current is applied to the film, the entire glass panel heats to about 600°F and emits radiation.

This heater has all the disadvantages of a low temperature emitter and in addition the panel is fragile and would break under mechanical shock.

5.2.1.4 Circular Quartz Lamp Heater

The final area source listed in Table VIII is made by the Hi-Shear Corporation and is basically a quartz lamp in the form of a spiral with a reflector behind the lamp (Figure 34). Since most quartz lamps are straight and therefore classified as line sources, they will be discussed in greater detail in the next section.

This heater has the highest operating temperature of all the area sources considered, approximately 4000°F, and a high radiation intensity. However the heaters occupy only a small fraction of the total surface area. As a result the mean output of the heater is approximately 8500 BTU/sq ft-hr.

5.2.2 Line Sources

5.2.2.1 Electric

(1) Quartz Lamp

The quartz lamp is a high temperature source of infrared radiation. It consists of a coiled tungsten filament in a quartz tube about 3/8 inch in diameter and from 5 to 38 inches long, depending on the wattage. The tube is filled with an inert gas and its ends are sealed.

The filament temperature of this lamp is about 4000°F, which is about 700° less than the operating temperature of the filaments in incandescent lamps. At 4000°F most of the infrared energy passes through the quartz enclosure and the lamp

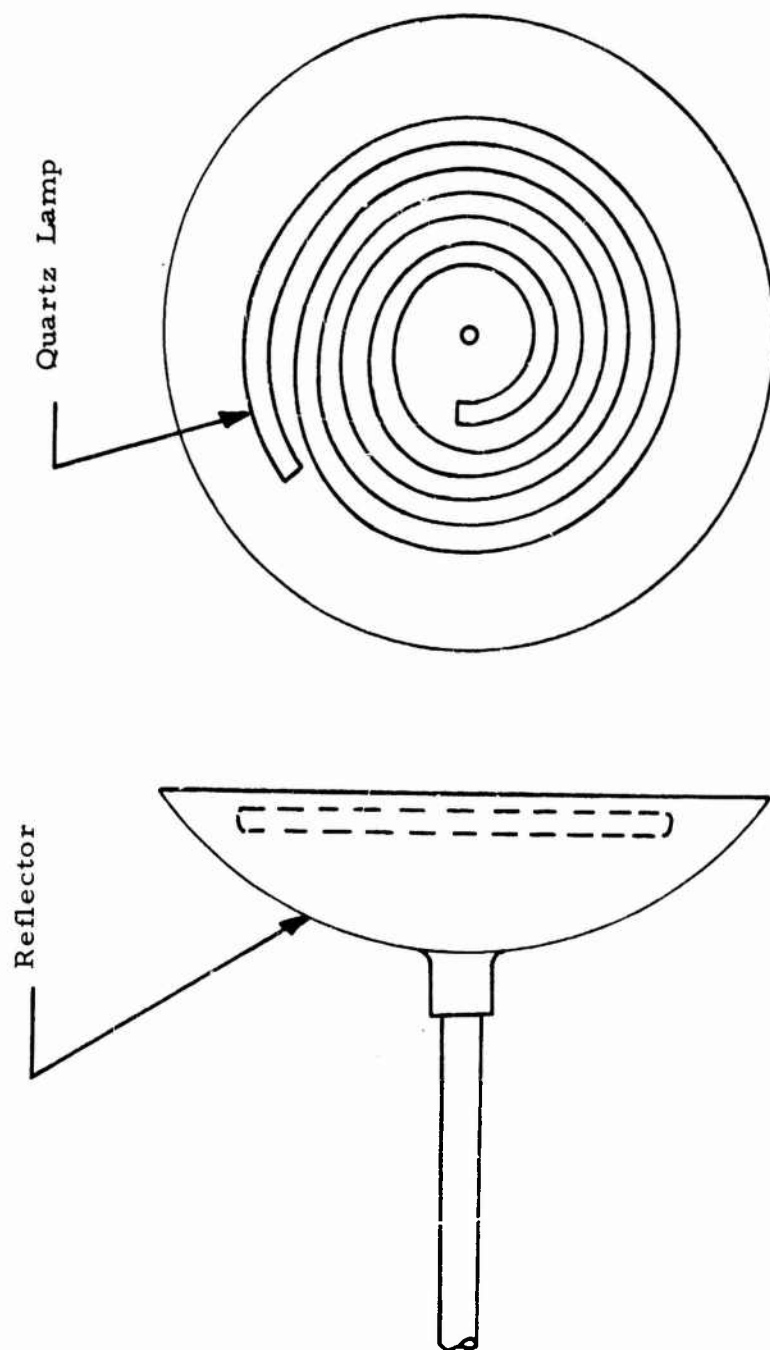


Figure 34 Sketch of Hi-Shear Corporation's Quartz Lamp Infrared Heaters

emits about 86 percent of its input energy as radiant energy. Part of this energy, approximately 8 lumens per watt, is radiated as visible light.

Quartz makes possible the compact size of these lamps because of the high temperatures it can withstand. Ordinary glass softens at about 840°F while the softening point of quartz is around 3000°F. This property of quartz enables the tungsten filament to operate very close to the tube walls. It is highly transparent to infrared radiation below 5 microns thus permitting its passage with little absorption. It is resistant to practically all chemical solvents, and it possesses excellent thermal shock resistance. It is claimed that quartz will not fracture if plunged into ice water from a temperature of 2000°F.

(2) Quartz Tubes

The quartz tube looks very much like the quartz lamp and the two are often confused. A quartz tube uses a nichrome wire filament instead of a tungsten filament, is not gas-filled and has a ceramic plug in each end which is not airtight.

The 3/8 inch diameter tube is rated at about 50 watts per inch. This is only half as much as the input per inch to the quartz lamp. For higher inputs the diameter of the tube is increased.

The filament in the quartz tube heater operates at about 1600°F which is close to the temperatures of most gas heaters. Because of this the spectral distribution of the energy emitted by the quartz tube and most gas heaters is similar.

(3) Metal Sheath Resistance Heater

The metal sheath heater is the most rugged of all electric heaters. It consists of an electrical resistance element embedded in a ceramic rod which is in turn enclosed by the metal sheath. When an electrical current is applied, the whole unit is heated to about 600°F.

(4) Comparison of Different Electric Line Source Heaters

The quartz lamp heater is probably the most efficient of all infrared generators. It operates at a high temperature and is very efficient in converting its input energy into radiant energy. The quartz envelope surrounding the filament does not absorb much of the radiant energy, thus minimizing convection losses to the environment. Figure 35 is a graph of radiation vs. air velocity for the three types of electric heaters. It shows that the quartz lamp and the quartz tube heaters are affected by the wind to a much lesser degree than the metal sheath heater whose radiating surface is exposed to the wind.

It appears that a quartz wind-break may be a desirable feature to add to any infrared heater. Quartz is transparent to much of the infrared energy given off by the heaters and would effectively shield the heaters from the wind. Its one drawback is, of course, its weakness to mechanical shock.

All of the electric heaters are produced in a fairly standardized form by several manufacturers such as the General Electric Co. and Westinghouse. They are then packaged in reflectors by a large number of companies.

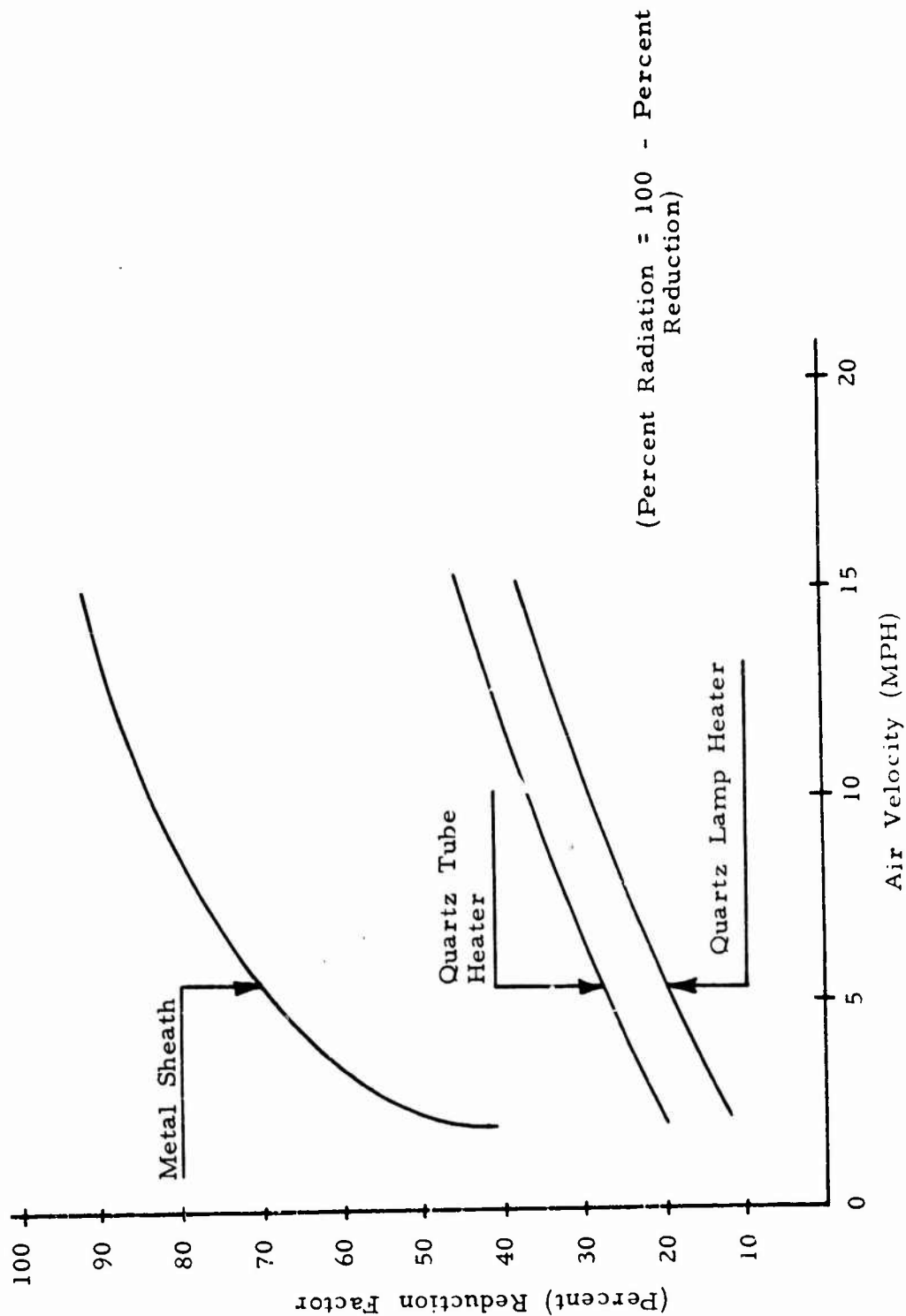


Figure 35 Radiation vs. Air Velocity Curves for Electrical Radiant Heaters

All of the quartz lamps and tubes manufactured by the major companies are straight. The heater produced by the Hi-Shear Corporation and discussed earlier was the only one found using a quartz lamp that was curved. Metal sheath heaters, on the other hand, can be easily bent and come in a variety of configurations.

5.2.2.2 Gas Heaters

(1) Radiant Tube Burner

Radiant Tube Burners use a tube or pipe as the radiating surface between the flame and the load. As an example the Roberts-Gordon system listed in Table VIII and shown in Figure 36 consists of a length of black iron pipe with a combustion chamber at one end and an eductor at the other to pull the hot gases through the pipe.

This particular heater was designed for heating buildings and is large and heavy. However, a radiant tube burner could be designed to be quite light and rugged.

The Roberts-Gordon heater has a maximum temperature of 1000°F. It is provided with a reflector to direct the radiation. The radiating surface of this heater is directly exposed to the environment; its operating temperature is relatively low. It is therefore likely to suffer a substantial reduction in radiant energy output when exposed to high wind.

5.2.3 Point Sources

Since true point sources do not exist, the

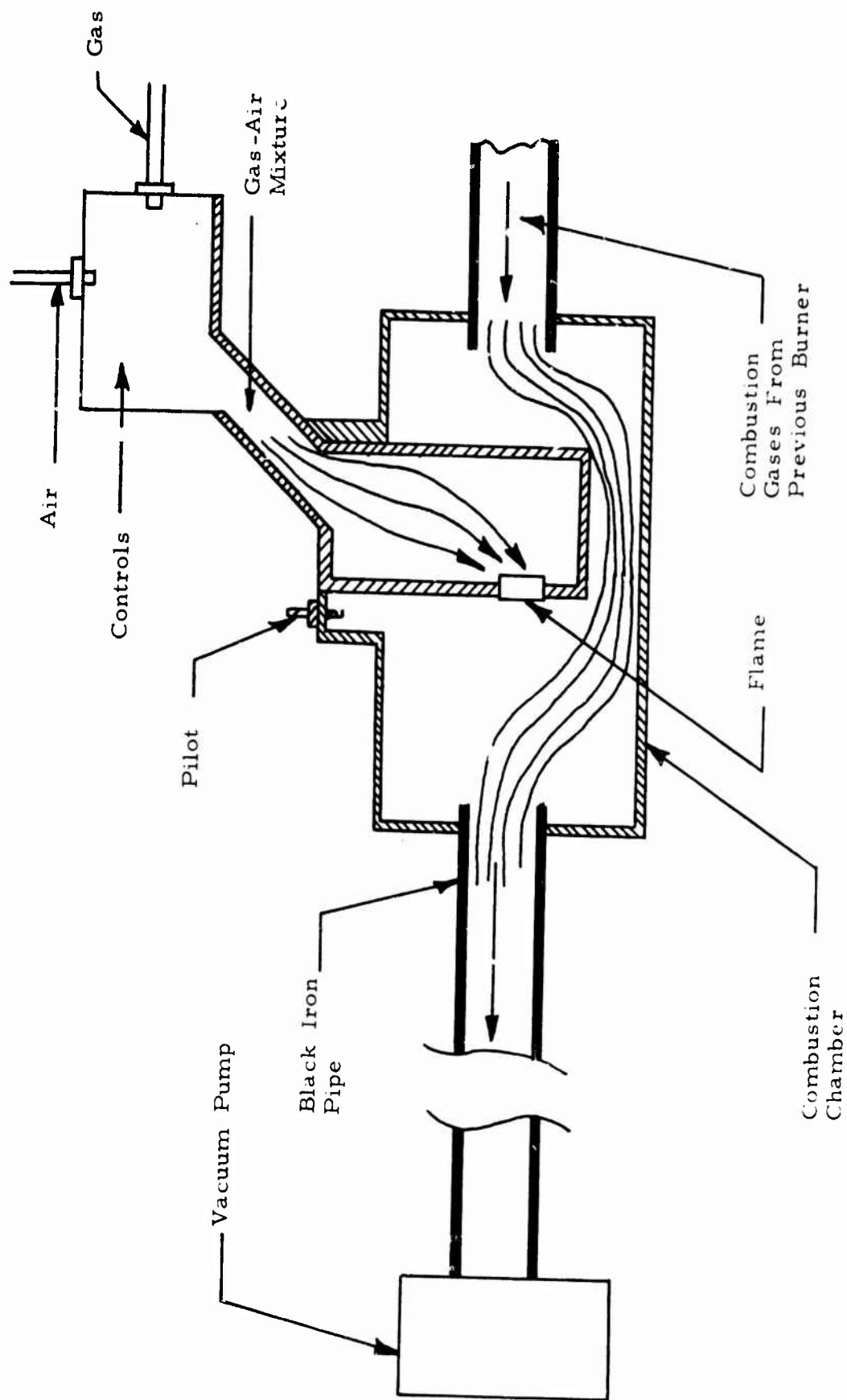


Figure 36 Schematic Drawing of the Roberts-Gordon Radiant Tube Heater

heaters discussed in this section are approximations to a point source. However, point sources are an interesting category because they lend themselves to a variety of reflector shapes and their energy can be aimed better than the energy from other types of sources.

5.2.3.1 General Electric R-40 Bulbs

Often called incandescent heat lamps, these are the most common electric infrared generators. These lamps are very similar to the common light bulb. They use a hot tungsten element as the energy source and usually have a built-in reflector. The infrared generating characteristics of this bulb are the same as those of the quartz lamp. The filament operating temperature is 4000°F and approximately 86 percent of the input energy is radiated with about 8 lumens per watt given off as visible light.

These lamps are efficient sources of radiant energy and are not affected by the wind; however, they are fragile and cannot take any mechanical shock.

5.2.3.2 Radiant System's Pyrocore

The Radiant System Pyrocore is a uniquely shaped surface combustion burner. The ceramic element is cylindrical with a pipe nipple connector at one end (Figure 37). It is surrounded by a nichrome wire reverberator screen and the entire unit is placed in a parabolic reflector. The burner operates without a blower at gas pressure of 10 to 30 psi.

The operating temperature and the output of the burner can be modulated by changing the gas pressure. The maximum continuous operating temperature is 2000°F.

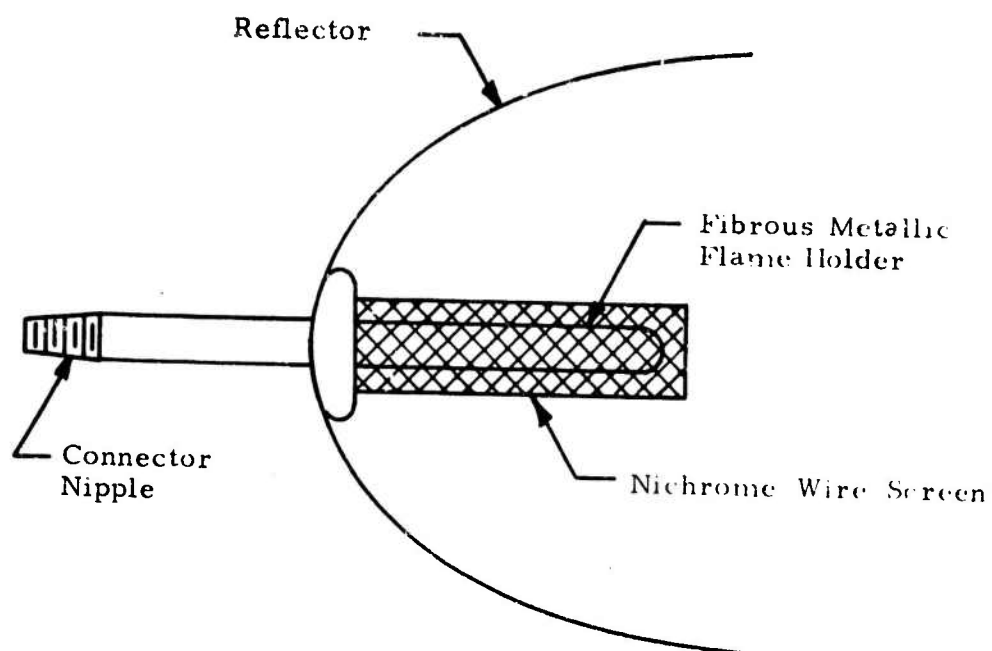


Figure 37 Radiant Systems Pyrocore Heater

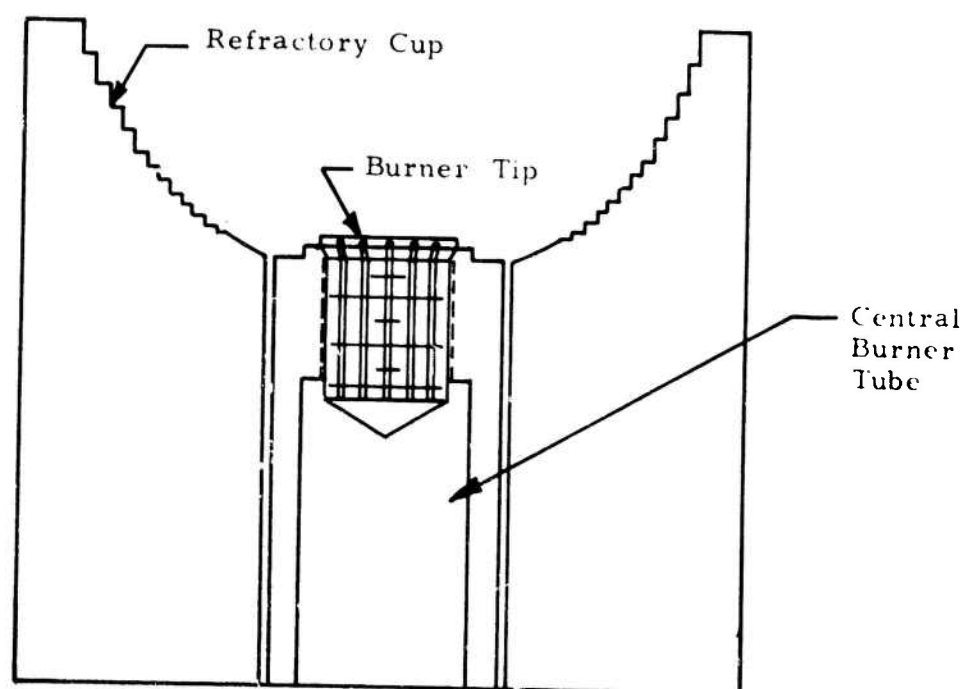


Figure 38 Drawing of the Selas Duradiant Burner

This unit approximates a point source and is surrounded by a parabolic reflector to direct the radiant energy. The manufacturer claims that the heater is windproof, very light, and resistant to mechanical shock.

5.2.3.3 Selas Duradiant Burners

The Selas Duradiant Burners are cup-shaped, ceramic burners with a wide variety of sizes. Each Duradiant burner is assembled around a central mixture tube of metal or ceramic material, according to the anticipated service temperature (Figure 38). A molded high temperature ceramic tip is screwed into the end of the mixture tube. With numerous narrow slots molded into its periphery, the tip functions essentially as the distributing head of a multiple-port burner. Surrounding the burner tip is a refractory, cup shaped block through which the tip protrudes.

The inner contour of the cup has been shaped so that its surface is always washed by hot combustion products, regardless of operating rates. Because the refractory cup is heated by the combustion products at their highest temperatures, it becomes highly incandescent. Combustion is completed within the cup.

The input to the burners can be varied by changing the input pressure of the propane or natural gas. With an input pressure of 18 inches water column, a 3 3/8" diameter burner has a capacity of 25,000 BTU/hr; therefore, these burners have a large capacity for their small size. For open applications the burners are enclosed by a stainless steel or cast iron casing which should greatly increase their strength.

For outdoor applications the burner is likely to be greatly affected by the wind.

5.2.4 Other Heaters

The Hupp Hot-Tot Heater shown in Figure 39 is a large high capacity personnel heater designed for indoor use. It is rated at a fuel input of 86,000 BTU/hr which is about 4 times larger than any other heater of the same size and weight. The Hot-Tot has a cylindrical source of the same general shape as the Pyrocore heater and operates at approximately the same surface temperature and radiant intensity. It differs from the Pyrocore in its burner design. In the Hot-Tot, combustion is complete before the hot gases pass through the perforated inconel cylinder; the latter then acts as only a heat exchanger extracting heat from the hot gases and radiating it out into space. In the Pyrocore, combustion occurs at the external surface of the fibrous metallic flame holder. The Hot-Tot is supplied without a reflector as it is designed to radiate uniformly into space. The surface area of the Hot-Tot burner is approximately 7 times that of the Pyrocore.

5.2.5 Commercial Heaters Selected for Experimental Evaluation

The selection of heaters for experimental evaluation was based on the following criteria:

1. Geometry of the source.
2. Reflector design to provide the spatial distribution of heat flux specified.

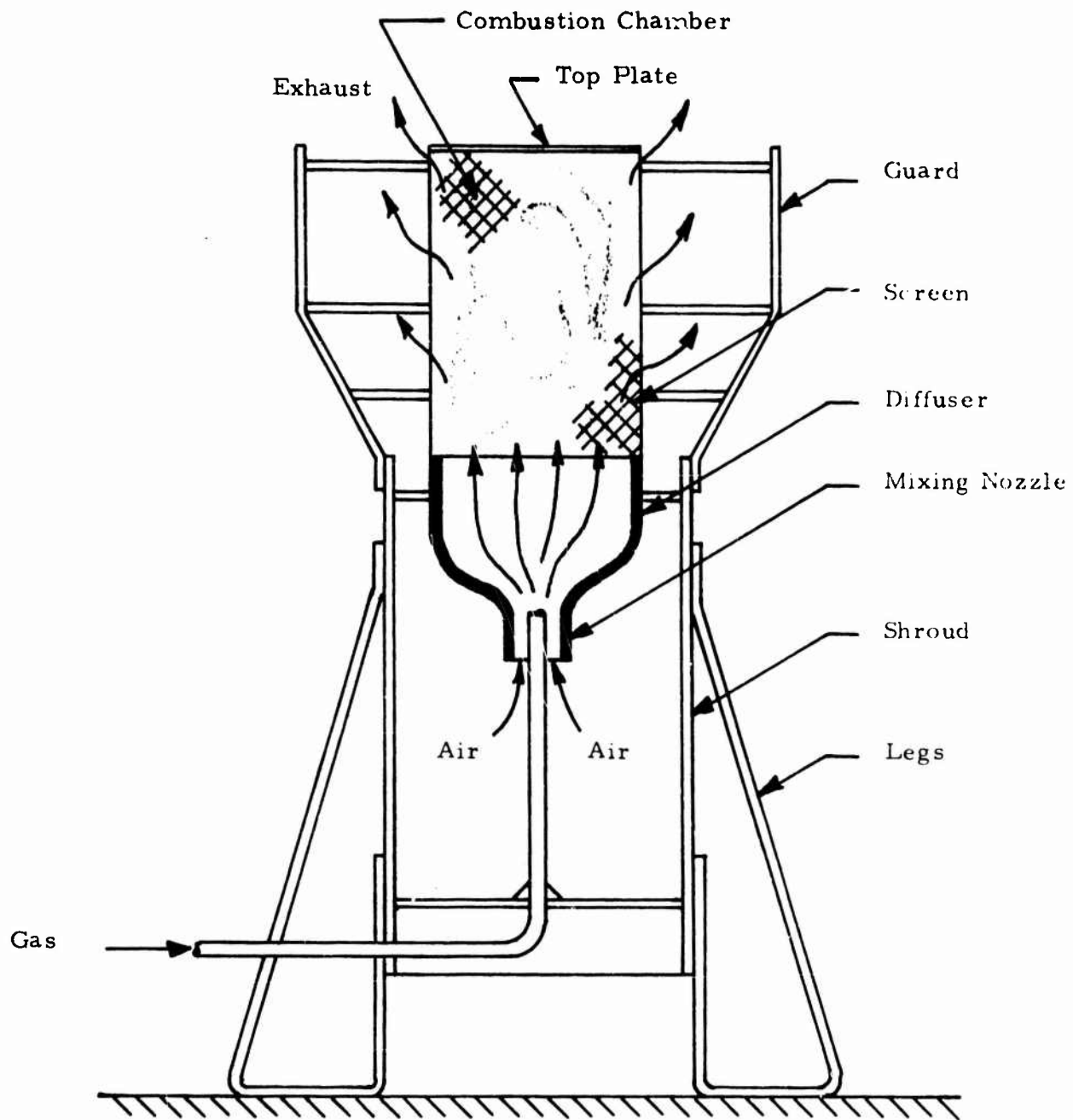


Figure 39 Schematic of Hupp Hot-Tot Heater

3. Design of the burner.
4. Material of construction of the emitter.
5. Wind resistant construction.

Of the fifteen heaters listed in Table VIII and the Hot-Tot heater, five were selected for further study and testing.

The Hupp Inc. surface combustion, area source type heater, with a parabolic reflector was selected. It has a ceramic emitter surface and is one of the more commonly used commercial units. Also, Hupp, Inc. has run a number of tests measuring the radiant flux output of their heaters. These test results would provide a useful comparison of the heat flux density measurements made as part of this program. It was initially planned to also test a similar Van Dorn heater with an inconel burner in order to study the effects of emitter material construction. However, as it was concluded early in the test program that source geometry, burner design, and reflector geometry are parameters more significant than the emissivity of the heater to the design of a heater for this program, the Van Dorn heater was eliminated in preference to the Foster-Miller heater.

Testing of electric heaters was de-emphasized, since the extra penalties of weight and inefficiency inherent to on-site electric power generation make the use of such heaters unattractive for Arctic application. However, the Hi-Shear Corporation's spiral quartz lamp was selected for testing due to its particular design, which simulates a high temperature area source. It is claimed to have a high wind resistance and would therefore provide a good relative comparison with other heaters having an exposed flame.

A straight line source is considered unsuitable to achieve a uniform spatial flux distribution over a circular receiver area. It was therefore eliminated from further consideration.

Two point sources were chosen. One is the Radiant Systems Pyrocore which is a light, powerful heater that is supposedly windproof. It is quite different from any other heater found in the survey and was therefore selected for further study. It is sold with a parabolic reflector but could be used with a variety of reflectors. The other burner chosen is the Sclas Duradiant Burner. This again is quite different in shape from any of the other burners in the study. One proposed use of the burner is shown in Figure 40. A burner is mounted with its radiating surface facing the reflector. This type of mounting is estimated to best direct all the energy radiated from the burner to the target area.

The Hupp Hot-Tot heater was also selected for further evaluation, being a larger cylindrical source of inconel which could be used for comparison with the Pyrocore heater.

Finally, the test results obtained during this program showed that no commercially available heater design could satisfy the spatial flux density distribution desired, as well as operate satisfactorily under the wind conditions specified. This led to the development of the Foster-Miller heater design, described in Appendix C which consists of a hemispherical source with a parabolic reflector. Tests were also conducted on this heater.

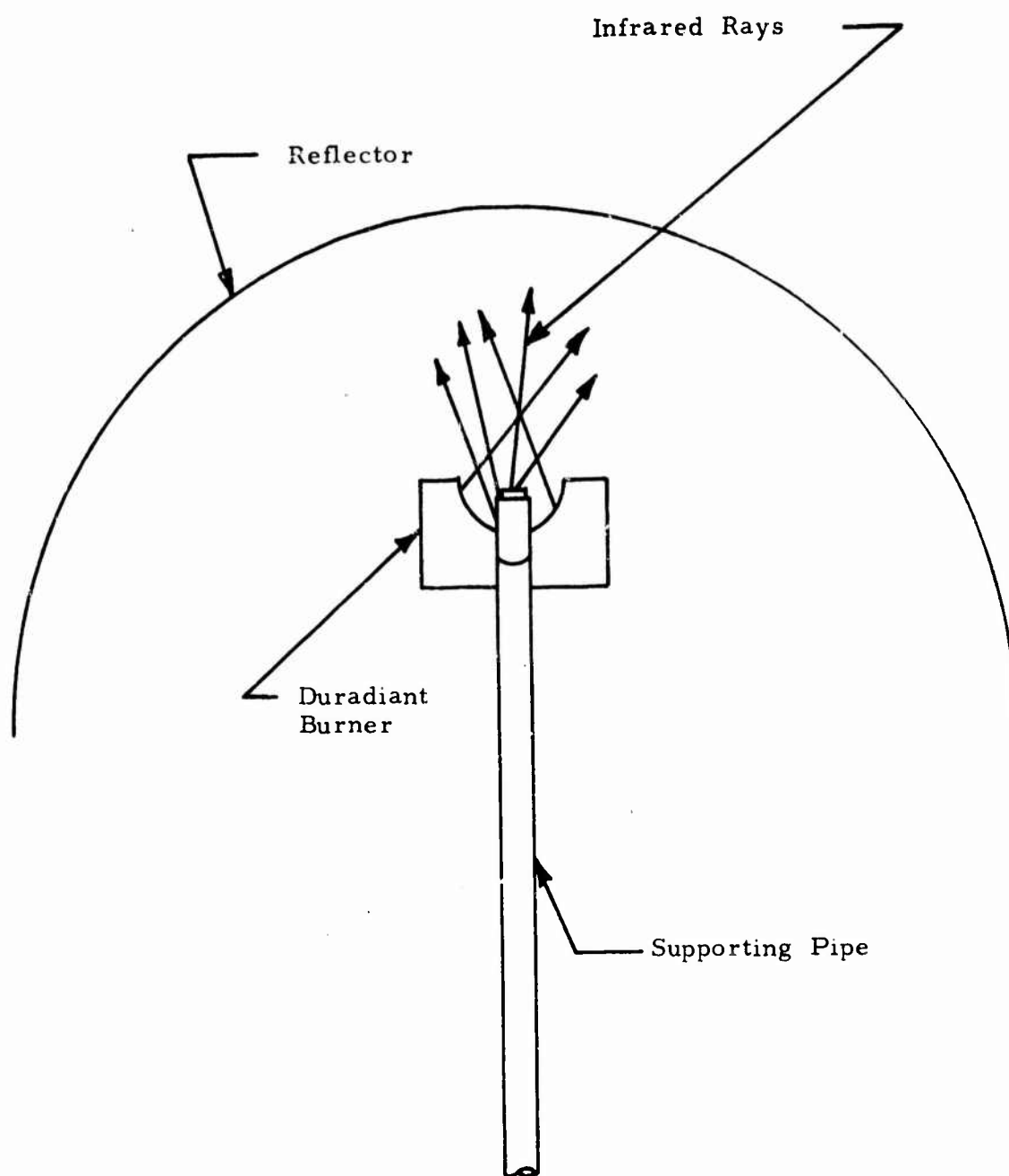


Figure 40 Schematic Arrangement of a Duradiant Burner to
Approximate a Point Source

6. Test Program

6.1 Scope of Test Program

A test program was conducted to measure the performance of the various heaters selected for experimental evaluation. The principal objective of this program is to measure the spatial distribution of radiant flux density on a target area 8 ft in diameter and located 4 to 10 ft away from the source. Tests were conducted under normal ambient conditions in the laboratory (70°F temperature) and with a 15 mph wind blowing at the surface of the heater from different directions. No tests were run at low ambient temperatures.

Tests were conducted on the following heaters:

1. Government Furnished Gasoline Heater
2. Pyrocore Propane Heater
3. Hupp Propane Heater
4. Hupp Hot-Tot Propane Heater
5. Hi-Shear Electric Heater
6. Selas Burner
7. Foster-Miller Radiant Heater

The following sections provide a description of the instrumentation selected for this study, a detailed description of the heaters, the test setup and procedures, and the test results.

6.2 Instrumentation for Measuring the Performance of the Radiant Heater

A survey was conducted of available instrumentation to measure the spatial distribution of the radiant heat flux intensity output of the radiant burner and of the radiant heat flux incident on the receiver area. These measurements are considered essential for the experimental evaluation of performance of the radiant heaters. From the various measuring techniques investigated a radiation pyrometer was selected to determine the radiant heater output and a radiometer to measure the radiant flux density distribution at the target.

The radiation pyrometer measures the intensity of radiation emitted from a small spot on the heater (say 0.25 inches in diameter) and, based on the emissivity of the emitter, produces a signal proportional to the emitter temperature. To get a true value of the emitter temperature it is essential to know the emissivity of the emitter, a value which is not particularly easy to measure. However, when using the radiation pyrometer to measure the spatial distribution of the radiant intensity of the source, it is only necessary to obtain the equivalent black body temperature of the emitter. This is easily achieved by setting the radiometer emissivity setting to 1 (i.e. a black body emitter) and measuring the effective black body temperature.

The radiant intensity,

$$I = \sigma T_b^4 \quad (7)$$

where

- I is the radiant intensity or flux density
- σ is the Stefan-Boltzmann constant
- T_b is the measured black body temperature

If the surface emissivity is ϵ , then the actual surface temperature, T_a will be higher and equal to,

$$T_a = \frac{T_b}{\sqrt[4]{\epsilon}} \quad (8)$$

Scanning the heater source area with the radiation pyrometer, a spatial distribution of the source black body temperature and hence the radiant heat output can easily be obtained.

The radiometer measures the intensity of radiation falling on a small detector area. Its output is directly in BTU/hr-ft² or radiant flux density. It can be used to measure the spatial distribution of flux density on the receiver area.

Table IX provides a summary of the essential characteristics of representative pyrometers made by various manufacturers. The Ircon 300 Series radiation pyrometer has the wide temperature range necessary for the test program, as well as a small target size, a continuous read out, and emissivity correction. It was selected for the test program.

An Eppley thermopile radiometer with a Keithley model 155 Microvoltmeter as the readout, was selected as the most suitable radiometer. The principle of operation and a description of these instruments is provided in the following sections.

6.2.1 Eppley Thermopile Radiometer

The basis of the radiometer is a thermopile

TABLE IX
COMPARISON OF PYROMETERS FOR TEMPERATURE MEASUREMENT

Instrument	Type	Accuracy	Read Out Device	Temperature Ranges	Minimum Target Size	Viewing Distance	Continuous Read Out	Correction for Emissivity
Leeds and Northrup 8641 Mark I	Automatic Optical	(1)	Recorder Needed	1400 - 2250° F 1950 - 3200° F 2700 - 5200° F	.1" Dia.	20" - ∞	Yes	No (2)
Pyro Model 81	Optical	0.5 to 1% of measured temperature	Direct Reading on Case	1400 - 2500° F	.055"	3' - ∞	No	No
Pyro	Micro-Optical	4 - 6° F	Direct Reading	1300 - 2500° F 2400 - 3400° F 3200 - 5800° F	.015	5' - ∞	No	No
Ironcon 300 Series	Radiation Pyrometer	2% of range	Read Out Indicator Included	-2200 - 300° F	.12	7" - ∞	Yes	Yes 0.2 - 1.0
Ironcon 1200 Series	Automatic Optical	1% of full scale	Read Out Indicator Included	1300 - 2600° F	1/2"	20" - ∞	Yes	Yes
Leeds and Northrup Spectray 90	Radiation Pyrometer	2% of range	Recorder Needed	1300 - 2300° F	.155"	12" - ∞	Yes	Yes
Bristol No. 9E9	Radiation Pyrometer	1% of full scale	Recorder Needed	1100 - 2200° F	1 1/3"	24" - ∞	Yes	On Recorder
Barnes Infrascopes Mark I	Radiation Pyrometer	1% of full scale	Indicator Included	750 - 4650° F	.010	6' - ∞	Yes	Yes .05 - 1.0
Thermo Electron Pistol Pyrometer	Radiation Pyrometer	± 7% of full scale	Direct Reading on Case	1200 - 2200° F	.01	6' - ∞	Yes	Yes .2 - 1.0

(1) Within standards set by National Bureau of Standards.

(2) In all optical pyrometers, corrections can be made for emissivities.

which consists of a number of thermocouples arranged in series. This arrangement has the advantage of providing a relatively large output signal for a given temperature difference between the hot and cold surfaces.

Figure 41 is a sketch of the Eppley radiometer with its circular thermopile. The thermopile has 8 bismuth-silver junctions with a lamp-black coating on the inner hot receiver junctions. The outer junctions are shielded from the incoming radiant energy and remain at the ambient temperature of the case. When the radiometer is aimed at a heater, for example, the infrared energy causes the temperature of the hot junctions to rise and the resulting EMF is a function of the differential temperature between the hot and cold junctions. Supplied with the radiometer is a calibration relating millivolts to radiant flux density, BTU/hr-ft^2 .

The Eppley radiometer consists of a cylinder with an opening in the front face and a thermopile mounted on the back face. The radiometer has a water-jacketed case to aid in maintaining a constant case temperature of 25°C . The water-jacketed case was deemed necessary to maintain the case temperature constant when measuring the high radiant flux density existing close to the heaters.

Figure 42 shows the response characteristics of several semiconductor detectors. Response is fairly uniform to all photons up to a particular wavelength. Photons beyond this wavelength will not have sufficient energy to liberate electrons to produce a signal. It can also be seen from Figure 42 that a thermal detector such as the thermopile used in the Eppley

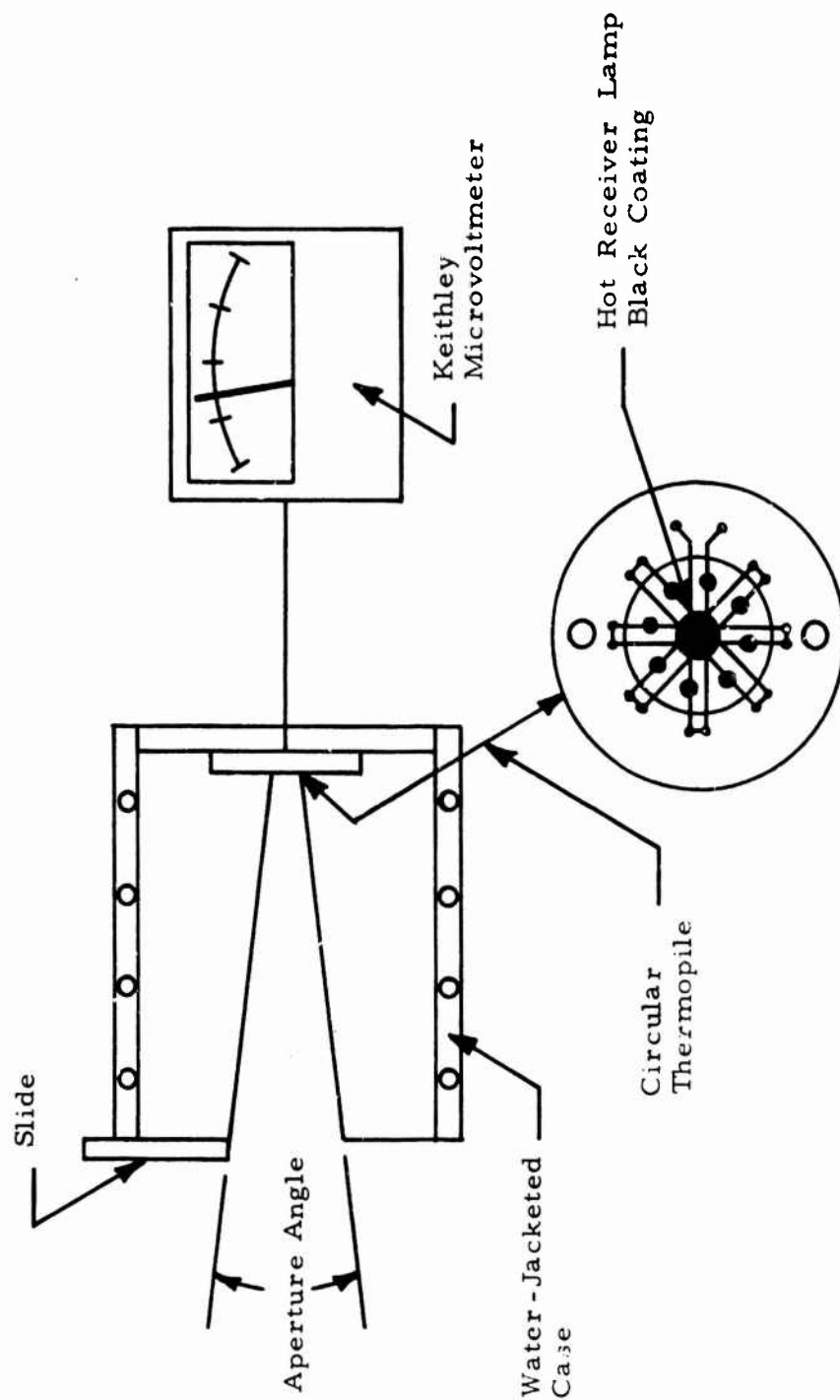


Figure 41 Eppley Thermopile Radiometer

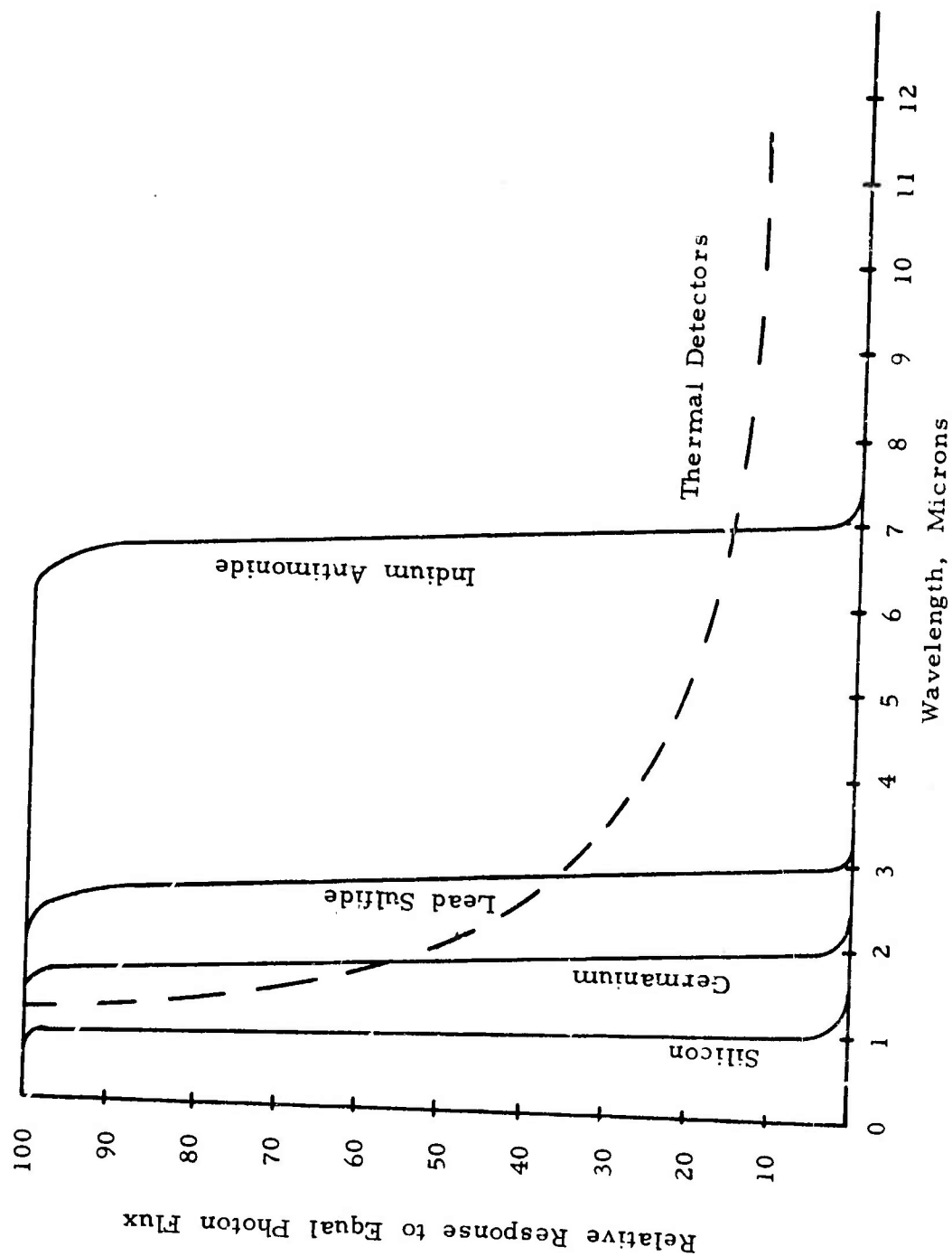


Figure 42 Spectral Response Characteristics of Several Infrared Detectors

Radiometer is sensitive to all wavelengths.

6.2.2 Ircon 300 Series Infrared Radiation Thermometer

The Ircon Infrared Radiation Thermometer is designed to measure the temperature of a body without contacting it. As shown in Figure 43, the infrared energy from a hot body passes through an objective lens (B), is reflected from the beam splitter mirror (C), and focused on the infrared sensor (D). The infrared sensor generates an electric signal proportional to this radiant energy. This signal is amplified at (E), to drive a meter (F), which is calibrated directly in °F.

Simultaneously with this operation the visible light from the object is transmitted by the mirror (C), focused in the plane of the telescope reticle (G), collimated by the eye lense (H), and viewed by the operator (I). The image appears with a circular pattern superimposed which shows the exact spot on the object being measured.

6.2.3 Keithley Model 155 Microvoltmeter

The Model 155 was used to measure the voltage given off by the Eppley Radiometer. It is a battery-operated meter with ranges from 1 microvolt full scale to 1000 volts.

6.3 Design of Test Apparatus

The test apparatus was designed to measure the following heater performance parameters:

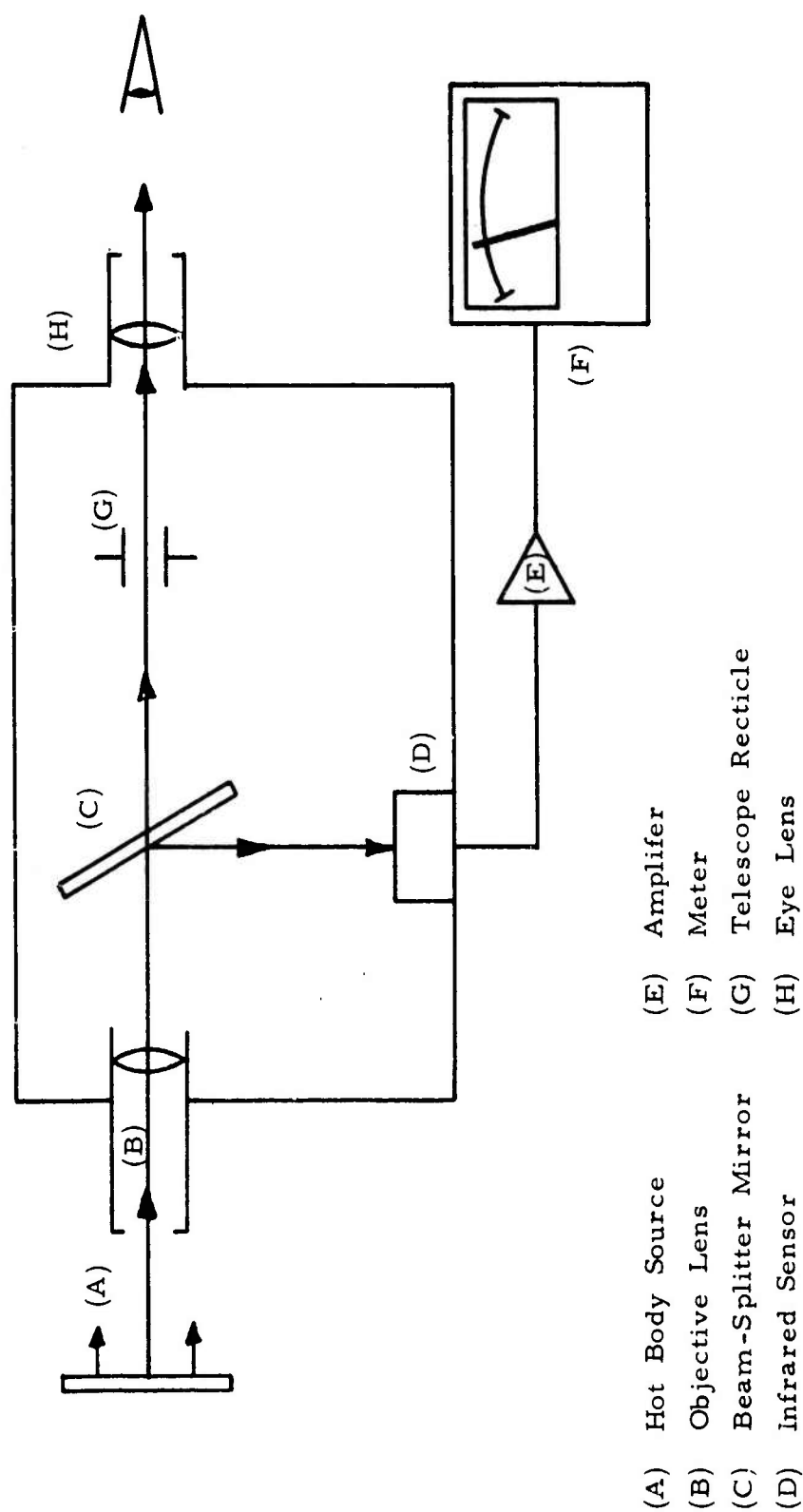


Figure 43 Schematic of the Ircon Model 300 Radiation Pyrometer

- (a) the spatial distribution of the radiant flux density (BTU/hr-ft^2) falling on a target four feet in radius and located 4 to 10 from the heaters emitting surface;
- (b) the temperature distribution of the emitting surface (providing an estimate of the total radiant energy output of the heater);
- (c) fuel flow-rate to the heater (providing a measure of the energy input to the heater).

Figure 44 shows a photograph of the test instrumentation.

6.3.1 Radiant Flux Measurement

The radiant flux distribution on the target surface was measured by the Eppley thermopile radiometer. The radiometer is mounted on an arm driven by a gear reducer, as shown in Figure 45. The mounting is designed to allow the radiometer to pivot on its mounting plate in order to direct its field of view at the heater. The arm is capable of rotation through a full circle, and the radial position of the radiometer is adjustable so that a complete map of the flux distribution on the target area can be obtained.

The radiometer is water-jacketed to maintain a constant cold junction temperature of the thermopile. The cooling water temperature is maintained at approximately $75^{\circ}\text{F} \pm 5^{\circ}\text{F}$ the calibration temperature. The exposure time of the thermopile to the incident radiation is limited to 30 seconds to minimize the effect of case heating and re-radiation of energy to the receiver.

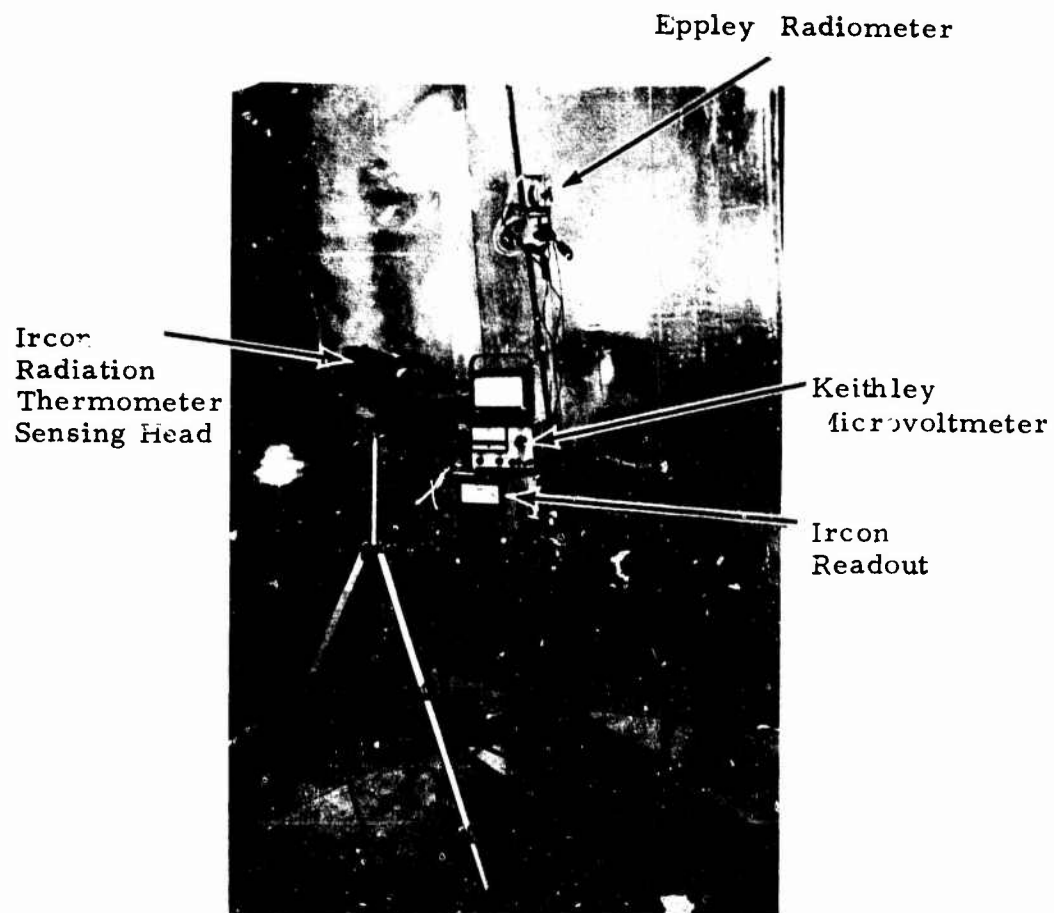


Figure 44 Test Instrumentation for Measuring
Radiant Heater Performance.

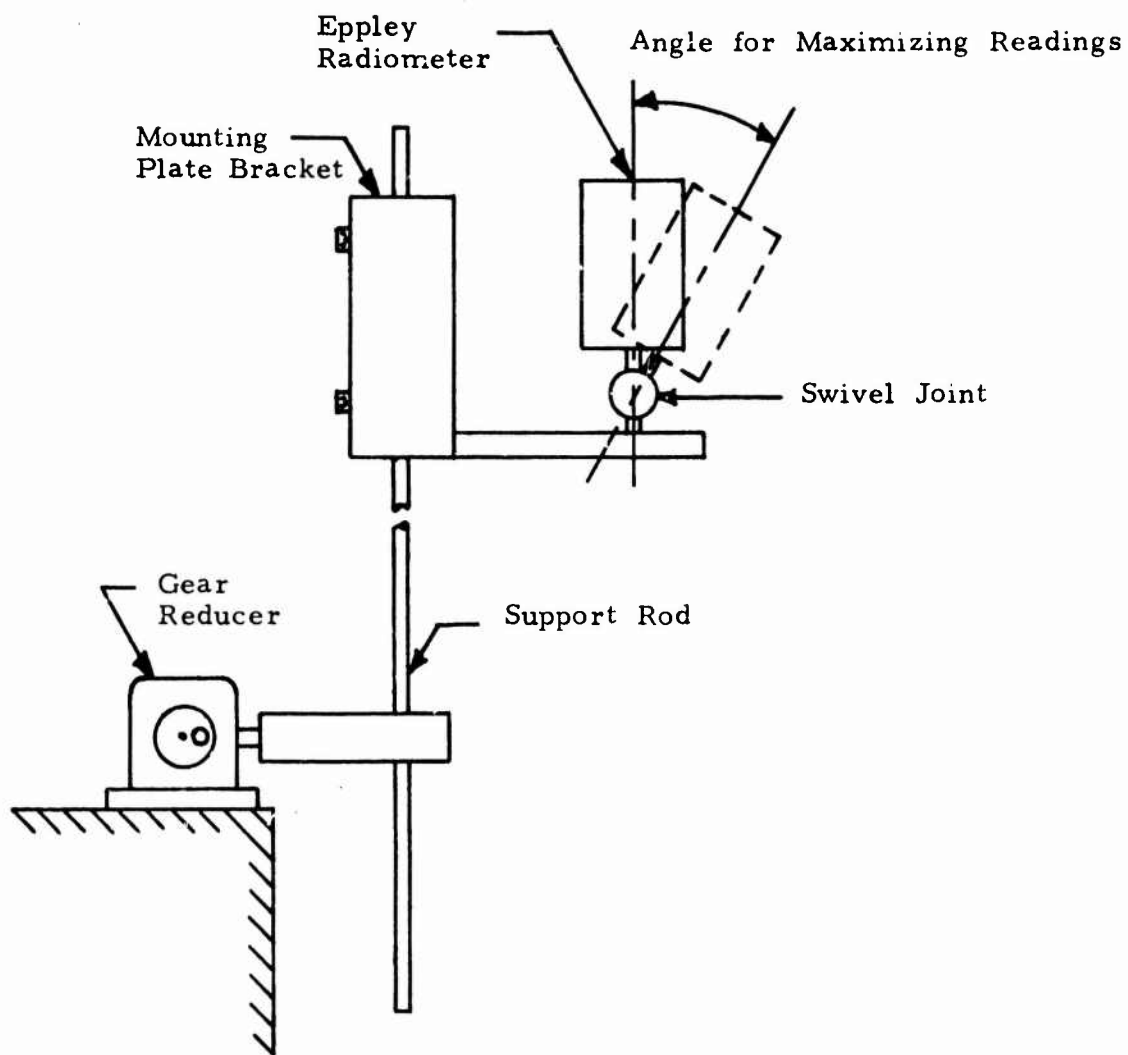


Figure 45 Radiometer Support Assembly

6.3.2 Temperature Measurement

The Ircon radiation pyrometer was used to measure the temperature distribution of the heater's radiating surface. From the temperature distribution, the total flux radiated from the heater was calculated.

6.3.3 Fuel Flow Rate

The fuel flow rate was determined and checked by the use of in-line flow meters for liquid and gaseous fuels and by measuring the weight of fuel consumed during the test. Difficulties were experienced when measuring gasoline fuel flow, because of fuel vaporization forming bubbles and causing meter fluctuations. Measurements of fuel consumption over the duration of the test were usually sufficient to provide an accurate and reliable indication of fuel flow rate.

6.3.4 Wind Test

A 15-mph wind condition was simulated in the laboratory by blowing air at the heaters with a fan. The air velocity was measured with an anemometer.

6.4 Experimental Results

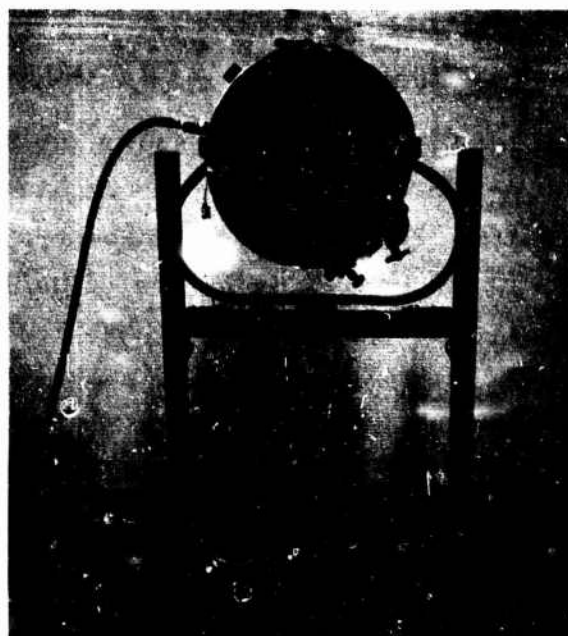
The results of performance tests conducted on the various heaters are presented in this section. Also provided is a short description of the heaters tested.

6.4.1 Government Furnished Gasoline Heater

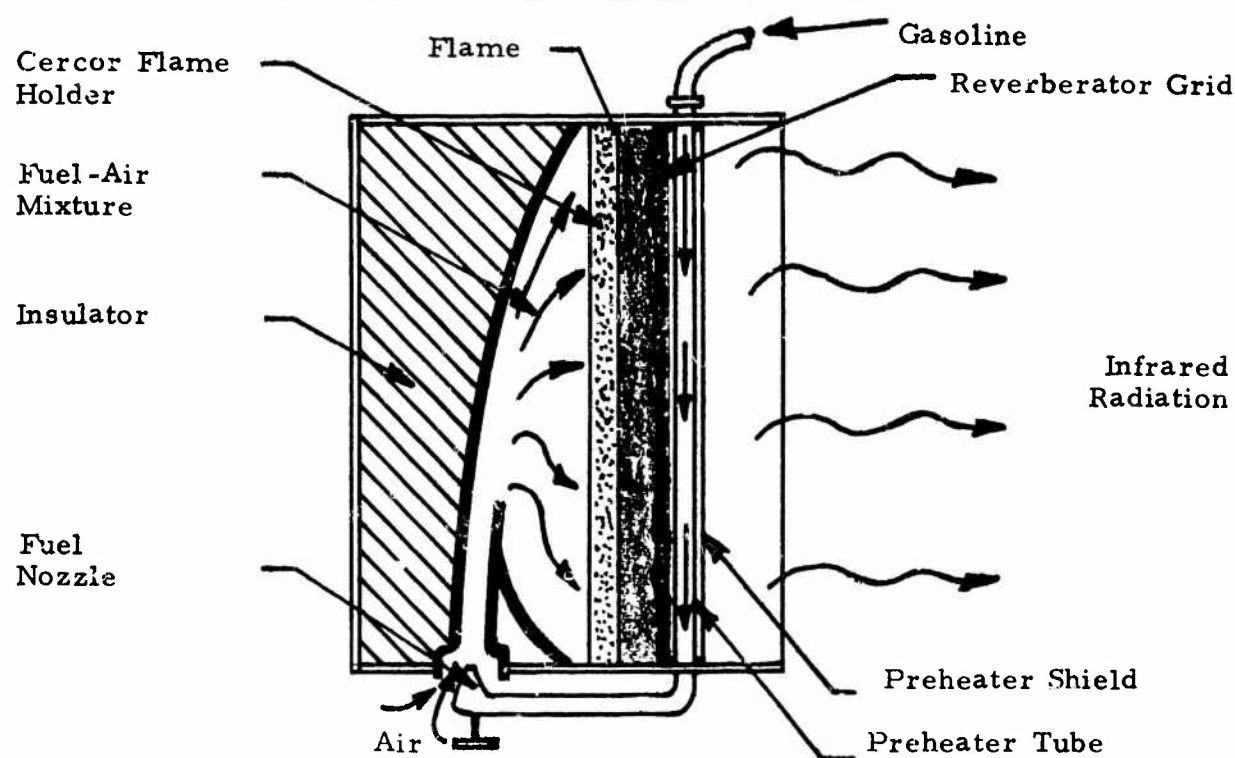
A photograph of the GFP Gasoline Heater is shown in Figure 46(a). It is an atmospheric burner using a Cercor element as the flame holder with a preheater to vaporize the liquid gasoline fuel. The fuel is fed to the heater at a pressure of approximately 25 psi from a pressurized fuel tank. The fuel is vaporized by passing through the preheater which in turn receives heat directly from the main Cercor burner surface. The pressurized fuel vapor in expanding through the nozzle of the eductor sucks in the required amount of air. The fuel-air mixture passes through a plenum chamber, from which it flows through the Cercor flame holder burning at its front surface as shown in Figure 46(b). The heat released by combustion heats the Cercor as well as the metal wire-mesh screen adjoining it. Both of these elements act as radiators to provide the necessary radiant energy.

Two GFP heaters were tested. Both units were difficult to light under the stationary ambient conditions of the laboratory. It would be extremely difficult to light one of these under the specified operating conditions of -50°F and 20-mph wind. Further the temperature of the burner surface was measured to be relatively nonuniform and variable. During the laboratory test program, the emitter surface temperature could not be increased above a black body surface temperature of 1350°F without the fear of a flashback.

A series of tests was conducted on these heaters, with and without a number of different reflectors. These results are presented in the subsequent sections.



(a) Photograph of CFP Gasoline Heater



(b) Schematic of Burner Head of GFP Gasoline Heater

Figure 46 GFP Gasoline Heater

6.4.1.1 Temperature Distribution of the Emitter Surface

Figure 47 shows the temperature distribution of the emitter surface. These readings represent the effective black body surface temperature as measured by the Ircon Radiation Pyrometer with an emissivity setting of unity. The mean temperature of the surface is approximately 1200°F, resulting in a total heat output of 8,060 BTU/hr from the heater surface. The mean fuel flow was measured to be approximately 1 lb/hr, corresponding to roughly 20,000 BTU/hr input and a fuel efficiency of approximately 40 percent.

6.4.1.2 Performance of Heater Without Reflector

The radiant flux distribution on target areas at various distances from the gasoline fired radiant heaters was measured using the Eppley thermopile radiometer. These tests were run at a gasoline supply pressure of 25 to 30 psi and a burner surface black-body temperature, as measured by the Ircon Radiation Pyrometer, of 1260°F. This temperature is measured in the middle of the burner face just above the preheater tube. The burner temperature was found to be a strong function of gasoline supply pressure and in order to hold the temperature constant during a test, the pressure was not allowed to drop below 25 psi. Operation at a temperature of 1260°F produces a relatively uniform burner face without the "overfire" condition that makes the heater unstable.

The heater used in most of the tests was very difficult to light and adjust. The main burner valve

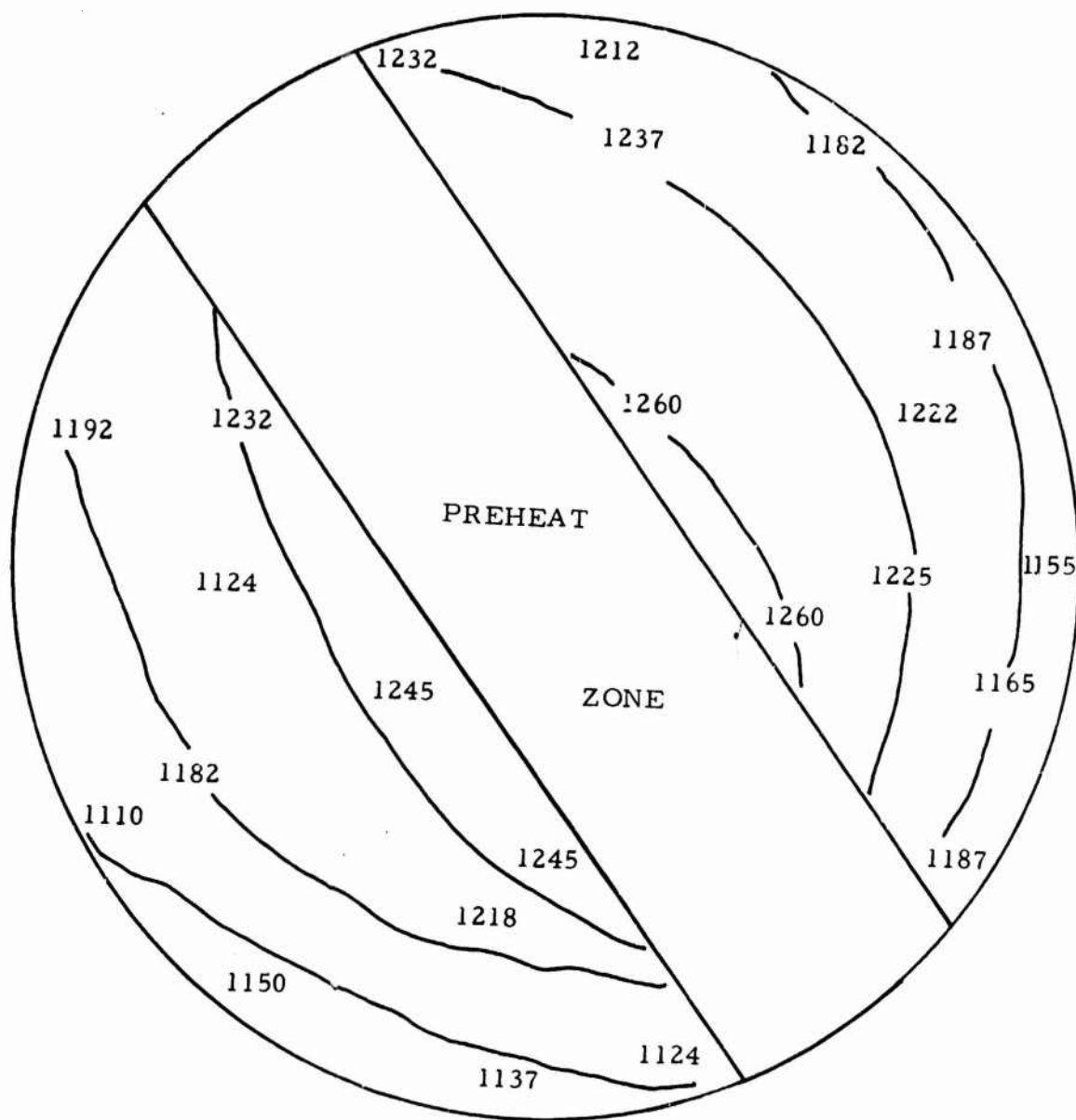


Figure 47 Black Body Temperature Map, °F. of the
Gasoline Heater

could be opened only $1/2$ to $3/4$ of a turn instead of the $2\ 1/2$ turns called for in the instructions. On firing, the burner required repeated adjustments to obtain a uniform burner face that was not too hot. However, once the heater was properly adjusted and warmed up, it would run well.

The heater was tested at a black body operating temperature of 1300°F . Radiant flux density distribution at target distances of 4, 6, 8 and 10 ft are shown in Figures 48 through 51. These show that at 4 ft a maximum intensity of $190\ \text{BTU/hr-ft}^2$ can be expected from this heater. This drops off to approximately $60\ \text{BTU/hr-ft}^2$ at the outer periphery of the 8 ft diameter receiver. At a target distance of 10 ft, this maximum flux density drops off to only $26\ \text{BTU/hr-ft}^2$. This is almost an order of magnitude smaller than the $200\ \text{BTU/hr-ft}^2$ considered necessary for heating.

The peculiar nonuniform distribution observed with these heaters, particularly at the shorter target distances, is due to the shadowing effect of the fairly large pre-heater which is located in the 4 o'clock position. It shields about 30 percent of the 1-ft-diameter Cercor emitter surface. At larger target distances its effect dies out, and the flux density distribution becomes quite uniform.

6.4.1.3 Performance of Heater with Conical Reflectors

Two types of conical reflectors were designed based on the analysis presented in Appendix A; a short and

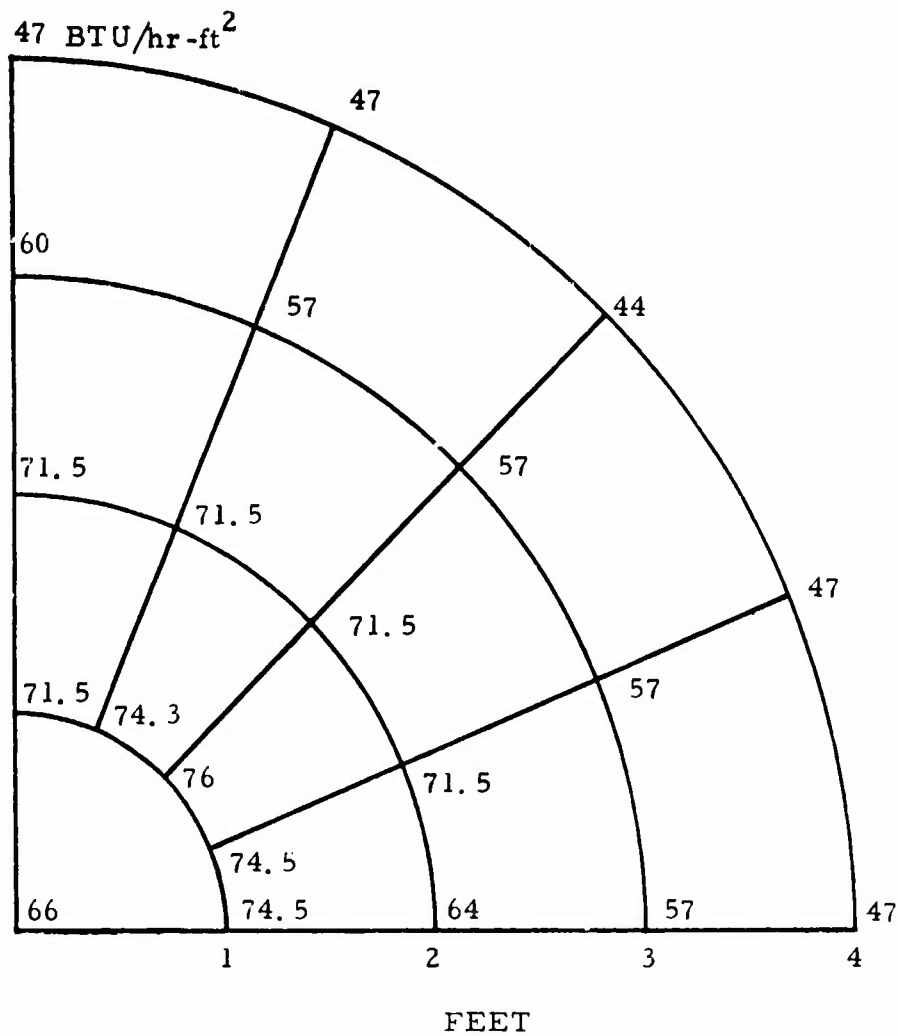


Figure 49 Radiant Flux Density Distribution, BTU/hr-ft²,

- GFP Gasoline Heater -

Target Distance, 6 feet.

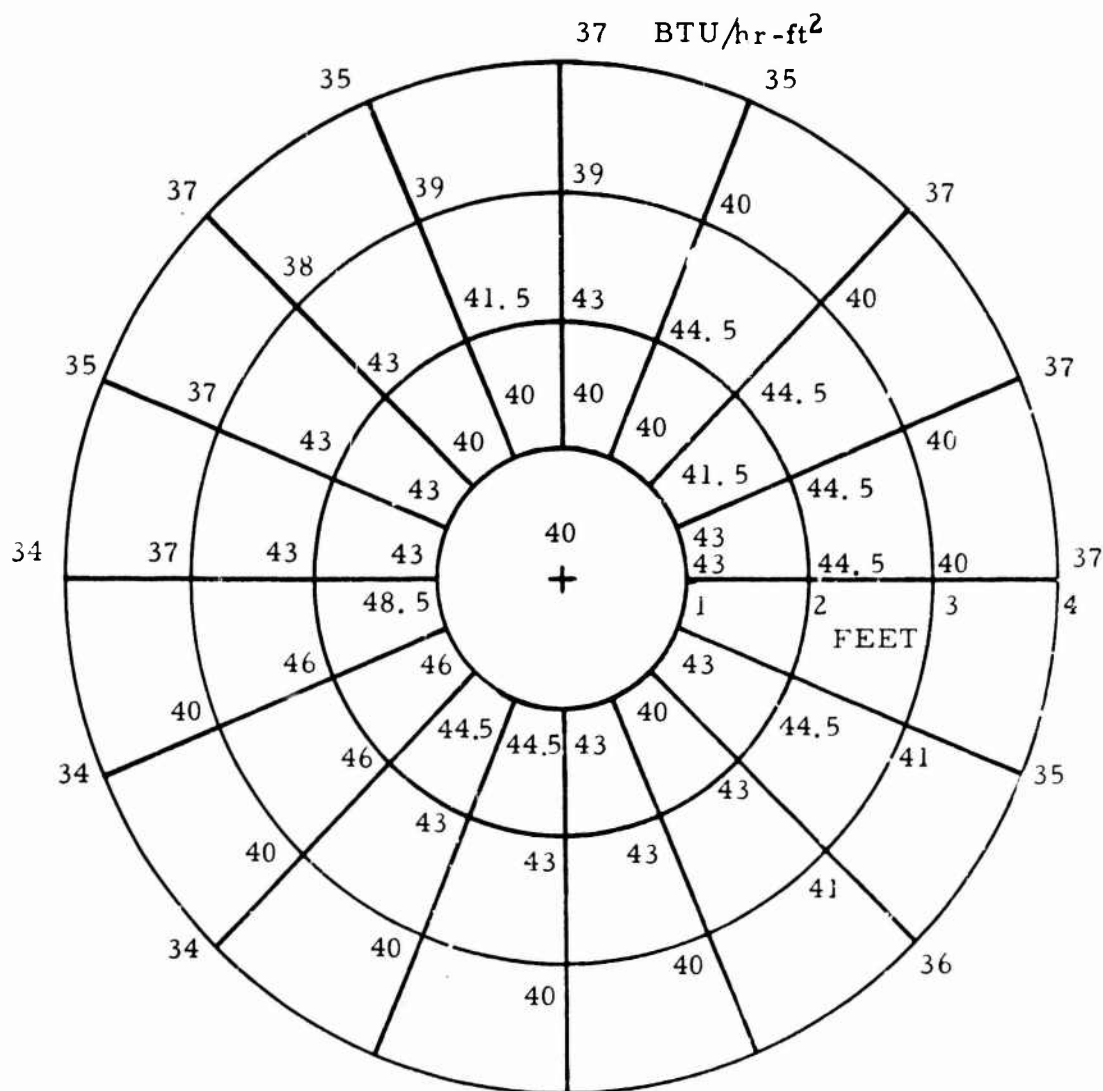


Figure 50 Radiant Flux Density Distribution, BTU/hr-ft²,

- GFP Gasoline Heater -

Target Distance, 8 feet.

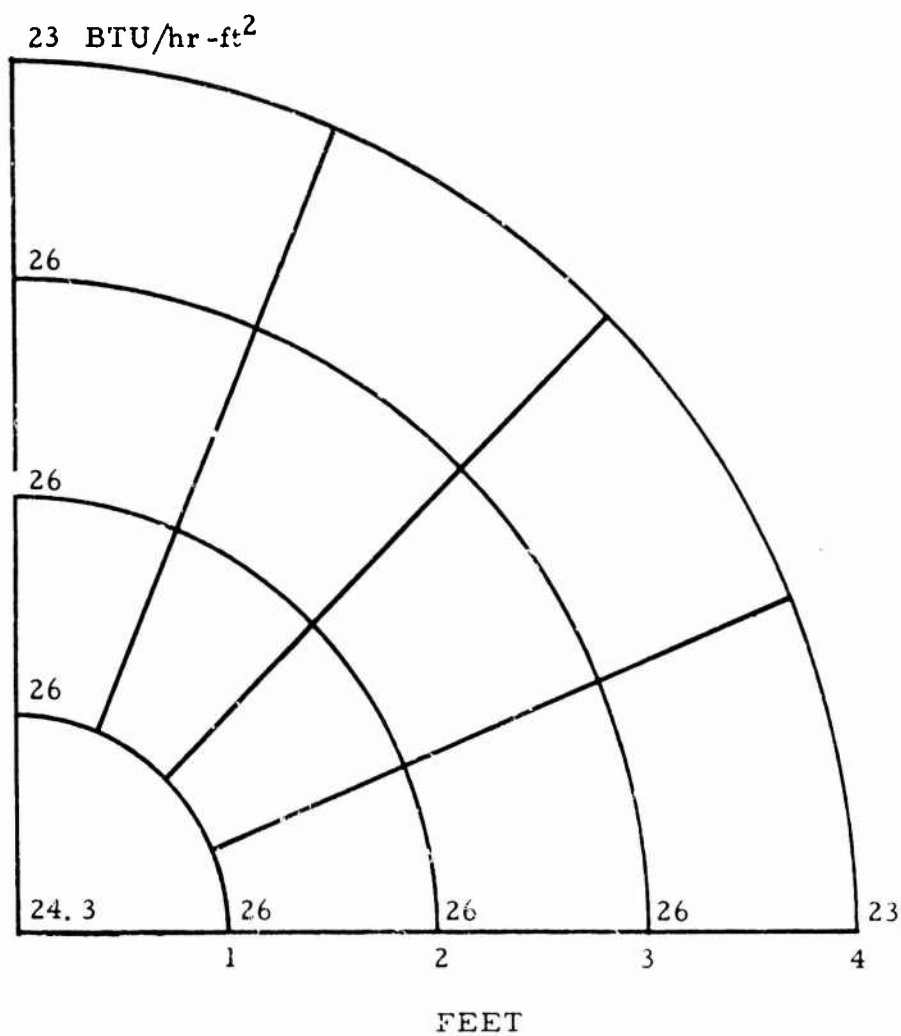


Figure 51 Radiant Flux Density Distribution, BTU/hr-ft².

- GFP Gasoline Heater -

Target Distance, 10 feet.

a long reflector. The reflector geometries are shown schematically in Figure 52. These were fabricated out of aluminum reflector sheeting manufactured by The Aluminum Corp. of America. Figure 53 shows a photograph of the two conical reflectors. Radiant flux density distributions were measured for target distances ranging from 4 to 10 feet. For these tests, measurements were principally restricted to the two axes in the first quadrant. Figure 54 shows these distributions at 4 and 10 ft with the short reflector, and Figure 55 shows similar results with the long reflector.

Figures 56 and 57 show a comparison of the flux density as obtained with and without the reflector, on targets at a distance of 4 and 8 ft respectively. The data shown are for the vertical axis starting at the centerline of the heater and moving up in 1-ft increments. These results show an increase in flux density by a factor of 2 for the short and 3 for the long reflector at the center point of the target. However, this increase is smaller at radial distances greater than 2.5 ft from the center. This is probably caused by shading of the radiation by the reflector and is more severe at target distances close to the heater.

6.4.1.4 Multicellular Conical Reflector

A multicellular conical reflector of the type shown in Figure 58 was designed and tested. This reflector has a number of small conical reflectors mounted on a plate whose rear face is also reflective. It was designed to fit inside the casing of the GFP gasoline heater, so as to cause no change in the overall heater diameter. The design was based on the assumption that each cone would act as the reflector for the small area of

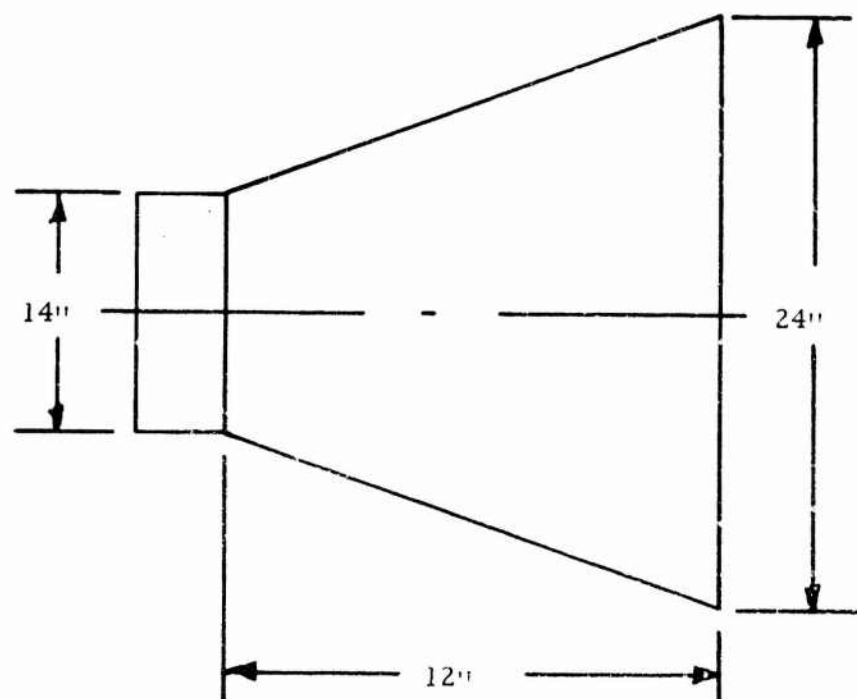
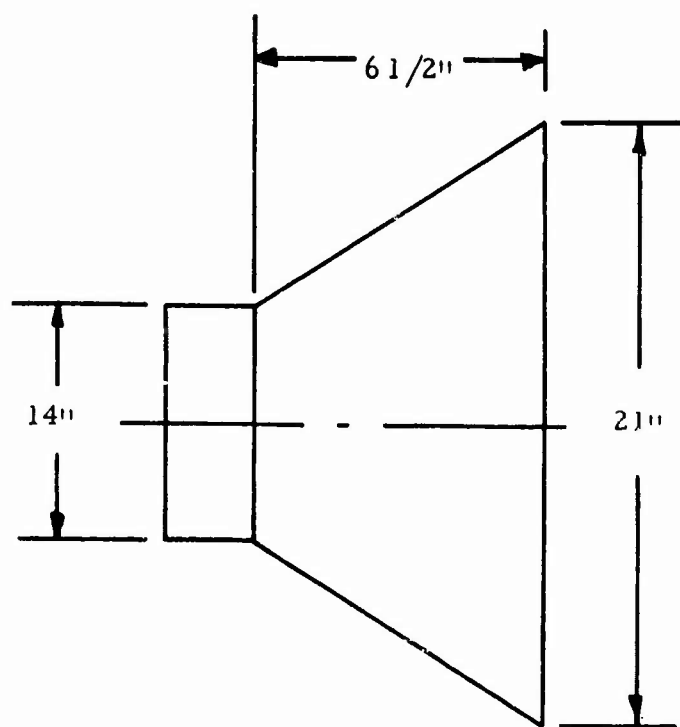


Figure 52 Schematic Drawings of Conical Reflectors

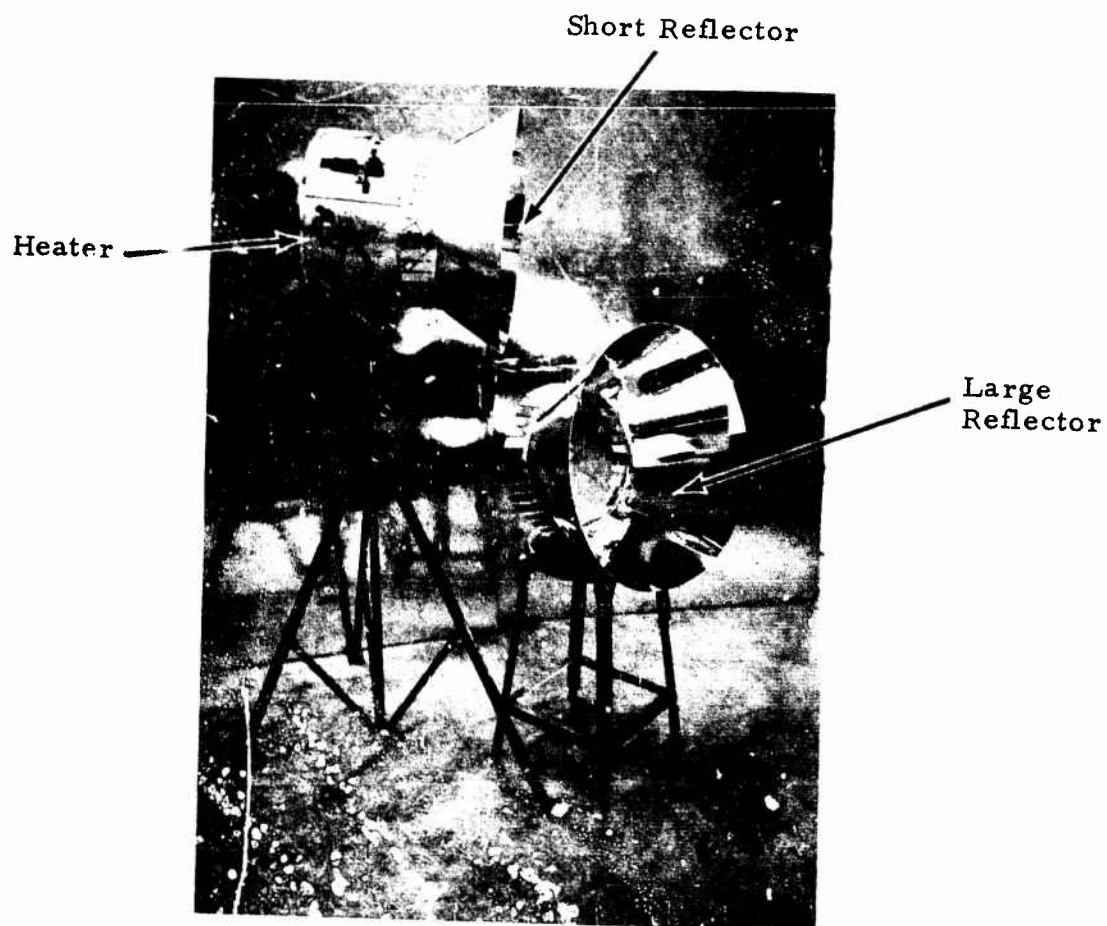
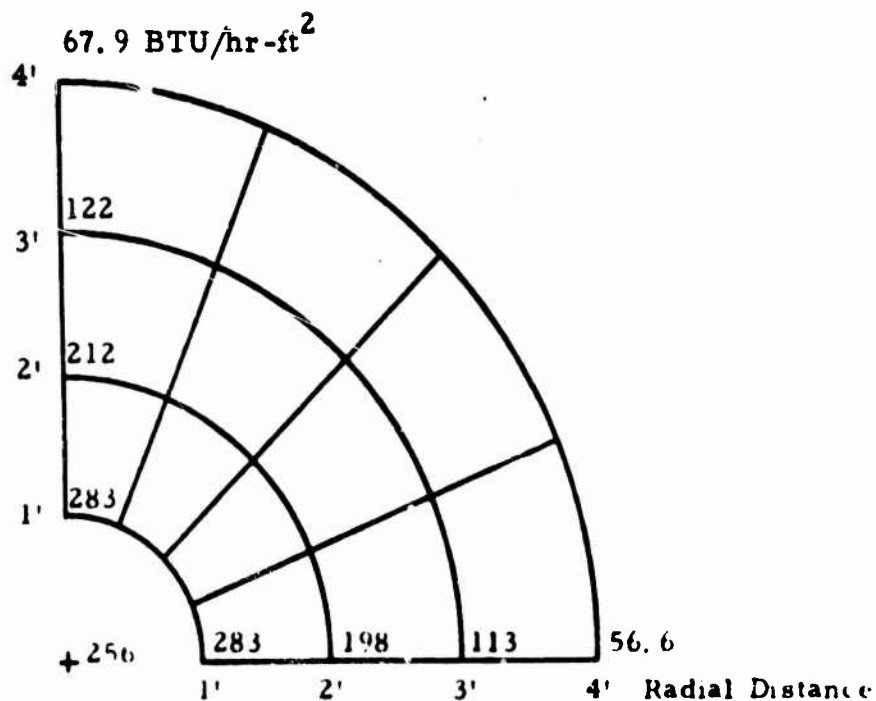
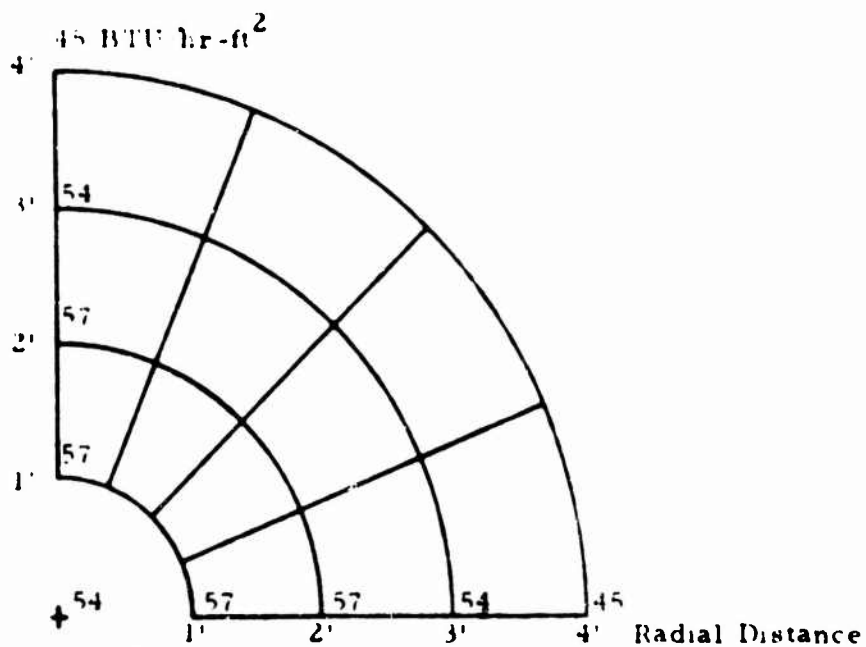


Figure 53 Reflectors for Gasoline Heater

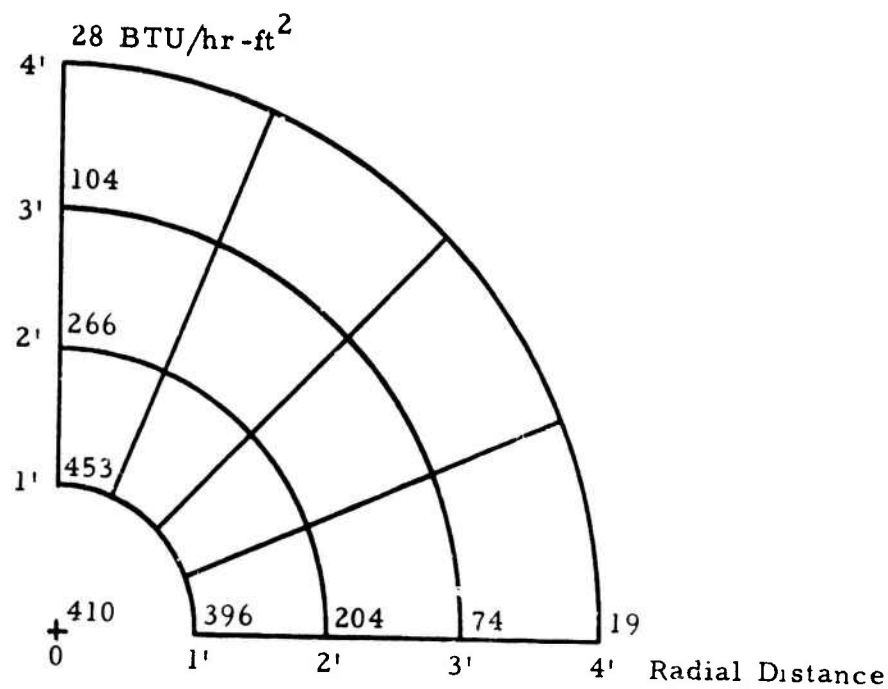


(a) Target Distance - 4 feet

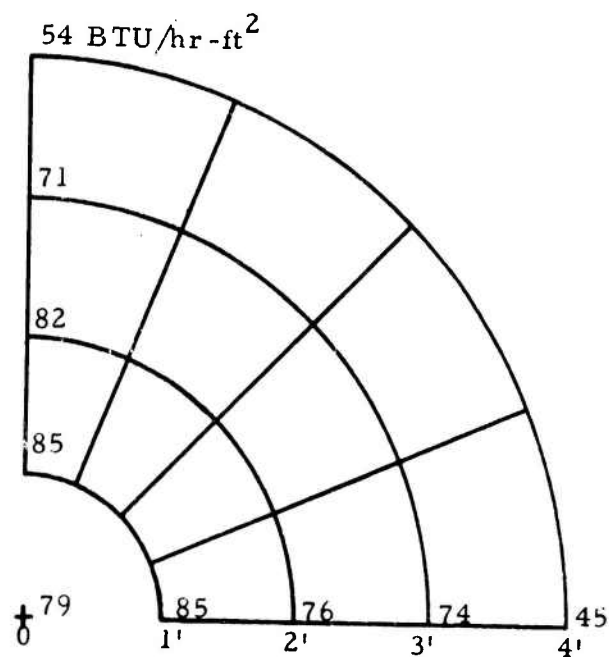


(b) Target Distance - 10 feet

Figure 54 Radiant Flux Density Distribution, BTU/hr-ft² - GFP Gasoline Heater with Small Conical Reflector



(a) Target Distance - 4 feet



(b) Target Distance - 10 feet

Figure 55 Radiant Flux Density Distribution, BTU/hr-ft² - GFP Gasoline Heater with Large Conical Reflector

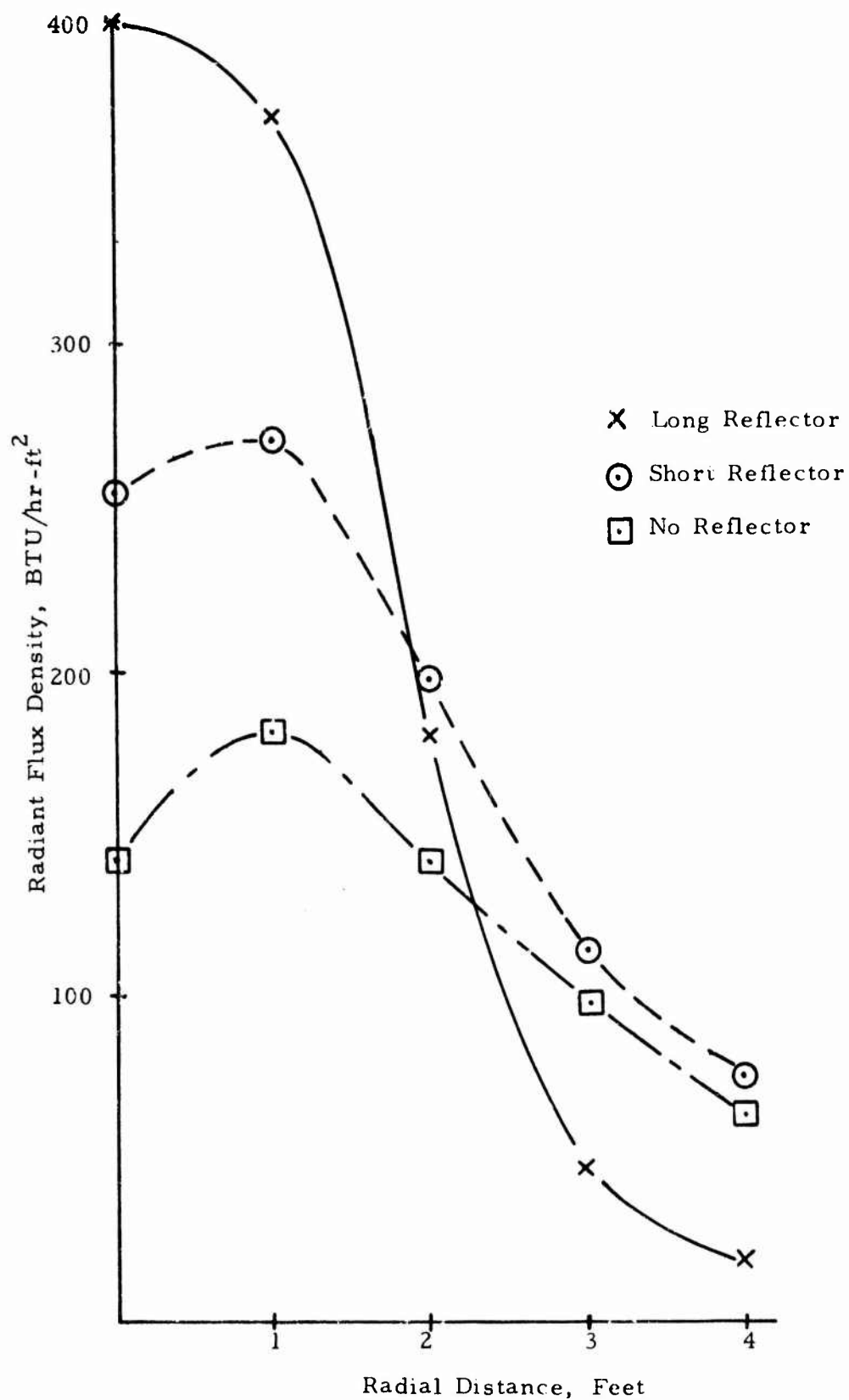


Figure 56 Variation in Flux Distribution Caused by the Addition of Reflectors to the Gasoline Heater - Target Distance, 4 feet

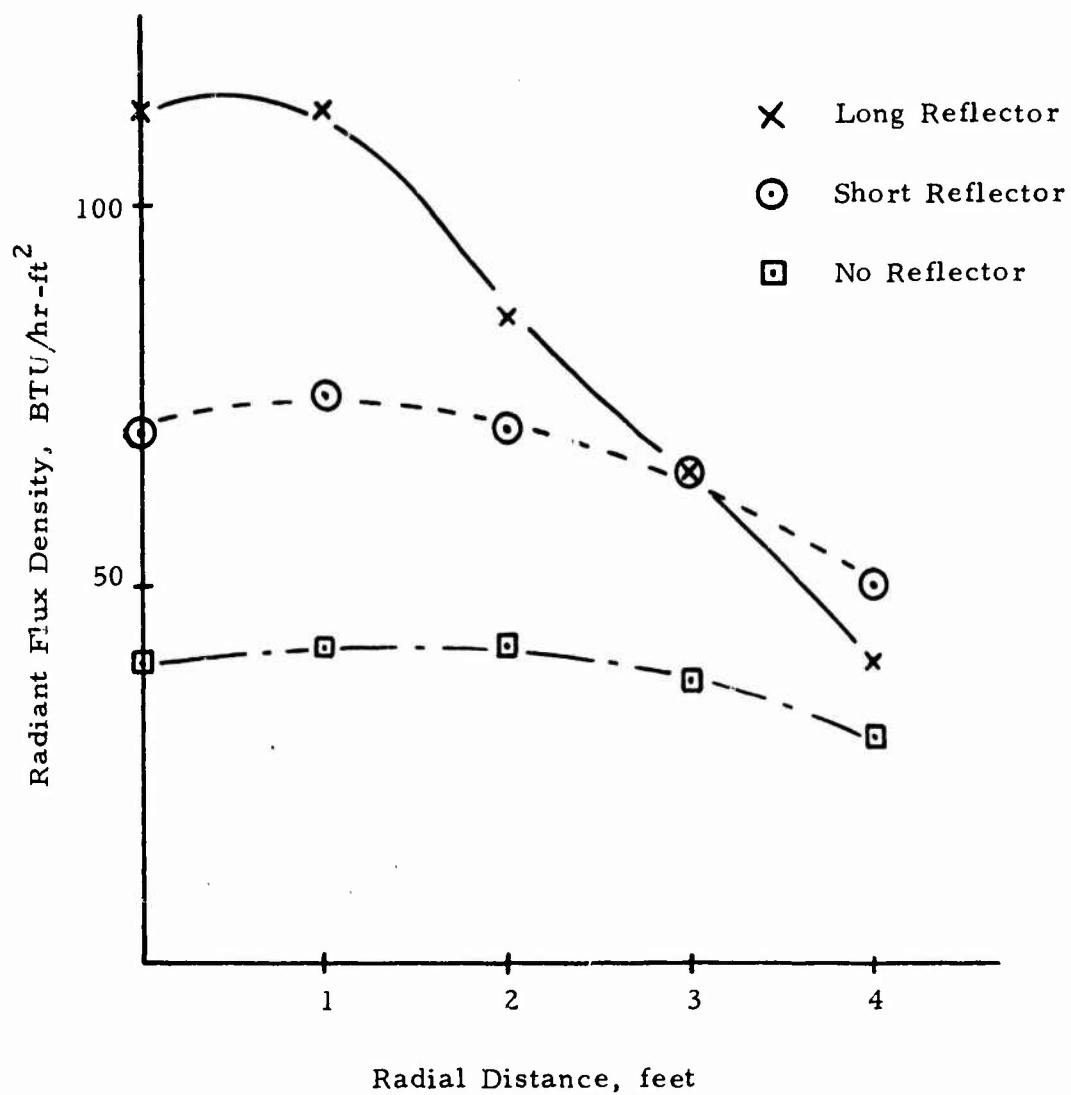
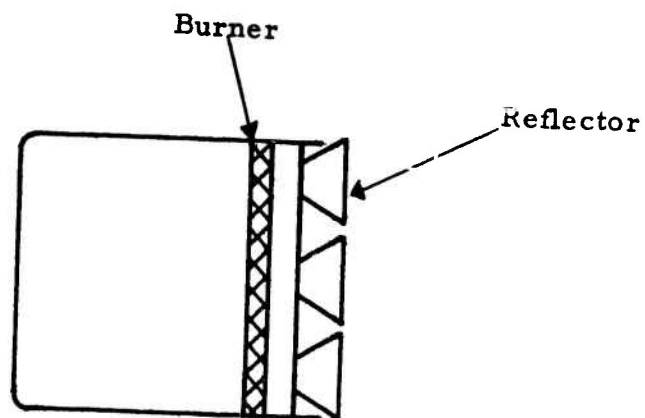


Figure 57 Variation in Flux Distribution Caused by the Addition
of Reflectors to the Gasoline Heater
Target Distance, 8 feet



(a) Schematic of Gasoline Heater with Multicellular Conical Reflector



(b) Photograph of Gasoline Heater with Multicellular
Conical Reflector

Figure 58 Multicellular Conical Reflector

source directly behind it. The solid part of the reflector plate would reflect the radiation falling on it back to the source, thus increasing the source temperature. The system would therefore result in a number of small high temperature area sources, each with its own reflector.

Tests showed that the temperature of the source did increase by approximately 200°F. However, the heater could not be operated under these conditions because of flash back. The concept does not appear to be suitable for the particular design of the gasoline heater.

6.4.1.5 Effect of Wind on Heater Performance

Tests were conducted to demonstrate the wind resistance of the gasoline heater. A fan was used to simulate the wind, with an average velocity across the face of the heater of approximately 15 miles per hour. The fan was aimed at the heater from 3 different locations: head-on, at a 45° angle to the burner face, and parallel to the burner face. When the fan was located in the first two positions, the heater would not operate. Flames shot out from the burner, and the radiant surface became dark.

When the wind was directed parallel to the face of the burner, a different phenomena occurred as shown in Figure 59. Part of the burner was dark and part was bright yellow, indicating an overfire condition. It is doubtful that the burner would operate in this mode for an extended period of time.

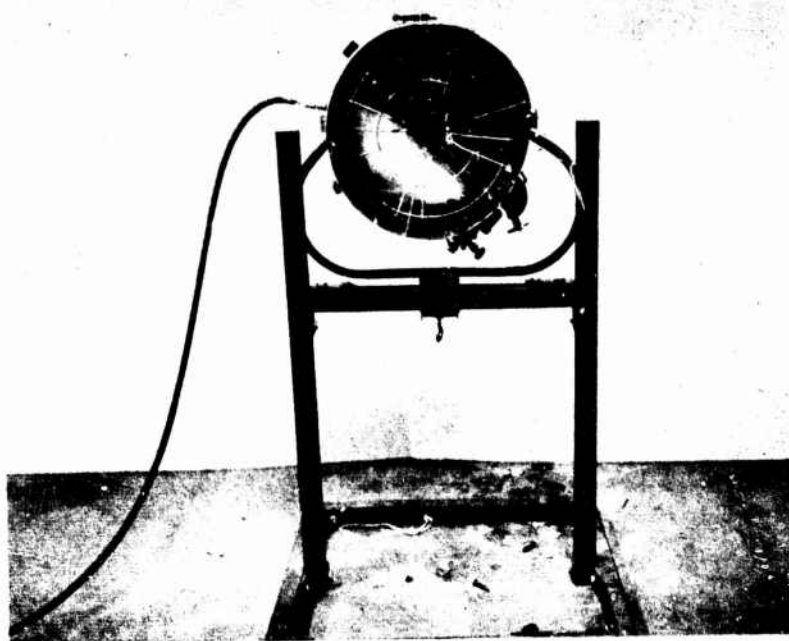


Figure 59 Gasoline Heater With Wind Blowing Parallel
to the Heater Face

The effect of wind on the heater fitted with a conical reflector was most severe. The conical reflector acts as a large collector directing the wind onto the burner surface and causing a flame-out.

A fine wire mesh screen was placed in front of the heater to act as a wind breaker. The screen did permit some operation with the wind blowing directly at the burner, but at a much reduced emitted power, so as to make it unacceptable. It appears that this basic type of burner design has extremely poor wind resistance.

6.4.2 Pyrocore Propane Heater

The Pyrocore Propane Heater Model RH-120 shown in Figure 60 was tested. It consists of a cylindrical source in a parabolic reflector. Propane under pressure is fed to the heater through an eductor where it mixes with air to form the desired fuel-air mixture as shown in Figure 37. The mixture passes through a flame holder consisting of a fibrous inconel mat and burns on its outside surface. A course screen surrounds the cylindrical flame holder and acts as a re-radiator increasing the temperature of the source and its radiant output.

Tests were made with a propane supply pressure of 40 psi giving a measured input of 12,500 BTU/hr. The emitter runs at a mean temperature of 1540°F which is substantially higher than the 1300°F possible with the GFP gasoline heaters. Based on a source area of 43 sq. inches this represents a fuel efficiency of 65.7 percent.



Figure 60 Pyrocore Propane Heater Under
Normal Operating Conditions.

6.4.2.1 Performance of Pyrocore Heater

Flux density distribution at target distances of 4, 6, 8 and 10 ft are shown in Figures 61 through 64. Due to the cylindrical geometry of the heater, the angular distribution of radiation was extremely uniform. Consequently, flux measurements were limited to those on the vertical and horizontal axes of the first quadrant. These tests show that the measured performance of this heater is comparable with that of the GFP gasoline heater without any reflectors. As seen from Figure 60, the parabolic reflector is very effective in increasing the virtual size of the radiating surface. The Pyrocore was very easy to light and adjust.

6.4.2.2 Performance of Pyrocore Heater with Modified Reflector Designs

In an attempt to improve the performance of the heater, several different reflector combinations were tested. A short conical reflector, shown in Figure 65, was added to focus the energy emitted by the end of the source that is normally lost through diffusion. However, as can be seen in Figures 66 and 67, this single reflector resulted in a decrease in the radiant flux received at a target 4' and 8' from the heater. The decrease was due to radiation hitting the back side of the cone and then diffusing. This problem was remedied by adding the outside conical reflector which, in effect, increased the length of the parabolic reflector and greatly increased the radiant flux measured at the center of the target.

These data also show that the addition of the conical reflector by itself also resulted in an increase in the flux density at the target centerline by almost a factor of 2.

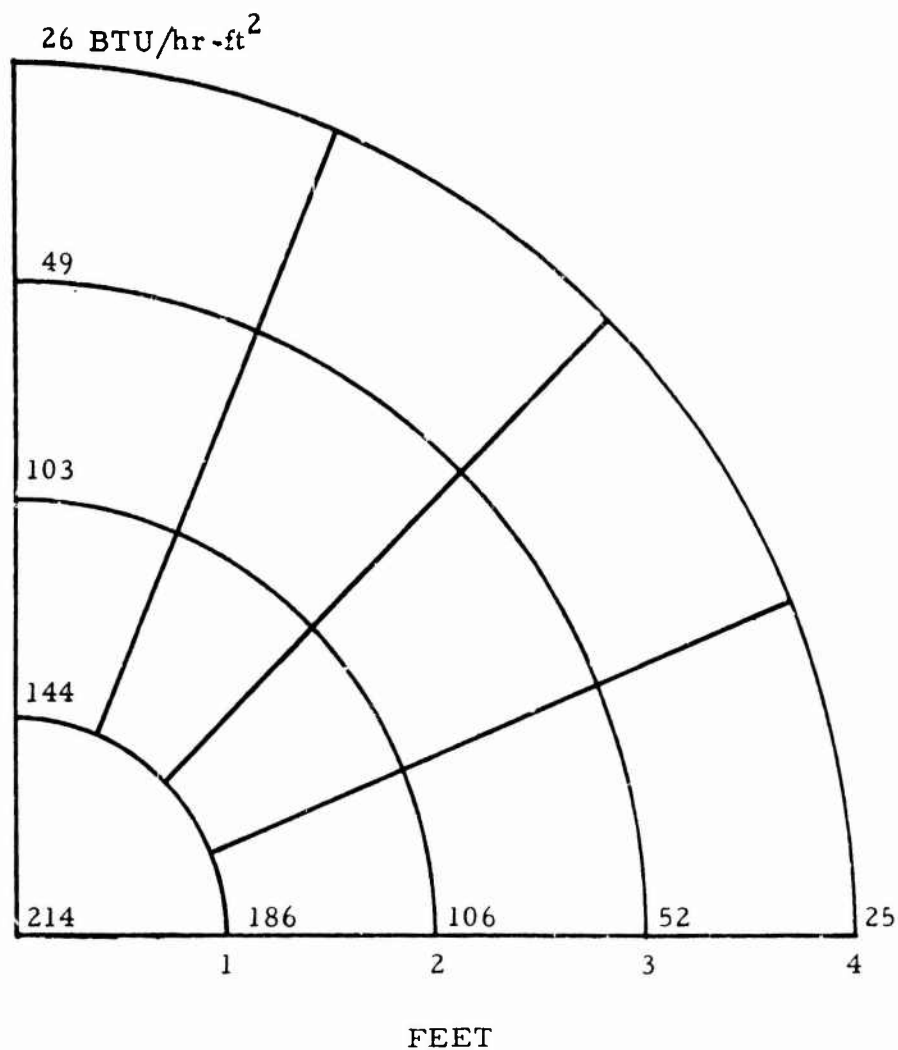


Figure 61 Radiant Flux Density Distribution, BTU/hr-ft²,

- Pyrocore Propane Heater -

Target Distance, 4 feet

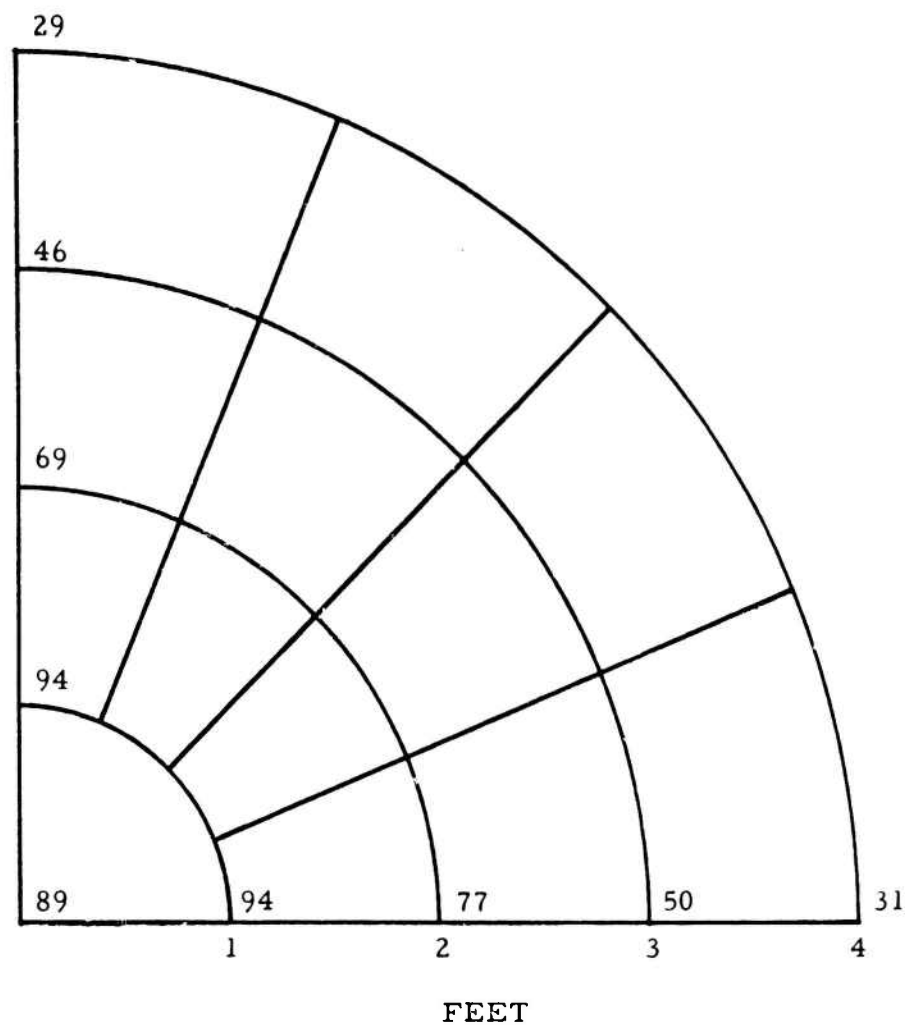


Figure 62 Radiant Flux Density Distribution, BTU/hr-ft².

- Pyrocore Propane Heater -

Target Distance, 6 feet

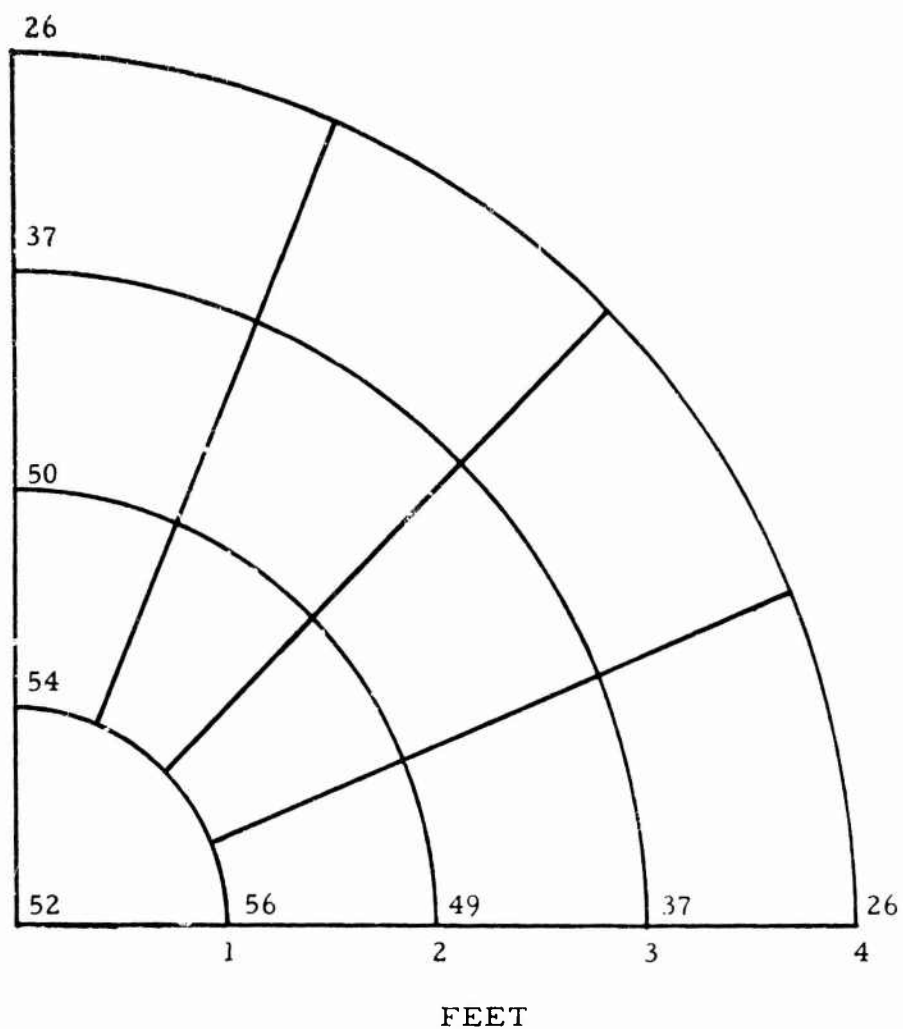


Figure 63 Radiant Flux Density Distribution, BTU/hr-ft²,
- Pyrocore Propane Heater -
Target Distance, 8 feet

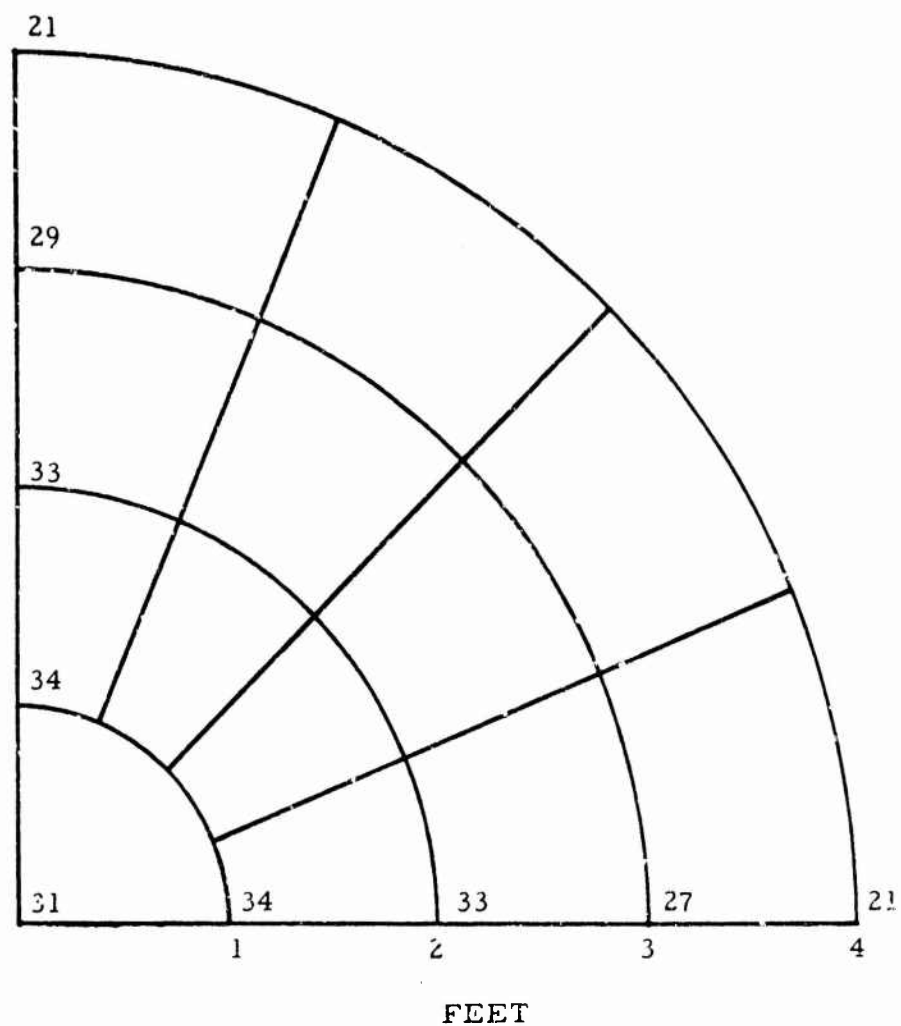


Figure 64 Radiant Flux Density Distribution, BTU/hr-ft²,

. Pyrocore Propane Heater -

Target Distance, 10 feet.

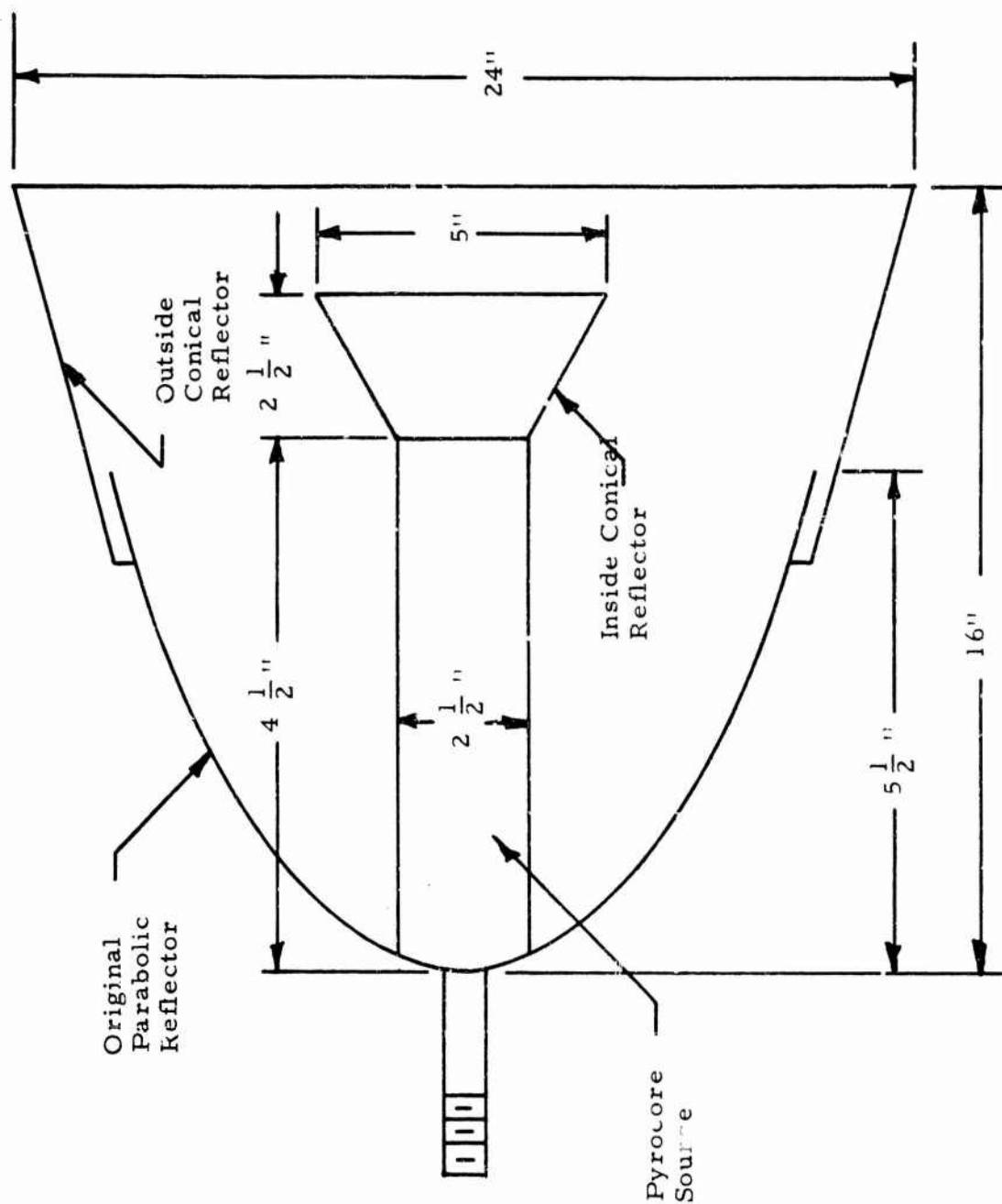


Figure 65 Reflector Combinations for Pyrocore Heater

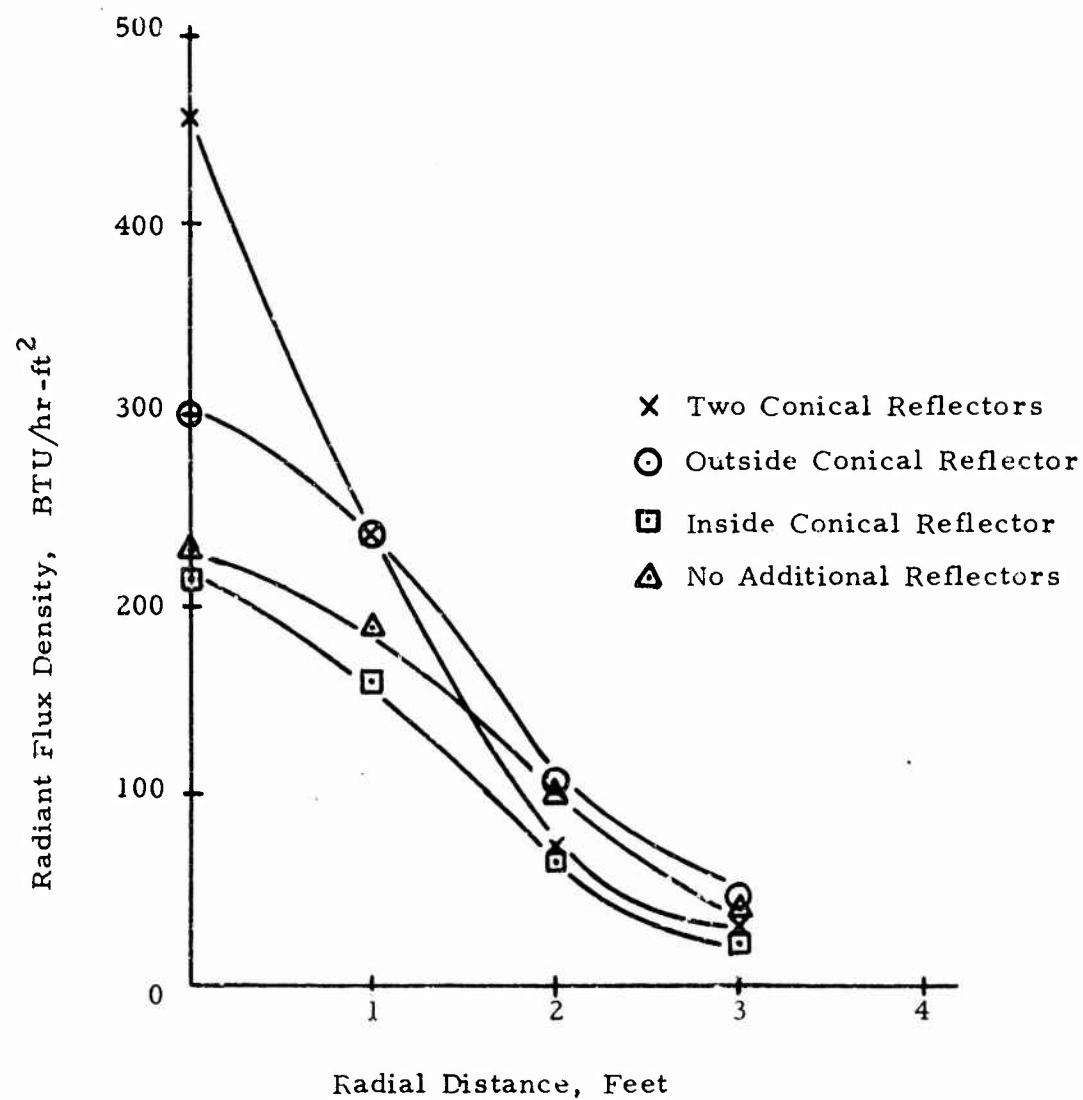


Figure 66 Comparison of the Effect of Additional Reflectors on the
Performance of the Pyrocore Propane Heaters
Target Distance, 4 feet

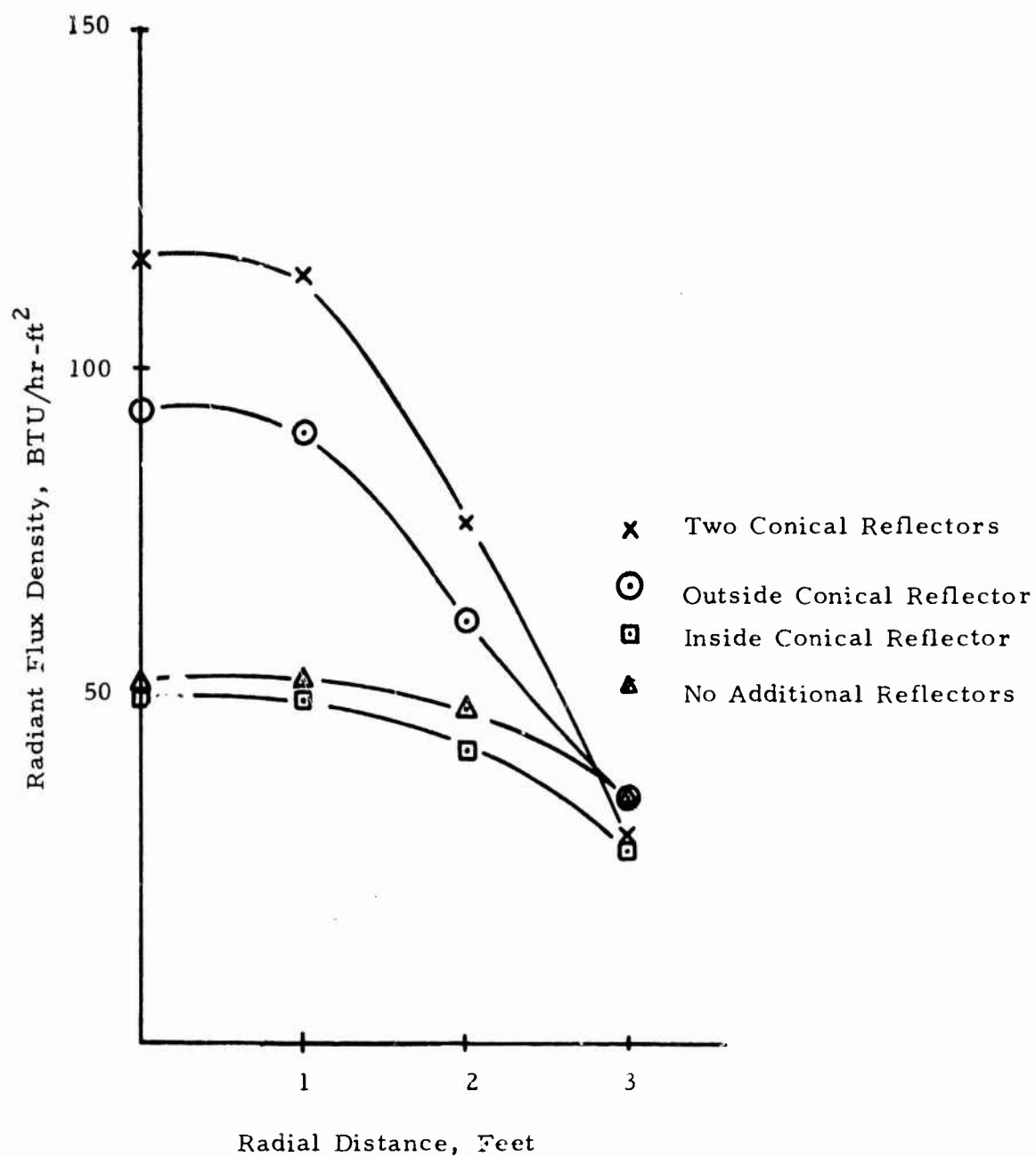


Figure 67 Comparison of the Effect of Additional Reflectors
on the Performance of the Pyrocore Propane Heaters
Target Distance, 8 feet

6.4.2.3 Effect of Wind on the Performance of the Pyrocore Heater

Possibly because of its high supply pressure, the Pyrocore was the most effective commercial heater tested in a windy environment. As in the case with the gasoline heater, the fan was placed in three locations: head-on, at a 45° angle to the burner, and blowing across the burner. For all three wind directions the heater would operate satisfactorily with, of course, a decrease in the surface temperature of the emitter and a consequent decrease in the total energy emitted. Figure 68 shows a photograph of the heater operating under a head-on wind and Figure 69 shows the black body temperature distribution of the emitter surface in a 15 mph, 45° wind. The temperature has decreased to a mean of 950°F from the original value of 1540°F.

The radiant flux distribution at 4 and 8 feet target distances is compared in Figures 70 and 71 for the heater operating with and without wind. The effect of a cross-wind is less severe than that of a head-on wind. The radiant flux density is approximately 30 percent of its value under a stationary ambient.

6.4.3 Hupp Propane Heater

The Hupp Model PJ2ALN propane heater manufactured by the Infrared Division, Hupp, Inc., Cleveland, Ohio has two rectangular burners enclosed in a parabolic reflector. The flame holders are made of cellular ceramic, like Cercor, and are each 5.25 x 7.25 inches in size. There is an inconel reverberator screen in front of the ceramic. Figure 72 shows a photograph of this heater in the fired condition.



Figure 68 Pyrocore Propane Heater with a 15 mph Wind
Blowing Directly at the Heater

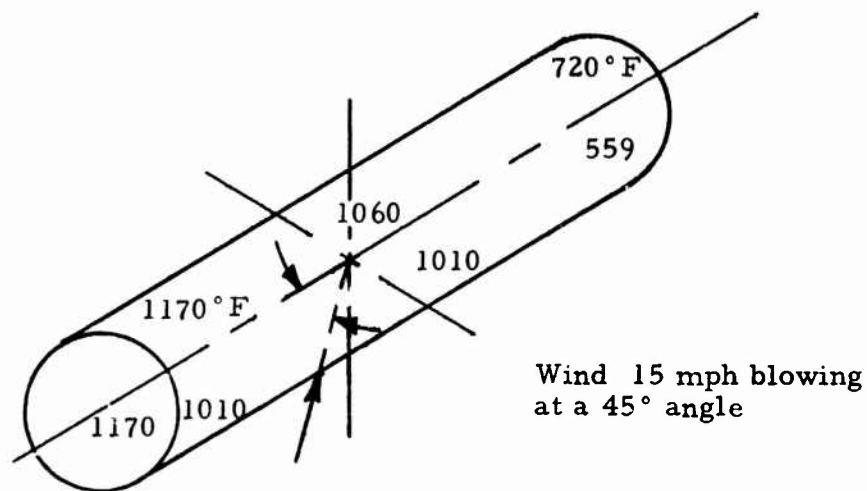


Figure 69 Temperature Map of the Emitter Surface of the
Pyrocore Heater in a Wind

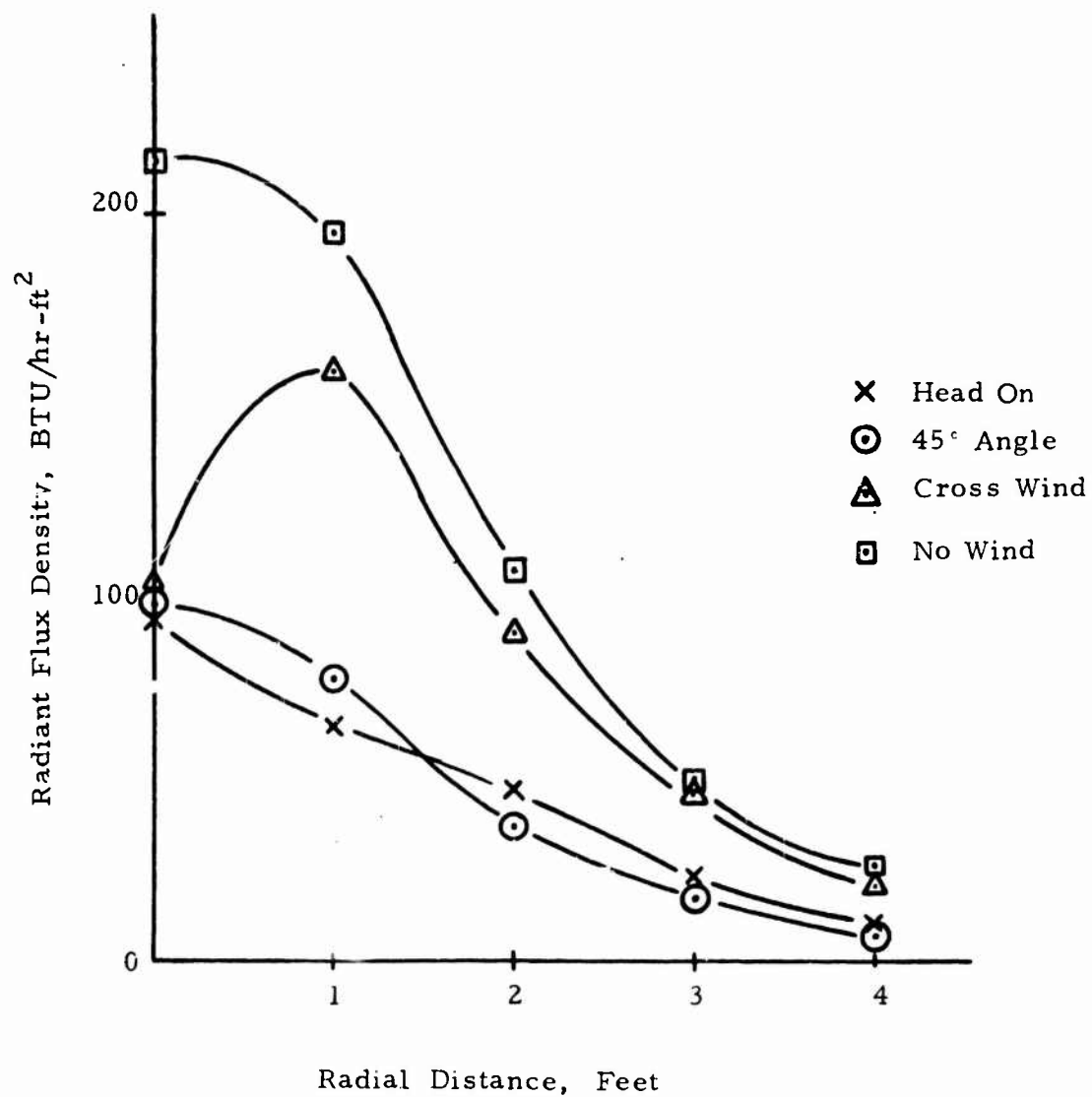


Figure 70 Comparison of the Effects of the Wind on the
Performance of the Pyrocore Heater
Target Distance, 4 feet

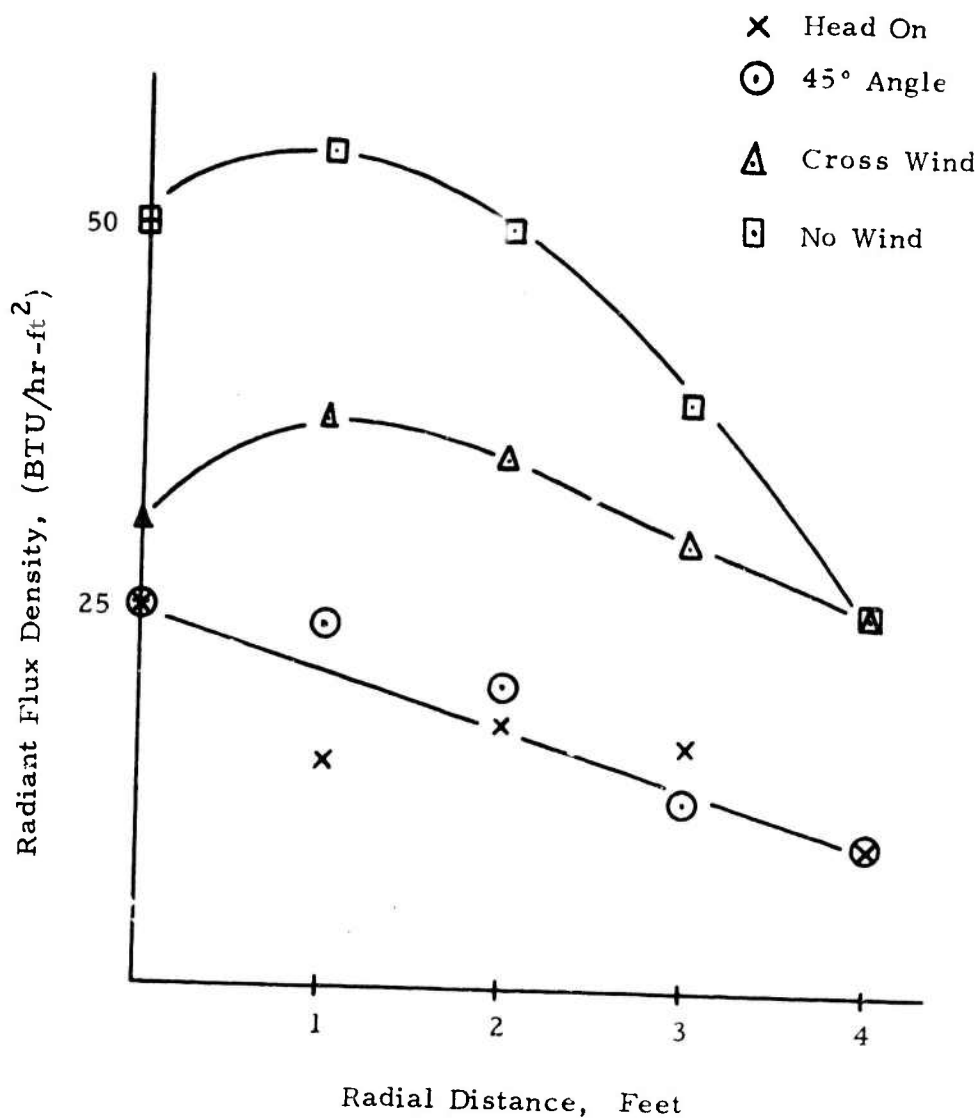


Figure 71 Comparison of the Effects of the Wind on the Performance
on the Pyrocore Heater
Target Distance, 8 feet

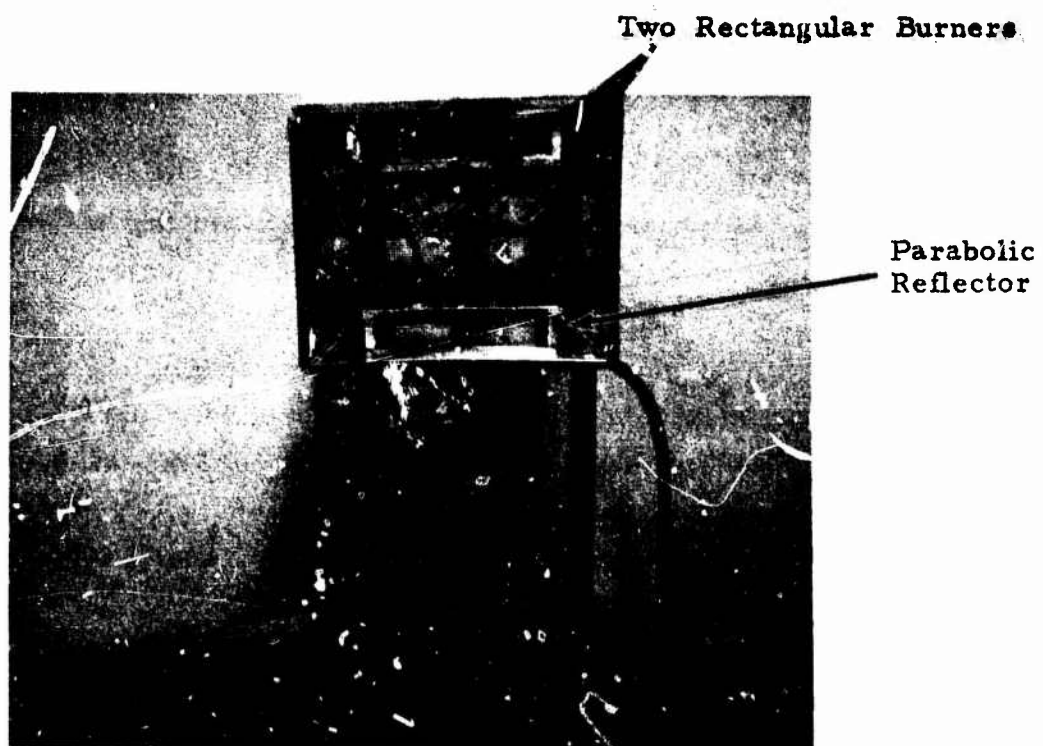


Figure 72 Hupp Propane Heater

The heater, as tested, had a measured fuel input of 20,000 BTU/hr at a gas pressure of 9.5 inches of water. This is a little lower than the rated 25,000 BTU/hr at 11 inches of water. However, the pressure regulator supplied with the heater could not be adjusted to provide the rated 11 inches of water.

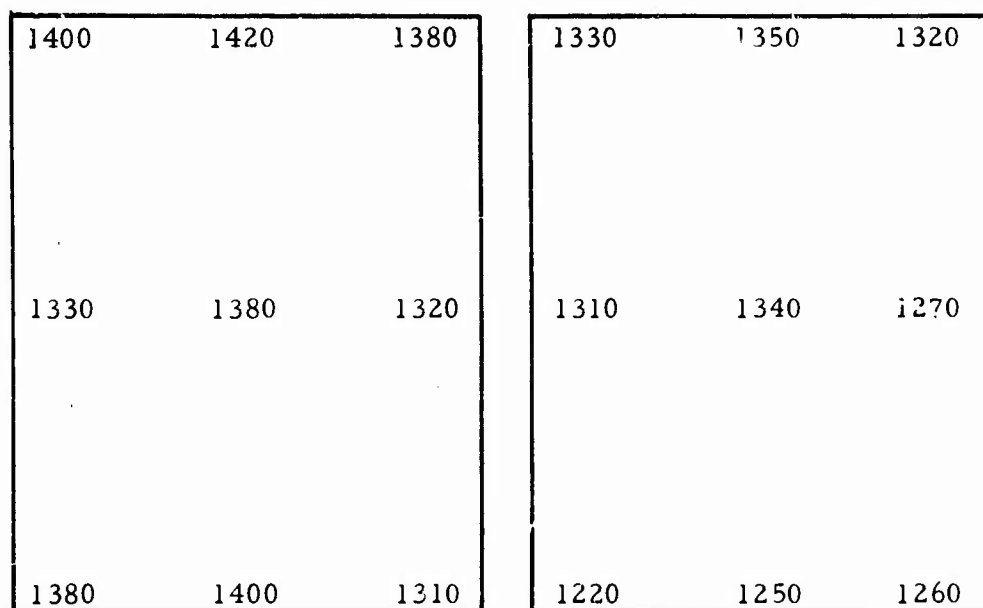
Figure 73(a) shows the black body temperature distribution of the two rectangular emitters as originally supplied with the heater. The left hand burner was about 50°F hotter than the right hand burner. When a very fine wire mesh screen (0.001" wire diameter, 0.007" spacing) was attached to the reverberator screen that is mounted about 1/2 inch off the ceramic burner face in order to study its effect as a wind breaker, the temperature of the right hand burner was raised and that of the left hand burner lowered, making the temperature distribution quite uniform, as shown in Figure 73(b).

6.4.3.1 Performance of Hupp Propane Heater

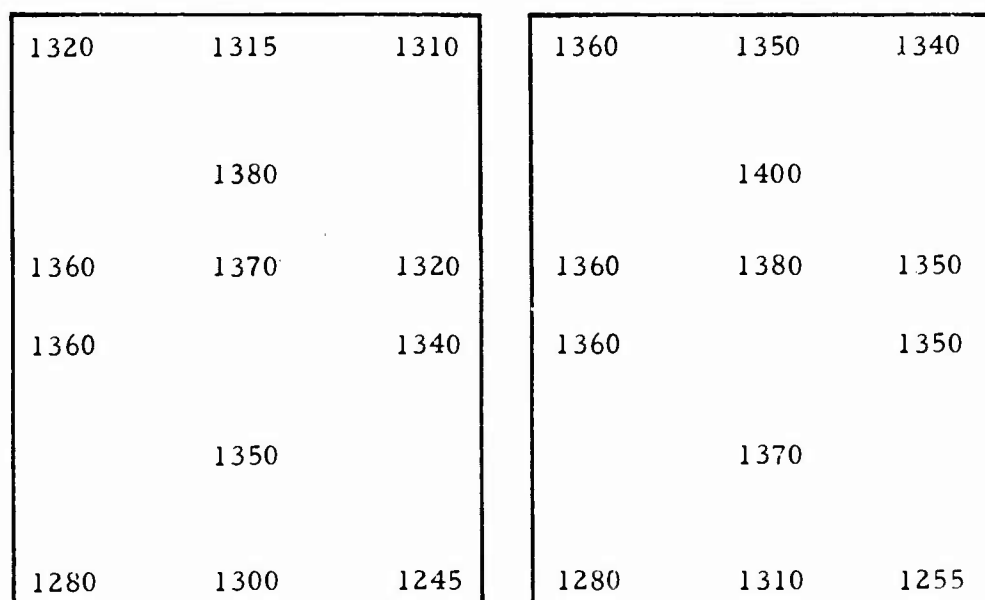
The radiant flux density distribution at target distances of 4, 6, 8 and 10 ft is shown in Figures 74 through 77. These results compare very well with the flux densities reported by Hupp. Due to the rectangular shape of the heater the flux density on the horizontal axis is higher than on the vertical axis. The radiant flux density at the target is almost twice that obtainable from the gasoline heater.

6.4.3.2 Effect of Wind

The heater would not operate with the wind blowing on it. The flame would blow out. The fine wire



(a) Without Fine Mesh Screens



(b) With Fine Mesh Screens

Figure 73 Hupp Propane Heater Temperature Map - °F

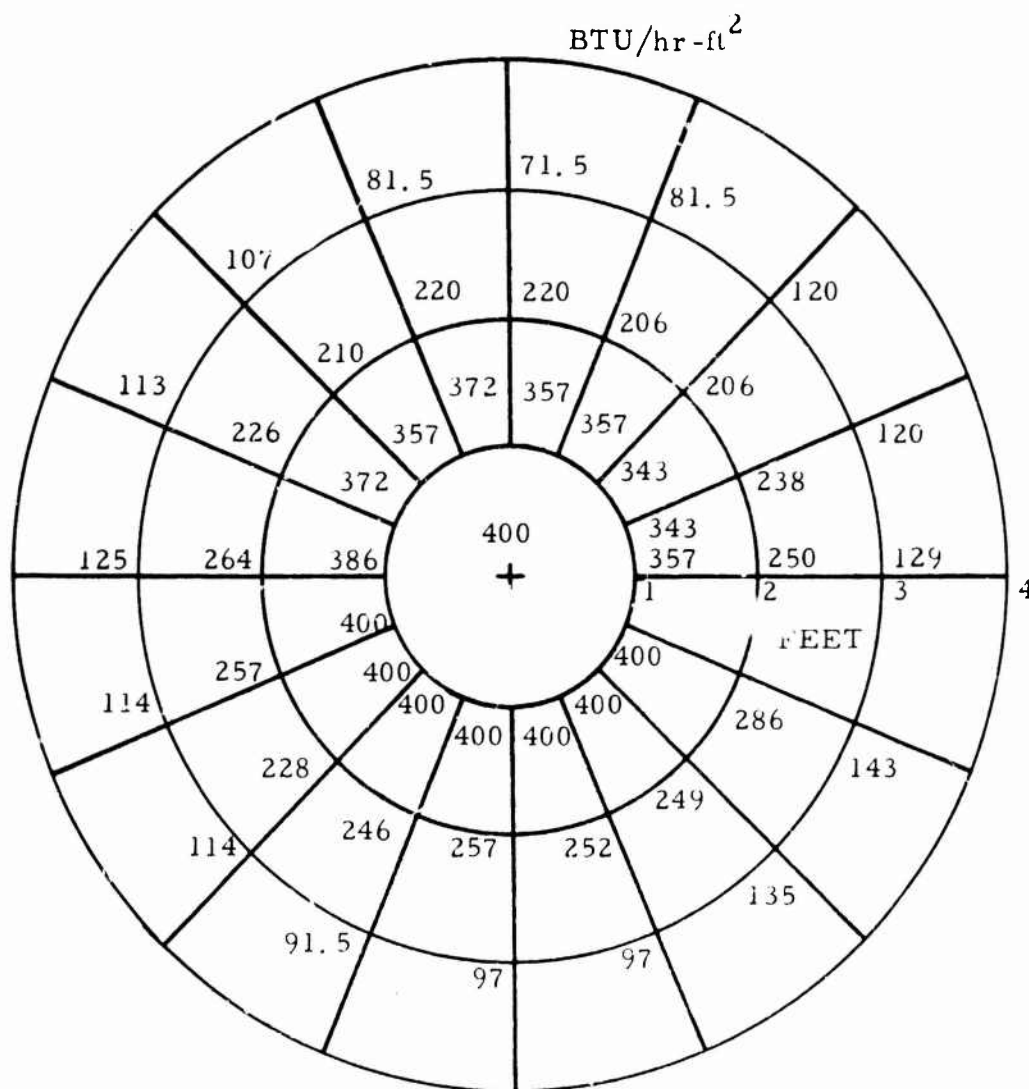


Figure 74 Radiant Flux Density Distribution, BTU/hr-ft^2 ,

- Hupp Propane Heater -

Target Distance, 4 feet

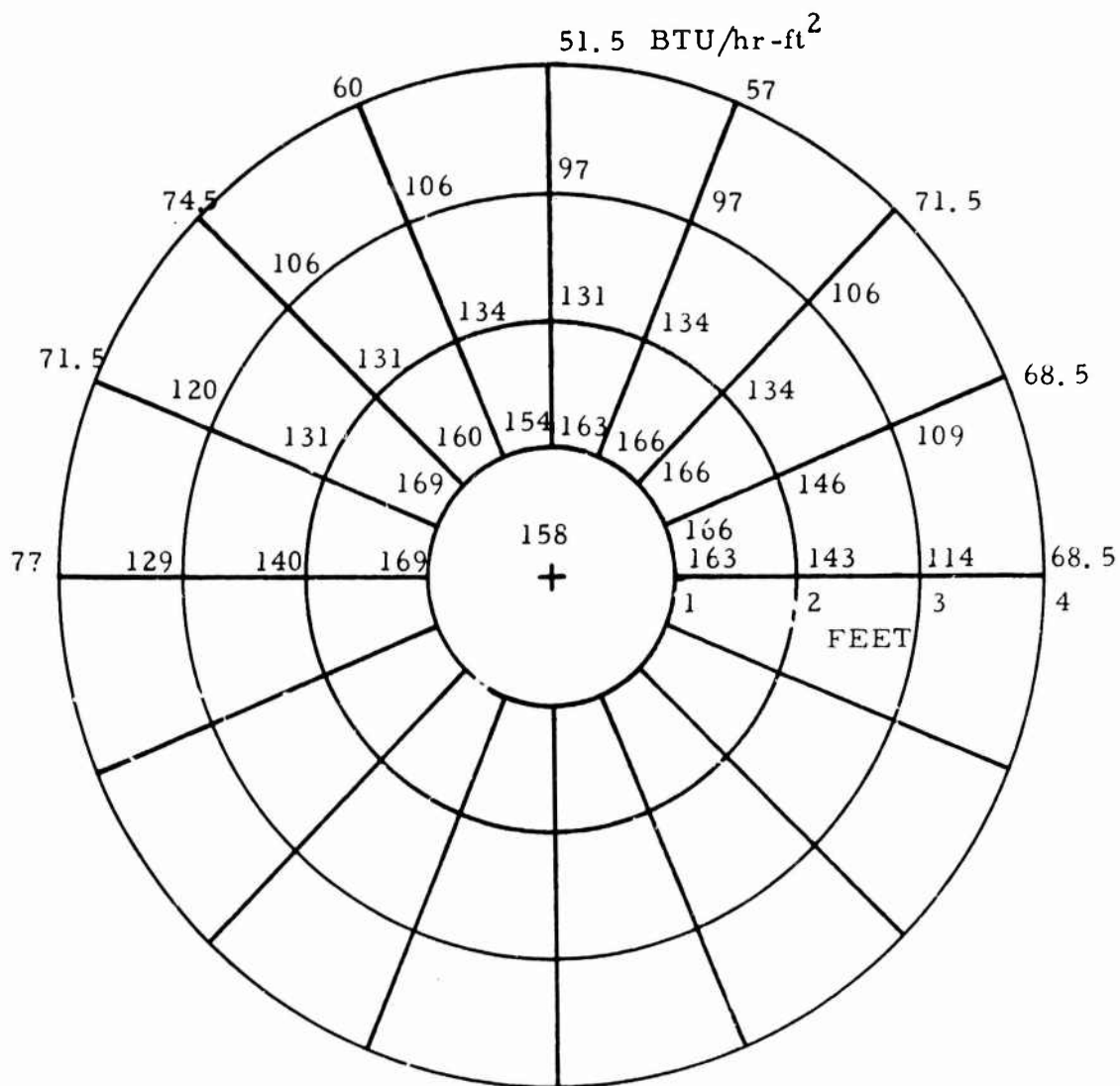


Figure 75 Radiant Flux Density Distribution, BTU/hr-ft²,

- Hupp Propane Heater -

Target Distance, 6 feet

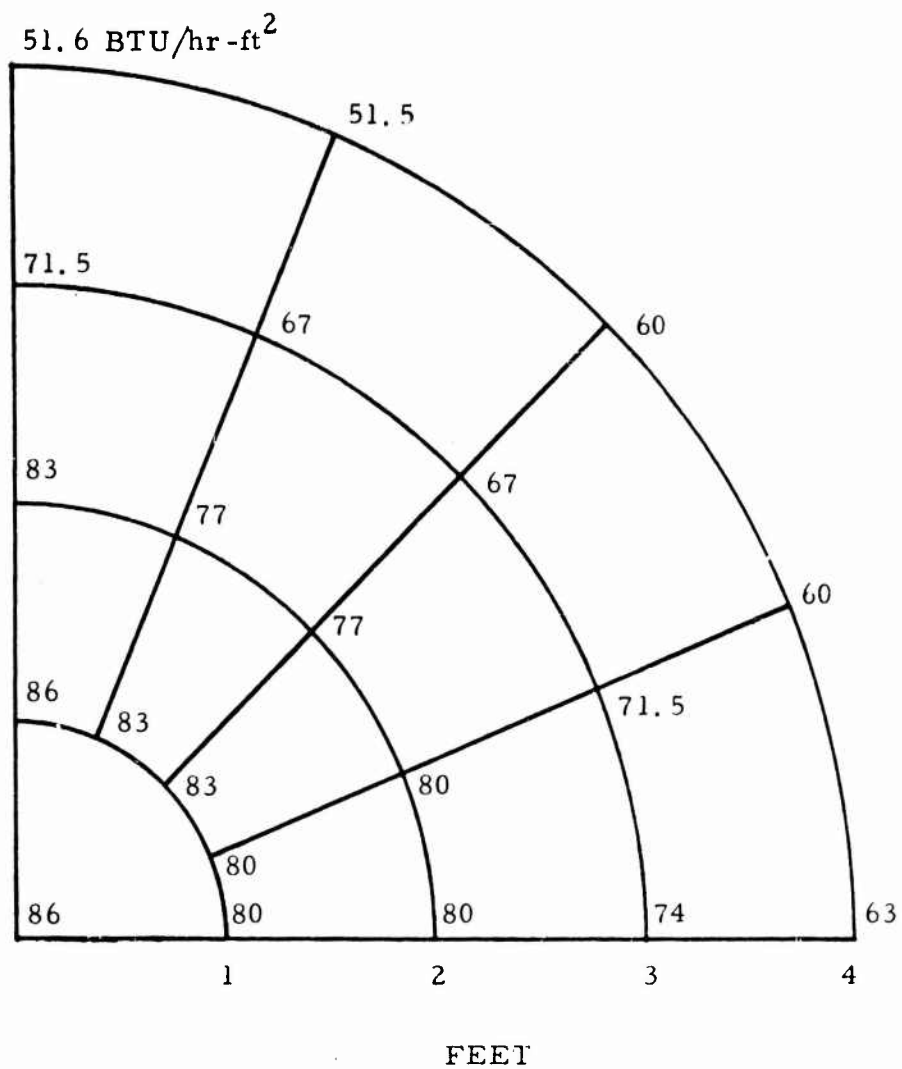


Figure 76 Radiant Flux Density Distribution, BTU/hr-ft²,

- Hupp Propane Heater -

Target Distance, 8 feet

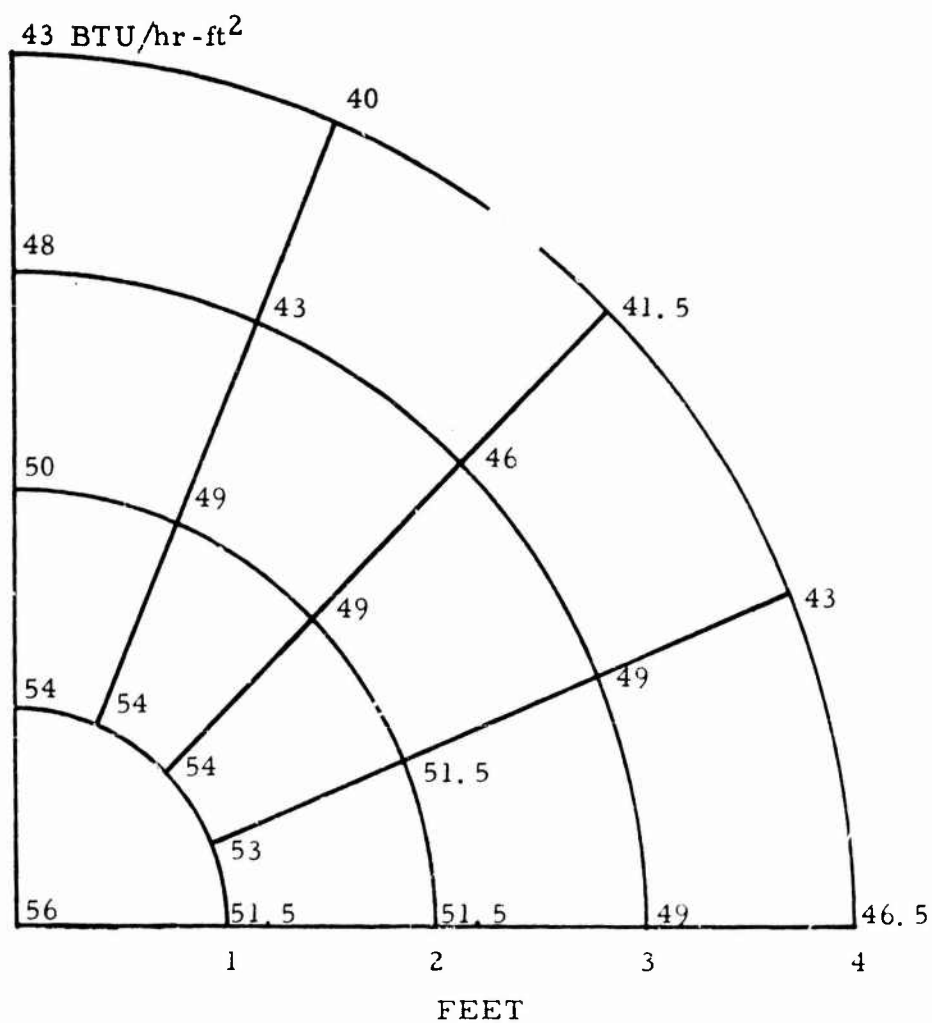


Figure 77 Radiant Flux Density Distribution, BTU/hr-ft².

- Hupp Propane Heater -

Target Distance, 10 feet

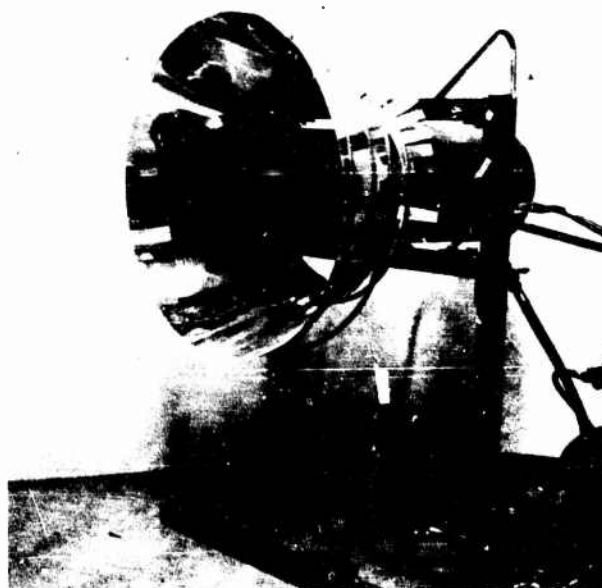
mesh screen was not effective as a wind breaker. It also caused a reduction in the total emitted flux under a stationary ambient.

6.4.4 Hupp Hot-Tot Heater

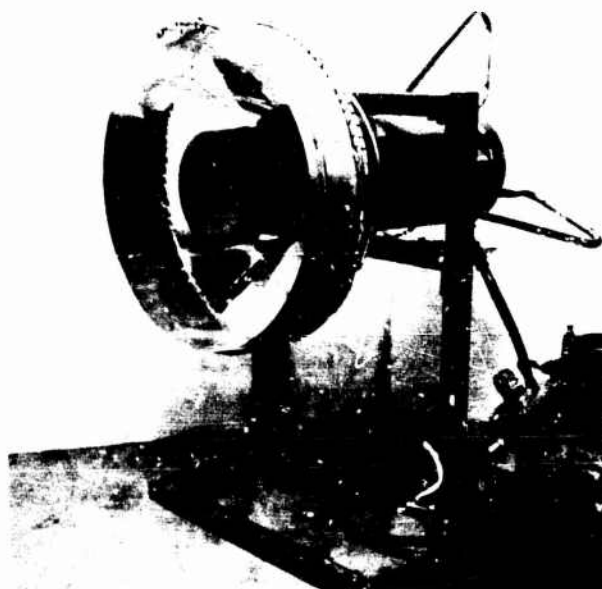
The Hupp Hot-Tot heater is a large high capacity personnel heater designed for indoor use. It does not have a reflector. It is rated at a fuel input of 86,000 BTU/hr which is about 4 times larger than any other heater tested. The Hot-Tot has a cylindrical source with the same general shape as the Pyrocore heater and operates at approximately the same surface temperature, 1500°F and same emitter intensity. The surface area of the Hot-Tot burner is approximately 7 times that of the Pyrocore. Since it does not come with a reflector, suitable reflectors were designed. The heater was operated horizontally as opposed to its normal upright position.

6.4.4.1 Performance of Hot-Tot Heater with Reflector

Two different reflector geometries were tried. The first series of tests were run using the long conical reflector of Figure 52. A second series of tests was conducted with a two-staged conical reflector designed to approximate a parabolic reflector. The Hot-Tot heater with these two reflectors is shown in Figure 78. Since the heater performance with both these reflectors was essentially the same, only that with the long conical reflector is presented in Figures 79 through 82. The heater was operating at an average emitter black body temperature of 1500°F.

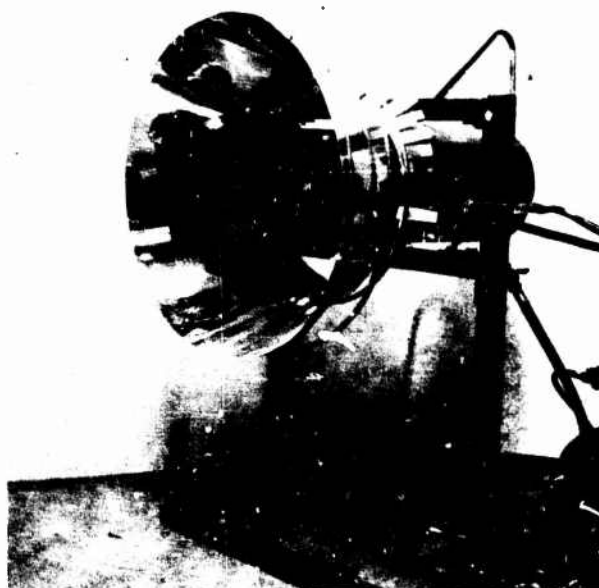


(a) Long Conical Reflector

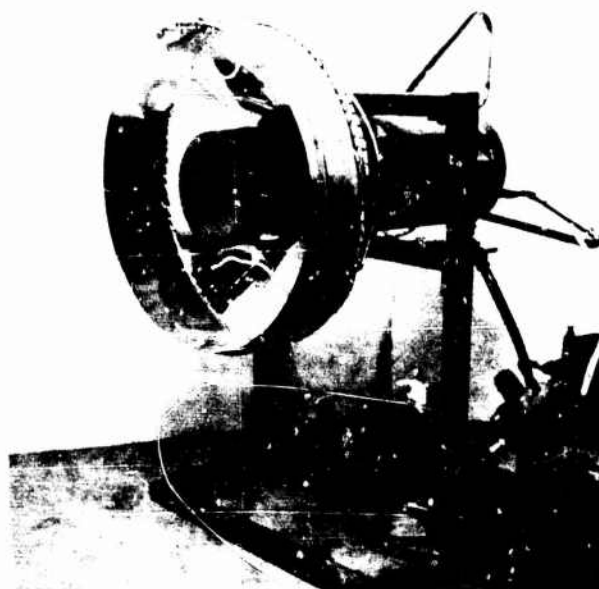


(b) Two-Staged Conical Reflector

Figure 78 Hot-Tot Heater with Conical Reflectors



(a) Long Conical Reflector



(b) Two-Staged Conical Reflector

Figure 78 Hot-Tot Heater with Conical Reflectors

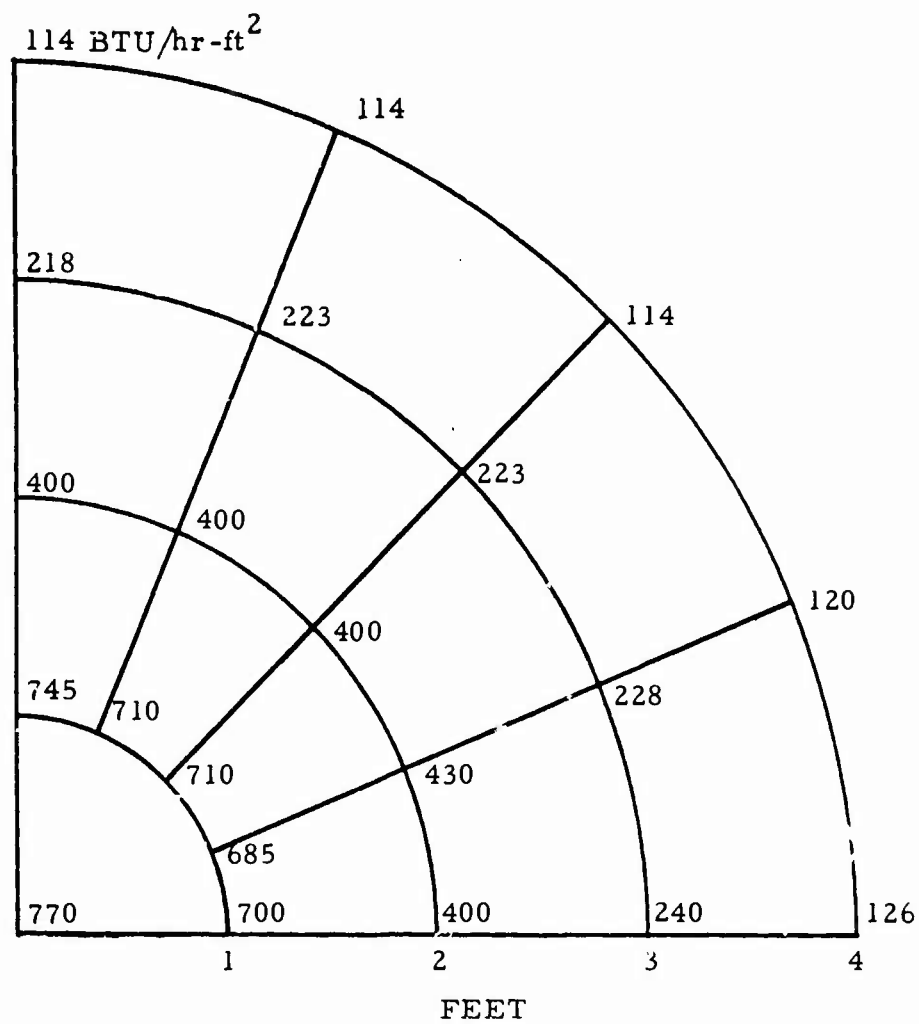


Figure 79 Radiant Flux Density Distribution, BTU/hr-ft²,
- Hupp Hot-Tot Heater with Long Reflector -
Target Distance, 4 feet

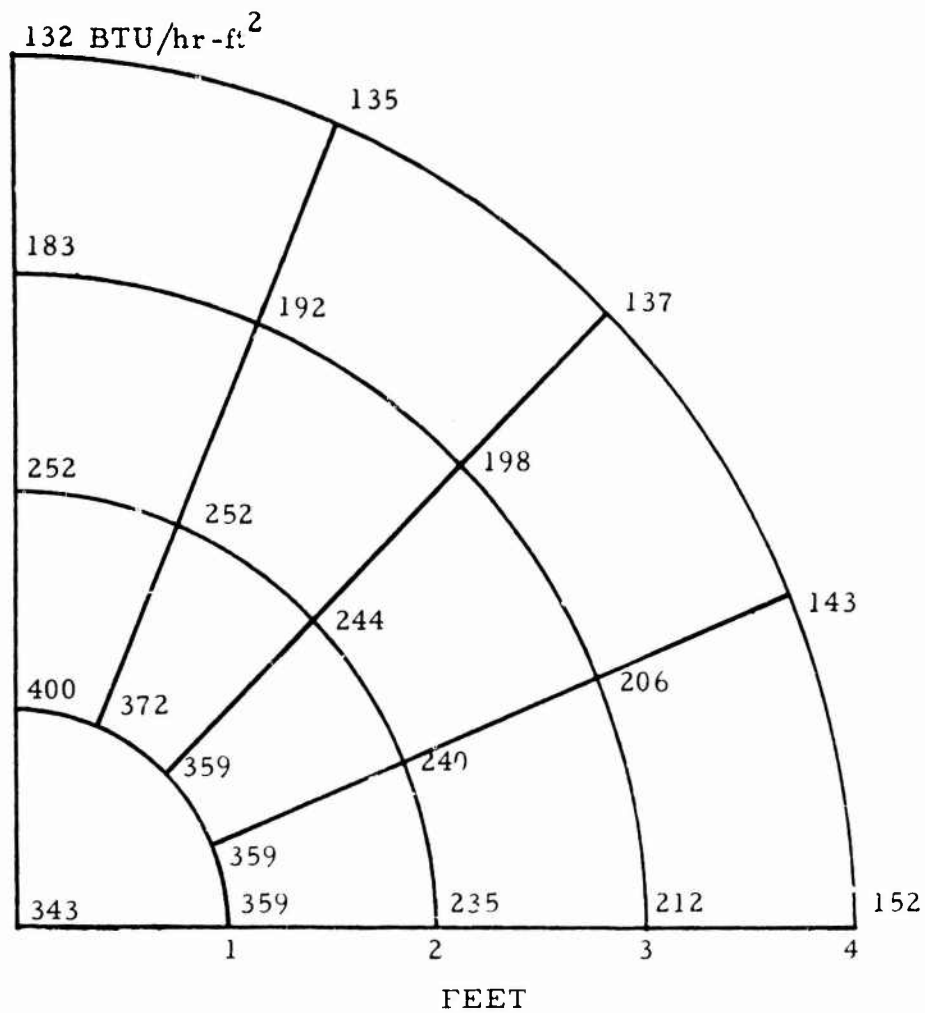


Figure 80 Radiant Flux Density Distribution, BTU/hr-ft²

- Hupp Hot-Tot Heater with Long Reflector -

Target Distance, 6 feet

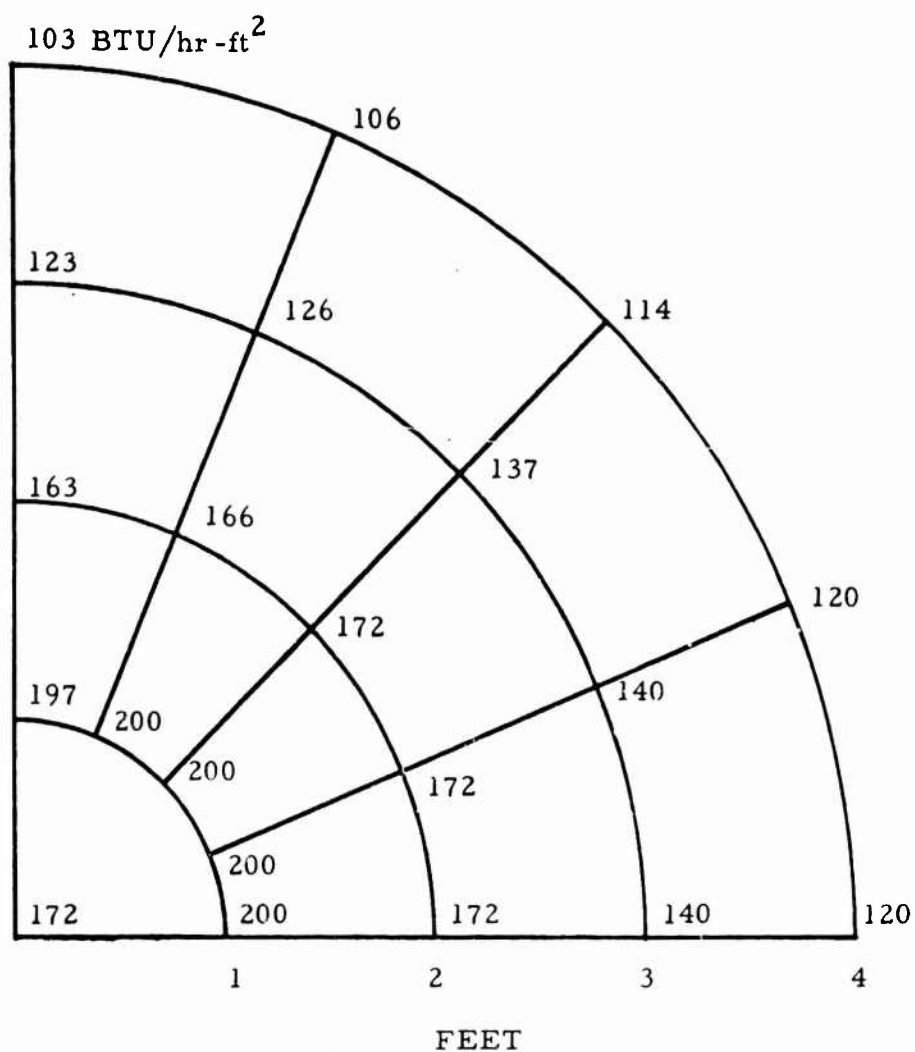


Figure 81 Radiant Flux Density Distribution, BTU/hr-ft²,

- Hupp Hot-Tot Heater with Long Reflector -

Target Distance, 8 feet

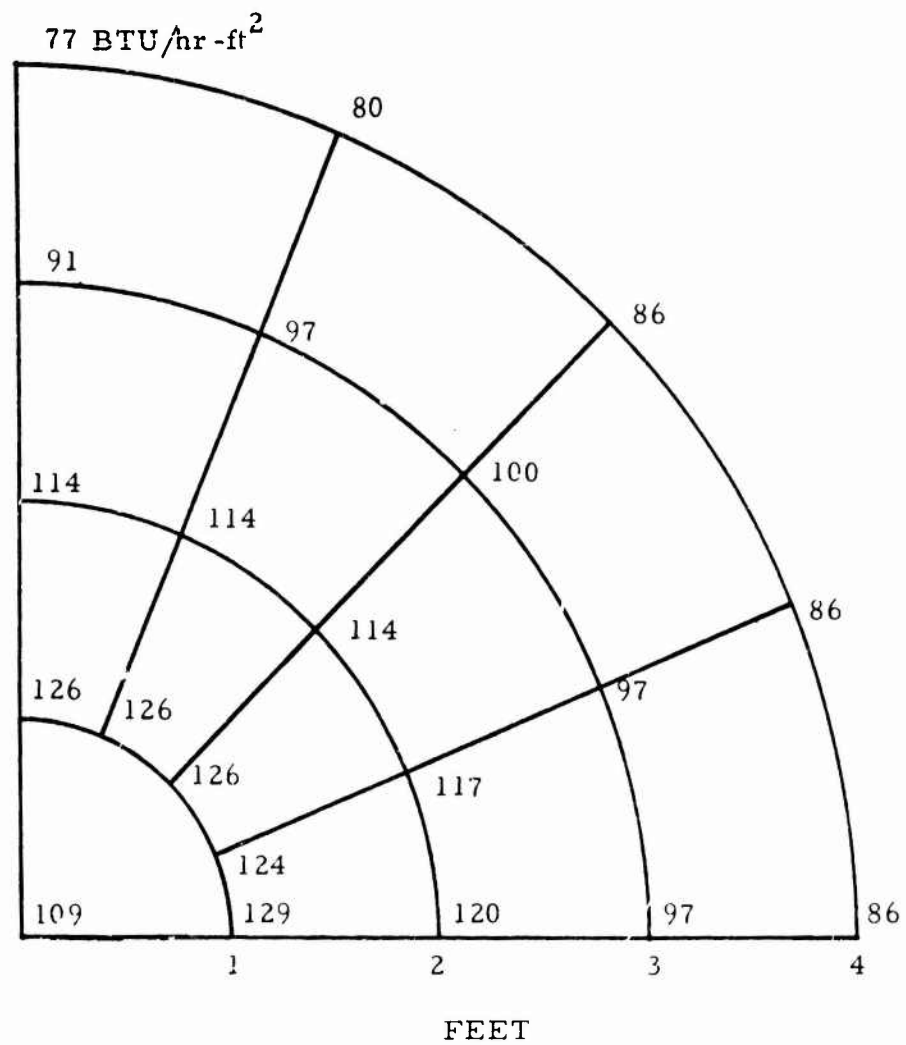


Figure 82 Radiant Flux Density Distribution, BTU/hr-ft²,

- Hupp Hot-Tot Heater with Long Reflector -

Target Distance, 10 feet

By comparing these results with those obtained with the Pyrocore heater, as shown in Figures 61 through 64, it is clear that this system is not as effective. The flux density at the target did not increase in proportion to the source area, that is by a factor of 7. It appears that a longer reflector would be required for better focusing. This would result in an increase in the overall volume of the heater.

6.4.4.2 Effect of Wind

Like the Pyrocore, this heater remained operational with a 15-mph wind, though with a reduced radiant output. Measurements show that with a 15-mph cross wind, the temperature of the part of the emitter facing the wind was reduced to 770°F while the other part was able to maintain its design temperature of 1500°F. Figure 83 shows the flux density distribution for the various target distances, with the heater operating in a 15-mph cross wind. The flux density is reduced by approximately 50 percent from that obtained in still air.

6.4.5 Foster-Miller Radiant Heater (FMA)

A special Foster-Miller (FMA) radiant heater was designed and developed for this program. It consists of a hemispherical source with a paraboloidal reflector. The source is designed to have extremely good wind resistance. Though such a design development was not specified within the scope of this program it was undertaken for the following reasons:

- (1) The results of theoretical analysis summarized in Section 4 and described in detail in Appendices A

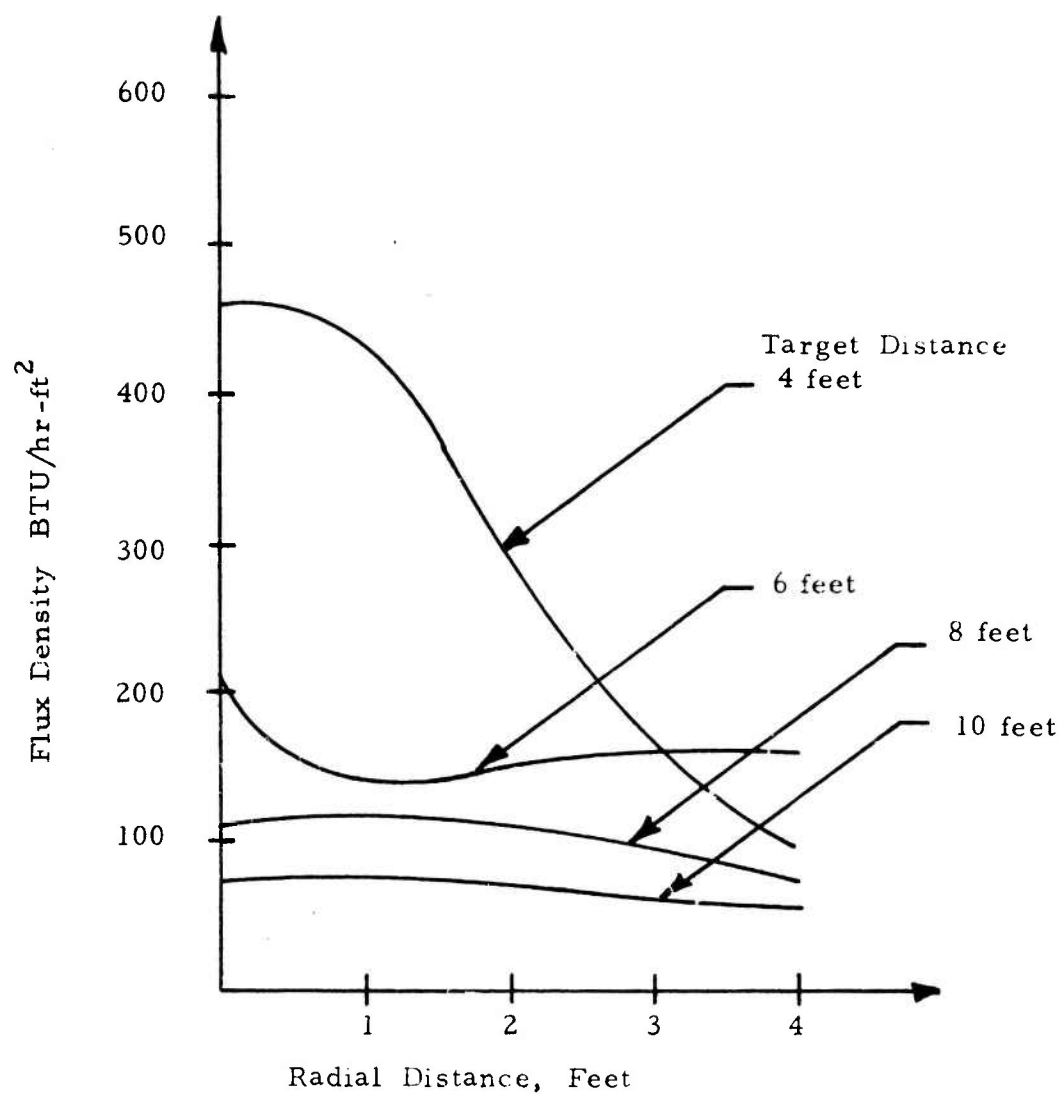


Figure 83 Performance of Hot-Tot Heater with Conical
Reflector in a 15 mph Cross-Wind

and B demonstrated that an optimum design of a hemispherical source-paraboloidal reflector radiant heater could provide a 50 percent increase in radiant flux density at the target, over that possible with an optimum design of a circular area source-conical reflector radiant heater.

(2) No commercially available radiant heaters could be found using a hemispherical source.

(3) All the commercially available heaters tested showed extremely poor wind resistance.

6.4.5.1 Description of the Foster-Miller Radiant Heater

The Foster-Miller (FMA) radiant heater is a propane fired heater which offers the potential of being modified for use on liquid gasoline. It is shown schematically in Figure 84 and consists basically of three parts, namely,

- (1) A high intensity Turbo-Torch burner.
- (2) A source which consists of a radiant emitter and a convective heat exchanger which is contiguous but not the same as the radiant surface.
- (3) A paraboloidal reflector with an internal reflector cone.

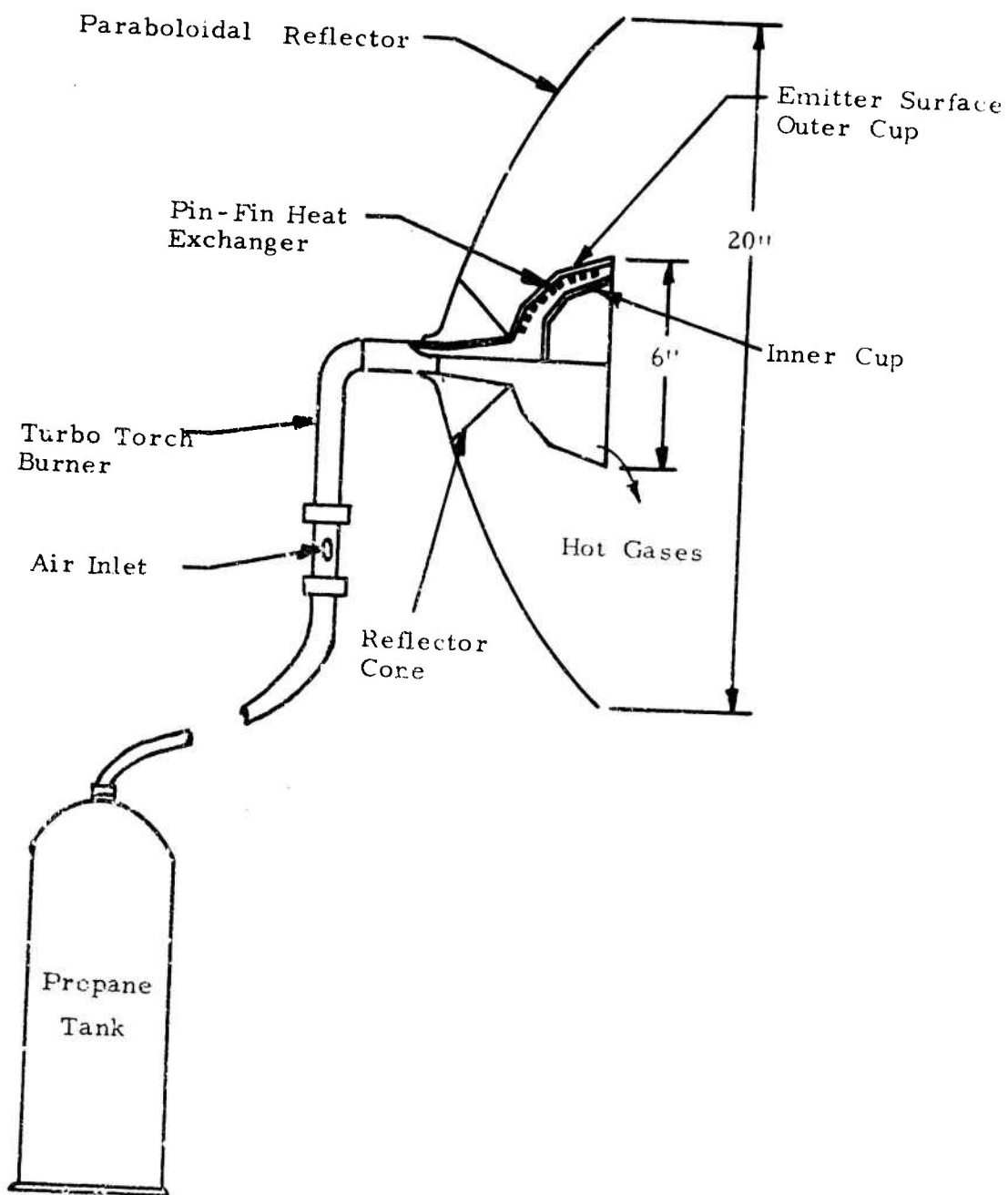


Figure 84 Schematic of Foster-Miller Radiant Heater

Figure 85 shows a photograph of the source and the burner.

The source is placed at the focal point of the paraboloidal reflector. The primary emitter surface of the source is the outer cup which is configured so as to radiate a large percentage of its total radiant output to the reflector which focuses the radiation on the target area. This particular configuration minimizes the diffusion loss due to direct radiation from the source. The inner cup radiates directly into space and its radiation is not controlled by the reflector. Consequently, it is desirable to design the source heat exchanger configuration to minimize the temperature of the inner cup and maximize the temperature and hence the heat radiated by the outer cup.

The prototype design as developed during this program is not to be considered to be optimum for any fixed criteria, but rather, it is an attempt to illustrate a compact burner-heat-exchanger that is suitable for a roughly hemispherical source-paraboloidal reflector system. Details of construction of the FMA radiant heater are presented in the following sections; the theoretical basis for the design is developed in Appendix C.

(a) Burner Design

The burner chosen is a propane burning "Turbo-Torch", manufactured by the Wingersheek Corp., Lynn, Mass. This burner is compact for its nominal heat rate of 30,000 BTU, and has a relatively high pressure jet pump in order to obtain the highest flame velocity for the maximum local surface

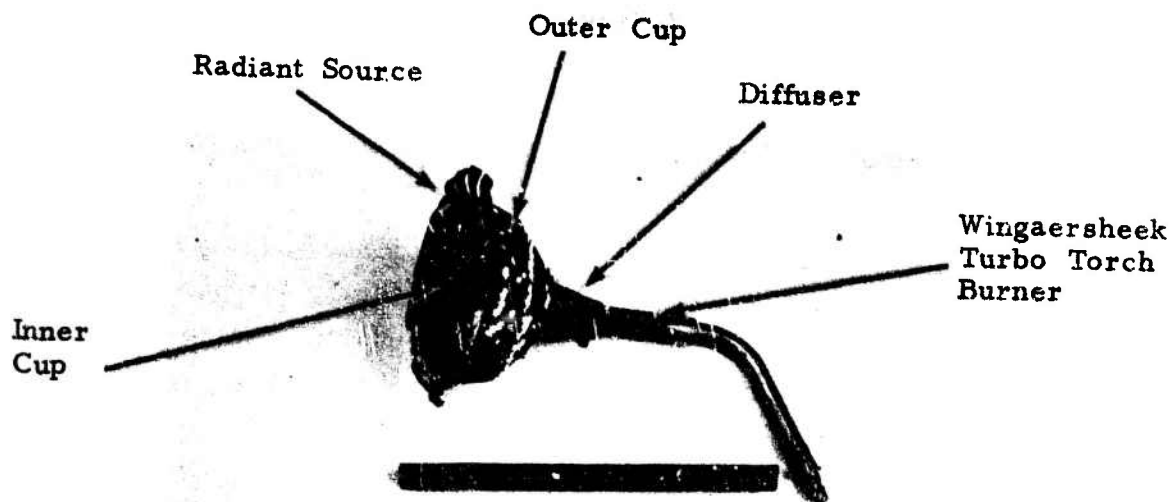


Figure 35 Photograph of the Foster-Miller Radiant Hemispherical Source and Wingaersheek Turbo Torch Burner

heating rate. This velocity is diffused in our design in order to recover the static pressure required to force the gases through the heat exchange matrix. Figure 86 shows a schematic of the Wingaersheek Turbo-Torch burner.

A burner designed specially for this application would be larger and would use a jet pump "trimmed" to develop maximum static pressure at the burner exit. This would minimize the inefficiency resulting from acceleration and diffusion of the burner flame.

(b) Radiant Source

The radiant source consists of an annular hemispherical cup with a pin-finned heat exchanger as shown schematically in Figure 87. The hot gases pass through the annulus at a high velocity, approximately 100 ft/sec, heating the pins by convection. The pins conduct the heat to the outer surface of the emitter for radiation out to the environment. In the present design both inner and outer cups act as emitters. The internal flow paths in the heat exchanger can be varied to vary the spatial temperature distribution of the emitter. In contrast to all the commercial gas-fired radiant burners tested, where the exhaust gas temperature is higher than the emitter temperature, with this particular heat exchanger configuration the exhaust gas temperature can be lower than the average emitter temperature, thus resulting in an increased fuel efficiency.

The heat exchanger design is based on the maximum permissible gas velocity in order to provide

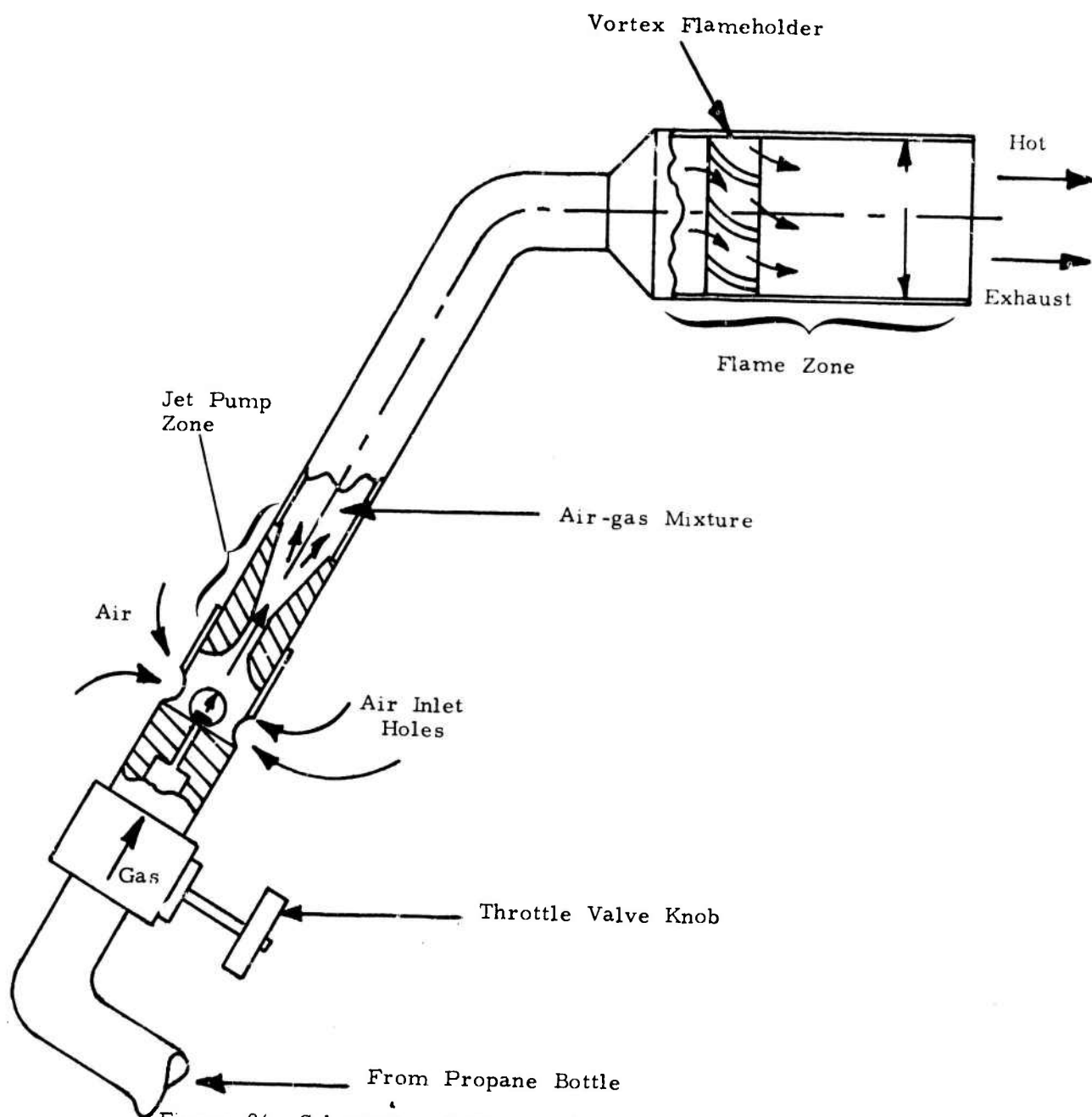


Figure 86 Schematic of Wingaersheek Turbo Torch Burner

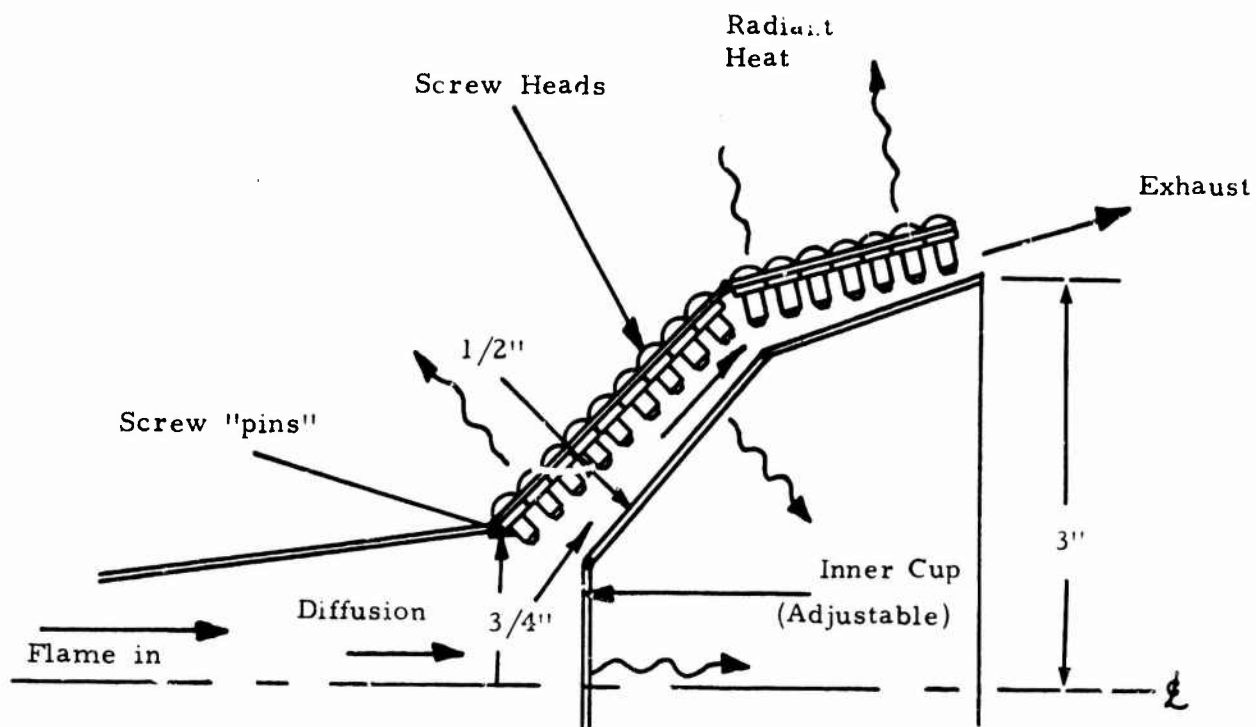


Figure 87 Schematic Section of Experimental Hemispherical
Heat Exchanger

the most compact size. The heat exchange surface consists of small pins spaced one or two diameters apart, staggered and roughly normal to the gas flow and the radiant surface. The heat exchanger was designed to have a mean radiant temperature of 1540°F. To achieve this mean radiant temperature with the particular burner design selected, it was necessary to design the heat exchanger to have a convective surface area equal to 1.5 times the radiant surface area. For the hemispherical design shown in Figure 87, this was achieved with the use of pins 0.06 inches in diameter, protruding 0.16 inches into the gas stream and spaced 45 per square inch.

The prototype developed had an outer cup of perforated mild steel fitted with mild steel screws and stainless steel nuts; the inner cup was also of mild steel. The particular choice of materials and method of construction was dictated by the need to demonstrate rapidly and at a minimum cost the feasibility of the concept and to obtain the necessary performance data. These items would have to be given careful consideration during the recommended further development program.

This particular design has the advantage of being able to vary the temperature distribution of the emitter surface so as to provide an optimum match with the reflector. This would be possible by appropriately varying the pin-fin heat exchanger effectiveness, namely, the pin diameter, protrusion length and spacing, and the gas velocity. The gas velocity can be adjusted by varying the cross-sectional flow area with a suitable inner cup design. With the prototype unit developed a limited variation in the flow area was possible by moving the inner cup in or out relative to the outer cup.

(c) Reflector Design

A paraboloidal reflector having a focal length of 5" and a maximum diameter of 20" was utilized. The effectiveness of the reflector system was increased by the addition of an inner cone to direct the radiation from those areas near the axis of the source, outwards and minimize internal reflections.

(d) Design for Wind Resistance

The radiant source and burner design of the Foster-Miller radiant heater is inherently capable of continuous operation in a windy environment. The likelihood of flame-outs is negligible. Combustion is essentially complete in the flame zone of the Turbo-Torch burner before the hot gases enter the heat exchanger section of the source. The outlet velocity of the hot gases emerging through the annulus between the outer and inner cups is designed to be high, approximately 100 ft/sec. At these velocities, even a 20 mph head-on wind would have little effect on the flow of the hot gases through the heat exchanger and the combustion in the burner. This is in direct contrast to most of the commercially available radiant heater designs which use a low through flow velocity through the flame holder making them highly susceptible to flame outs in a windy environment.

6.4.5.2 Performance of Foster-Miller Radiant Heater

A photograph of the FMA radiant heater in operation is shown in Figure 88. It shows the effectiveness of

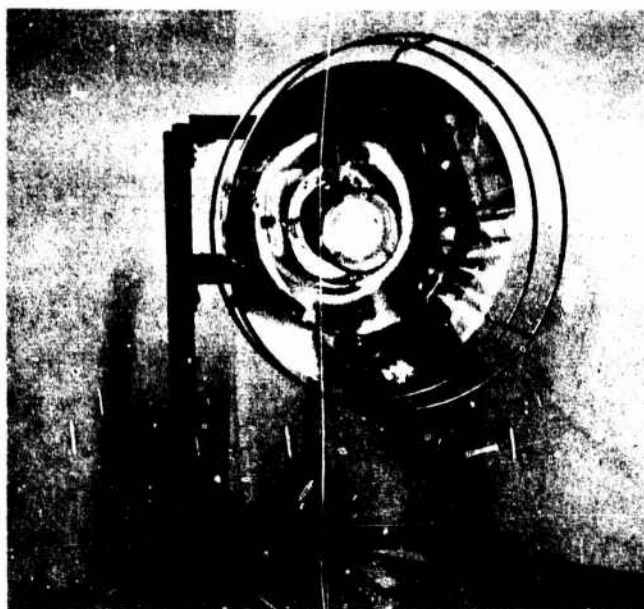


Figure 88 Foster-Miller Radiant Heater

the reflector in increasing the virtual size of the source as well as the high intensity of the radiant source.

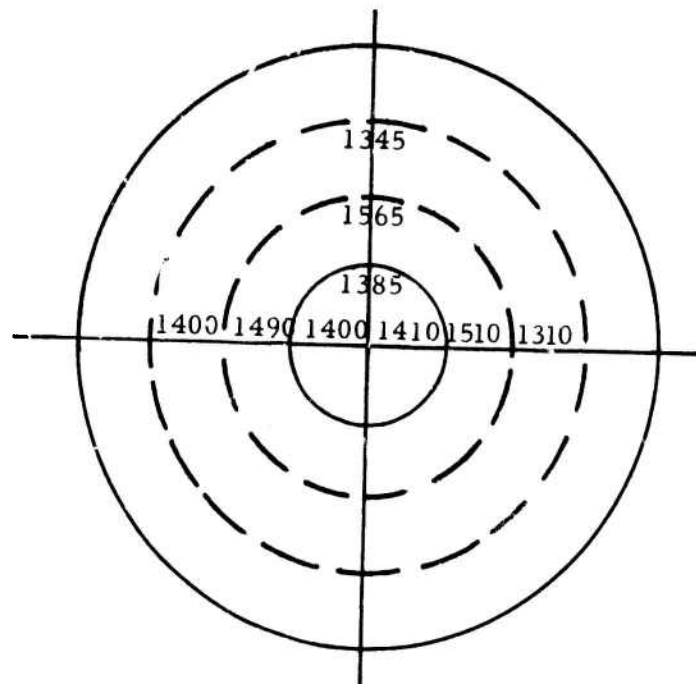
(1) Temperature Distribution of
Emitter Surface

The black body temperature distribution of the inner and outer cups obtained without the reflector in place is shown in Figure 89. The outer cup had a mean temperature of approximately 1400°F. Since the design was not optimized, the surface temperature of the outer periphery was low, only 1200°F. This could be increased to 1400°F by better design. Further, the high temperature and radiant intensity of the inner cup is ineffectively utilized in the present design. Subsequent designs should try to keep this temperature as low as possible.

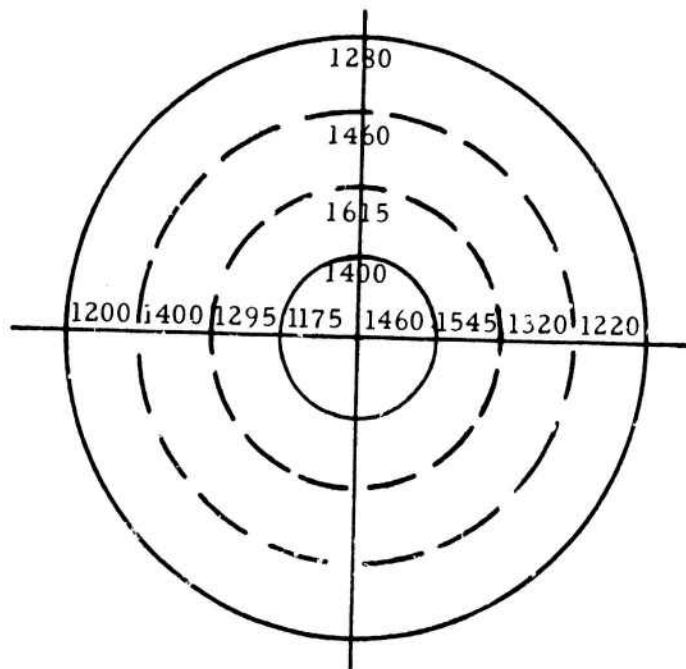
(2) Flux Density Distribution at
the Target

The performance of the radiant heater was measured at a fuel input rate of 20,000 BTU/hr. Figure 90 shows the flux density distribution at target distances of 4, 6, 8 and 10 ft. Due to the symmetrical geometry of the reflector and the source, the angular distribution of the flux density was extremely uniform.

The flux density at the center of the target is extremely high and comparable to that obtained with the large Hot-Tot heater operating at a fuel input of 86,000 BTU/hr. The flux density drops off very rapidly at larger target radii. This is considered to be a limitation of the particular design



(a) Outer Cup



(b) Inner Cup

Figure 89 Black Body Temperature Distribution of the Foster-Miller Hemispherical Radiant Source, °F

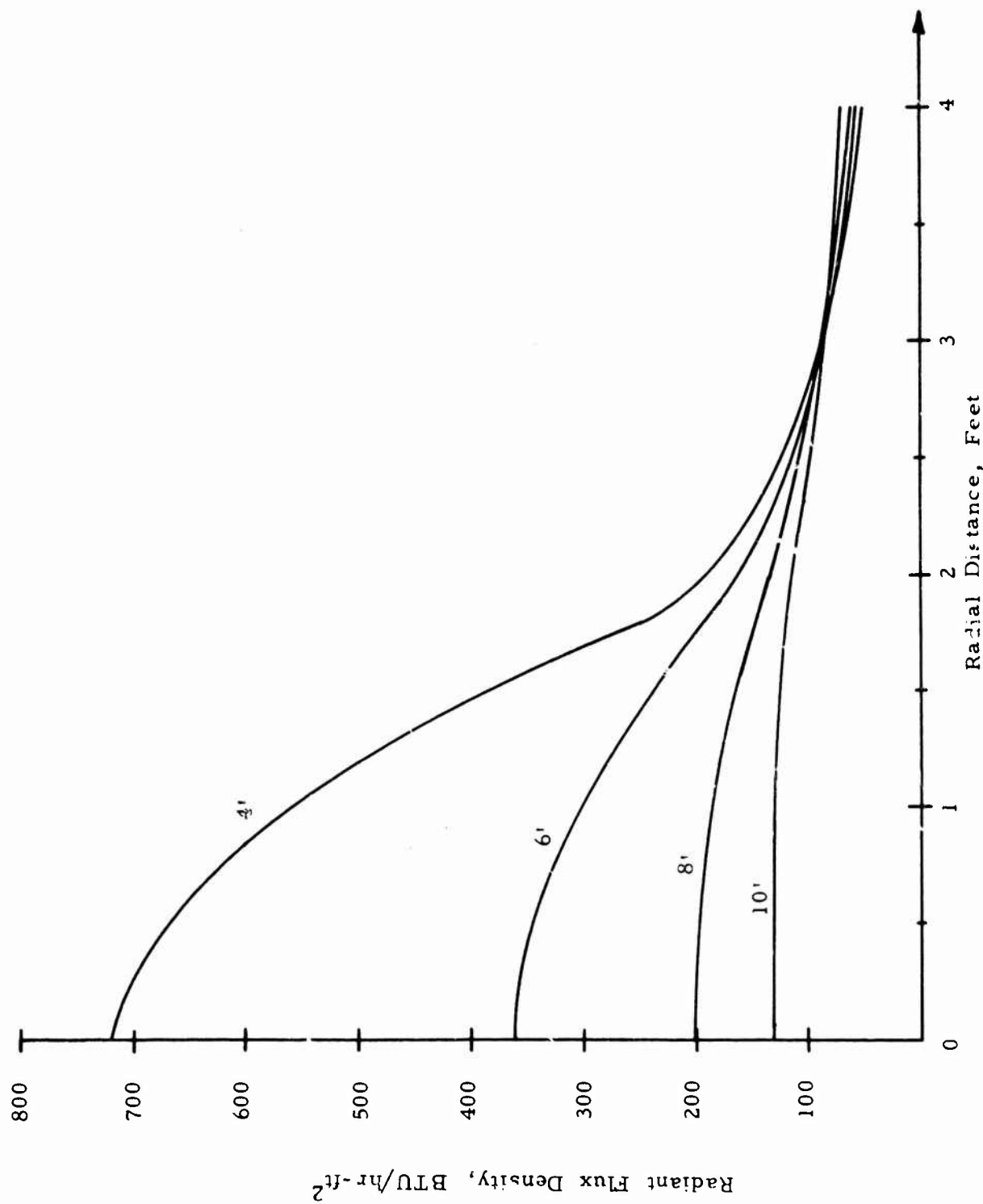


Figure 90 Radiant Flux Density Distribution, BTU/hr-ft^2 - Foster-Miller Radiant Heater

of the paraboloidal reflector. A higher, and more uniform distribution could be obtained with a different paraboloidal design or even a hyperboloidal reflector design. These designs could not be tested during the course of this program.

(3) Effect of Wind

The Foster-Miller radiant heater showed extremely good performance when operating with a 15-mph head wind. The measured flux density distribution at target distances of 6 and 10 ft is shown in Figure 91. Also shown are the performance curves under a stationary ambient. The net reduction in performance is a maximum of 30 percent at the target center and becoming less at the larger target radii. The flux density under these conditions is still almost comparable to the maximum obtainable with the GFP gasoline heater fitted with the long conical reflector and operating in a stationary ambient.

6.4.6 Selas Burner

The Selas burner is a powered burner requiring pressurized air to supply the burner with the proper fuel-air mixture. In this manner it differs from the other burners tested which use pressurized fuel supplies to aspirate the necessary air.

To operate the burner, air is supplied to the mixture at 1 to 3 psi, the propane is reduced in pressure from 7" water column to close to zero pressure, and the fuel-air mixture is supplied at a pressure of approximately 10" water column to the burner, as shown in Figure 92. Considerable difficulty was experienced in adjusting the air and fuel flows to obtain the necessary

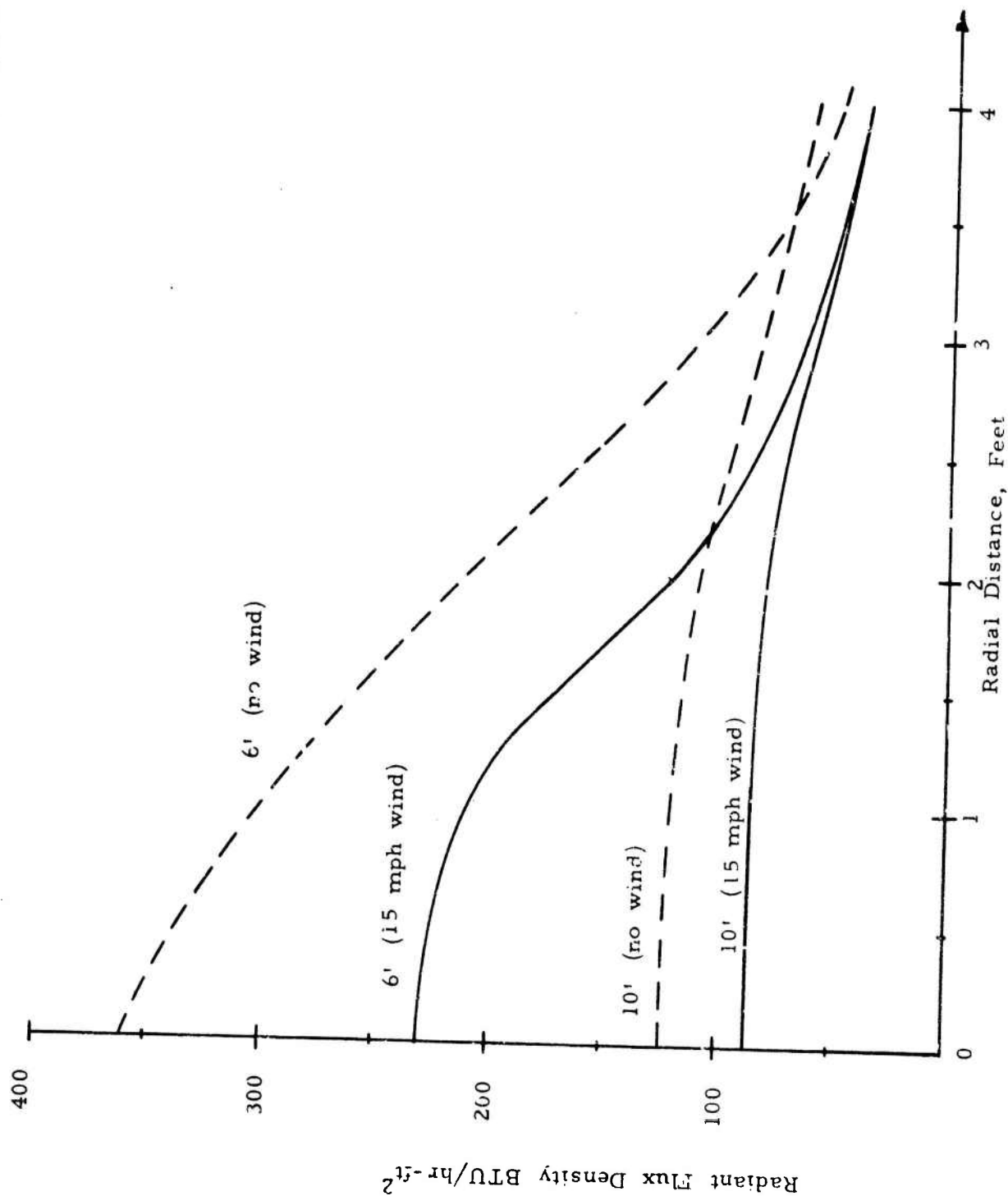


Figure 91 Effect of Wind on the Radiant Flux Density Distribution - Foster Miller
Radiant Heater

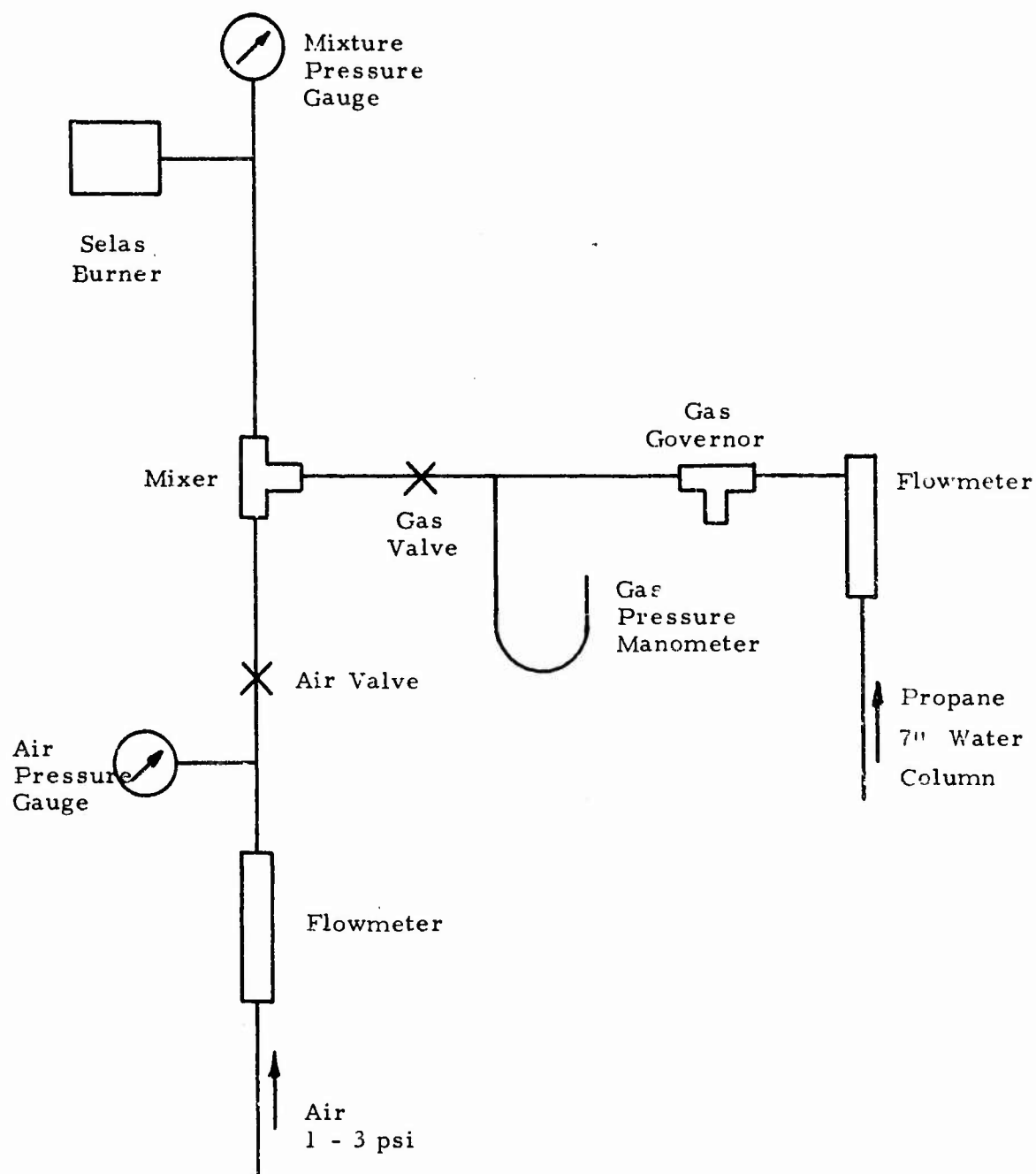


Figure 92 Schematic Diagram of Gas-Air Mixer for Selsas Burner

flow rates at the specified fuel-air mixture ratio. With the burner operating at the optimum setting, the black body temperature of the ceramic has been measured to be as high as 1900°F. However, due to its small size it is not an effective radiator. A large fraction of the total energy input is lost in the exhaust gases. Preliminary attempts to extract heat from the exhaust gases using various types of screens in front of the burner have proven to be unsatisfactory. In view of the complexity of operation of the burner, further work with this burner was abandoned.

6.4.7 Hi-Shear Electric Heater

The Hi-Shear electric quartz tube radiant heater described in Section 5.2 of this report was tested. The operating black body temperature of the quartz radiant tube was measured to be approximately 1100°F. The maximum flux density at a target distance of 4 ft was only 50 BTU/hr-ft². This is considered too small for this application and the heater was eliminated from further testing.

6.5 Summary of Test Results

Test results for the heaters evaluated during this program are summarized in Table X. This table includes a comparison of the heater source temperature, the total radiant energy output, the fuel efficiency and the radiant flux density at target distances of 4 and 8 feet when operating in both stationary and windy environments. The salient results of this experimental program are discussed here.

TABLE X
SUMMARY OF EXPERIMENTAL RESULTS FOR PERFORMANCE OF VARIOUS HEATERS

Heater Specifications						Heat Flux Density at the Target Area (BTU/hr-ft ²)																							
Type of Heater	Mean Black Body Source Temp. (° F)	Area of Source (in. ²)	Total Fuel Input (BTU/hr)	Total Heat Radiated (BTU/hr)	Fuel Efficiency (Percent)	Description of Reflector	No Wind						15 mph Head On Wind																
							Target Distance			Target Distance			Target Distance			Target Distance													
							2 feet	Mean Value	R= 1ft	R= 4ft	Mean Value	R= 1ft	R= 4ft	Mean Value	4 feet	Mean Value	R= 1ft	R= 4ft	Mean Value	8 feet	Mean Value	R= 1ft	R= 4ft	Mean Value					
Government Furnished Gasoline Heater	1200	70	20,000	8,660	40	As received	186	65	135	43	35	40	N-O																
						Small conical reflector	270	73	190	75	50	67	N-C																
						Large conical reflector	372	20	205	115	45	85	N-O																
Pyrocor Propane Heater	1540	43	12,300	8,210	65.7	As received	166	25	116	55	30	45	70	44	20	12	17												
						Added inner cone	155	20	93	48	25	40	N-M																
						Added outer cone	240	60	142	90	50	60	N-M																
						Added both inner and outer cones	240	30	143	120	25	70	N-M																
Hupp Propane	1360	76	20,000	9,980	50	As received	375	38	235	83	58	77	N-O																
Hupp Hot-Tot Propane Heater	1500	334	80,000	59,200	69	Long conical	710	120	497	200	114	162	530 (a)	110 (a)	200 (a)	25 (a)	35 (a)	78 (a)											
FMA Heater	1400	113	20,000	14,906	74.5	Three stage	560	50	313	195	58	145	210 (b)	55 (b)	35 (b)	78 (b)													

Notes: R = Radial Distance at the Target (a) Data for Cross Wind
N-O = Not Operational (b) Measured at 6 feet
N-M = Not Measured (c) Measured at 10 feet

(1) Source Temperature and Fuel Efficiency

The mean source temperature and fuel efficiency are direct measures of the effectiveness of the burner and emitter design of the radiant heater. In general it is desirable to have a high mean source temperature together with a high fuel efficiency.

The surface combustion heater designs, such as, the GFP gasoline heater and the Hupp propane heater, where the flame holder is both the heat exchanger and the emitter, have a poor heat exchange effectiveness. This results in a high exhaust gas temperature, low emitter temperature and poor fuel efficiency. The measured fuel efficiency of the GFP gasoline heater is only 40 percent at a mean source temperature of 1200°F. Similar values for the Hupp propane heater are 50 percent and 1360°F.

The FMA heater and the Hupp Hot-Tot heater designs have separate burner and heat exchange surfaces thus resulting in higher fuel efficiencies and emitter temperatures. The FMA heater has the highest measured efficiency of 74.5 percent at a mean source temperature of 1400°F. The Hupp Hot-Tot is equally efficient at 69 percent at a source temperature of 1500°F.

The Pyrocore heater is a good design of a surface combustion type burner operating at a fuel efficiency of 65.7 percent at a source temperature of 1540°F. It has the highest source temperature of all the heaters tested.

The FMA heater design has not been optimized. An improved heat exchanger design for the source is likely to result

in a source having a mean black body temperature of 1600°F with a small reduction in fuel efficiency but a 50 percent increase in the total heat flux radiated.

(2) Heat Flux Density at the Target Surface -
Effect of Reflectors

The measured flux density distribution at the target surface from the various heater source and reflector configurations is seen to confirm the theoretical predictions of their relative performance. For comparable fuel inputs, the highest flux density is obtained with the hemispherical-source-paraboloidal-reflector FMA heater and the lowest with the area-source-conical-reflector GFP gasoline heater. The cylindrical or line source with a paraboloidal reflector, such as the Pyrocore heater, is intermediate in value.

The flux density distribution over the target was generally nonuniform for all heaters, with a peak along the axis and a minimum at the outer radius of the target. This ratio of maximum to minimum flux density was largest at target distances close to the heater, such as 4 feet. At the larger target distances, such as 8 feet, the flux density distribution would tend to be more uniform. The addition of reflectors to direct the radiation at the target would generally result in an increase in both the mean flux density and the ratio of maximum to minimum flux density. Thus suitable trade-offs must be made to optimally match source and reflector designs in order to achieve both maximum uniformity and mean value of the flux density distribution at the target.

The target heating performance of the GFP gasoline heater was found to be extremely poor. At a target distance of 4 feet a peak heat flux density of 186 BTU/hr-ft^2 was measured at a target radius of 1 foot which dropped off to a value of 65 BTU/hr-ft^2 at a target radius of 4 feet and a mean value of 135 BTU/hr-ft^2 . As the original heater came with no reflector for focusing of the radiation, the flux density at a target distance of 8 feet dropped off to 45 and 35 BTU/hr-ft^2 at target radii of 1 and 4 feet and a mean value of 40 BTU/hr-ft^2 . This heating performance was increased substantially when the GFP heater was fitted with conical reflectors designed to optimize the radiant heat flux density at the target. With the large conical reflector, having a maximum diameter of 24 inches and a length of 12 inches, the flux density at the target was almost twice that of the original heater. The flux density at a target distance of 8 feet is still quite low having a mean of 85 BTU/hr-ft^2 , compared with the 200 BTU/hr-ft^2 desired from each heater unit. It is unlikely that further substantial increases could be made with improved reflector designs. The source temperature is also limited and cannot be increased with the present Cercor flame holder design due to the danger of flash backs.

The FMA radiant heater, with the exception of the much larger Hot-Tot heater, gave the highest flux density at the target area. At a target distance of 4 feet this varied from 560 to 50 BTU/hr-ft^2 over target radii of 1 to 4 feet with a mean value of 313 BTU/hr-ft^2 and at a target distance of 8 feet this similarly varied from 195 to 58 BTU/hr-ft^2 with a mean value of 145 BTU/hr-ft^2 . These results show that the heater performance is approaching the desired value of 200 BTU/hr-ft^2 . The radial flux

density distribution as obtained from this source-reflector combination is highly concentrated along the axis and is seen to fall off very rapidly at the larger target radii. We feel that the radial flux density distribution could be made more uniform by using a hyperboloidal reflector instead of the paraboloidal one. As discussed earlier, it is likely that with an improved source design, the source temperature could be increased to 1600°F resulting in a 50 percent increase in the flux density at the target. With both these modifications incorporated into the FMA heater, a mean flux density of 200 BTU/hr-ft² at a target distance of 8 feet appears to be achievable.

The Pyrocore propane heater had the best performance of all the commercial heaters tested. At 60 percent of the fuel input of the GFP gasoline heater, it provided a flux density on the target which was comparable to that of the gasoline heater. The performance of the original Pyrocore heater was substantially improved with the addition of the large conical reflector so as to increase the overall diameter of the paraboloidal reflector and a small inner cone to control the radiation from the front end of the cylindrical source. Thus, mean flux densities of 143 and 70 BTU/hr-ft² at target distances of 4 and 8 feet respectively were obtained.

(3) Heater Performance in a 15 MPH Wind

The GFP gasoline heater and the Hupp propane heater would not operate with a 15 mph head on wind due to flame-outs. This is a characteristic of all surface combustion burners. The Pyrocore, though a surface combustion burner, has good wind resistance, due possibly to its high operating gas pressure. It remained operational at approximately 30 percent of its original flux density.

The FMA radiant heater has extremely good wind resistance. There was no danger of a flame out with this heater design. The heater was extremely easy to light. The flux density obtained from this heater when operating in a 15 mph head wind was about 70 percent of its value in a stationary ambient.

(4) Conclusions

To summarize, the test program has shown that the Foster-Miller Radiant heater has by far the best performance of all the heaters tested. It has extremely good wind resistance. It offers the potential for the development of a compact, rugged radiant heater to meet the needs of personnel working in an Arctic environment.

7. Emitter Materials for Radiant Heater Construction

The choice of an emitter material is based on the following considerations:

1. Emissivity: The material should have a high emissivity at its operating temperature.
2. Resistance to Thermal Degradation: The material should be capable of prolonged periods of operation at its operating temperature without excessive oxidation and spalling.
3. Resistance to Mechanical Shock: The material should be capable of withstanding normal mechanical shock during handling without mechanical failure or cracking.
4. Thermal Conductivity: For those cases where the emitter also acts as the flame holder, the material should have a poor thermal conductivity to prevent flashback.

The two most commonly used materials for the emitter surface are a glass-ceramic material, such as Cercor manufactured by Corning Glass Works, Corning, New York, and inconel. Both of these materials have practically the same emissivities, in the range of 0.65 to 0.78^{10, 12}. Further, as seen from Table VI, measured values of the total emissivities (including the effect of gas radiation) of ceramic and inconel surfaces indicate essentially no difference.

At the normal temperature of operation of these burners, 1500 to 1800°F, the inconel is oxidized and thus has a high emissivity. In general all metals in their oxidized state and other refractory type metals have high emissivities.¹² For example, high emittance coatings developed for AISI-310 stainless steel include iron-titanate and calcium-titanate which are capable of increasing the emissivity to 0.89 while remaining well bonded to the substrate.¹³

Inconel is superior to the ceramic for mechanical shock resistance. It would be the preferred material of construction for the personnel heater under evaluation. The ceramic is too brittle and fragile to withstand the rough handling normal to operation under these stringent environmental conditions.

As the emissivity of the emitter materials used in the construction of the radiant heaters tested was found to be reasonably high, the search for materials and coatings of high emissivity was eliminated. Instead, efforts to optimize source and reflector geometry were emphasized during the course of this program.

8. Special Design Requirements for a Liquid-Fuel Fired Radiant Heater

A radiant heater developed for this application is required to operate on liquid fuels, such as gasoline. It must also have adequate controls for safety during operation. Special design features to satisfy these requirements are discussed in the following sections.

8.1 Burner Design for Liquid Fuel Operation

The burner of a liquid fuel fired radiant heater should be designed to have the following characteristics:

- (a) Burn several different liquid fuels.
- (b) Require no external power for air or control except for the fuel tank pressure.
- (c) Be simple to operate and adjust for a particular fuel.
- (d) Have inherent or automatic safeguards against flash back and external fire.

These requirements are most effectively satisfied by a burner which uses the burner heat to prevaporize the fuel. The fuel vapor provides the jet-pump action to induce the air. Thus, any gas burning design can be trimmed to operate satisfactorily with the fuel.

The fuel vaporization can be accomplished by leading the fuel tube through or around the burner, or by bleeding a small amount of combustion gases from the burner to a separate vaporizer section. Temperature of the vaporizer can then be maintained with a temperature sensitive transducer to regulate the hot gas bleed flow.

For best operation, some controls for regulation of the fuel vaporization heat should be provided.

Start-up with liquid fuel is a problem which could be solved by either one of the following two methods or a combination there of:

- (a) providing an open wick or pool of volatile fuel to burn underneath and heat up the fuel vaporizing tube;
- (b) providing a separate air-atomizing pilot-burner nozzle in the main burner or in the fuel-vaporizer region that will ignite and burn long enough to start vaporization for the main burner fuel supply.

The start-up or pilot-flame can be manually controlled and shut off, or automatically controlled by temperature or pressure sensitive elements.

8.2 Safety Controls for Liquid-Fuel Operation

Several different safety controls for a liquid-fuel-fired

radiant heater are possible and should be suitably incorporated into a liquid-fuel radiant heater design. These are:

- (a) A simple quick disconnect-shut-off on the fuel tank to shut off fuel flow and remove the tank in case of a fire, thus minimizing the explosion danger.
- (b) A control to shut-off the fuel in case of a flame out. Such a control would consist of a temperature-sensing element in the burner which provides enough force and displacement to operate a shut-off valve, such as, a bimetallic spring or a liquid-filled tube and bellows similar to common thermostats. This safety valve could be incorporated into a subsystem that also controls prevaporization of the fuel to the main burner.
- (c) With a low intensity burner, such as the GFP gasoline heater, flash-back of the flame into the considerable volume upstream can be hazardous. An automatic over temperature shut-off, similar to the flame-out device, is recommended. With a high intensity burner, such as the Wingaersheek Turbotorch used with the FMA radiant heater, the chance of flash-back upstream of the flame holder is small and the associated explosion hazard negligible due to the small enclosed volume.

9. Conclusions and Recommendations

9.1 Conclusions

The major conclusion from the studies reported in the preceding section is that there is no commercially available heater capable of operating in the specified Arctic environment of -50°F and 20 mph winds and supplying the necessary heating rate to keep personnel and equipment warm. The GFP gasoline heater is totally unsuitable for this application.

With a limited amount of design effort, a novel radiant heater design has been developed, called the FMA radiant heater, which has the best performance of all the heaters tested. The radiant flux density at the target from this heater configuration was found to approach the minimum considered necessary for personnel and equipment heating. This design offers the potential of being developed into a portable, rugged, compact, high intensity, high efficiency radiant heater for Arctic operations.

The specific major conclusions derived from this study are presented as follows:

(1) Calculations indicate that a flux density from a heater on the order of 200 Btu/hr-ft^2 to the clothed maintenance personnel will be required to prevent a drop in body temperature when working at -50°F even when exposure to wind is prevented by use of suitable windbreaks. Estimates indicated that even higher flux densities will be required on the hands and tools to maintain hand temperature at 55°F or greater.

(2) This heat input can best be achieved by use of several radiant heaters. For example, two large units might be used as large area heaters to cover the maintenance personnel and help maintain body temperature. Each should provide about 200 Btu/hr-ft^2 at the target area from about 8 feet away and should be suitably placed to equalize coverage of the target. Additional smaller heaters might operate from 2 to 4 feet distance from the target to help maintain higher flux levels in the immediate working area of the hands.

(3) The theoretical radiant heat transfer analysis developed during this program is capable of predicting the radiant flux density distribution at the target from various heater configurations, consisting of area, cylindrical and hemispherical sources and conical, paraboloidal, and hyperboloidal reflectors. The correlation between theoretical predictions and experimental measurements of flux density distribution at the target is extremely good.

(4) A hemispherical source with a paraboloidal or hyperboloidal reflector is considered to be the most effective configuration for meeting the design requirements. It is capable of providing a 50-percent higher flux density at the target surface than possible with an optimum disc source, conical reflector configuration of the same source area, source temperature and overall reflector size. A cylindrical source with a paraboloidal reflector is intermediate in performance between the above two configurations.

(5) The design charts developed can be used for the preliminary design of a heater configuration to provide any specified flux density requirement at the target. Though the charts have been developed for a source temperature of 1500°F, designs for other source temperatures can easily be obtained by suitable scaling of the radiated emissive power (i. e. scaling by the fourth power of the absolute temperature).

(6) A source temperature in the range of 1400°F to 1800°F is considered desirable to optimize the radiant energy absorption at the target.

(7) The GFP gasoline heater is considered unsuitable for operation in the specified Arctic environment. It is extremely difficult to light and will not operate with a head wind blowing on it. In a stationary ambient it operates at a mean black body emitter temperature of 1200°F. Its source temperature could not be increased due to the danger of a flash back. The heating performance of the original gasoline heater was extremely poor with a mean flux density of 40 BTU/hr-ft² at a target distance of 8 feet. This can be improved by the use of a conical reflector having a maximum diameter of 24 inches and a length of 12 inches, to 85 BTU/hr-ft². This is still substantially less than 200 BTU/hr-ft² required. Substantial increases above this value with improved reflector designs do not appear to be possible.

(8) The Foster-Miller radiant heater consisting of a high intensity Wingaersheek Turbo Torch burner, a hemispherical shaped heat-exchanger and emitter, and a paraboloidal reflector showed the best performance of all the heaters tested. It is easy

to light and operates extremely well in a windy environment. The heater-source configuration design is one where a high mean source temperature can be achieved with a relatively high fuel efficiency. The heater operated at a mean black body temperature of the emitter of 1400°F and a fuel efficiency of 74.5 percent. The mean flux density at a target distance of 8 feet was 145 BTU/hr-ft² which is 72 percent of the 200 BTU/hr-ft² required.

(9) The Foster-Miller radiant heater continued to operate in a 15 mph head-on wind with a mean flux density at 8 feet estimated to be 100 BTU/hr-ft². This represents a 30 percent reduction in its radiant power output. This performance was found to be superior to any of the other heaters tested and is attributable to the special design features of the hemispherical source.

(10) The source configuration and the reflector design of the Foster-Miller heater have not been optimized. Improved heat exchanger design of the source could result in an increase in the mean temperature to 1600°F resulting in a 50 percent increase in the radiant flux radiated. Thus, a value of 210 BTU/hr-ft² for the mean flux density at an 8 feet target distance could be obtained. An improved reflector, such as a hyperboloidal design, could result in a more uniform flux distribution at the target and possibly a higher flux density.

(11) The burner design used with the Foster-Miller heater can be modified to liquid fuel design with the addition of a prevaporization section. It is inherently safe. The chance of a flash-back upstream of the flame holder leading to an explosion is negligibly small.

(12) The most commonly used materials for emitter construction are inconel and a ceramic, such as, Cercor. Their emissivities at the high temperatures of 1400 to 1600°F are comparable. Cercor, being fragile and brittle is likely to be damaged by mechanical shock due to rough handling. It is therefore, not recommended for this application. Inconel is the better choice. The FMA radiant heater design lends itself to fabrication with inconel.

(13) Radiant System's Pyrocore heater was the best of all the commercially available heaters tested. It has a cylindrical source of inconel in a paraboloidal reflector. The mean flux density at a target distance of 8 feet was 45 BTU/hr-ft² at a source temperature of 1540°F and a fuel input which is 60 percent of the input value to the GFP and FMA heaters. The mean flux density at the target was increased to 70 BTU/hr-ft² with the addition of the 24 inch (large) conical reflector used for the GFP heater and an inner conical reflector. The heater was easy to light and has good wind resistance.

9.2 Recommendations

The preliminary prototype model of the Foster-Miller radiant heater has clearly demonstrated its superiority over all other commercially available designs for the specified application of heating personnel and equipment in an Arctic environment. It is therefore recommended that a development program be undertaken to optimize the design and to modify it for liquid fuel operation. Such a development program would have as its specific objectives;

- (a) Optimization of the burner and heat exchanger to increase the mean source temperature to 1600°F from the presently achieved 1400°F . This would result in an increase in the radiant intensity of the source by 50 percent and result in a mean radiant flux density of 210 BTU/hr-ft^2 at a target distance of 8 feet.
- (b) Optimization of the reflector design to achieve a more uniform radial distribution over the target area, such as, with a hyperboloidal reflector.
- (c) Detailed design of the heat exchanger configuration, including selection of material of construction, mode of construction and fabrication to minimize weight and cost.
- (d) Modification of the burner design for liquid-fuel operation by incorporating a prevaporization section for the liquid fuel.
- (e) Optimization of the configuration design for portability, reliability of operation, resistance to shock and rough handling and finally good wind resistance.
- (f) Design for safety and controls to optimize operation in the specified Arctic environment.

LITERATURE CITED

1. Gaydor, H. F., "Effect on Complex Manual Performance of Cooling the Body while Maintaining the Hands at Normal Temperatures," J. Appl. Physiol., V. 12, p. 373-376, 1958.
2. Adams, Thomas., "The Control of Body Temperature," Technical Report 59-21. Arctic Aeromedical Laboratory, Ladd Air Force Base, Fairbanks, Alaska, July 1960, AD-249 794.
3. Stinchfield, R. M., and Rohr, A., Personal Communication.
4. Carlson, Loren D., "Man in Cold Environment - A Study in Physiology," Arctic Aeromedical Laboratory, Ladd Air Force Base, Fairbanks, Alaska, August 1954, AD-67874.
5. Bruce, W., "Man and his Thermal Environment," Technical Paper No. 84, Division of Building Research, National Research Council, Ottawa, Canada, February 1960, AD-236020.
6. Adams, Thomas, "Environmental Factors Influencing Thermal Exchange," Arctic Aeromedical Laboratory, Ladd Air Force Base, Fairbanks, Alaska, September 1960, AD 251856.
7. Lyman Fourt, et al., "The Comfort and Function of Clothing," Harris Research Laboratories, Rochville, Md. June 1969, AD-703143.
8. Gagge, A. P., "Configuration Factors and Comfort Design in Radiant Beam Heating of Man by High Temperature Infrared Sources," Paper No. 2048 presented at the ASHRAE 74th Annual Meeting, June 1967.
9. DeWirth, D. W., "Literature Review of Infra-Red Energy Produced with Gas Burners," Research Bulletin 83, American Gas Association Laboratories, Cleveland, Ohio.
10. DeWirth, D. W., "A Study of Infra-Red Energy Generated by Radiant Gas Burners," Research Bulletin 92, American Gas Association Laboratories, Cleveland, Ohio.
11. Harwood, K. J., "Focusing and Transmitting Gas-Fired Infra-Red Energy, Research Report No. 1432, American Gas Association Laboratories, Cleveland, Ohio.

12. Hottel, H. C. and Sarofin, A. F., "Radiative Transfer," McGraw Hill Book Company, New York, 1967.
13. Cleary, R. E., Emanuelson, R., et al., "Properties of High Emittance Materials," United Aircraft Corporation, East Hartford, Conn., NASA CR-1278, Feb. 1969.

APPENDIX A

THEORETICAL ANALYSIS OF THE AXIAL DISTRIBUTION OF THE RADIANT HEAT FLUX DENSITY FROM VARIOUS EMITTER AND REFLECTOR COMBINATIONS

1. Introduction

The analysis of this Appendix is designed to calculate the axial distribution of the radiant heat flux density as a function of target distance from the heater source for various emitter and reflector combinations. The different radiation emitter configurations analyzed include point, line, and area sources. These sources were coupled with reflector shapes such as cylindrical, conical, parabolic or paraboloidal, elliptic or ellipsoidal, hyperbolic or hyperboloidal. These results are further utilized to calculate and compare the relative effectiveness of the various heater-source-reflector combinations. The radial distribution of the heat flux over the target area is analyzed in Appendix B.

2. General Description of Radiant Heat Transfer

The thermal energy radiated from a hot body is given by the Stefan-Boltzman Law which for a gray body is written as,

$$e = \epsilon \sigma T^4 \quad (A-1)$$

where

- | | | |
|------------|---|--|
| e | = | emissive power, BTU/hr-ft ² |
| ϵ | = | emissivity of the surface |
| σ | = | Stefan-Boltzman constant, BTU/hr-ft ² °R ⁴ |
| T | = | absolute temperature of the surface, °R |

A typical radiant heat transfer situation is shown in Figure A-1. The net rate of heat transferred from the source to the receiver is expressed as

$$Q = \sigma A_s \mathcal{F}_{sr} (T_s^4 - T_r^4) \quad (\text{A-2})$$

where

- Q = rate of heat transfer to the object BTU/hr
- σ = radiation constant
- T_s and T_r are the absolute temperatures of the source and the receiver
- \mathcal{F}_{sr} = overall view factor for gray surfaces

where

$$\mathcal{F}_{sr} = \frac{1}{\frac{1}{F_{sr}} + \left(\frac{1}{\epsilon_s} - 1\right) + \frac{A_s}{A_r} \left(\frac{1}{\epsilon_r} - 1\right)} \quad (\text{A-3})$$

This factor \mathcal{F}_{sr} is an overall factor which depends on

- (a) The geometric configuration between source and load
- (b) The reflecting effect of walls confining the process
- (c) The deviation of the real source and the receiver from black bodies.

The term F_{sr} is the geometrical view factor between the radiator and the receiver when the surfaces are black. These values have been tabulated in the literature for some typical configurations. However, the presence of reflectors will make the actual intensity higher than the calculated intensity using these factors.

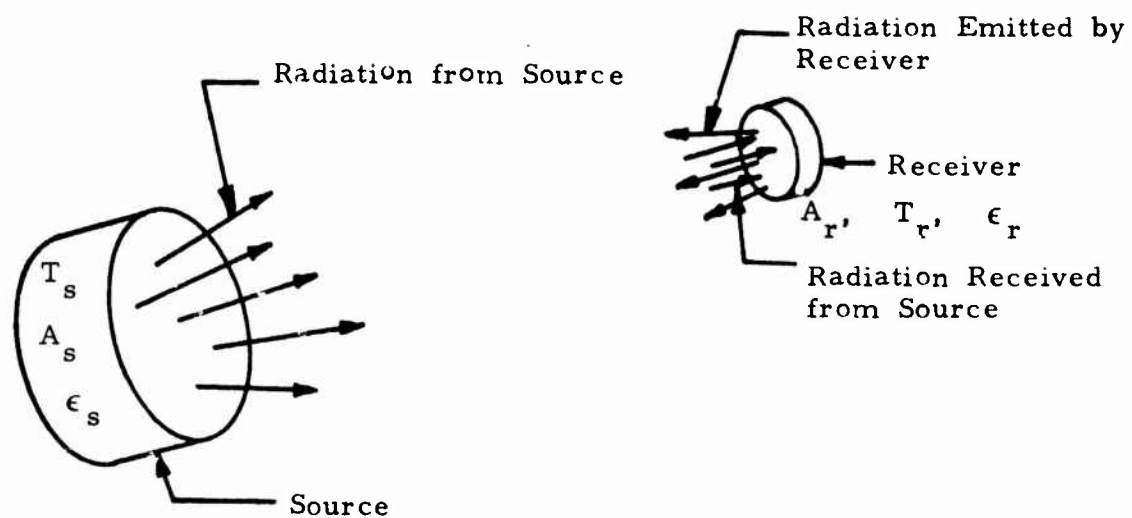


Figure A-1 Radiation Heat Transfer Between Source and Receiver

For a black body,

$$\mathcal{F}_{sr} = F_{sr} \quad (A-4)$$

and by definition of the view factor, $\bar{\Gamma}$,

$$A_s F_{sr} = A_r F_{rs} \quad (A-5)$$

Then, for radiant interchange between a black body source and receiver, Equation (A-3) reduces to

$$I_r = \left(\frac{Q}{A_r}\right) = F_{rs} \sigma (T_s^4 - T_r^4) \quad (A-6)$$

where I_r is the radiant heat intensity at the receiver.

An evaluation of this relationship is fairly simple except for the calculation of the view factor. This represents the major effort in the solution of any radiant heat transfer problem and will form the basis of the analyses of the sections to follow. The effect of the inclusion of a reflector to direct the radiant energy can be looked upon as a change in the view factor between the source and the receiver.

By definition, the view factor between an element dA_r at the receiver and the source A_s is given by,

$$F_{rs} = \frac{1}{\pi} \int_{A_s} \cos \beta_r \cdot d\omega_r \quad (A-7)$$

where β_r = angle between the radiation direction and the normal to the plane of the receiver.

$d \omega_r$ = solid angle the source subtends at the element $d A_r$ of the receiver.

For the case of a source with a reflector, this relationship has to be modified to include the radiant energy received after reflection in addition to that received directly from the source.

Thus,

$$\overline{F}_{rs} = \frac{1}{\pi} \int_{A_s'} \cos \beta_r d \omega_r \quad (A-8)$$

where \overline{F}_{rs} is now referred to as the radiant interchange factor

$$\text{and } A_s' = A_s + A_i$$

$$A_i = \text{image of the source area as seen through the reflector.}$$

The reflector magnification can then be defined as,

$$M = \frac{\overline{F}_{rs}}{F_{rs}} \quad (A-9)$$

3. Direct Radiation from a Source without a Reflector

The radiation intensity at the receiver from typical source geometries was calculated. This formed the basis for evaluating the relative efficiencies or magnification factors of various reflectors. The source geometries analyzed were chosen to represent typical commercial or Government heaters.

3.1 Plane Area Source

Plane area sources are generally of two types: circular discs such as used in the Government furnished gasoline heater, and rectangular such as used with commercial gas-fired heaters.

3.1.1 Circular Disc Source

The view factor, F_{rs} between the receiver element dA_r and a circular source of radius R , shown in Figure A-2 is given in Reference 1* as

$$F_{rs} = \frac{1}{2} \left\{ 1 - \frac{\bar{H}^2 + \bar{r}^2 - 1}{\sqrt{(\bar{H}^2 + \bar{r}^2 + 1)^2 - 4\bar{r}^2}} \right\} \quad (A-10)$$

where

$$\bar{r} = \frac{r}{R}$$

$$\bar{H} = \frac{H}{R}$$

and H = normal distance between source and receiver

R = radius of the source

r = offset of receiver area from the source center

Along the axis of the source, $r = 0$ and

$$F_{rs} = \frac{1}{1 + \bar{H}^2} \quad (A-11)$$

Figure A-2 shows a plot of the view factor as a function of \bar{H} and \bar{r} .

* Numbers refer to literature cited at the end of Appendix A.

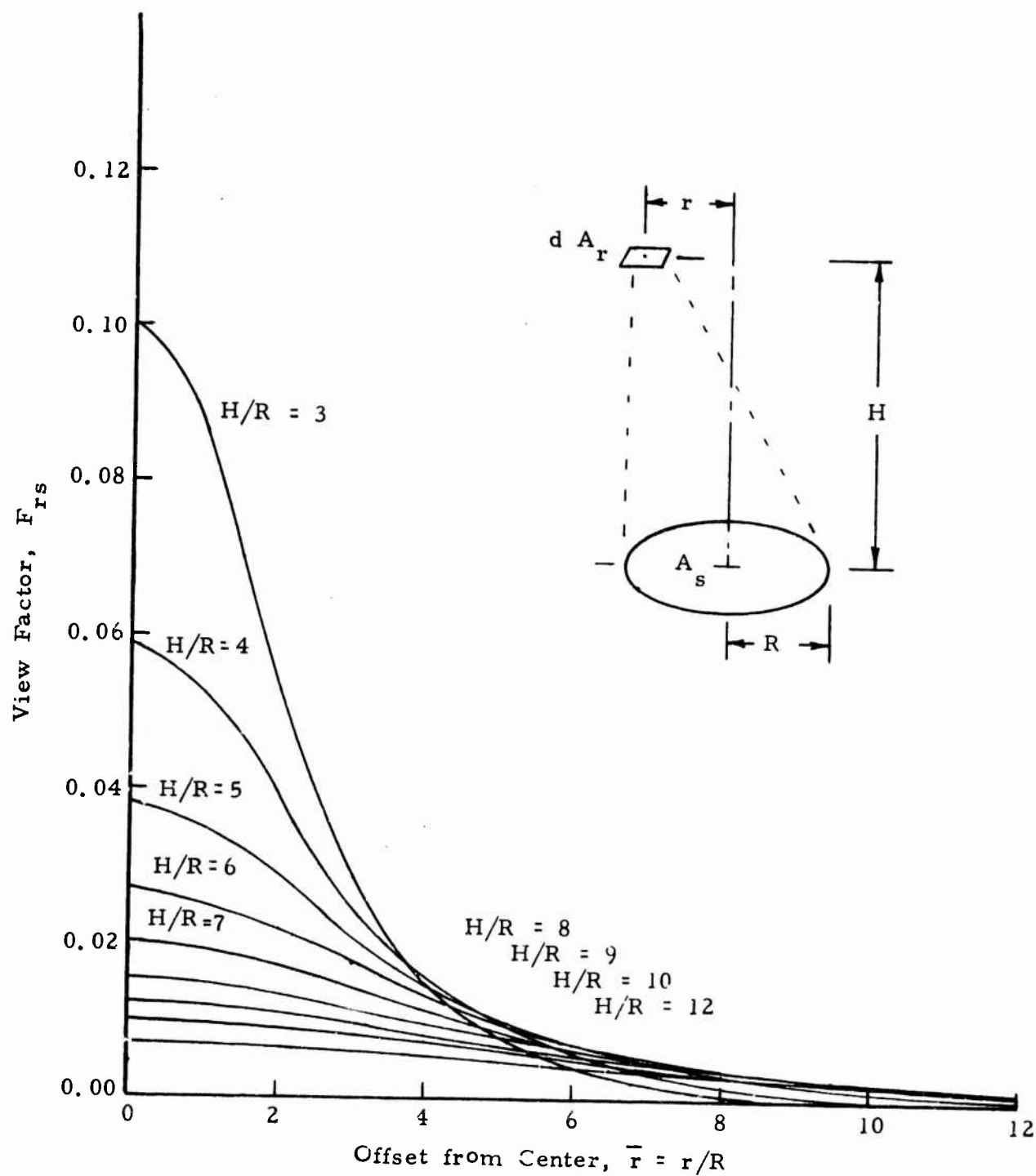


Figure A-2 View Factor F_{rs} , for Direct Radiation
Between an Element and a Circular Disc

3.1.2 Rectangular Area Source

The view factor for a receiver element located at x, y receiving direct radiation from a rectangular source of length a and width b , as shown in Figure A-3, is obtained by summation of the view factors between the receiver element and the source areas 1 to 4. This is given by,

$$F_{rs}(x, y) = \sum_{i=1}^4 F_i \quad (A-12)$$

$$F_i = \frac{1}{2\pi} \left[\frac{x_i}{\sqrt{x_i^2 + H^2}} \tan^{-1} \frac{y_i}{\sqrt{x_i^2 + H^2}} + \frac{y_i}{\sqrt{y_i^2 + H^2}} \tan^{-1} \frac{x_i}{\sqrt{y_i^2 + H^2}} \right] \quad (A-13)$$

where F_i is the view factor between the receiver element and the source areas, $i = 1$ to 4 as obtained from Reference 4.

$$x_1 = x_4 = \frac{a}{2} + x_r$$

$$y_1 = y_2 = \frac{b}{2} + y_r$$

$$x_2 = x_3 = \frac{a}{2} - x_r$$

$$y_3 = y_4 = \frac{b}{2} - y_r$$

The view factor is shown graphically in Figure A-3 for a rectangular source having $a/b = 2$.

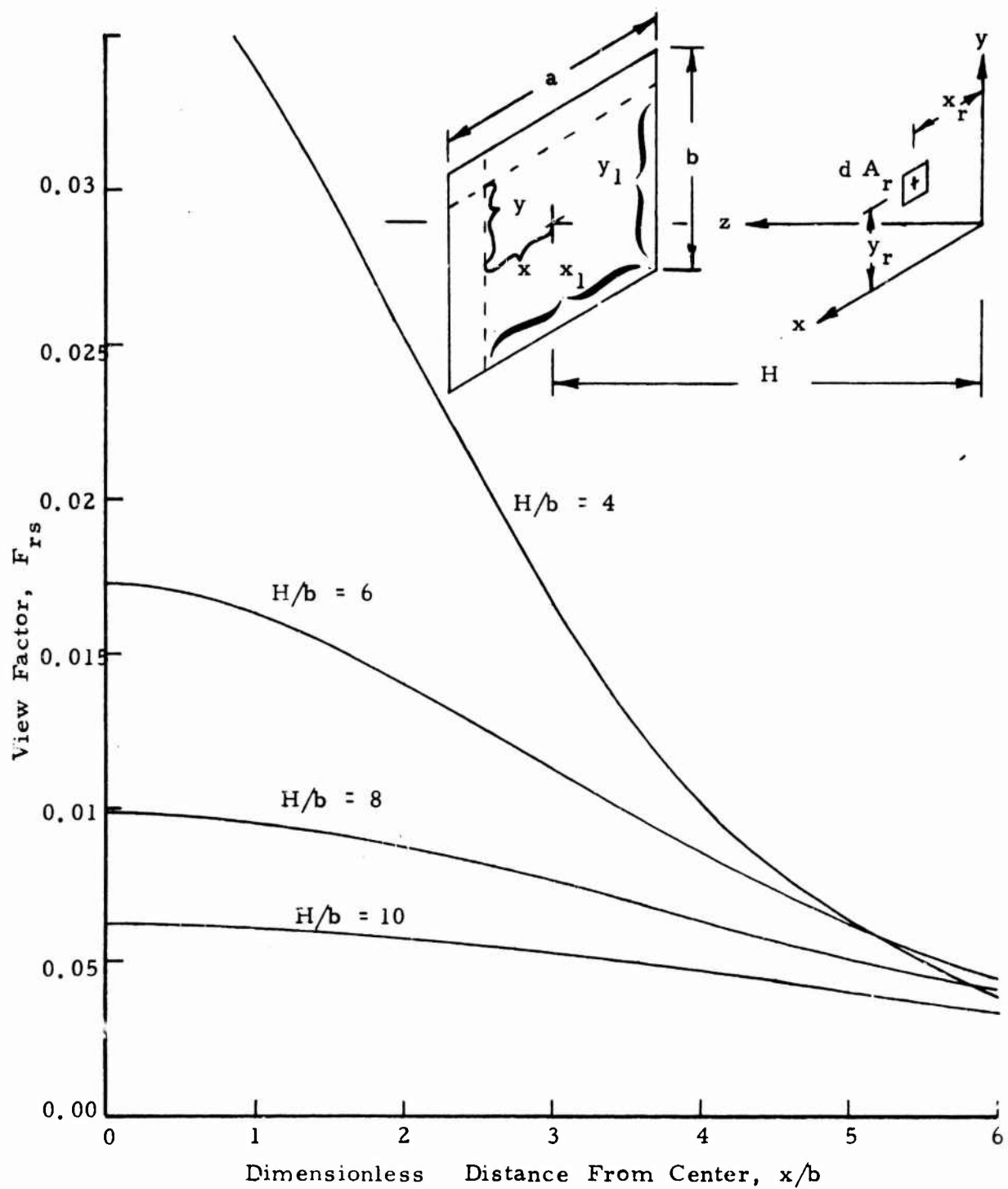


Figure A-3 View Factor for Direct Radiation Between an Element and a Rectangular Source

3.2 Line Source

This is a cylindrical source with length much larger than its diameter as shown in Figure A-4. Using this co-ordinate definition, the view factor between the source and a receiver element at H, y_r, z_r is computed to be,

$$F_{rs} = \frac{Hd}{2 \pi s^2} \left[\frac{s \sin \phi_1}{s_1} + \frac{s \sin \phi_2}{s_2} + \phi_1 + \phi_2 \right] \quad (A-14)$$

where

$$\begin{aligned} s &= (H^2 + y_r^2)^{1/2} \\ s_1 &= \left\{ H^2 + y_r^2 + \left(z_r + \frac{L}{2} \right)^2 \right\}^{1/2} \\ s_2 &= \left\{ H^2 + y_r^2 + \left(z_r - \frac{L}{2} \right)^2 \right\}^{1/2} \\ \sin \phi_1 &= \frac{1}{s_1} \left(\frac{L}{2} + z_r \right) \\ \sin \phi_2 &= \frac{1}{s_2} \left(\frac{L}{2} - z_r \right) \end{aligned}$$

3.3 Spherical or Point Source

A spherical area source would be equivalent to a point source when the distance between the source and the receiver is much larger than the diameter of the source. For the case shown in Figure A-5 the view factor is given by

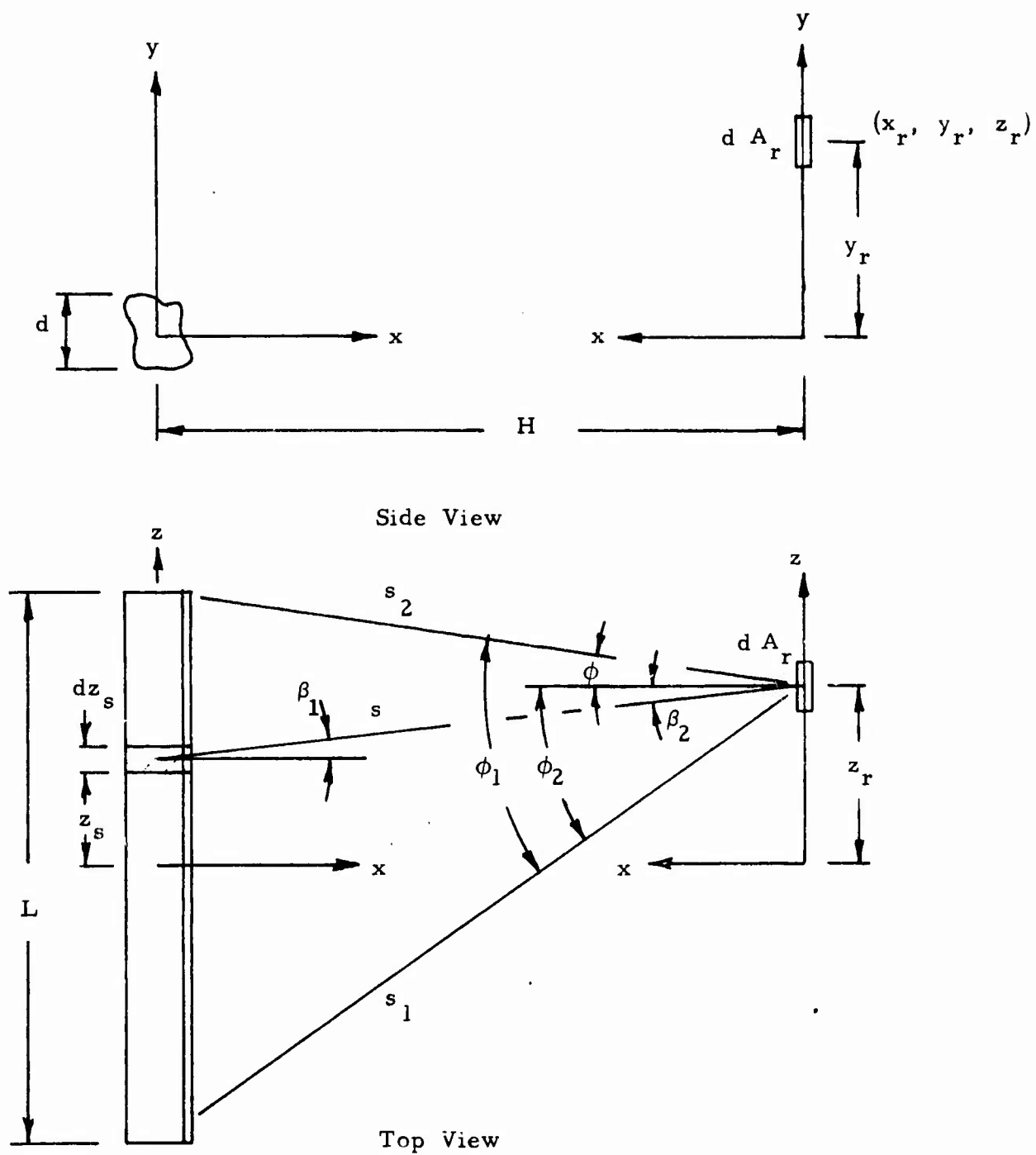


Figure A-4 Coordinate System for the Analysis of a Line Source

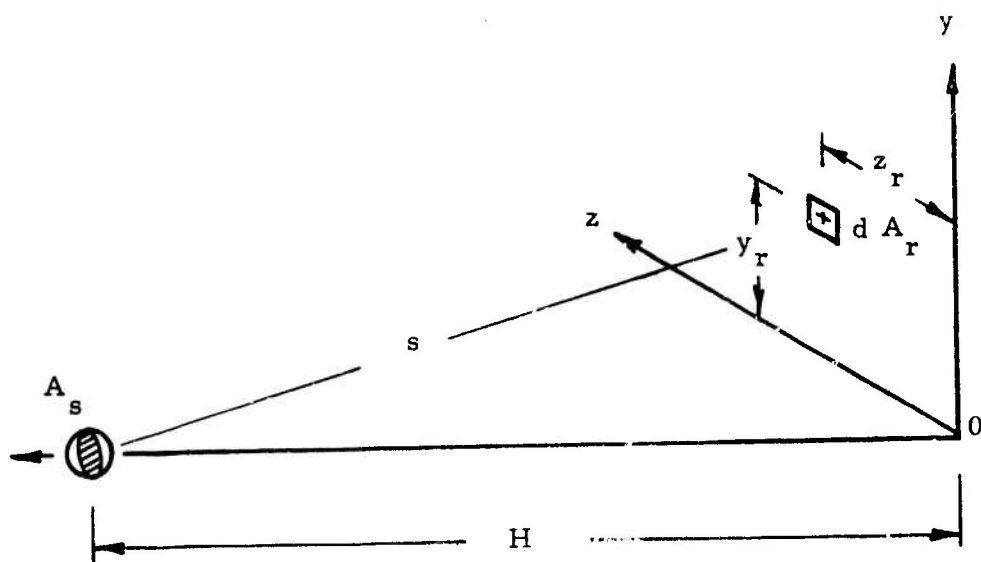


Figure A-5 Coordinate System for the Analysis of
a Spherical Point Source

$$F_{rs} = \frac{1}{\pi} \int_{A_s} dA_s \cos \beta_1 \cdot d\omega_1$$

$$\cong \frac{1}{\pi} \frac{A_s}{s^2} \quad (A-15)$$

where

$$s = (H^2 + y_r^2 + z_r^2)^{1/2}$$

$$A_s = \text{projected area of source}$$

3.4 Comparison of Radiant Heating Performance of Different Source Geometries

For the purposes of comparison of the performance of various heater geometries it is convenient to express heater performance in terms of the following factors.

1. Heat transfer efficiency, η_T defined as

$$\eta_T = \frac{\text{Total heat flux received by the target}}{\text{Total heat flux emitted by the source}}$$

2. Flux density ratio, R_{FD} , defined as

$$R_{FD} = \frac{\text{Heat flux received per unit area of the target}}{\text{Heat flux emitted per unit area of the source}}$$

3. i_T = Radiant flux density at the target generated by a source of unit area, i_T , BTU/hr-ft².

The performance comparison is based on the following assumptions:

- (1) The source temperature was constant and uniform over the total source area as well as for all different source types. An assumed temperature of 1500°F and an emissivity of 1 results in an emissive power of 25,000 BTU/hr-ft².
- (2) The target is 6 ft in diameter and 10 ft away from the source. It has an absorptivity of 1.
- (3) The radiant flux densities calculated represent a mean over the target area.

Source geometries assumed are:

- (1) Circular disc area source 1 ft in diameter
- (2) Line source 2 ft long, 0.1 ft in diameter
- (3) Spherical point source, 0.1 ft in diameter

The heat transfer efficiency parameters, η_T , R_{FD} and i_T for these sources are tabulated in Table A-1.

The results show that the larger disc source is more efficient than the line and point sources alone when there are no reflectors. The effect of reflectors on the performance of these sources is discussed in the next section.

4. Radiation from a Source with a Specular Reflector

The square law dispersion of radiation from the source results

TABLE A-I

COMPARISON OF PERFORMANCE OF VARIOUS SOURCE GEOMETRIES

Source	η_T Percent	R_{FD}	i_T BTU/hr-ft ⁴
Disc	9.45	0.25×10^{-2}	83
Line	2.83	0.063×10^{-2}	25.2
Point	0.57	0.25×10^{-4}	5.05

in a significant reduction in the radiant intensity at the receiver. This intensity decreases as the receiver moves farther away from the source. In other words the view factor for the net interchange of heat between the receiver and the source decreases, resulting in a reduction in the net radiant heat transfer. One common way to increase the radiant intensity at the receiver is to direct or focus the radiation from the source to the receiver by fitting the source with a suitably designed specular reflector. Subsequent sections of this Appendix analyze the design and performance of a number of different reflector designs suitable for the basic source geometries considered in the previous section.

4.1 Characteristics of Specular Reflection

With specular reflection, the directional history of the incident radiation is retained on reflection, the angle of incidence of the incident ray being equal to the angle of reflection of the reflected

ray. Consequently, it is necessary to account for the directional paths of radiant energy transfer between the source, the reflector, and the receiver.

For analytical simplification, the reflector is idealized to be a perfect reflector, having a reflectivity equal to one which is independent of angle of incidence and the wave length of the incident radiation. Most actual reflectors deviate from this ideal in all three respects; their reflectivity is generally less than one and it is a function of the angle of incidence and the wave-length of the radiation.

As a further simplification, this analysis has been restricted to calculating the radiant intensity distribution along the longitudinal axis joining the center of the source and the receiver. In addition, radiant energy transfer to the receiver by multiple reflections from the source-reflector system has been excluded from the analysis.

4.2 Radiation from a Disc Source with a Conical Reflector

4.2.1 Analytical Formulation of Radiant Interchange

The geometry of a conical reflector for the circular disc source is shown schematically in Figure A-6. The commonly used optical image technique is utilized to calculate the radiation intensity at a target point along the axis.¹⁴ The reflected image of the source as seen through the reflector from the target point is shown in Figure A-6 and is seen to be a cone with a cone angle equal to twice the cone angle of the reflector. Depending on the location of the target point (or the separation between the source and the receiver) and the size of the conical reflector, two cases are possible: one, where the source image completely fills the reflector, and second, where it only partially fills the reflector. This condition is defined analytically in terms of

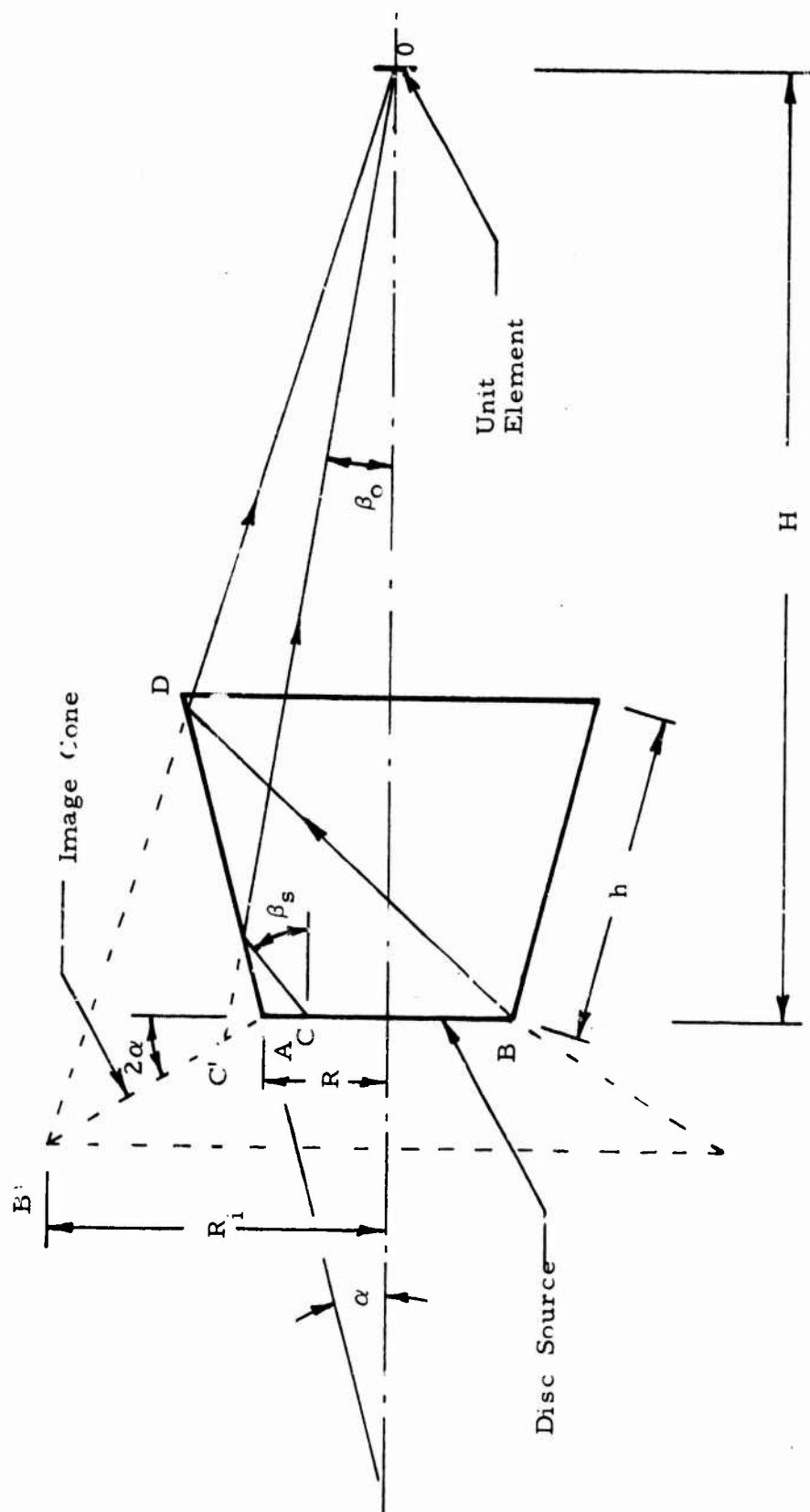


Figure A-6 Definition of Nomenclature for Conical Reflector

$$p \equiv \frac{\bar{H} (1 + \bar{h} \sin \alpha) - (\bar{H} - \bar{h} \cos \alpha)}{(\bar{H} - \bar{h} \cos \alpha) \cos 2 \alpha - (1 + \bar{h} \sin \alpha) \sin 2 \alpha} \quad (\text{A-16})$$

where $\bar{H} = \frac{H}{R}$ and $\bar{h} = \frac{h}{R}$ and the other variables have been defined in Figure A-6. Then $p > 2$ is the condition for a full image and $p \leq 2$ for a partial image.

The radiant interchange for these two cases is discussed separately in the following sections.

4.2.1.1 Radiant Interchange for Full Image Conditions

The emissive power of the reflected source image is assumed to be uniform over the image cone. Then, the radiation received at the target by reflection is given by ¹, as

$$I_{ri} = e_r \left\{ \frac{(1 + 2 \cos 2 \alpha)^2}{(1 + 2 \cos 2 \alpha)^2 + (\bar{H} + 2 \sin 2 \alpha)^2} - \frac{1}{1 + \bar{H}^2} \right\} \quad (\text{A-17})$$

where

e_r = average emissive power of the image

I_{ri} = radiation intensity at the target due to reflected radiation

The radiation received by the target directly from the source is given by. ¹

$$I_{rs} = e_s \left(\frac{1}{1 + \bar{H}^2} \right) \quad (A-18)$$

where

e_s = emissive power of the source.

Then the total radiation received by the target is given by

$$I_r = I_{ri} + I_{rs}$$

$$= e_s \left\{ \frac{1}{1 + \bar{H}^2} (1 - \gamma) + \frac{\gamma (1 + 2 \cos 2\alpha)^2}{(1 + 2 \cos 2\alpha)^2 + (\bar{H} + 2 \sin 2\alpha)^2} \right\} \quad (A-19)$$

where

$\gamma = \frac{e_r}{e_s}$, the ratio of the emissive power of the image to that of the source.

The magnification factor M , for the reflector, which is defined as the ratio of the radiant flux density at the target with a reflector to that without one is given as

$$M = (1 - \gamma) + \gamma \frac{(1 + 2 \cos 2\alpha)^2 (1 + \bar{H}^2)}{(1 + 2 \cos 2\alpha)^2 + (\bar{H} + 2 \sin 2\alpha)^2} \quad (A-20)$$

For the case where $\bar{H} \gg 1$, this simplifies to

$$M \cong (1 - \gamma) + \gamma (1 + 2 \cos 2\alpha)^2 \quad (A-21)$$

The ratio γ is approximately estimated as follows:

A ring element on the source on reflection results in two image rings as shown schematically in Figure A-7. Since the image area is larger than the source area, the emissive power of the image has to be lower than the emissive power of the source, in the ratio of its areas in order to maintain the total heat flux the same. Then the emissive power of the image rings are given by

$$\left. \begin{aligned} \frac{e_{r1}}{e_s} &= \frac{1 - Y}{1 + Y \cos 2\alpha} & \text{for } Y < 1 \\ \text{and} \\ \frac{e_{r2}}{e_s} &= \frac{Y - 1}{1 + Y \cos 2\alpha} & \text{for } Y > 1 \end{aligned} \right\} \quad (A-22)$$

where

$$Y = \frac{y}{R}$$

$$y = R + r$$

r = radius of source ring

Then on the average,

$$\begin{aligned} \gamma = \frac{e_r}{e_s} &= \frac{1}{2} \left[\int_0^1 \frac{e_{r1}}{e_s} dY + \int_1^2 \frac{e_{r2}}{e_s} dY \right] \\ &= \frac{1 + \cos 2\alpha}{\cos^2 2\alpha} \log \left[\frac{1 + \cos 2\alpha}{\sqrt{1 + 2 \cos 2\alpha}} \right] \end{aligned} \quad (A-23)$$

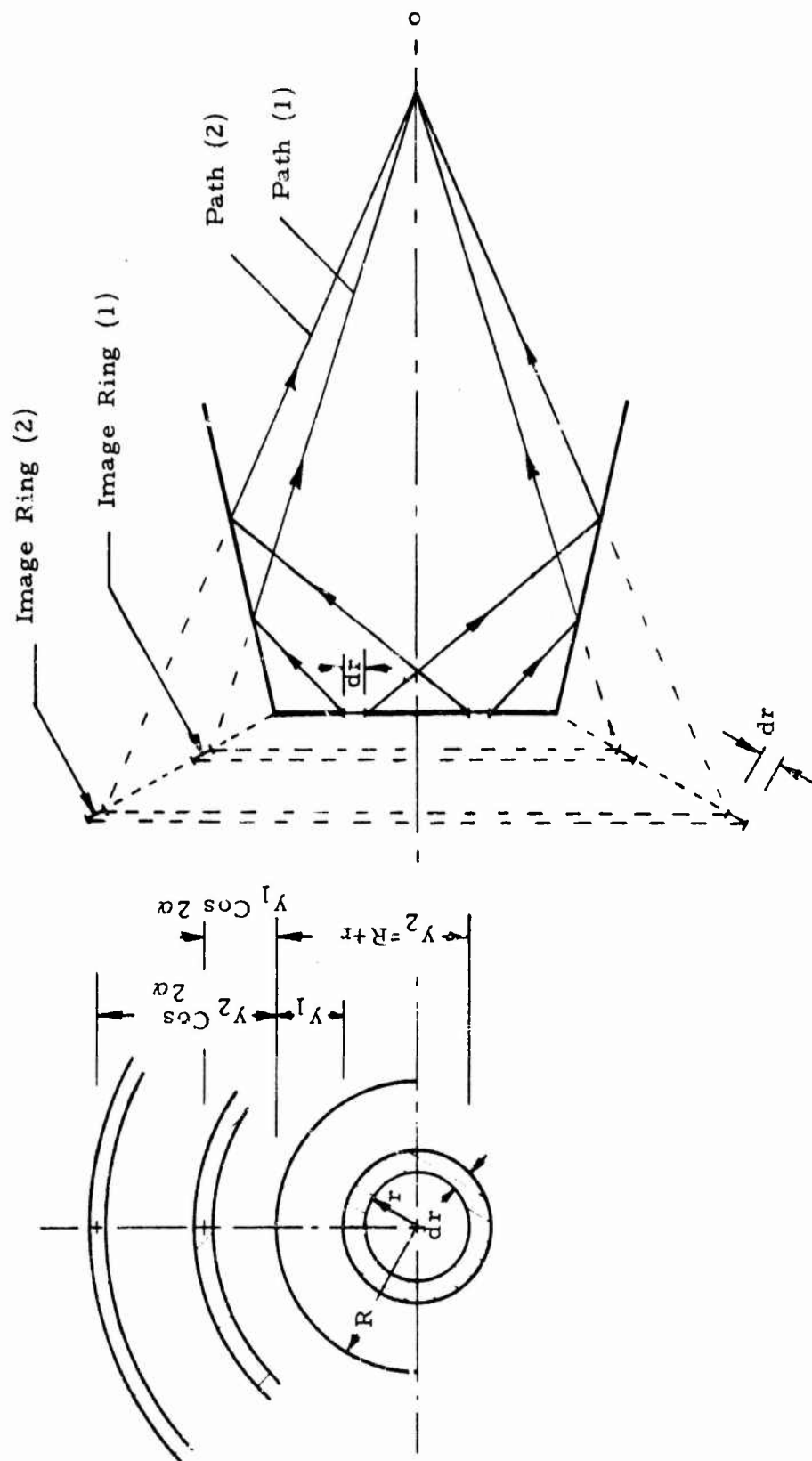


Figure A-7 Image Rings Produced by Source Ring Elements

The value of γ as given by Equation (23) is substituted in Equations (A-19) and (A-21) to calculate I_r and M .

4.2.1.2 Radiation Interchange for Partial Image Conditions

The analysis of the previous section is repeated but with the image partially cut off as shown in Figure A-8.

The image cone length, h_i , can be obtained in terms of the reflector length h and target distance H as

$$\bar{h}_i = \frac{\bar{H} (1 + \bar{h} \sin \alpha) - (\bar{H} - \bar{h} \cos \alpha)}{(\bar{H} - \bar{h} \cos \alpha) \cos 2 \alpha + (1 + \bar{h} \sin \alpha) \sin 2 \alpha} \quad (\text{A-24})$$

where

$$\bar{H} = \frac{H}{R}, \quad \bar{h} = \frac{h}{R}, \quad \bar{h}_i = \frac{h_i}{R}$$

Then

$$I_{ri} = e_r \left\{ \frac{(\bar{h}_i \cos 2 \alpha + 1)^2}{(\bar{H} + \bar{h}_i \sin 2 \alpha)^2 + (1 + \bar{h}_i \cos 2 \alpha)^2} - \frac{1}{1 + \bar{H}^2} \right\} \quad (\text{A-25})$$

I_{rs} is the same as given in Equation (A-18) and

$$I_r = e_s \left\{ \frac{1}{1 + \bar{H}^2} (1 - \gamma) + \frac{\gamma (1 + \bar{h}_i \cos 2 \alpha)^2}{(1 + \bar{h}_i \cos 2 \alpha)^2 + (\bar{H} + \bar{h}_i \sin 2 \alpha)^2} \right\} \quad (\text{A-26})$$

The magnification factor M for $\bar{H} \gg 1$ reduces to

$$M \approx (1 - \gamma) + \gamma (1 + \bar{h}_i \cos 2\alpha)^2 \quad (\text{A-27})$$

The ratio γ is similarly calculated to be

$$\begin{aligned} \gamma &= \frac{1}{\cos 2\alpha} \left[\frac{1}{\bar{h}_i} \left(\frac{1 + \cos 2\alpha}{\cos 2\alpha} \right) \log (1 + \bar{h}_i \cos 2\alpha) - 1 \right] \text{ for } \bar{h}_i \leq 1 \\ &= \frac{2}{\bar{h}_i \cos 2\alpha} \left[\left(\frac{\bar{h}_i}{2} - 1 \right) + \left(\frac{1 + \cos 2\alpha}{\cos 2\alpha} \right) \log \frac{(1 + \cos 2\alpha)}{\sqrt{1 + \bar{h}_i \cos 2\alpha}} \right] \text{ for } \bar{h}_i \geq 1 \end{aligned} \quad (\text{A-28})$$

These relationships are sufficient to calculate I_r and M .

4.2.2 Optimum Design of a Conical Reflector

An optimum conical reflector will be designed to provide a full image of the source in the reflector for all design target distances. This will maximize the radiant flux density at the target. This design procedure includes setting $p = 2$ in Equation (A-16) to solve for α for a reflector length h and maximum target distance H . This equation is best solved graphically as shown in Figure A-9 where the optimum cone angle is given by the intersection of the loci of \bar{h} and \bar{H} . Values obtained for typical cases are summarized in Table A-II.

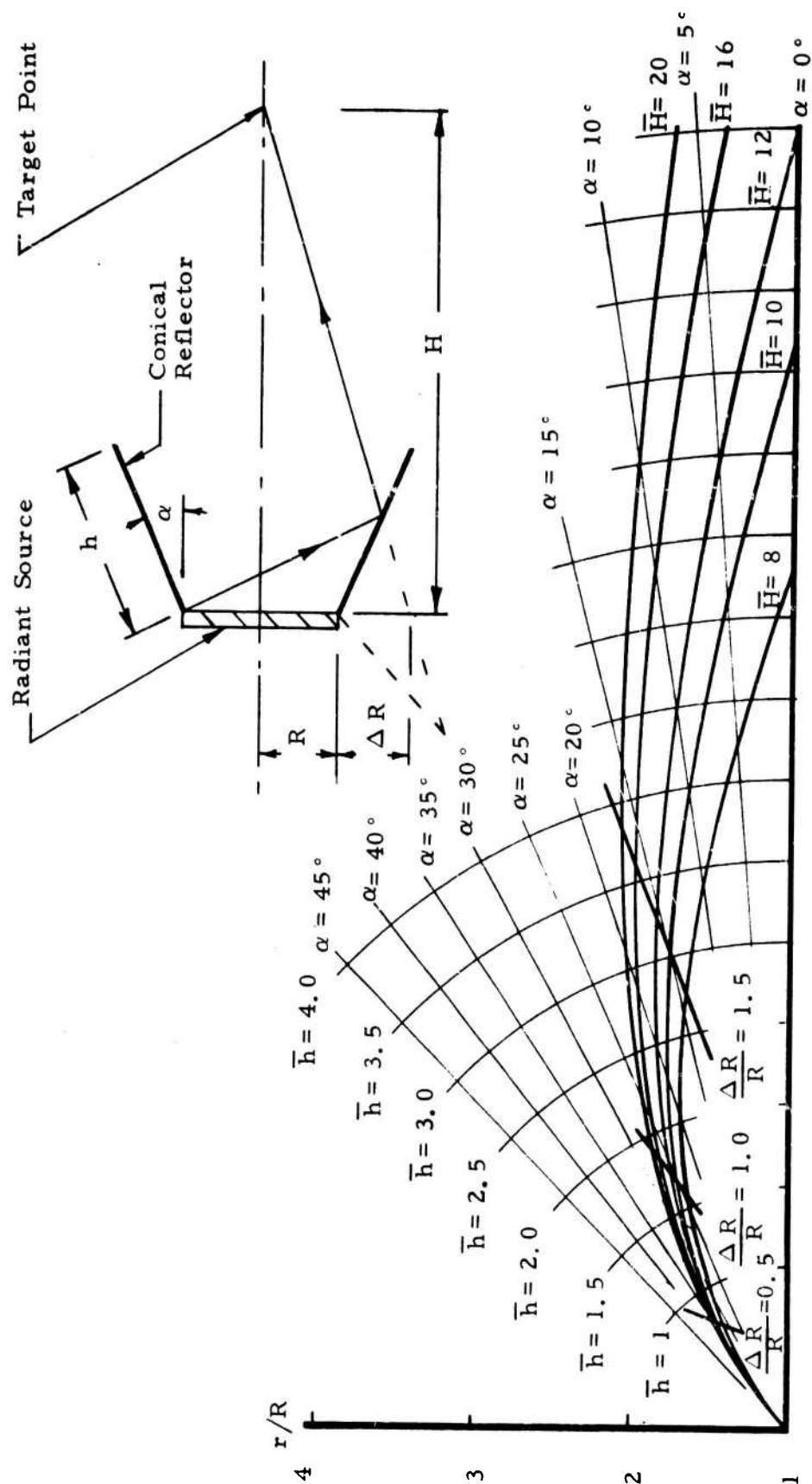


Figure A-9 Selection Chart For Optimum Dimensions for Conical Reflector

TABLE A-II

OPTIMUM CONE ANGLE FOR CONICAL REFLECTOR

Reflector Length $\bar{h} = \frac{h}{R}$	Target Distance $\bar{H} = \frac{H}{R}$	Optimum Cone Angle °
1	10	30°
1	20	35°
2	10	22.5°
2	20	27.5°

4.2.3 Parametric Variation of Reflector Performance

The parametric variation of reflector performance was calculated using a digital computer program. The effect of cone angle and reflector length on the axial distribution of the magnification factor were studied and the results shown graphically in Figures A-10 and A-11. The results show that with the use of an optimum conical reflector, the radiant flux intensity can be approximately doubled. The cylindrical reflector shows a comparatively poor performance.

4.2.4 Estimated Performance of the Government
Furnished Radiant Heater with a Conical
Reflector

The radiant flux intensity from the Government furnished radiant heater was calculated for a variety of conical reflector designs. The results are shown in Figure A-12 for the

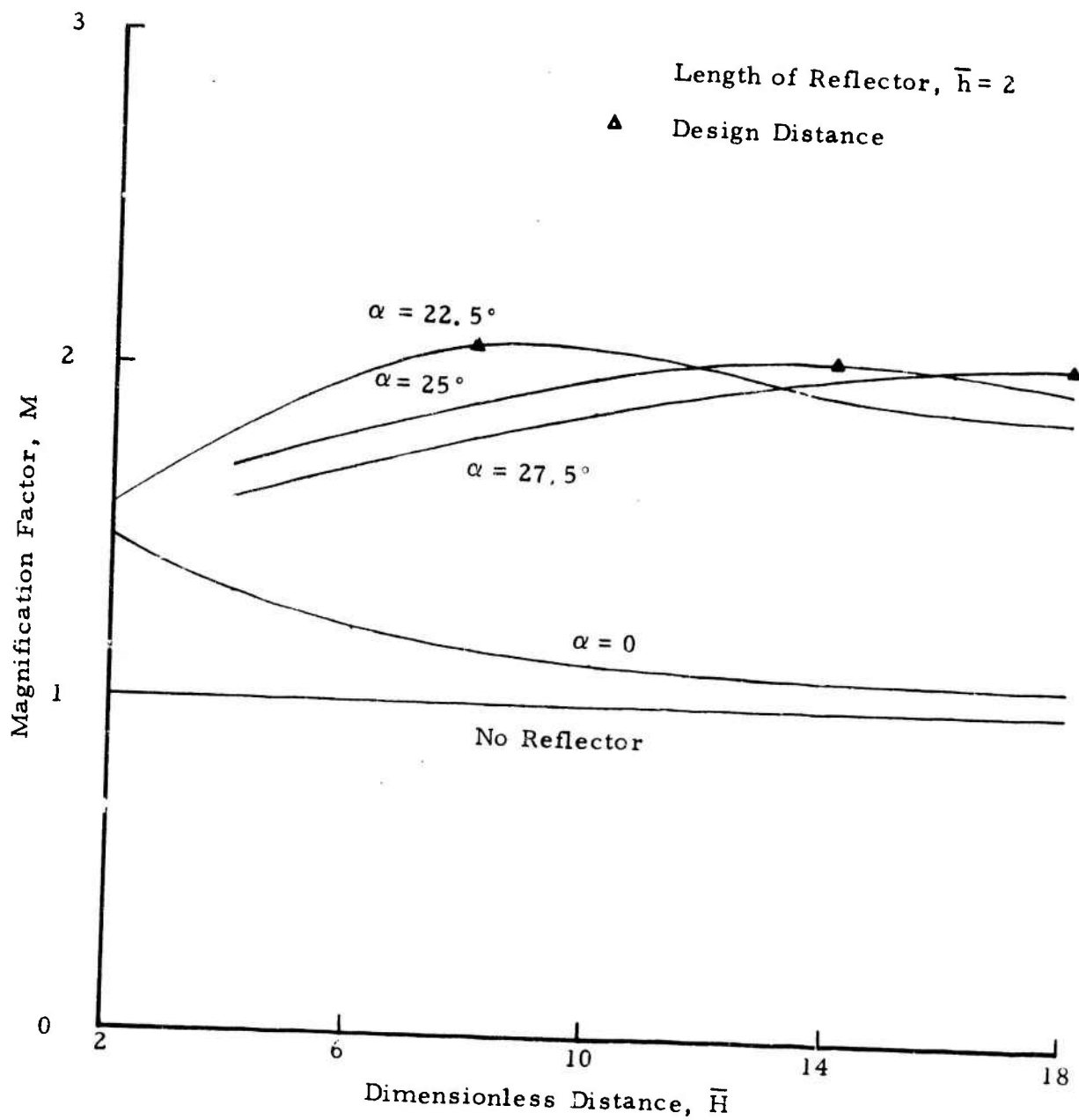


Figure A-10 Effect of Cone Angle, α on Reflector Performance

Conical Angle is based on design
length $\bar{H}_f = 10$

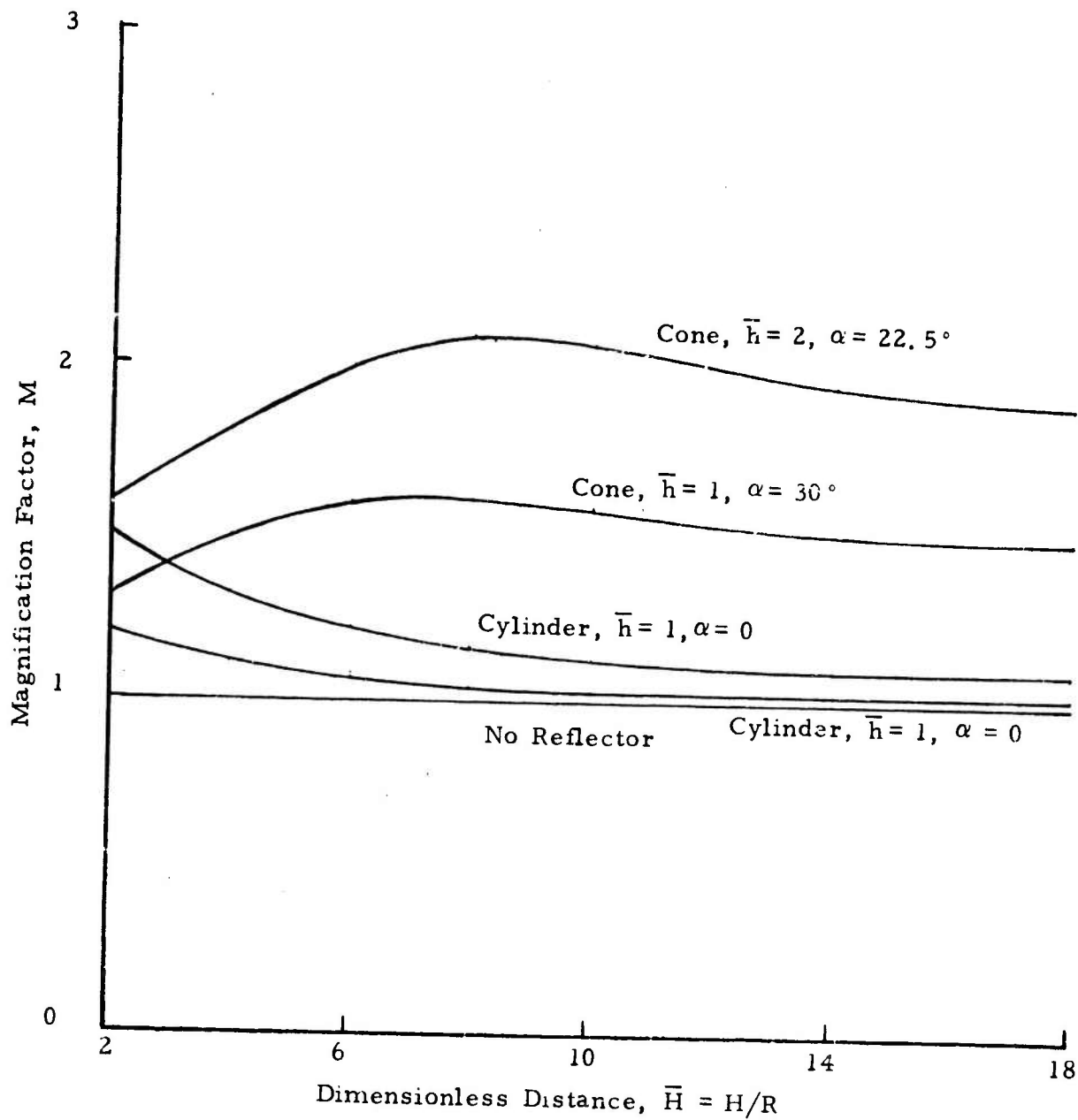


Figure A-11 Effect of Reflector Length on Reflector Performance

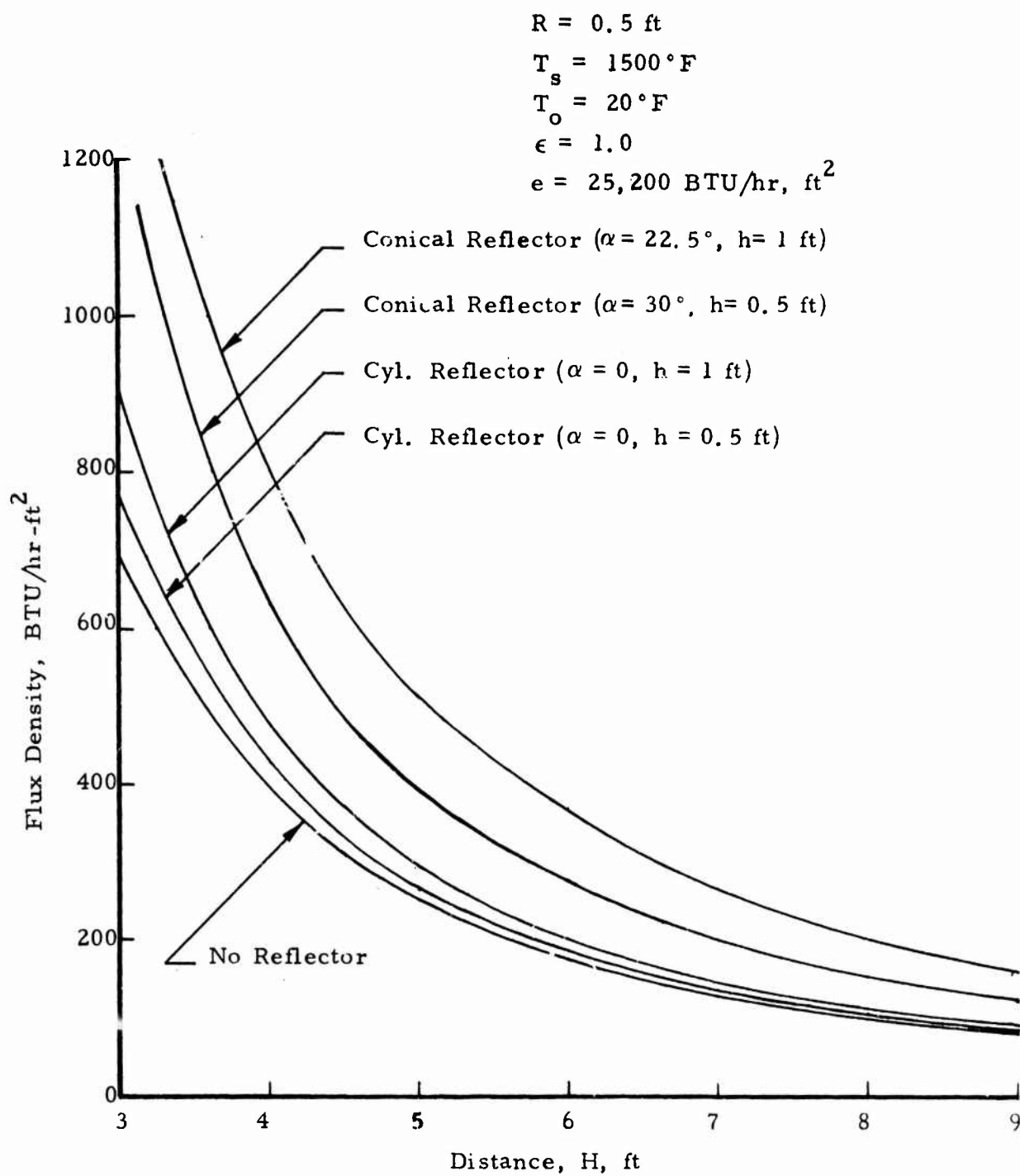


Figure A-12 Flux Density Distribution for Various Reflectors

specified conditions. Table A-III shows a comparison between theoretically predicted and experimentally measured values. The correlation is seen to be fairly good.

4.2.5 Heat Transfer Efficiency

The flux density ratios, R_{FD} of the heat flux from a unit area source to a target of unit area is given by

$$R_{FD} = \left(\frac{1}{1 + \bar{H}^2} \right) \bar{M} \quad (A-28)$$

where \bar{M} is the average magnification factor over the design target area.

To determine the average magnification factor it is necessary to take into consideration the radial distribution of the flux density over the receiver area. As a first approximation the source-reflector system is assumed to be replaced by an equivalent source of area equal to the projected area of the conical image and located at the plane of the source. The radial distribution can then be obtained from Figure A-2, and a correction factor, f , calculated such that

$$\bar{M} = M_o f$$

where M_o is the magnification factor along the axis. Then, η_T as defined in Section 3.4 of this Appendix, is given by

$$\eta_T = \frac{A_r}{A_s} \bar{R}_{FD}$$

TABLE A-III

COMPARISON OF THEORETICALLY PREDICTED AND
EXPERIMENTALLY MEASURED VALUES OF THE MAGNIFICATION FACTOR

Distance From Source (ft)	Reflector *	Magnification Factor	
		Theoretical Prediction	Measured Value
4	Short Reflector	1.6	1.475
	Long Reflector	2.1	2.0
8	Short Reflector	1.6	1.66
	Long Reflector	2.1	2.5

* Refer to Figure 52 for size and geometry of the reflectors.

where A_r is the area of the receiver.

Numerical Calculations:

For the design having, $h = 0.5$ ft, $\alpha = 35^\circ$, $H = 10$ ft, $R_t = 3$ ft and $T_s = 1500^\circ\text{F}$, calculations show that $M_o = 1.6$, $f = 0.93$, $R_{FD} = 0.0038$, $\eta_T = 13.8$ percent; and $i_T = 116$ BTU/hr-ft⁴.

For the design having, $h = 1$ ft, $\alpha = 30^\circ$, $H = 10$ ft, $R_t = 3$ ft, $T_s = 1500^\circ\text{F}$ calculation show that $M_o = 2.1$, $f \cong 1.0$, $R_{FD} = 0.0055$, $\eta_T = 19.7$ percent and $i_T = 166$ BTU/hr-ft⁴.

4.3 Radiation from a Circular Disc Source with an Ellipsoidal Specular Reflector

An ellipsoidal reflector is capable of focusing the energy radiated from a point source located at one focal point to a target point located at the second focal point as shown in Figure A-13. This type of a system is often used in solar energy simulators to obtain extremely high intensity beams for heating of small localized areas. However, for a finite area source the radiant energy, instead of being sharply focused, is distributed over a larger area and could possibly represent a method of heating the specified receiver area.

4.3.1 Geometry of Ellipsoidal Reflector

The shape of the ellipsoidal reflector illustrated in Figure A-13 designed to enclose the disc source at one focal point with the receiver located at the other focal point is given by,

$$\frac{(x - \frac{H_f}{2})^2}{a^2} + \frac{y^2}{b^2} + \frac{z^2}{b^2} = 1 \quad (\text{A-29})$$

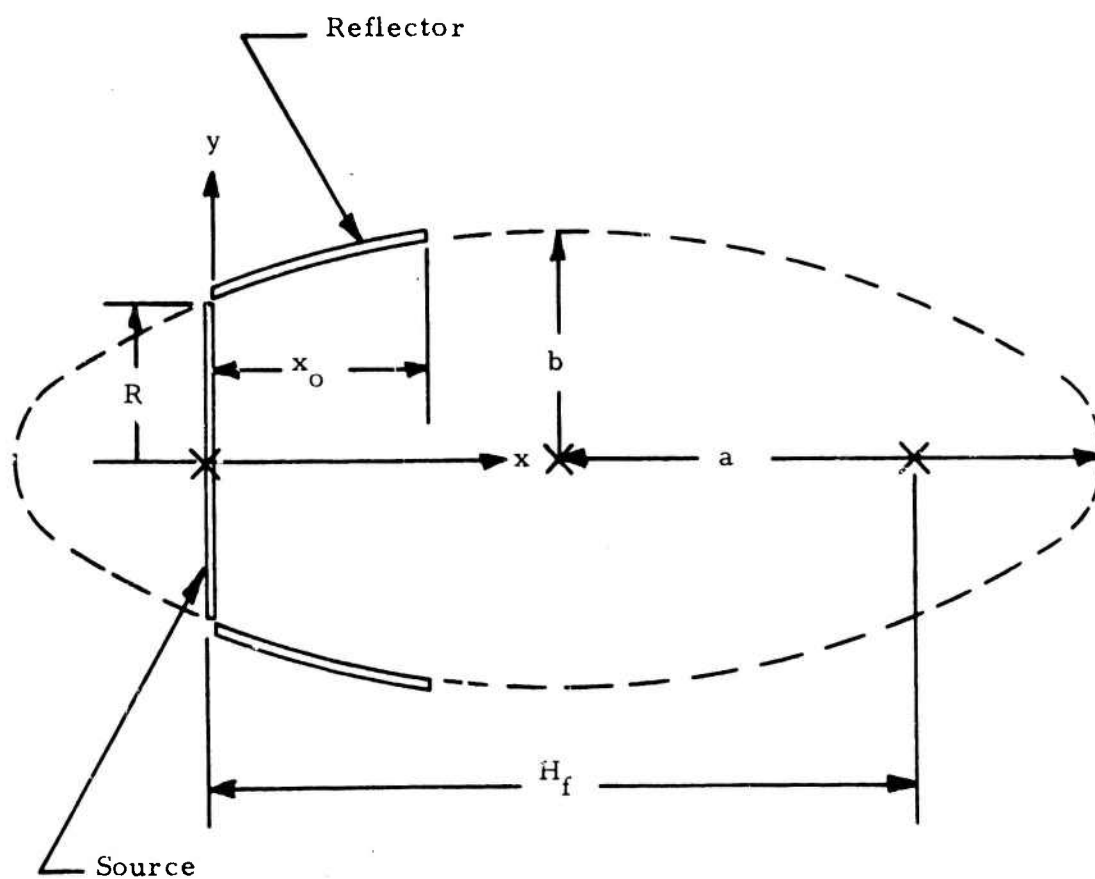


Figure A-15 Geometry of Ellipsoidal Reflector

where

a is the major radius
b is the minor radius
 H_f is the distance between the foci

Then from geometry,

$$R = \frac{b^2}{a} \quad \text{and} \quad \frac{H_f}{2} = \sqrt{a^2 + b^2} \quad (\text{A-30})$$

Solving for a and b gives

$$\left. \begin{aligned} \frac{a}{R} &= \frac{1}{2} \left[1 + \sqrt{1 + \left(\frac{H_f}{R}\right)^2} \right] \\ \left(\frac{b}{R}\right)^2 &= \frac{1}{2} \left[1 + \sqrt{1 + \left(\frac{H_f}{R}\right)^2} \right] \end{aligned} \right\} \quad (\text{A-31})$$

Substituting Equation (A-31) into (A-30) yields

$$\frac{4 \left(\bar{x} - \frac{\bar{H}_f}{2}\right)^2}{\left(1 + \sqrt{1 + \bar{H}_f^2}\right)^2} + \frac{2}{1 + \sqrt{1 + \bar{H}_f^2}} (\bar{y}^2 + \bar{z}^2) = 1 \quad (\text{A-32})$$

where $\bar{x} = \frac{x}{R}$; $\bar{y} = \frac{y}{R}$; $\bar{z} = \frac{z}{R}$; $\bar{H}_f = \frac{H_f}{R}$

At the plane $\bar{z} = 0$, this equation reduces to

$$\bar{y}^2 = \frac{(1 + \sqrt{1 + \bar{H}_f^2})}{2} \left(1 - \frac{4 \left(\bar{x} - \frac{1}{2} \bar{H}_f\right)^2}{1 + \sqrt{1 + \bar{H}_f^2}} \right) \quad (\text{A-33})$$

Figure A-14 shows the shape of the ellipsoidal reflector for various values of H_f . For a typical target distance of $\bar{H}_f = 10$ to 20 and a practical design limitation on the reflector length of $\frac{x}{R} \approx 2$ to 3, the shape of the ellipsoid is not much different than the cone. Consequently results may be expected to be similar.

4.3.2 Analytical Formulation of Radiant Interchange

The analysis once again utilizes the optical image technique described in Section 4.2.1 of this Appendix. As discussed in that section, full image and partial image conditions are possible depending on the location of the receiver relative to the second focal point. As seen from Figure A-15 full image conditions occur for all $H \geq H_f$ and partial image conditions for all $H < H_f$. These are discussed separately in the following sections. The analyses is similar to that of Section 4.2.1.1

4.3.2.1 Radiant Interchange for Full Image Conditions

The radiation received at the target by reflection is given by

$$I_{ri} = e_r \left\{ \frac{\bar{y}_o^2}{\bar{y}_o^2 + (\bar{H} - x_o)^2} - \frac{1}{(1 - \bar{H}^2)} \right\} \quad (A-34)$$

where

I_{ri} = radiation intensity at the target due to reflected radiation

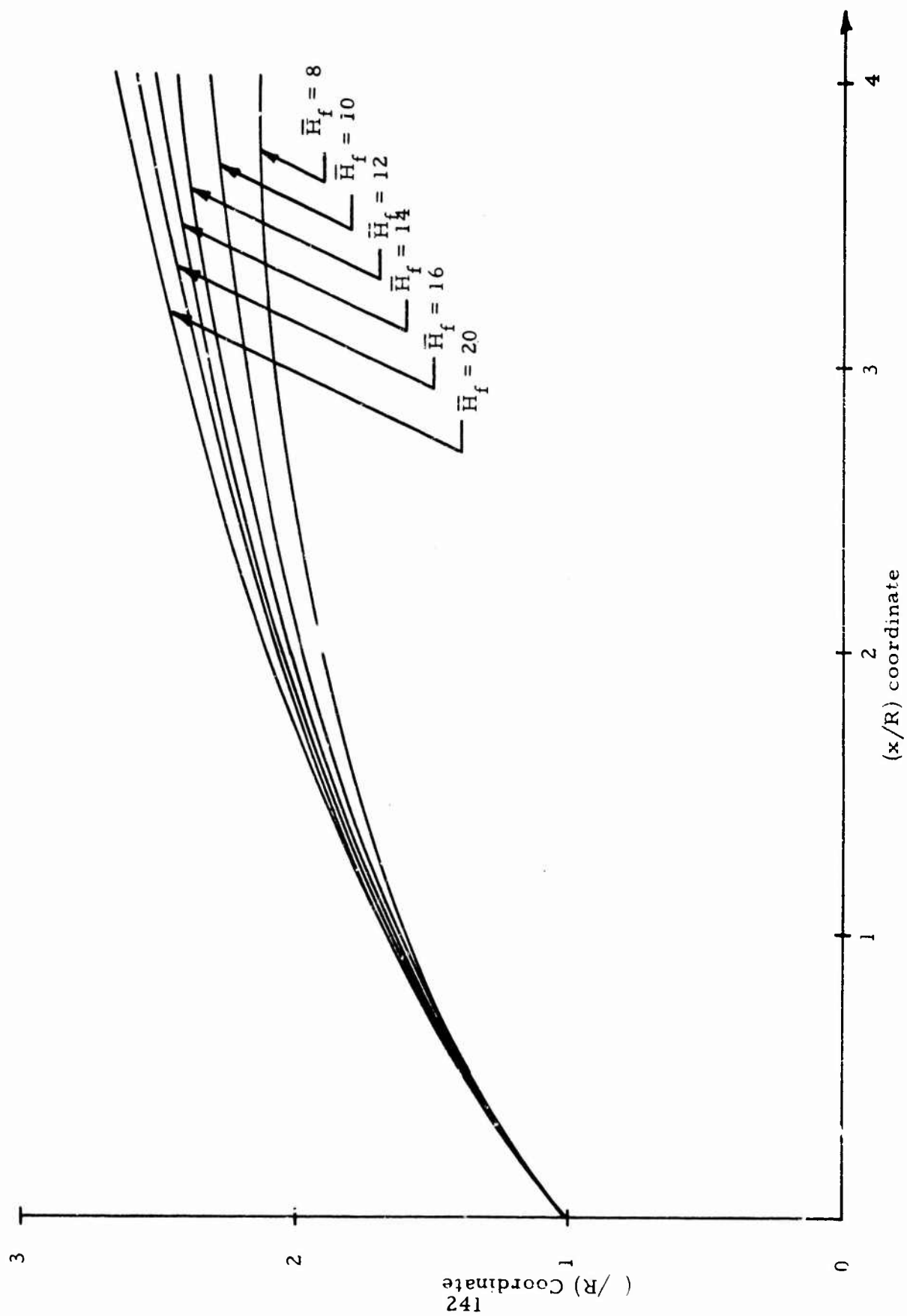


Figure A-14 Geometry of Ellipsoid for Various Focal Distances, \bar{H}_f

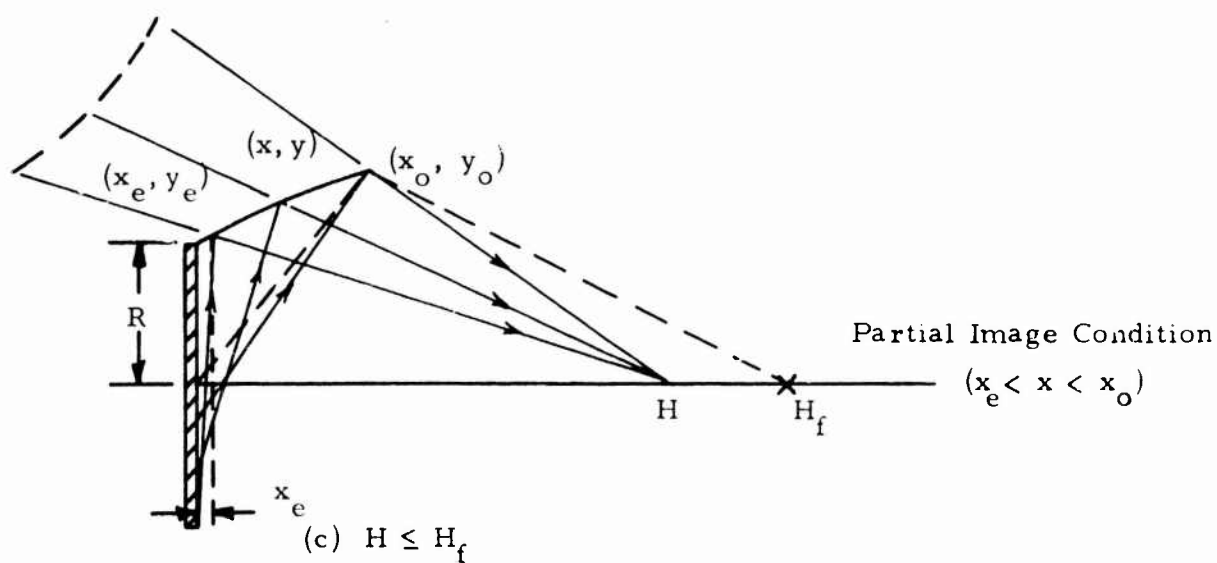
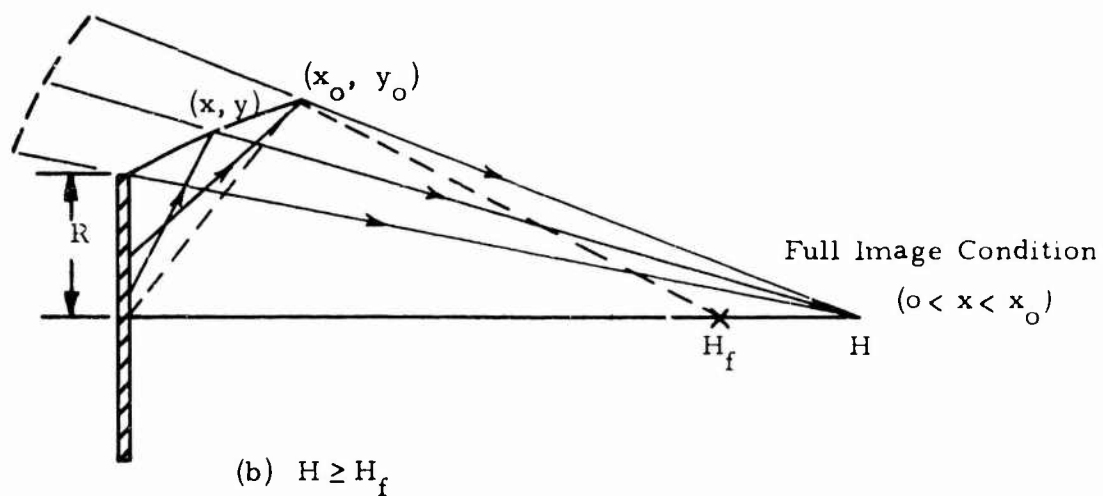
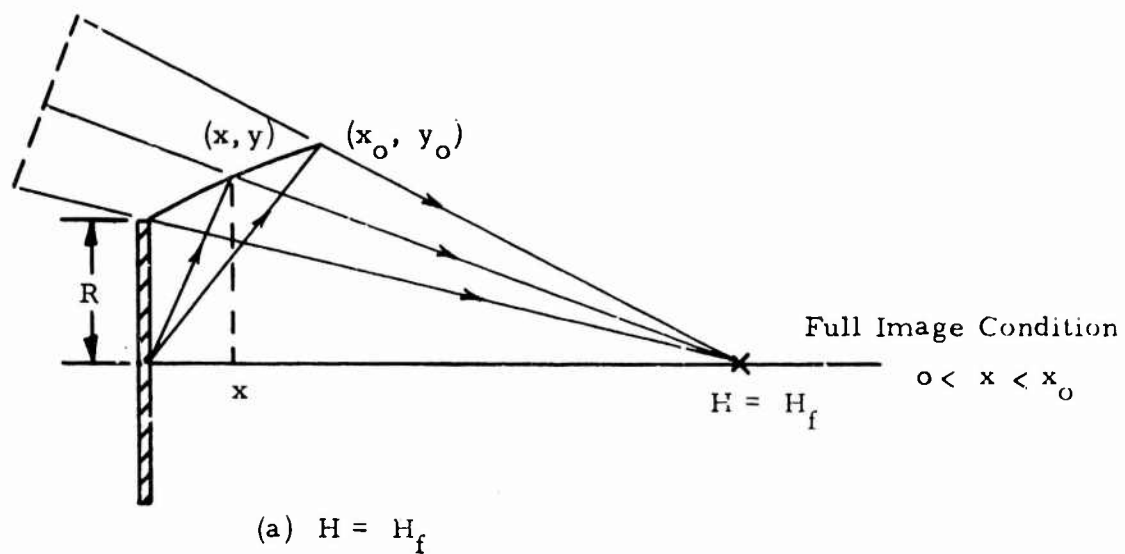


Figure A-15 Image of Source as Seen from Various Target Distances

e_r = average emissive power of the image

$\bar{x}_o = x_o/R$; $\bar{y}_o = y_o/R$ and $\bar{H} = H/R$

The radiation received by the target directly from the source is given by Equation (A-18) as

$$I_{rs} = e_s \left(\frac{1}{1 + \bar{H}^2} \right)$$

and

$$I_r = I_{ri} + I_{rs}$$

$$= e_s \left\{ \frac{1}{1 + \bar{H}^2} (1 - \gamma) + \frac{\gamma \bar{y}_o^2}{\bar{y}_o + (\bar{H} - \bar{x}_o)^2} \right\} \quad (A-35)$$

where

$$\gamma = \frac{e_r}{e_s}$$

An approximate value of γ is calculated by approximating the ellipsoid as a cone with an average half cone angle given by

$$\alpha = \frac{1}{2} (\alpha_o + \alpha_{x_o}) \quad (A-36)$$

where

α = average half cone angle
 α_o = half cone angle at $x = 0$
 α_{x_o} = half cone angle at $x = x_o$

α_o and α_{x_o} are obtained from

$$\tan \alpha_x = \left(\frac{b}{2} \right) \left(\frac{H_f}{2} - x \right) \left\{ 1 - \frac{1}{a^2} \left(\frac{H_f}{2} - x \right)^2 \right\}^{-1/2} \quad (A-37)$$

Then y can be obtained from Equation (A-23) using the α calculated from Equation (A-36).

4.3.2.2 Radiant Interchange for Partial Image Conditions

For the partial image condition, define the effective zone as given by $x_e < x < x_o$, where x_e is obtained from the condition,

$$\left(\frac{x_e}{y_e + R} \right) \tan (\beta_{x_e} + 2 \alpha_{x_e}) = 1 \quad (A-38)$$

where the nomenclature is defined for an arbitrary point x, y in Figure A-16.

The angle α_{x_e} is obtained from Equation (A-37) and β_{x_e} from

$$\tan \beta_{x_e} = \left(\frac{y_e}{H - x_e} \right) \quad (A-39)$$

Then, the total radiant intensity at the target due to the reflected and direct components is derived to be

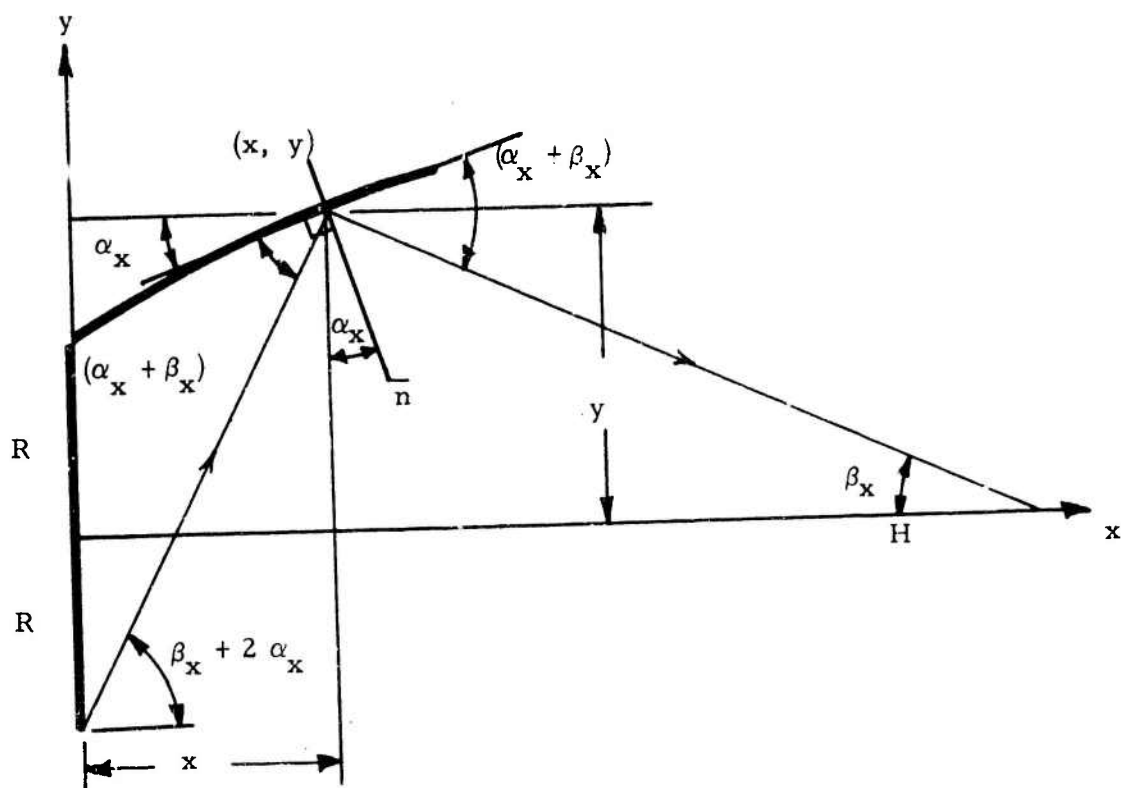


Figure A-16 Nomenclature Definition for Partial Image Conditions

$$I_r = \frac{e_s}{1 + \bar{H}^2} \left\{ 1 + \gamma \left[\frac{\bar{y}_o^2}{(\bar{H} - \bar{x}_o)^2 + \bar{y}_o^2} - \frac{\bar{y}_e^2}{\bar{y}_e^2 + (\bar{H} - \bar{x}_e)^2} \right] \right\} \quad (A-40)$$

The value of γ is obtained by using an equivalent conical reflector with a half cone angle equal to the average over $x = x_e$. The relationship is similar to that of Equation A-28.

4.3.3 Sample Designs

The theoretical relationships describing the performance of the ellipsoidal reflector are complex. A digital computer program was utilized to calculate sample designs. The following four design cases were evaluated.

Design Case Number	Local Design Distance, H_f	Reflector Length, \bar{x}_o
1	10	1
2	10	2
3	20	1
4	20	2

Radius of source, $R = 0.5$ ft

Source Temperature, $T_s = 1500^\circ\text{F}$

Room Temperature, $T_o = 20^\circ\text{F}$

Emissive power of source, $e_s = 25,204$ BTU/hr-ft²

The results of the computations are presented in Figures A-17 and A-18.

The computed performance is seen to be similar to that obtained with a conical reflector. The magnification factor is sensitive to the ellipsoidal reflector length but relatively insensitive to the focal distance. The ellipsoidal reflector is less effective when the receiver is located close to the heater. A conical reflector is therefore recommended over an ellipsoidal, being similar in performance and less expensive to fabricate.

4.4 Radiation From a Cylindrical or Tubular Source with a Parabolic Reflector

The parabola can be visualized as an ellipse whose second focal point is at infinity. Thus radiation emanating from a point (or small diameter) source located at the focal point emerges as a parallel beam of radiation after reflection. This reflector has the potential capability of providing a uniform radiant intensity on target areas located from 4 to 10 ft away from the source. However, for such a case the source area would have to be small (i.e. a high intensity source), and the diameter of the parabola be as large as the target diameter, which is impractical. Dispersion of the beam due to finite area effects need to be considered. The analysis for a tubular source is discussed in this section and that for a point source in Section 4.6 of this Appendix.

4.4.1 Line Source with Parabolic Reflector

Using the coordinate system shown in Figure A-19 a parabolic reflector can be described mathematically as

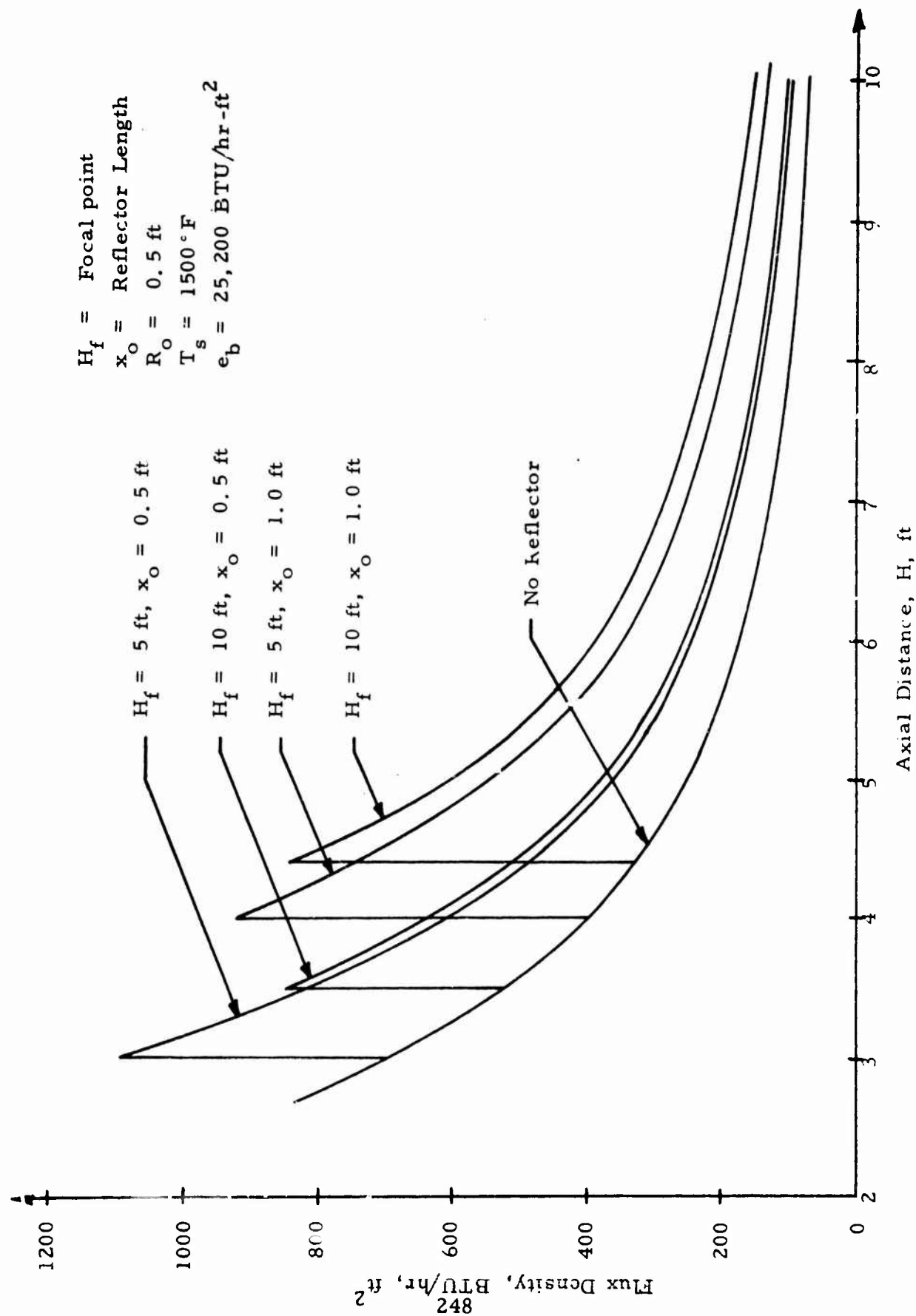


Figure A-17 Axial Flux Density Distribution for Ellipsoidal Reflector with Circular Disc Source

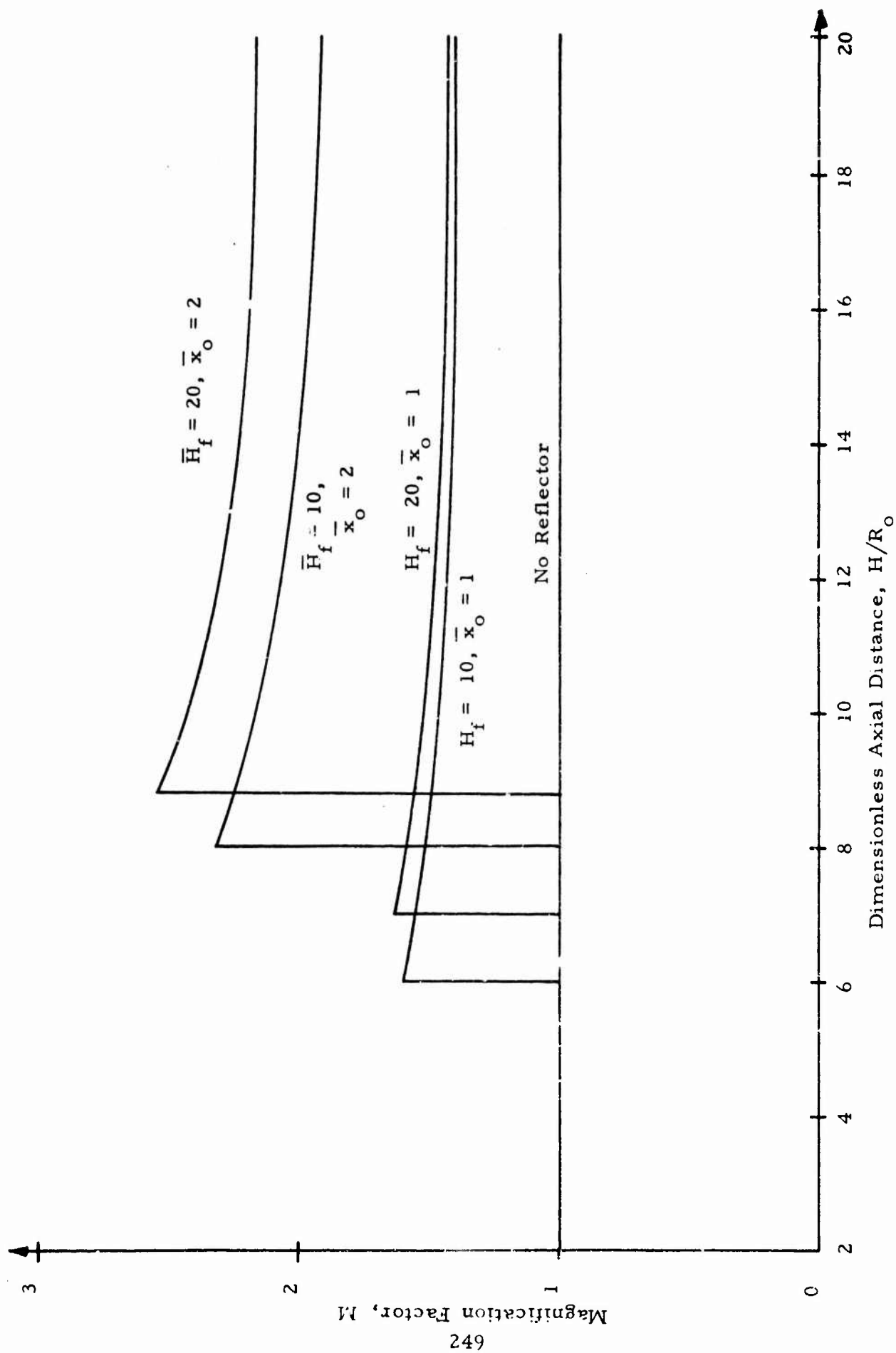


Figure A-18 Magnification Factor for Ellipsoidal Reflector for Disc Source

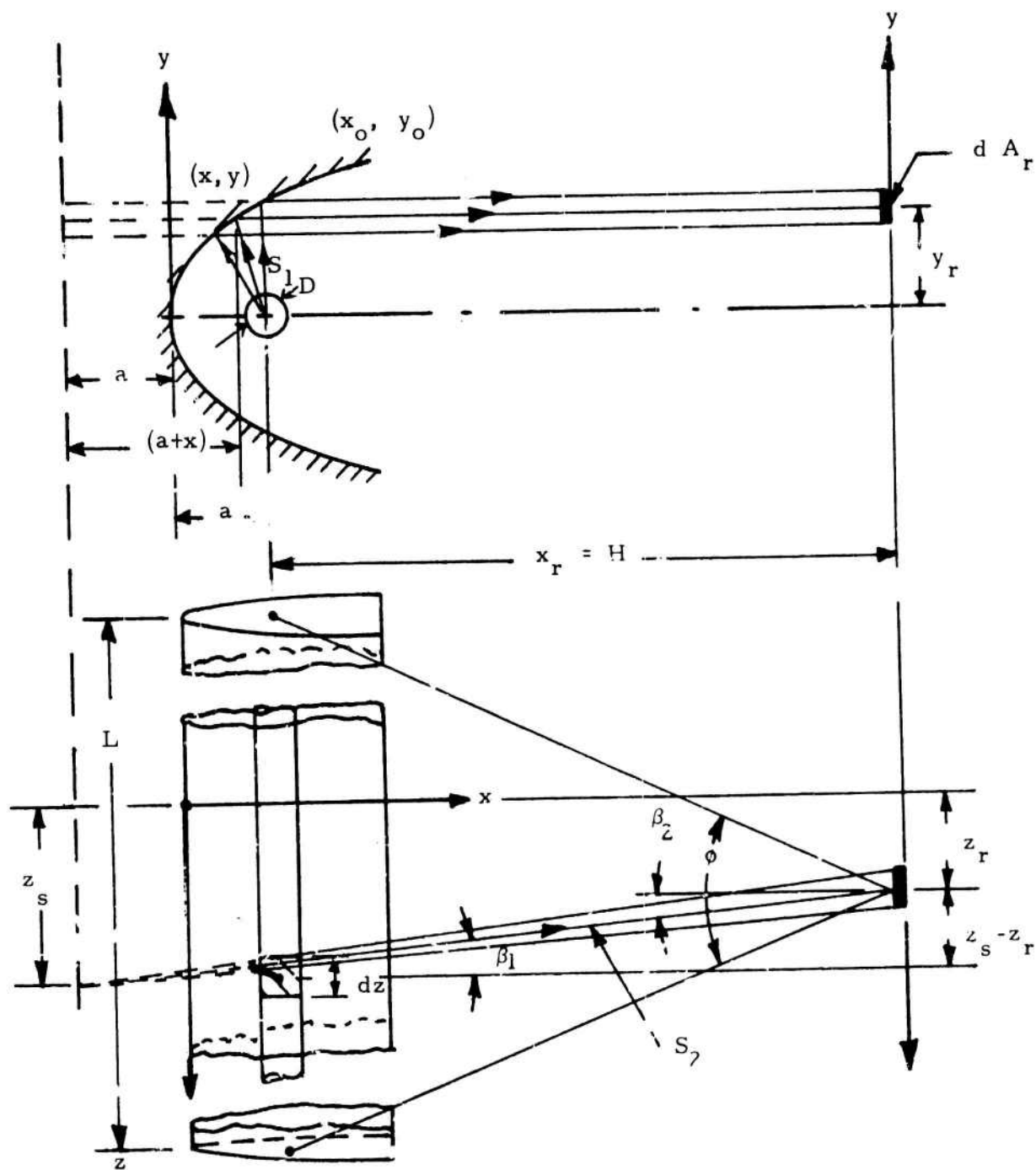


Figure A-19 Geometry of Line Source-Parabolic Reflector

$$y = \sqrt{4 a x} \quad (A-41)$$

where

a = focal length

A tubular source of very small diameter can be considered to be a line source for all practical purposes. The reflected beam from a line source located at the focal point of the parabola will be parallel in the plane normal to the source axis but will disperse in the plane of the source axis as shown in Figure A-19.

Now the heat transferred from an elemental length dz of the source located at $z = z_s$ to an elemental receiver area dA_r through the reflector is given by

$$dI_{ri} = (D dz, d\omega_1) \frac{e_s}{\pi} \cos \beta_1 \quad (A-42)$$

where

- D is the diameter of the tubular source
- dz is the elemental length of the source
- $d\omega_1$ is the solid angle subtended by the receiving area dA_r located at x_r, y_r, z_r
- e_s is the emissive power of the source
- β_1 is defined in Figure A-19

The solid angle, $d\omega_1$, is given by

$$d\omega_1 = \frac{dA_r \cos \beta_2}{S_1 (S_1 + S_2)} \quad (A-43)$$

where

$$\begin{aligned} S_1 &= \left\{ (a+x)^2 + \left[\frac{S_1 (z_s - z_r)}{S_1 + S_2} \right]^2 \right\}^{1/2} \\ S_2 &= \left\{ (H-x)^2 + (z_s - z_r)^2 \left(1 - \frac{S_1}{S_1 + S_2} \right)^2 \right\}^{1/2} \end{aligned} \quad (\text{A-44})$$

$$\cos \beta_1 \cong \cos \beta_2 = \frac{H-x}{\sqrt{(H-x)^2 + (z_s - z_r)^2}}$$

When the receiver distance H is much larger than the size of the reflector, $S_1 \ll S_2$ and the equations can be approximated by

$$\left. \begin{aligned} S_1 &= a+x \\ S_2 &= \sqrt{(H-x)^2 + (z_s - z_r)^2} \\ \text{and } d\omega_1 &= \left(\frac{H-x}{x+a} \right) \left\{ \frac{dA_r}{(H-x)^2 + z_r^2} \right\} \end{aligned} \right\} \quad (\text{A-45})$$

The total heat flux from the entire source to a unit receiving area $dA_r \cos \beta_2 = 1$ is

$$I_{ri} = \frac{e_s}{\pi} D \left(\frac{H-x}{x+a} \right) \int_{-\frac{L}{2}}^{\frac{L}{2}} \frac{dz_s}{(H-x)^2 + (z_s - z_r)^2} \quad (\text{A-46})$$

thus,

$$I_{ri} = \frac{e_s}{\pi} \frac{D}{x+a} \cdot \phi \quad (\text{A-47})$$

$$\text{where } \phi = \tan^{-1} \left(\frac{z + \frac{L}{2}}{H - x} \right) + \tan^{-1} \left(\frac{\frac{L}{2} - z}{H - x} \right) \quad (\text{A-48})$$

The heat transferred due to direct radiation from the source is given by

$$I_{rs} \cong \frac{e_s H D}{\pi \sqrt{H^2 + y_r^2}} \quad (\text{A-49})$$

Thus the total radiation heat transferred to the receiver is

$$I_r = \frac{e_s}{\pi} D \left[\frac{\phi}{x + a} + \frac{H}{\sqrt{H^2 + y_r^2}} \right] \quad (\text{A-50})$$

and the magnification factor M is given by

$$M = 1 + \frac{(H^2 + y_r^2) \phi}{H (x + a)} \quad (\text{A-51})$$

For a parallel beam, $x = \frac{y_r^2}{4a}$

This solution is valid for $y_r \leq \sqrt{4ax_0}$. When $y_r > \sqrt{4ax_0}$ the radiant intensity drops off to zero.

The view factor,

$$F_{sr} = \frac{D}{\pi} \left[\frac{\phi}{(x + a)} + \frac{H}{\sqrt{H^2 + y_r^2}} \right] \quad (\text{A-52})$$

This view factor distribution is calculated as a function of y_r and z_r for the numerical case specified in Figure A-20. The heat flux distribution (which follows the same pattern as the view factor) along the y_r axis drops off sharply. This could be improved by either using a larger source area and relying on dispersion for area coverage, as discussed in the following section, or wrapping the source-reflector system into a spiral of the type described in Section 5.2 of this report.

4.4.2 Large Diameter Cylindrical Source with Parabolic Reflector

For a source of diameter the same as the focal length of the parabolic reflector, the reflected beam is no longer parallel but disperses to provide a larger area coverage. The dispersion angle is shown in Figure A-21 and is expressed as

$$\sin \theta = \frac{r}{x + a} \quad (\text{A-53})$$

The dispersion angle becomes smaller as x increases. Therefore, the minimum dispersion will occur when $x = x_0$.

This dispersion angle has to be the same as the dispersion angle of the target. Thus,

$$\frac{x_0}{r} \leq \frac{\sqrt{H^2 + R^2}}{R} - \frac{a}{r} \quad (\text{A-54})$$

where R is the radius of the receiver.

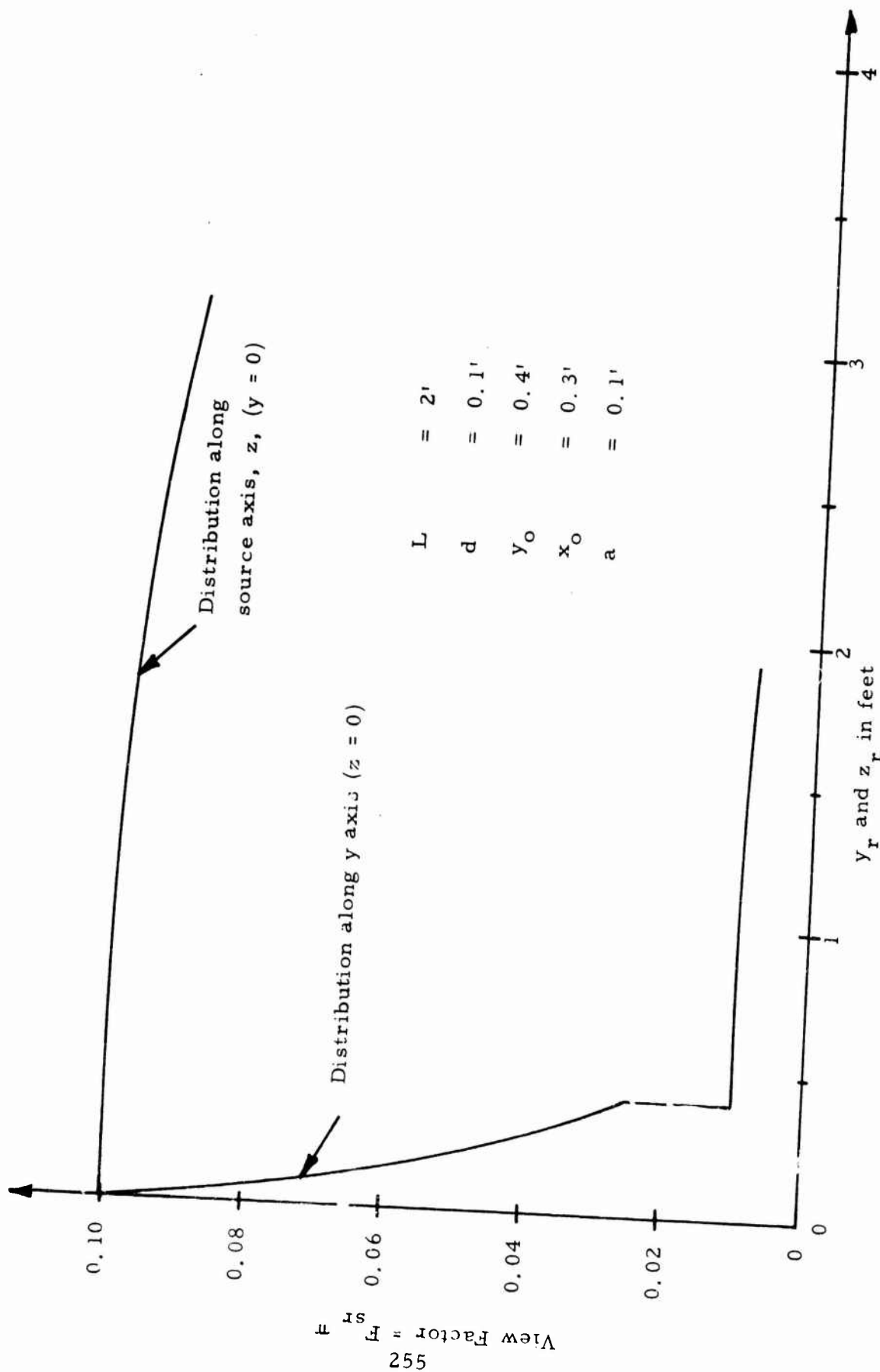


Figure A-20 Distribution of View Factor for a Tubular Source Parabolic Reflector Geometry

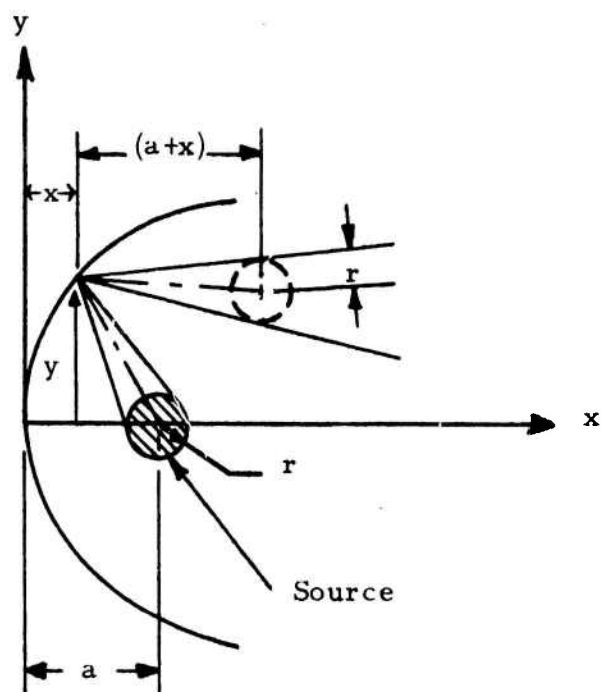


Figure A-21 Dispersion Due to Finite Source Area

The radiant heat flux including dispersion is obtained from Equation A-47 as

$$I_r = \frac{e_s}{\pi} \left(\frac{D}{x+a} \right) \left(\frac{r}{R} \right) \phi \quad (A-55)$$

The average \bar{R}_{FD} is given by

$$\bar{R}_{FD} = \frac{1}{\pi D L R} \int_0^{y_o} \frac{\phi}{\pi} \frac{D}{x+a} dy \quad (A-56)$$

For large values of L and x , ϕ is independent of x , hence,

$$\bar{R}_{FD} = \frac{2}{\pi R L} \left(\frac{\phi}{\pi} \right) \tan^{-1} \left(\frac{y_o}{2a} \right) \quad (A-57)$$

The heat transfer efficiency η_T is

$$\eta_T = R_{FD} \frac{A_T}{A_s} = \pi R^2 R_{FD} / A_s \quad (A-58)$$

For the design case where,

$D = 0.1$ ft; $L = 2$ ft; $H = 10$ ft and $R = 3$ ft;

$a = 0.1$ ft; $y_o = 0.284$ ft; $x_o = 0.2$ ft;

\bar{R}_{FD} is calculated to be 0.392 and $\eta_T = 17.65$ percent. Similarly, where $a = 0.1$ ft; $y_o = 0.4$ ft; $x_o = 0.4$ ft, $\bar{R}_{FD} = 0.5$ and $\eta_T = 20.8$ percent.

4.5 Hyperbolic Reflector with Tubular Source

4.5.1 Geometry of Hyperbolic Reflectors

Using the coordinate system of Figure A-22 the equation for the hyperbola is written as

$$\frac{(x - a)^2}{a^2} + \frac{y^2}{b^2} = 1$$

This can also be expressed in terms of the eccentricity e and focal length c as

$$\left(\frac{x}{c} - \frac{1}{e-1}\right)^2 + \frac{\left(\frac{y}{c}\right)^2}{(e+1)^2} = \frac{1}{(e-1)^2} \quad (\text{A-60})$$

where

$$e = \frac{\sqrt{a^2 + b^2}}{a}$$

$$c = \sqrt{a^2 + b^2} - a$$

As per the analysis of Section 4.4, the source dispersion angle, θ_s for a finite reflector length is expressed by

$$\tan \theta_s = \frac{\frac{y_o}{c}}{2 \left(\frac{e}{e-1}\right) - 1 + \left(\frac{x_o}{c}\right)} \quad (\text{A-61})$$

To disperse the radiation over the whole receiver area the source dispersion angle θ_s must equal the receiver dispersion angle θ_r given by,

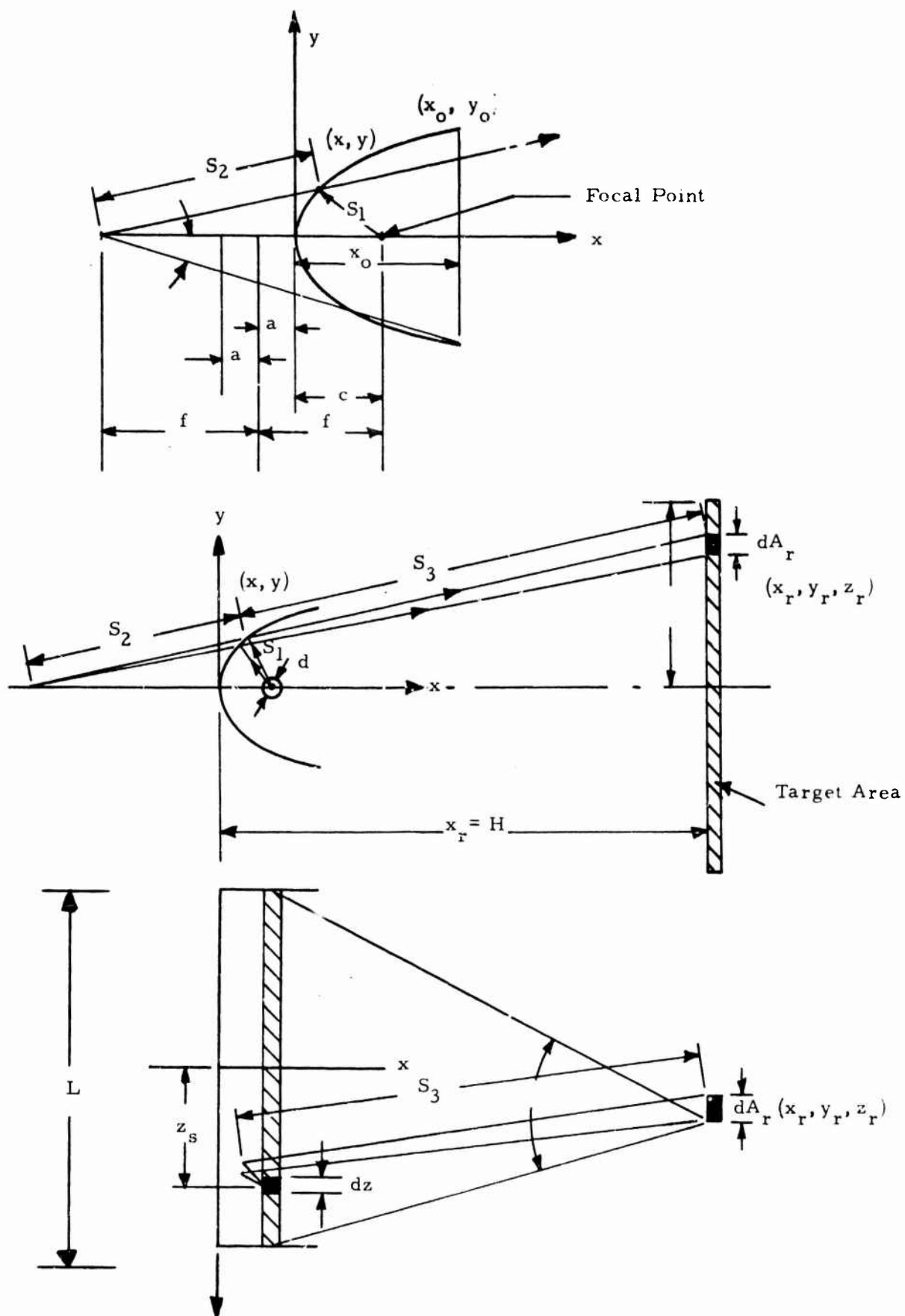


Figure A-22 Coordinate System for the Hyperboloidal Reflector

$$\tan \theta_r = \frac{R}{H}$$

where

R = radius of receiver

H = distance of receiver from the source

A solution of this equality results in the following relationships.

$$\frac{a}{f} = (1 + p) \sqrt{1 + \left(\frac{R}{H}\right)^2} - \sqrt{\left(\frac{p}{1 + p}\right)^2 + \left(\frac{R}{H}\right)^2}$$

$$\frac{c}{f} = \frac{1}{\left(1 - \frac{1}{e}\right)} \quad (\text{A-62})$$

and

$$p = \left(\frac{H - c}{2f}\right)$$

These relationships are sufficient to size a suitable hyperbolic reflector.

4.5.2 Analytical Formulation of Radiant Heat Transfer for a Small Source Diameter

The nomenclature used in the analysis is as defined in Figure A-22.

The radiant heat flux received by a unit area of the receiver located at x_r, y_r, z_r , is given by

$$d I_r = e_s \int_{A_s} d A_s \cos \beta_1 d \omega_1 \quad (A-63)$$

For $S_1, S_2 \ll S_3$, the solid angle $d\omega_1$ is approximated by

$$d\omega_1 \cong \frac{S_1 S_2}{S_3^2} \frac{\cos \beta_2 d A_r}{S_1^2} \quad (A-64)$$

where

$$\begin{aligned} S_3 &= \sqrt{x_r^2 + y_r^2 + z_r^2} \\ S_1 &= \left\{ (x - c)^2 + y^2 \right\}^{1/2} \\ S_2 &= \left\{ (2c + x - 1)^2 + y^2 \right\}^{1/2} \approx 2f \end{aligned} \quad (A-65)$$

Substitution of Equation (A-65) into Equation (A-63) and integrating over the source area A_s yields.

$$I_r = e_s d A_r \left(\frac{2f}{S_3} \right) \left(\frac{D}{S_1} \right) \phi \quad (A-66)$$

where

$$\phi = \tan^{-1} \left(\frac{z_r + \frac{L}{2}}{x_r} \right) + \tan^{-1} \left(\frac{\frac{L}{2} - z_r}{x_r} \right)$$

and the view factor \bar{F}_{rs} becomes

$$\bar{F}_{rs} = \frac{2 f D}{S_1 S_3} \left(\frac{\phi}{\pi} \right) \quad (A-67)$$

The heat transfer by direct radiation is negligibly small.

The flux density ratio R_{FD} is given by

$$R_{FD} = \frac{1}{\pi L} \left(\frac{2f}{S_3} \right) \left(\frac{1}{S_1} \right) \left(\frac{\phi}{\pi} \right) \quad (A-68)$$

Taking into account symmetry of the radiant intensity distribution over the receiver, an average value for R_{FD} is obtained

$$\bar{R}_{FD} = \left(\frac{1}{\pi L} \right) \left(\frac{2f}{S_3} \right) \frac{\phi}{\pi} \frac{1}{R} \int_0^R \frac{d y_r}{S_1} \quad (A-69)$$

The equation for η_T is difficult to integrate explicitly. A sufficiently accurate approximation is obtained by a linear variation for S_1 between $0 < y \leq y_0$.

As an example, for the sample design case of $L = 2$ ft, $D = 0.1$ ft, $f = 0.5$ ft, $a = 0.4$ ft, and $c = 0.1$ ft $H = 10$ ft, $R = 3$ ft and $\phi = 0.2$, calculations show that $\bar{R}_{FD} = 0.35$ and $\eta_T = 15.8$ percent.

4.6 Spherical Source with Paraboloidal Reflector

Using methods similar to that described for the line source, the radiant intensity at an elemental area $d A_r$ of the receiver due to the source is given by

$$I_r = e_s \frac{r^2}{S_1^2} d A_r \quad (A-70)$$

where

r = radius of the source and

$$S_1^2 = (x + A)^2 = \left[\left(\frac{y}{2a} \right)^2 + 1 \right] a^2$$

The average \bar{R}_{FD} is calculated on the assumption that the radiant heat flux contained in the parallel beam of radius y_o is uniformly distributed over the receiver of radius, R . Thus,

$$\begin{aligned} \bar{R}_{FD} &= \frac{1}{2 \pi R^2} \int_0^{y_o} \frac{y \, dy}{\left[\left(\frac{y}{2a} \right)^2 + 1 \right] a^2} \\ &= \frac{1}{\pi R^2} \left[\frac{\frac{x_o}{a}}{\frac{x_o}{a} + 1} \right] \end{aligned} \quad (A-71)$$

Typical Numerical Cases:

Case 1: $D = 0.1$ ft; $a = 0.1$ ft; $y_o = 0.284$ ft;
 $x_o = 0.2$ ft, $R = 3$ ft.

Calculated: $\bar{R}_{FD} = 0.074$ percent and $\eta_T = 67$ percent

Case 2: $D = 0.1$ ft; $a = 0.1$ ft; $y_o = 0.4$ ft; $x_o = 0.4$ ft;
 $R = 3$ ft

Calculated: $\bar{R}_{FD} = 0.089$ percent and $\eta_T = 80$ percent.

4.7 Spherical Source with Hyperboloidal Reflector

Using methods similar to those described for the line source, the R_{FD} is given by

$$\bar{R}_{FD} = \left(\frac{2f}{x}\right)^2 \frac{1}{4 \pi S_1^2} \quad (A-72)$$

where S_1 is given by Equation (A-65).

The average value of \bar{R}_{FD} is

$$\bar{R}_{FD} = \left(\frac{2f}{x}\right)^2 \frac{1}{4 \pi} \frac{2}{R^2} \int_0^R \frac{y_r d y_r}{S_1^2} \quad (A-73)$$

For the design case specified as

$$a = 0.4 \text{ ft}, b = 0.3 \text{ ft}, c = 0.1 \text{ ft}, x_0 = 0.2 \text{ ft}, y_0 = 0.3 \text{ ft}, \\ L = 2 \text{ ft}, \text{ and } D = 0.1 \text{ ft}.$$

The \bar{R}_{FD} is calculated to be 0.08 percent and η_T to be 72 percent.

APPENDIX A

LITERATURE CITED

1. Siegel Robert, and Howell, John R., "Thermal Radiation Heat Transfer," Vols. 1 and 2, NASA SP-14

APPENDIX B

SPATIAL DISTRIBUTION OF RADIANT FLUX DENSITY OVER THE RECEIVER AREA - THEORETICAL ANALYSIS AND COMPARISON WITH EXPERIMENTAL DATA

1. Introduction

The analysis of the previous sections has been devoted to investigating the design parameters affecting reflector design and the variation of the radiant heat flux intensity along the heater axis. Its utility for studying the relative performance of various source geometries and sizes and to predict the radiant flux distribution over the specified receiver area is limited. Accordingly, an approximate analysis was developed which predicts the flux distribution as obtained from these finite area sources. The results of this analysis were compared with actual measurements obtained as part of the experimental program. The good correlation obtained established the reliability of the predictive model. Various source-reflector combinations were sized to meet the specified heating requirements. The hemispherical heater source with a paraboloidal reflector was found to be the optimum. This data was subsequently utilized in the prototype design and testing of the hemispherical heater developed during this program.

This Appendix describes the analytical development of the approximate predictive model.

2. Analysis

Three common source shapes were analyzed:

- (1) Plane circular disc source

- (2) Cylindrical source with axis directed normal to the receiver area.
- (3) Hemispherical source.

The analysis was based on the following assumed conditions:

- (1) The radiating surface area of the source and its surface temperature are the same for all the source geometries so that they all emit the same total radiation.
- (2) An optimum reflector design is utilized, as discussed in Appendix A , so that the image of the source as seen from any point on the receiver area fills the whole reflector.
- (3) The reflectors are designed to lie within an overall size envelope defined by $R_0 L$, where R_0 is the maximum radius of the reflector and L is its maximum length as shown in Figure B-1.
- (4) The source and the receiver are perfect black bodies and the reflectors are perfect with reflections of unity.

Then the radiation intensity at any point, A, on the receiver as shown in Figure B-1 is given by,

$$I_R = I_0 \omega_d + I_r \omega_r \quad (B-1)$$

where

$$I_0 = \text{radiant intensity of the source}$$

$$= \frac{\sigma}{\pi} (T_s^4 - T_o^4) \text{ BTU/hr-ft}^2\text{-rad}$$

I_r = radiant intensity of the image of the source.

ω_d = solid angle for direct radiation from the source area.

ω_r = solid angle for radiation from reflected image area.

T_s = black body temperature of the source

T_o = temperature of the ambient

The solid angles are obtained as,

$$\omega_d = \frac{\pi R_s^2 \cos \beta}{\left(1 - \frac{L_s}{H}\right) s^2} \quad (\text{B-2})$$

$$\begin{aligned} \text{with } s^2 &= (H^2 + y_r^2) \\ \text{and } \omega_r &= \frac{\pi (R_o^2 - R_i^2)}{s^2 \left(1 - \frac{L_s}{H}\right)} \cos \beta \end{aligned} \quad (\text{B-3})$$

The radiation intensity I_r of the image has to be such that the total flux radiated from the image is equal to the total flux incident on it from the source. Thus if the image area is larger than the source its intensity would necessarily be reduced.

The image area is a function of both the meridional and longitudinal curvatures of the reflector. However for the geometries under consideration the

meridional curvature is very small, and for these conditions the intensity of the image can be approximated as

$$I_r = I_o \left(\frac{\bar{R}_s}{\bar{R}_e} \right) \quad (B-4)$$

where \bar{R}_s = average radius of the source area

$$\begin{aligned} \bar{R}_e &= \text{average radius of effective reflector area} \\ &= \frac{1}{2} (R_o + R_i) \end{aligned}$$

Combining these equations results in

$$I_R = \frac{J_o}{s^2} \left\{ \frac{\pi R_s^2}{\left(1 - \frac{L_s}{H}\right)^2} + \frac{\pi (R_o^2 - R_i^2)}{\left(1 - \frac{L}{H}\right)^2} \left(\frac{\bar{R}_s}{\bar{R}_e} \right) \right\} \cos \beta \quad (B-5)$$

$$\text{where } \cos \beta = \frac{1}{\sqrt{1 + \left(\frac{Y}{H}\right)^2}}$$

For off-axis points on the receiver, this relationship has to be corrected to allow for shading of the image area by the reflector, as shown in Figure B-2. For $y > R_o$, this effect causes a reduction in the flux intensity at the receiver.

From Figure B-2, the reduction in maximum radius of the image due to shading is given by

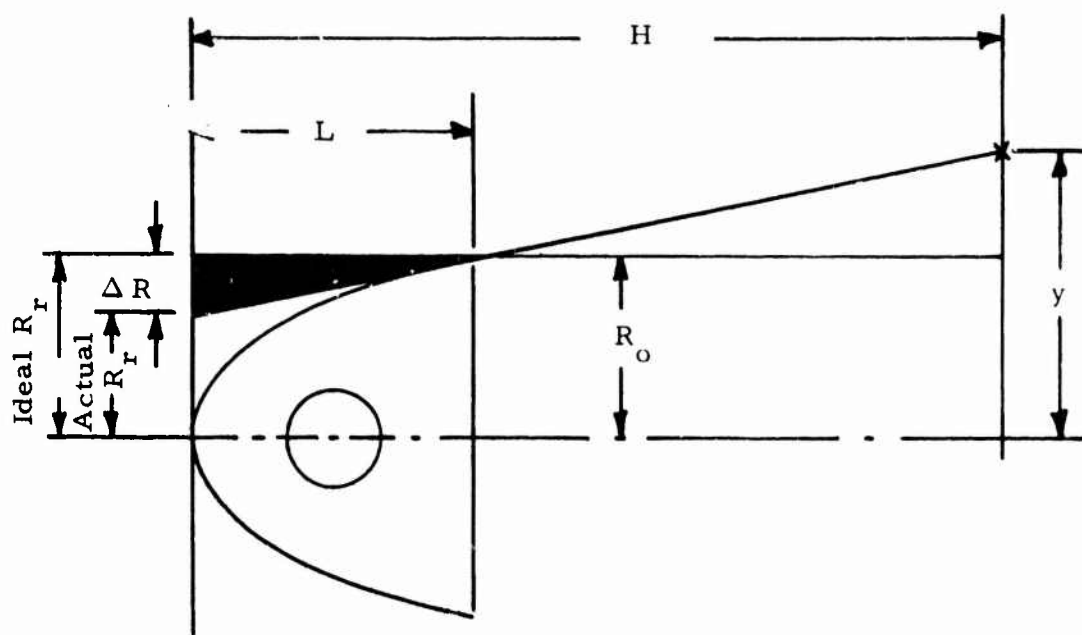


Figure B-2 Reduction in Image Area due to Shading of Reflector

$$\Delta R = L \left(\frac{y_r - R_o}{H - L} \right) \quad (B-6)$$

This is accounted for in Equation B-5 by a shading correction factor f_s defined by

$$f_s = \frac{A_{es}}{A_e} \quad (B-7)$$

where

A_e = ideal effective image area

A_{es} = actual effective image area allowing for shading

Using Equation (B-6) this can be written as

$$f_s = 1 - \frac{\frac{y_r}{R_o} - 1}{2 \left(\frac{H}{L} - 1 \right)} \quad \text{for } y_r > R_o$$

$$= 1 \quad \text{for } y_r \leq R_o \quad (B-8)$$

and Equation B-5 is rewritten as

$$I_R = \frac{I_o}{s^2} \left[\frac{\pi R_s^2}{\left(1 - \frac{L_s}{H}\right)^2} + \frac{\pi (R_o^2 - R_i^2)}{\left(1 - \frac{L}{H}\right)^2} \cdot \frac{\bar{R}_s}{\bar{R}_e} \right] f_s \cos \beta \quad (B-9)$$

This is an approximate equation to calculate the radiant flux density distribution at the receiver.

3. Numerical Calculation of Radial Flux Density Distributions at the Receiver for Various Source Geometries

The radial flux density distribution was calculated using Equation B-9 for the radiant heaters tested in the experimental program and the results compared with experimental data.

3.1 Disc Source (GFP Gasoline Heater)

The GFP gasoline heater with the large conical reflector, shown in Figure 52 was used for comparison. Its representative dimensions in inches are:

$$R_o = 12, R_i = 7, L = 12, R_s = 6, \\ \text{and } \bar{R}_e = 9.5, \bar{R}_s = 3$$

The preheater caused a reduction in the effective source area of 30 percent. Test measurements were made at an average black body source temperature, $T_s = 1200^\circ\text{F}$ and a corresponding $I_o = 3660 \text{ BTU/hr-ft}^2\text{-rad}$.

Figure B-3 shows a comparison of experimental and theoretical values for radiant flux density for the gasoline heater at receiver distances of $H = 4$ and 8 ft . The error between calculated and measured values is seen to be quite small.

3.2 Cylindrical Source (Pyrocore Heater)

The Pyrocore heater with its original parabolic reflector has the following dimensions in inches:

$$R_o = 5.75, R_i = 1.25, R_s = 1.25, L = 5.5, L_s = 2.5 \\ \text{and } \bar{R}_s = 1.25, \bar{R}_e = 3.5$$

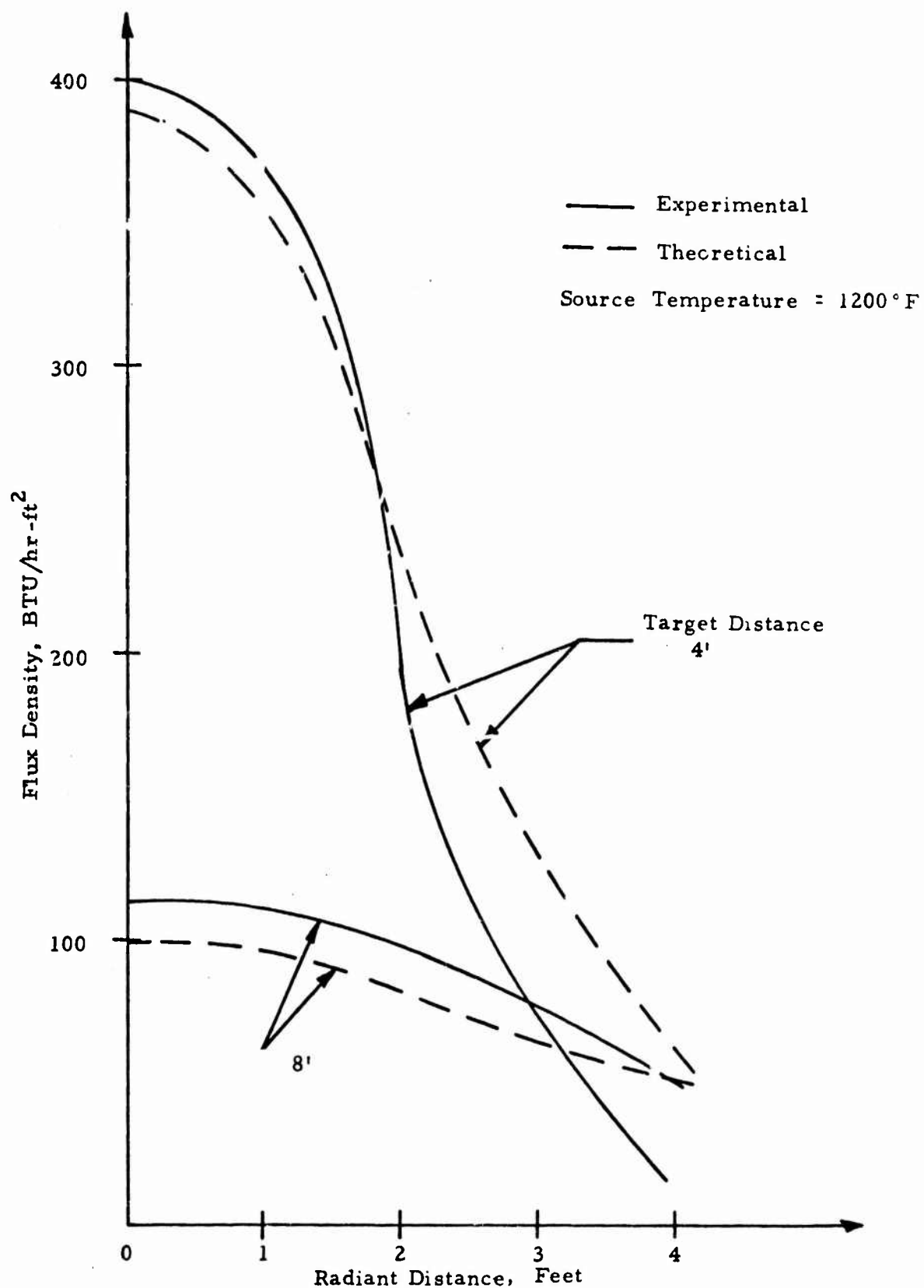


Figure B-3 Comparison of Experimental and Theoretical Values of the Radiant Flux Density Distribution at the Target from the GFP Gasoline Heater with the Long Conical Reflector

Test measurements were made at an average black body source temperature, $T_s = 1570^\circ\text{F}$ and a corresponding $I_o = 9300 \text{ BTU/hr-ft}^2\text{-rad}$. Figure B-4 shows a very good correlation between calculated and measured values of the radiant heat flux distribution at receiver distances of 4 and 8 feet from the heater.

3.3 Cylindrical Source (HOT-TOT)

The Hot-Tot heater with the conical reflector has the following dimensions in inches:

$$R_o = 11.5, R_i = 5, R_s = 4.25, L = 12, L_s = 6$$

$$\text{and } \bar{R}_s = 4.25, \bar{R}_e = 4.25$$

Test measurements were made at an average black body source temperature $T_s = 1540^\circ\text{F}$ and a corresponding $I_o = 8750 \text{ BTU/hr-ft}^2\text{-rad}$. Figure B-5 shows a good correlation between calculated and measured values of the radiant heat flux distribution at receiver distances of 4 and 8 feet from the heater.

3.4 Hemispherical Source

The Foster-Miller Associates radiant heater using a Turbo-Torch burner, a hemispherical source, and a paraboloidal reflector has the following dimensions in inches:

$$R_o = 12, R_i = 2, R_s = 3, L = 8, L_s = 5$$

$$\text{and } \bar{R}_s = 1.5, \bar{R}_e = 7$$

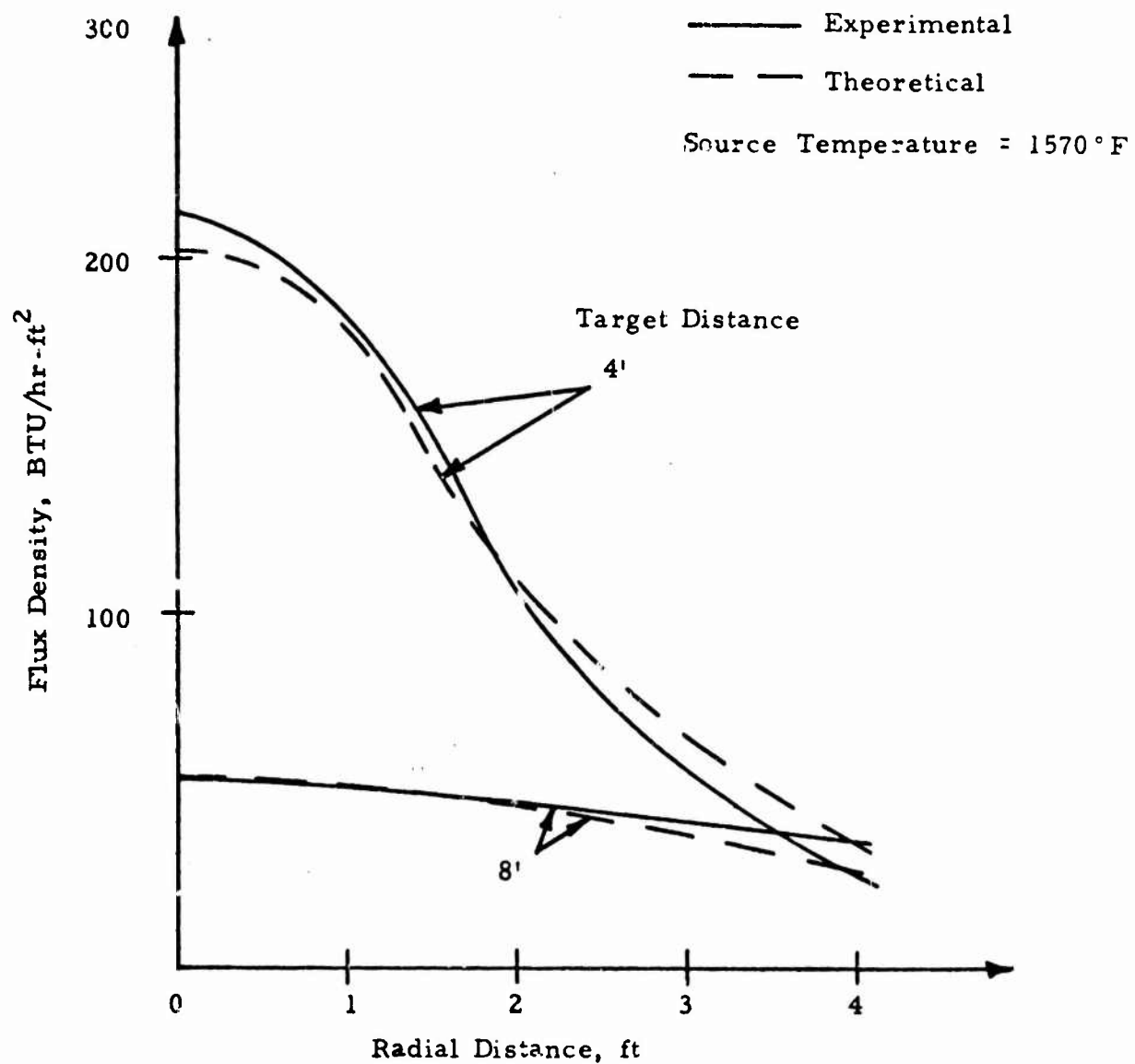


Figure B-4 Comparison of Experimental and Theoretical Values of the Radiant Flux Density Distribution at the Target from the Pyrocore Heater

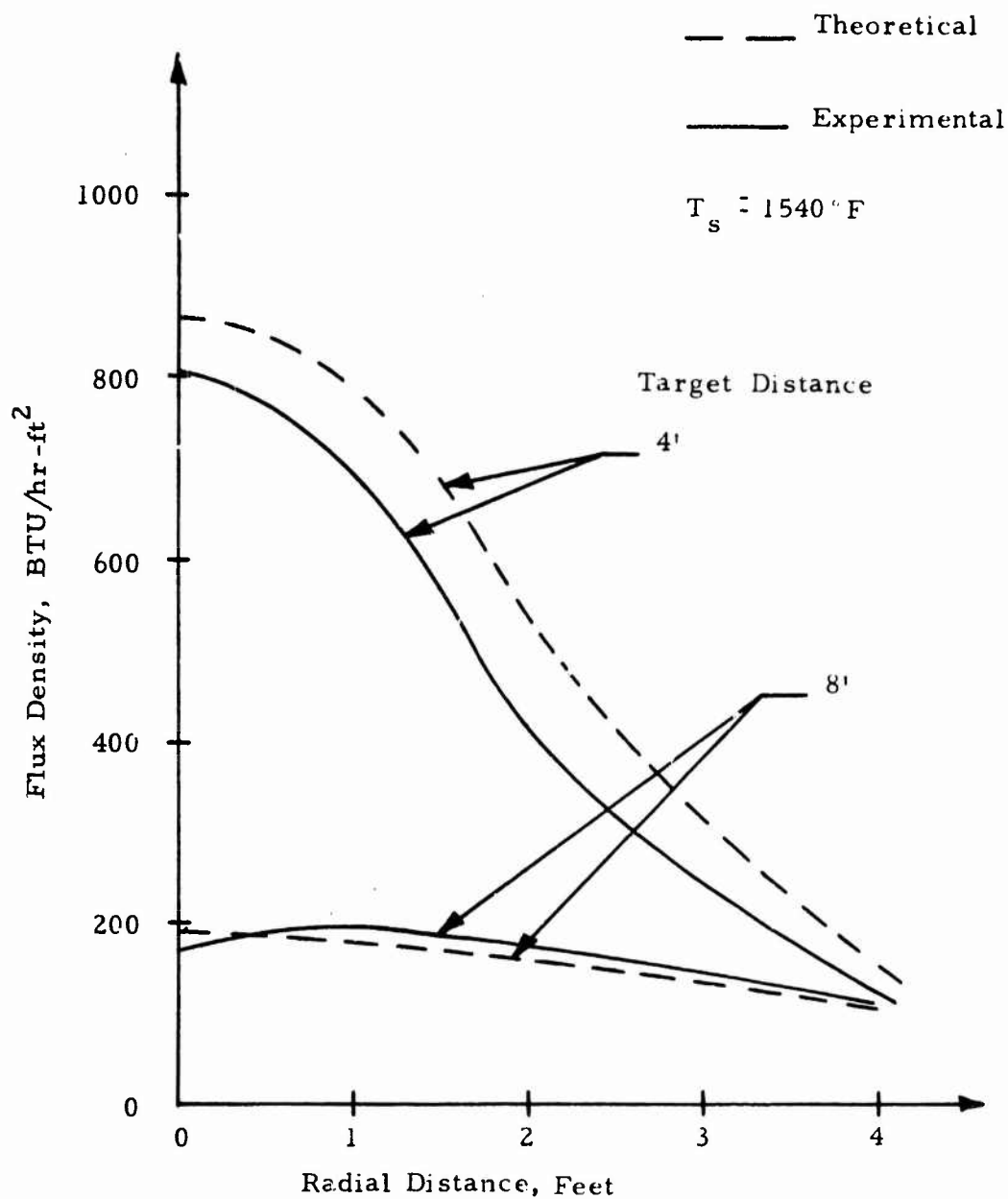


Figure B-5 Comparison of Experimental and Theoretical Values of the Radiant Flux Density Distribution of the Hupp Hot-Tot Heater

Test measurements were made at an average black body source temperature of $T = 1450^{\circ}\text{F}$ and a corresponding $I_o = 6960 \text{ BTU/hr. ft}^2 \text{ rad.}$ Figure B-6 shows a comparison between calculated and measured values. The measured performance is seen to be much lower than theoretical predictions. This is felt to be due to a non-optimum reflector. As discussed in Section 6.4.5 a hyperboloidal reflector design would possibly result in improved performance.

3.5 Conclusions

Based on the good correlation between calculated and measured values of the radiant heat flux distribution at the receiver for a variety of source geometries and reflectors it is concluded that Equation (B-9) is a good approximation for use in heater design.

4. Selection of Optimum Source - Reflector Design

Three source geometries, disc, cylindrical and hemispherical were theoretically compared under identical conditions of total heat flux radiated, that is source area and temperature, to select the optimum design. Each source was assumed to have an optimum reflector design to fit within the same overall envelope as discussed in Section 2 of this Appendix.

For the purposes of comparison, the values for the hemispherical heater were taken as standard, that is,

$$\text{source area} = A_s = 113 \text{ in}^2$$

$$\text{envelope} = LR_o = 96 \text{ in}^2$$

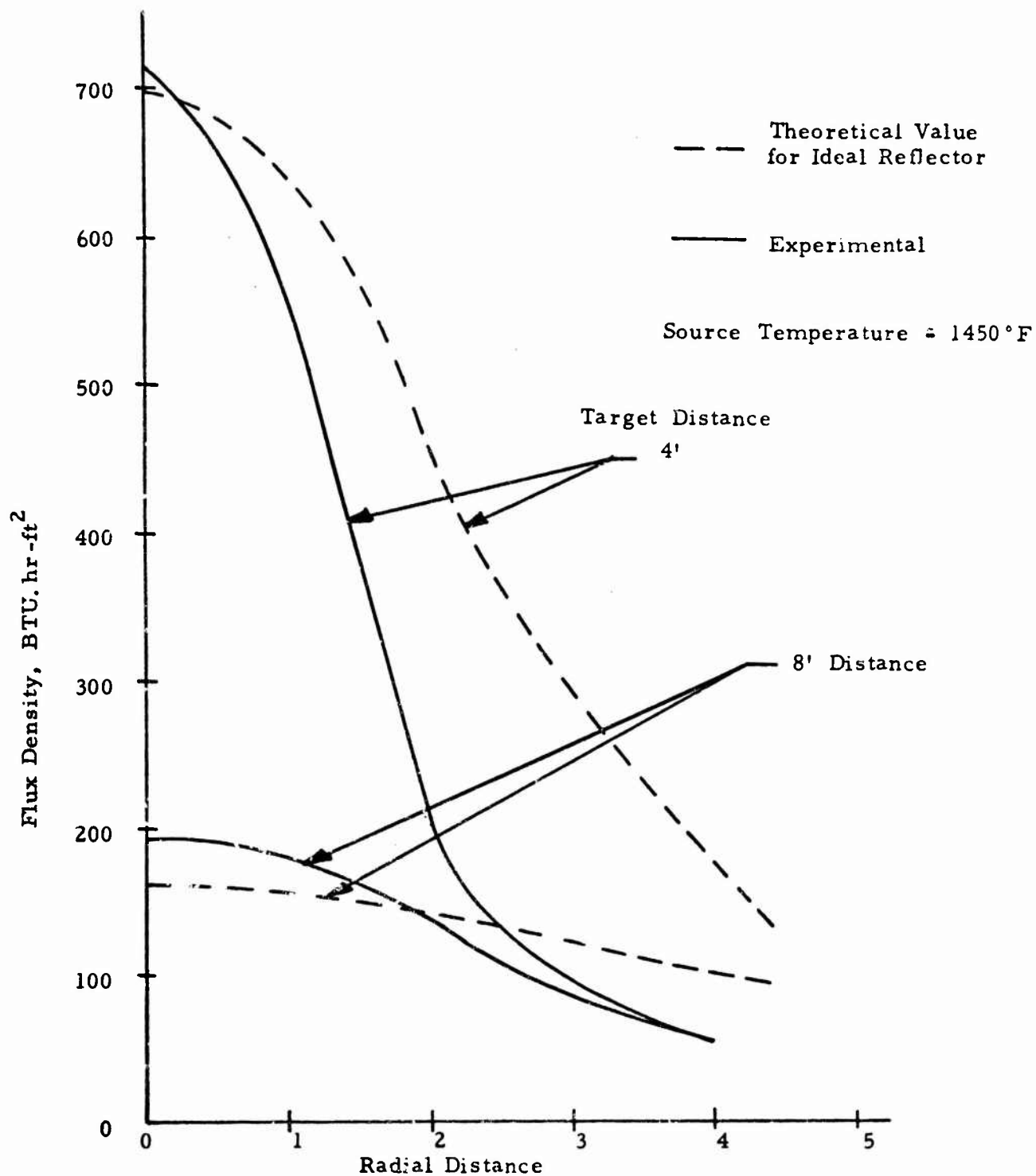


Figure B-6 Comparison of Experimental and Theoretical Values of the Radiant Flux Density Distribution at the Target from the Foster-Miller Hemispherical Source Radiant Heater

The corresponding heater dimensions in inches are:

- (1) Disc Source with Optimum Conical Reflector:

$$R_o = 8, R_s = 6, L = 9.5, \text{ cone angle} = 23^\circ$$

- (2) Cylindrical Source with Optimum Paraboloidal Reflector:

$$R_o = 12, R_s = 2, L = 8, L_s = 9$$

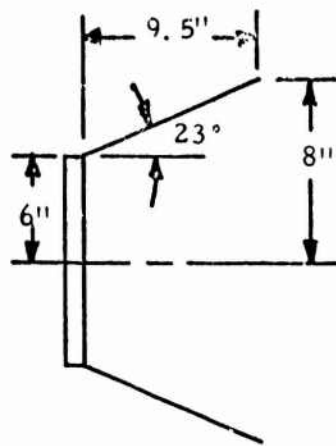
- (3) Hemispherical Source with Optimum Paraboloidal Reflector:

$$R_o = 12, R_s = 3, \text{ and } L = 8$$

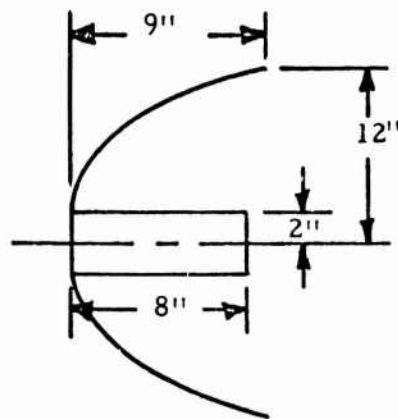
Figure B-7 shows schematically the relative size and configuration of these heaters.

The heater performance is compared in terms of the R_{FD} which represents the ratio of the flux density at the target to that of the source. Figure B-8 shows the distribution of R_{FD} over the target area for target distances of 4 and 8 feet.

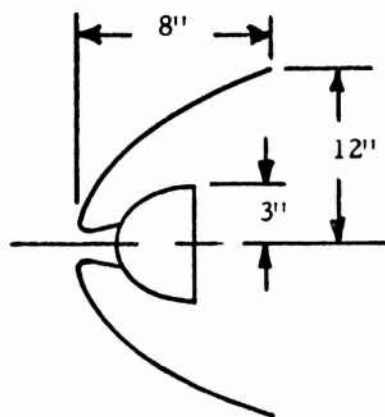
The results show that the R_{FD} from the hemispherical source heater is almost twice that from the disc source at a target distance of 4 ft and at least 50 percent greater at a target distance of 8 feet.



(a) Disc Source with Conical Reflector



(b) Cylindrical Source with Paraboloidal Reflector



(c) Hemispherical Source with Paraboloidal Reflector

Figure B-7 Optimum Source-Reflector Configurations

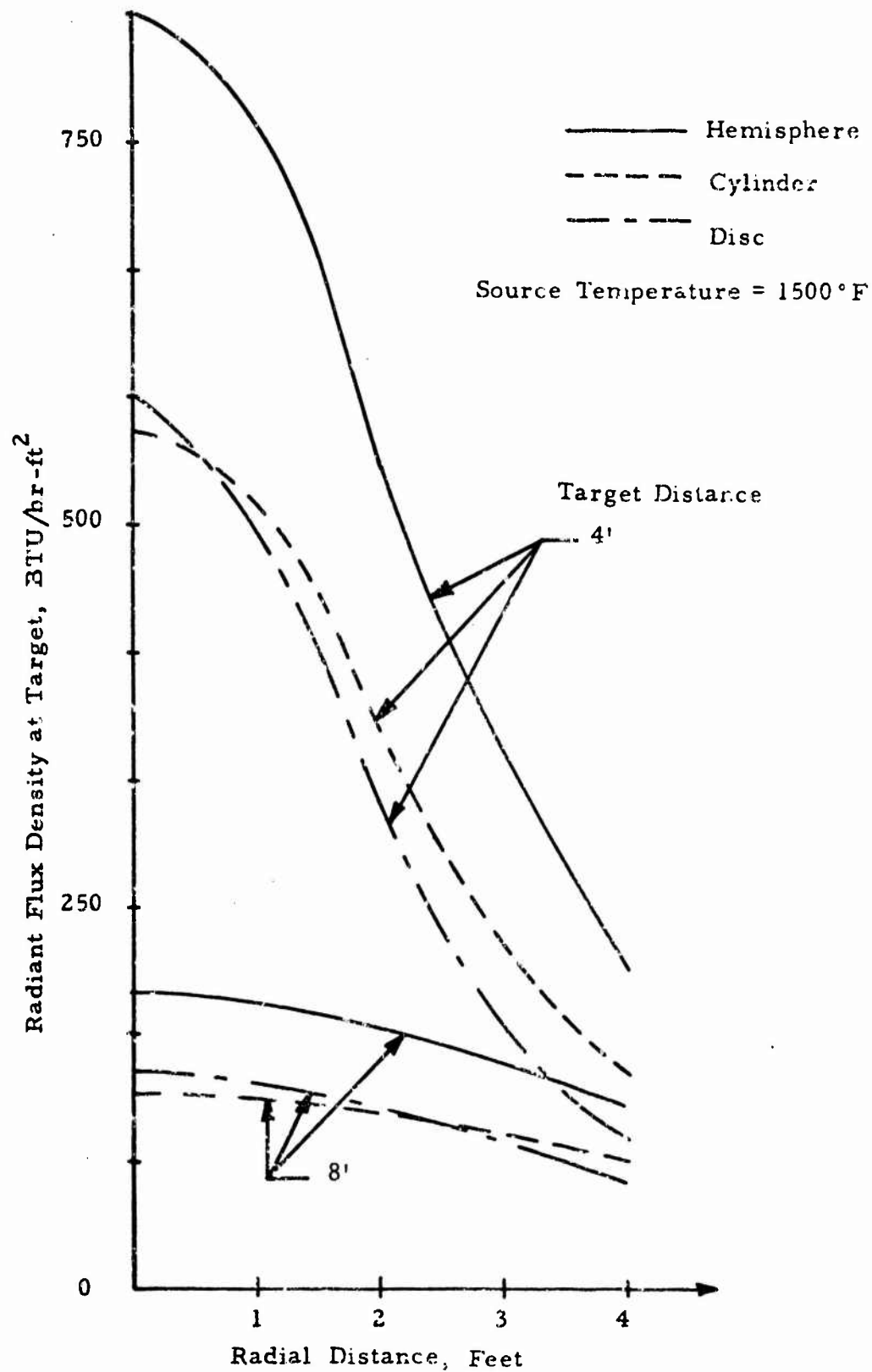


Figure B-8 Comparison of Relative Heating Performance of Different Source-Reflector Configurations

APPENDIX C

DESIGN SYNTHESIS OF A RADIANT BURNER

This Appendix discusses the development of a mathematical model to describe the operation of a fuel fired radiant burner. The analysis formed the basis for the design synthesis of a hemispherically shaped radiant burner.

1. Radiant Burner - System Description

A radiant heating system involves a radiant source, a target to receive heat, and usually a reflector or lens for beaming energy from one to the other. Beaming and reception are complex subjects discussed in Appendices A and B. However a radiant burner can be described rather independently.

A radiant burner system may be thought to consist of these components:

- (1) A mechanical energy source to force the air, fuel and mixed gases through the system;
- (2) A burner to react the fuel and stabilize the flame position;
- (3) A heat exchanger to extract the heat from the flame products by convection and deliver the heat by radiation.

Although it may not appear so for all radiant burners, the three functions are quite distinct, especially in a parametric description. In addition to the pumping, burning and heat transfer functions, some provisions are also required for start-ups and control.

Figure C-1 is the flow diagram of a most complex radiant burner system with mechanical pumping, air preheat and gas products re-heat. It illustrates the ultimate in radiant burner for these reasons:

- (1) Unlimited pumping head permits effective heat exchange.
- (2) Air preheat, unlimited heat exchange effectiveness and re-heat allow the radiant surface to be maintained near maximum possible material temperature.
- (3) Air preheating by exhaust gases minimizes the heat uselessly lost in the exhaust gases thereby minimizing fuel consumption.

These factors can lead to a compact burner and a small radiant surface, hence small reflector, without sacrificing fuel efficiency. However, this system is complex and costly to build. Consequently all portable radiant burners are simplified and consist of the following simple functional features:

- (1) A fuel-jet air inducer or "venturi" pump;
- (2) A single burner or flame-holding zone; and
- (3) Convective heat transfer from the exhaust gases to the radiator only (no air pre-heat)

The parameters and trade-offs for this latter type of radiant burner are described in the following sections.

A schematic arrangement of a simple radiant burner is shown in Figure C-2. Normal operation is as follows:

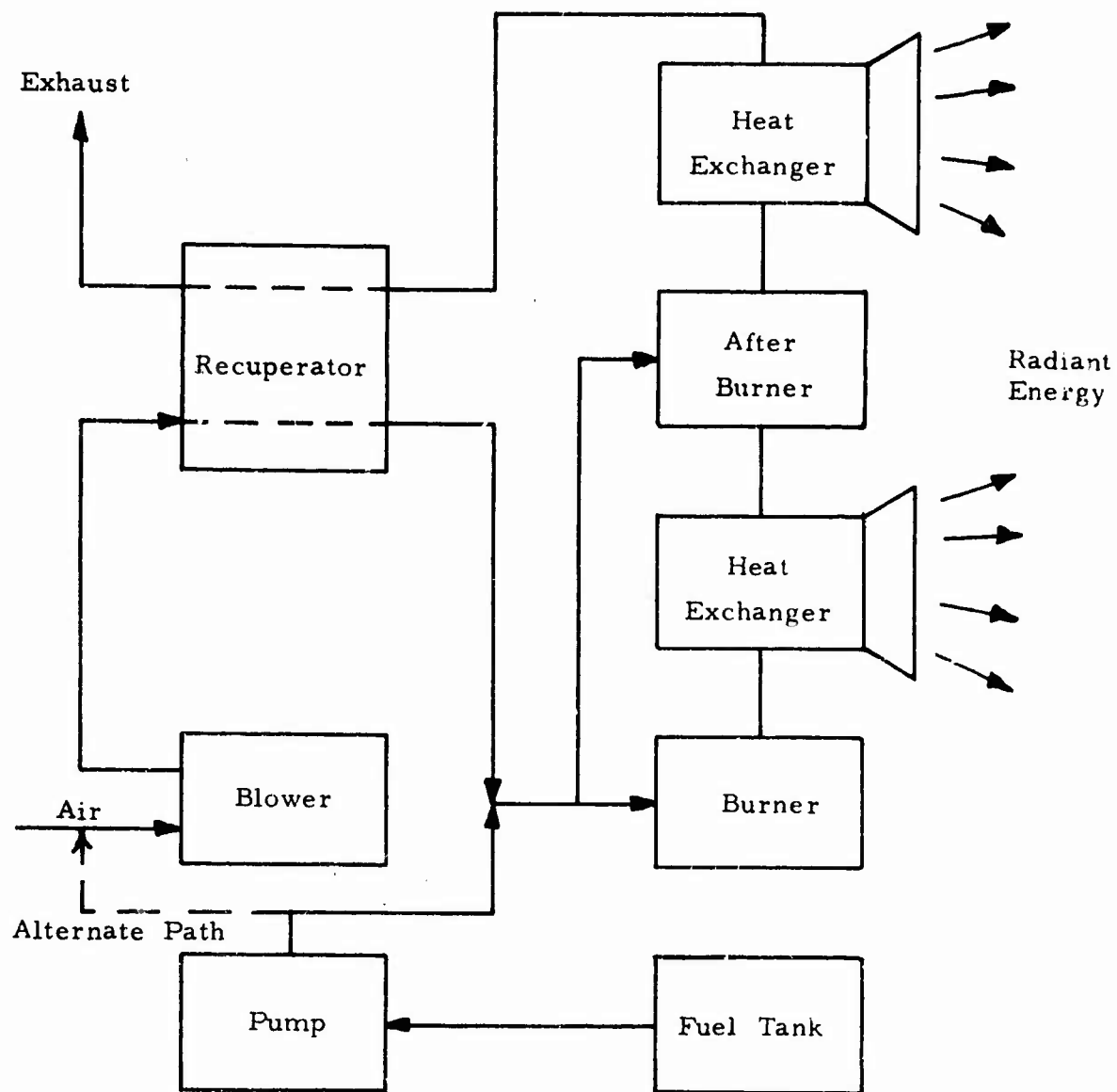


Figure C-1 Schematic of a Radiant Burner Showing Possible System Options

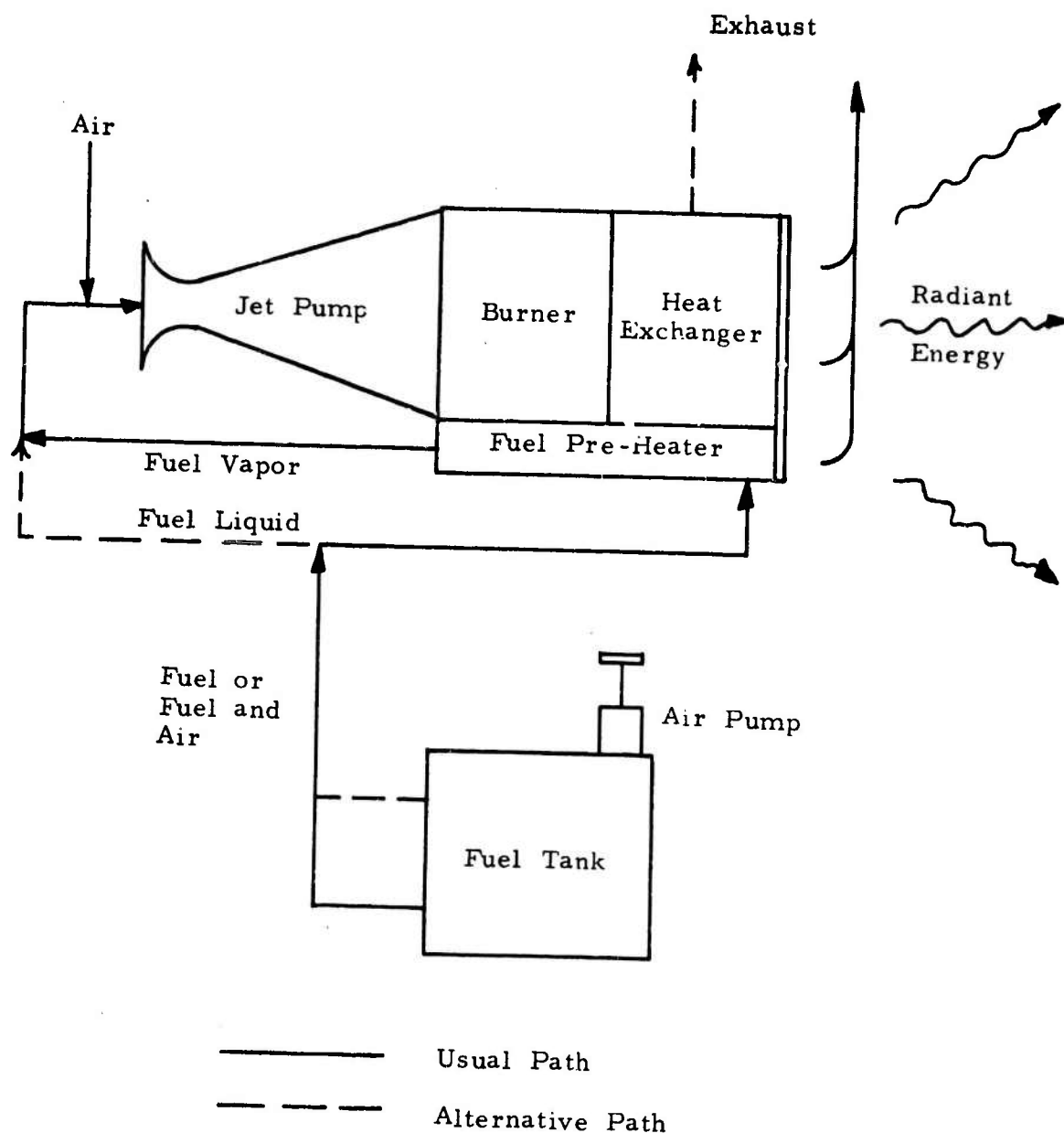


Figure C-2 Schematic of the Usual Simple Radiant Burner System

- (1) Pressurized air in the fuel tank causes liquid to flow to the fuel pre-heater;
- (2) Some heat extracted from the burned products vaporizes the fuel;
- (3) The jet momentum of the fuel vapor from the nozzle entrains air and produces pumping "total head" in the mixture;
- (4) The burner converts chemical to thermal energy, with some head loss;
- (5) The heat exchange surface extracts heat convectively from the products, with temperature differential and head loss;
- (6) The radiant surface, coincident with or conducting from the convection surface, delivers the heat extracted from the products.

The important points in this discussion are that the motive power, the burning, and the heat exchange are considered separately, and the jet pump must provide all the head for the latter functions.

The system can be described quantitatively in a fairly simple manner taking into account certain practical factors which limit or constrain the system design.

- (1) all of the typical fuels to be used in the present application have about the same heating value at

about the same stoichiometric air-fuel mass ratio.
(20K BTU/lb fuel at 15/1 air-fuel mass-ratio).

Richer or leaner mixtures will not burn properly and yield lower temperature products, which is always undesirable for fuel economy and heat transfer intensity.

- (2) The jet pumping properties, (sonic velocities and specific heat ratios) of the fuel vapor, inlet air and combustion products do not vary significantly with variable operation or different configurations.
- (3) The temperature range for operation of the radiating surface do not vary greatly for all good radiant burners, say between 1400 and 2100° F. Low radiant intensity is undesirable at the one extreme, material and heat transfer problems and high exhaust heat loss limit the upper temperature. Since this temperature range is small compared to the peak temperature of the burner products, about 3500°F, then the heat exchanger effectiveness can be adequately determined using a constant or mean temperature for the radiant surface.

2. Parametric Design of a Radiant Burner

The parametric design of a simple radiant burner must combine the following major factors:

- (1) the pressure rise in the fuel-air jet pump;

- (2) the pressure drop of the flow through the burner and through the convective heat exchange surface;
- (3) convective and conductive heat exchange to the radiant surface;
- (4) radiant release of heat.

These four factors are analyzed separately. The appropriate parameters are then matched to achieve an optimum design synthesis.

2.1 Jet Pump Design

As discussed in several reference works the maximum pressure rise possible in a jet pump is a function of mass flow ratios and inlet properties.¹ In dimensionless form

$$p_e/p_a = \theta (w_a/w_f, p_a/p_f, T_a M_f / T_f M_a, k_a/k_f, c_{pa}/c_{pf}) \quad (C-1)$$

where the symbols refer to

w	=	weight flow
p	=	pressure
T	=	temperature
M	=	Molecular weight
k	=	ratio of specific heats
c _p	=	specific heat, constant pressure

and the subscripts refer to

* Numbers refer to literature cited at the end of Appendix C.

a - ambient air
 f = fuel
 e = jet pump outlet

In the simple burner, many of the ratios are nearly fixed, and in addition, the optimum performance is rather insensitive to the more independent variables, such as fuel pressure and temperature. For instance, for typical fuel pressures, fuel preheat, and jet nozzle designs, the jetting velocity remains about 1000 fps. In our case the pressure rise is quite small, so the air flow is nearly of constant density, and the fuel flow is only about 7 percent of the air flow. Consequently, a very simplified analysis of the jet pump will illustrate its action and estimate the pressure rise adequately.

Referring to Figure C-3, the approximate expressions for momentum balance and fluid flow are:

$$(P_2 - P_1)g A = W_f (C - V) + W_a (V_a - V)$$

or

$$(P_2 - P_1)g A \approx W_f (C - V) + 0$$

$$(P_2 - P_1) \approx \frac{W_a}{gA} (C - V) \frac{W_f}{W_a}$$

$$(P_2 - P_1) \approx \frac{\rho V}{g} (C - V) \frac{W_f}{W_a} \quad (C-2)$$

$$P_3 = P_2 + \eta \frac{\rho}{2g} V^2 \quad (C-3)$$

$$P_a = P_1 + \frac{\rho}{2g} V^2 \quad (C-4)$$

$$\Delta P = P_3 - P_a \quad (C-5)$$

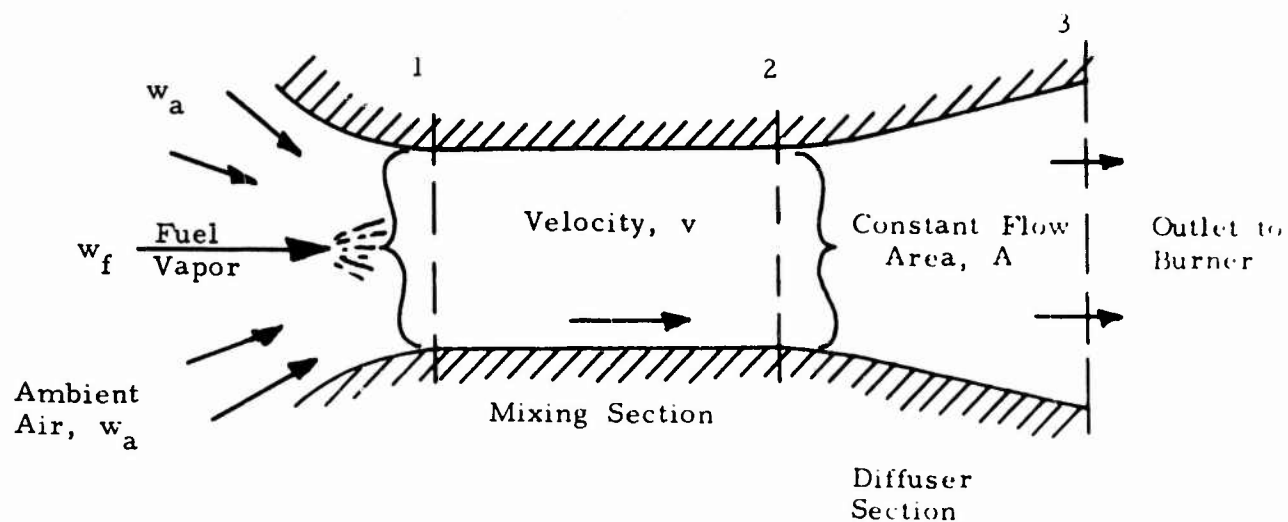


Figure C-3 Schematic of Jet Pump

where

P = pressure lb_f/ft^2

ρ = density lbm/ft^3

V = velocity in mixing section ft/sec

C = fuel vapor jetting velocity, near sonic ft/sec

g = gravitational constant $32.17 \frac{\text{lbm ft}}{\text{lb}_f \text{ sec}^2}$

η = diffuser efficiency dimensionless

ΔP = net pressure rise lb_f/ft^2

(This analysis neglects the change in air velocity in the mixing section, and includes all wall friction losses with diffuser efficiency.) If $c = 1000 \text{ fps}$, $w_a/w_f = 15$, and $\eta = 0.7$, the equations combine to:

$$\Delta p = \frac{\rho}{2} (133 v - 0.433 v^2) \quad (\text{C-6})$$

for which Δp is a maximum and equal to just over 2 inches of water gage when $v = 300 \text{ fps}$. This value compares well with experimental results obtained by the Wingaersheek Co., for air-fuel jet pumps designed for maximum Δp .²

The major conclusion from the above discussion is that in a typical radiant burner design a total pumping head of about two inches of water is available.

If less head is required for the system, a non-optimum jet pump design or an inlet damper valve may be used. If more head appears very desirable, slight gains may be achieved with higher fuel preheat, supersonic fuel nozzles, and multiple-staged pumps, but the effort may not be worth the cost.

2.2 Basic Burner Design

Burner design is a complex and rather experimental art. However, most design problems concern construction, control,

life, noise, and cleanliness, rather than the basic parameters of efficiency of burning and pressure drop. With premixing of air and fuel vapor, energy efficiency is usually above 95 percent, and pressure drop can be reduced simply by designing for a low through-flow velocity, if the geometric constraints are not severe.

Burner volume is little problem in the present application. For example, the low velocity burning zone of the Government furnished heater is about 1/4 inch deep by 12 inches in diameter (between honey-comb flame holder and wire screen) with a burning intensity of about $2 (10)^6$ BTU/hr ft³. At the other extreme, the high velocity Wingaersheek Turbo Torch flame zone is about 3 x 1 inch length by diameter, with an intensity of about $25 (10)^6$ BTU/hr ft³. Both burners have efficient combustion to near-stoichiometric flame temperature with about 30,000 BTU/hr heat release from the fuel. Between these extremes, a burner can be configured conveniently for any radiant heater with an acceptable pressure loss.

The pressure drop in a burner is caused in two ways: by fluid friction in the flameholder section and perhaps flame tube, and by acceleration of the flow due to temperature rise. Flame holding usually occurs at the end of a flow restriction (e.g. laminar flow tube matrix, porous sheet, bluff body, sudden expansion, or swirl vanes). From experimental correlations for fluid flow or drag the pressure loss is:

$$\Delta p = C_L \frac{\rho}{2g} v^2 = C_L \frac{G^2}{2\rho g} \quad (C-7)$$

where

C_L = dimensionless loss coefficient
 ρ = density

g = gravitational constant, $32.17 \frac{\text{lb}_m}{\text{lb}_f} \frac{\text{ft}}{\text{sec}^2}$
 G = weight flow rate per cross-sectional area, lb_m/ft^2
 v = velocity, ft/sec

The pressure drop due to burning acceleration in a constant area section (typical) is:

$$\Delta p = \left(\frac{1}{\rho_2} - \frac{1}{\rho_1} \right) G^2 / g =$$

$$(T_2/T_1 - 1) \frac{G^2}{\rho_1 g} \approx 7 \frac{G^2}{\rho_1 g} \quad (C-8)$$

where 1 and 2 subscripts are for up- and downstream condition. This pressure drop is usually a total loss because recovery or diffusion of the downstream dynamic head, $G^2/2 \rho_2 g$, is not accomplished.

Clearly, both forms of pressure loss can be reduced by reducing mass flow velocity, G_1 . For example the Wingaersheek Turbo Torch burner (1 in dia.) has a high-velocity burner pressure drop of about 2 inches of water, equal to the total pressure rise in the jet pump. If burner diameter were doubled for the same flow rate, pressure loss would be only about 1/8 inch.

2.3 Convective Heat Transfer

The objective for convective heat transfer design is to extract the maximum heat from the gases without exceeding the flow pressure drop available, using a geometry suitable for the radiant surface and convenient for mechanical design. There are many factors, analytic and practical, and many configurations may be investigated.

However, if a generally desired configuration is proposed for the radiant surface, the convective parameters can be studied in a fairly direct manner.

Specification of the radiant surface for the purpose of designing the convection surface requires a statement of the following:

- (1) Radiant area and general shape,
- (2) Surface temperature,
- (3) Heat rate per unit area

In addition there are two possible approaches to design based on whether (a) the gases flow through the radiant surface, or (b) the gases flow past but not through the radiant surface. These two basic approaches are shown in Figure C-4. The fundamental difference between the two approaches is that in (a) all, or most of the radiant surface will be cooler than the exhaust gas temperature; in (b) the radiant temperature of the surface can decrease as the hot gases cool, with only the terminal section of the radiant surface cooler than the exhaust gases. With method (b) either fuel efficiency can be increased, with a given mean radiant temperature but lower exhaust heat loss, or radiator size can be reduced with a higher mean temperature and the same efficiency, but not both independently. For preliminary design purposes it is usually satisfactory to consider the radiant surface at a constant temperature for either flow scheme, (a) or (b).

The heat extracted from the gases may be expressed simply as

$$Q_c = \eta_h w c_p (T_g - T_r) \quad (C-9)$$

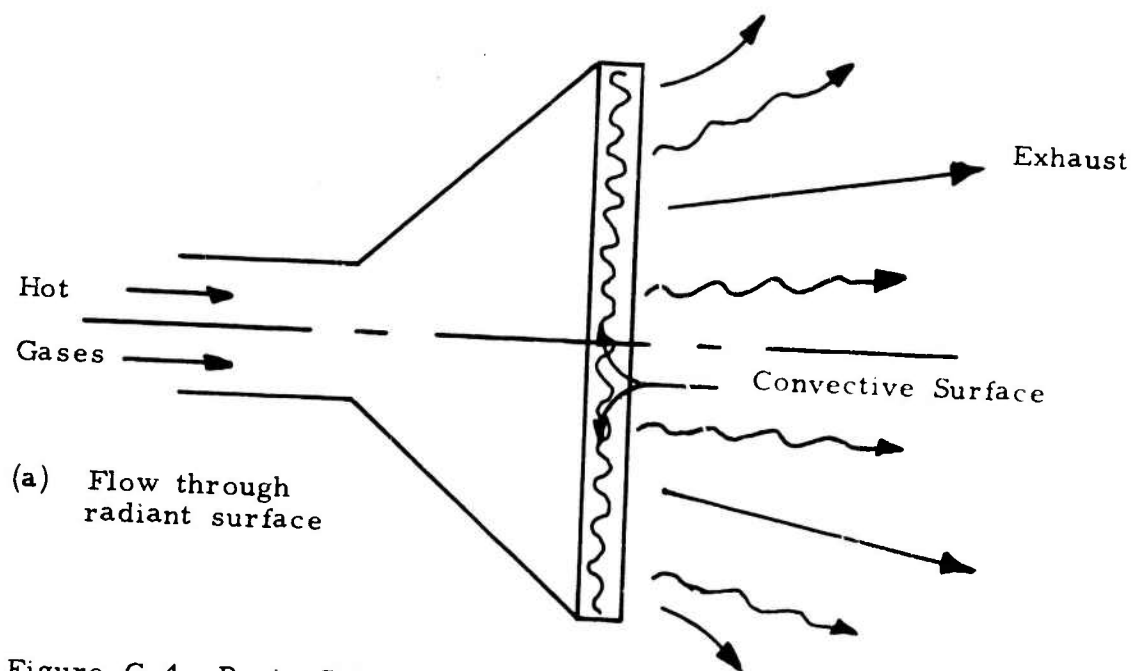
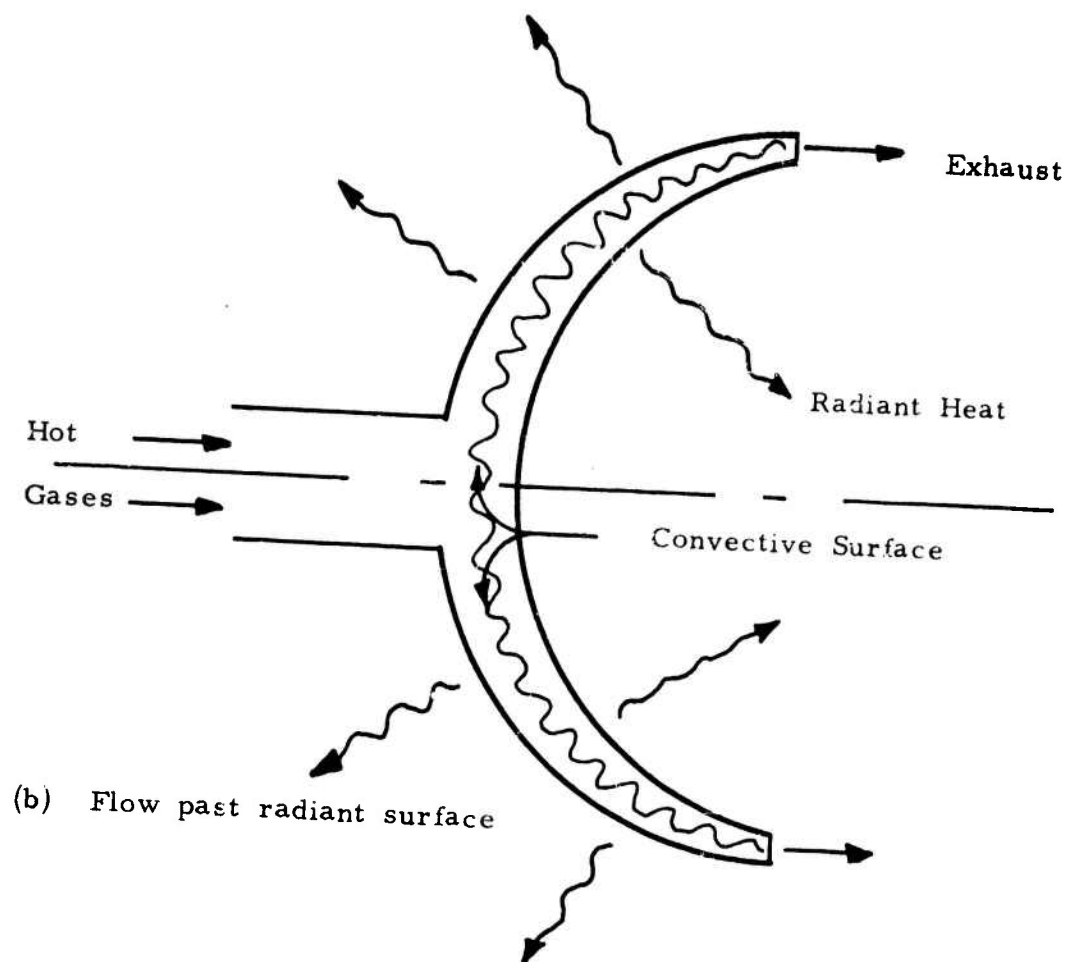


Figure C-4 Basic Schemes for Convective to Radiant Heat Exchange

where

η_h	=	heat exchanger efficiency, dimensionless
w	=	gas weight flow, lb_m/sec
c_p	=	gas specific heat, constant pressure, $\text{Btu}/\text{lb}_m^\circ\text{F}$
T_g	=	maximum or inlet gas temperature, $^\circ\text{F}$
T_r	=	average, lowest, or exit radiant temperature, $^\circ\text{F}$

Heat exchanger efficiency may be expressed as a function of net transfer units, NTU, as discussed in standard texts.³ This factor is defined as $UA/w c_p$, where U is a net conductance of the heat transfer area, A . The analysis can include effects of varying metal temperature and metal conduction. However, for most situations of present interest it is satisfactory to use the approximations:

$$U \approx h \quad (\text{C-10})$$

$$\eta_h \approx 1 - \exp(-\text{NTU}) \approx 1 - \exp(-hA/w c_p) \quad (\text{C-11})$$

where h is the surface or gas film conductance

This is the simple exponential function in which one NTU yields 63 percent efficiency and 3 NTU yields 95 percent efficiency. If fuel efficiency, hence exhaust heat loss, is of some concern, NTU between 1 and 3 must be employed.

The previous equations are used to match the heat extracted convectively to that delivered by radiation. In a typical situation, the gas inputs and desired efficiency are known, and it remains only to provide the required NTU or (hA) . There are very many forms of surfaces or matrices that are used to develop conductance, or forced convection from the gas stream boundary layer

or film, such as flat plates, tubes, fins, pins, screens, fused spheres, etc. Data for these surfaces are given in the literature compiled as dimensionless variables.^{1, 3} For present purposes the correlations are usually given as N_{St} or N_{Nu} and f versus N_{Re} and N_{Pr} .

$$N_{St} = h/C c_p ; N_{Nu} = hD/k ; N_{Re} = GD/\mu ; N_{Pr} = \mu c_p/k$$

where

- h = film coefficient, Btu/ft²hr⁰F
- G = weight flow per unit area lb/hr ft²
- f = gas flow friction factor
- c_p = gas specific heat, constant pressure, Btu/lb_m⁰F
- $D/4$ = hydraulic radius, $A_c L/A$
- L = length of gas flow path, or depth of matrix, ft
- k = gas thermal conductivity, Btu/hr ft⁰F
- μ = gas viscosity, lb_m/ft sec
- A = total area "wetted" by the gas, ft²
- A_c = cross-sectional area for flow (minimum, usually), ft²
- N_{St} = Stanton Number
- N_{Nu} = Nusselt Number
- N_{Re} = Reynolds Number
- N_{Pr} = Prandtl Number

The above nomenclature is defined in Figure C-5

Since desired NTU and available pressure drop, Δp , are given, a very significant approximation (exact in differential form) can be used, namely:

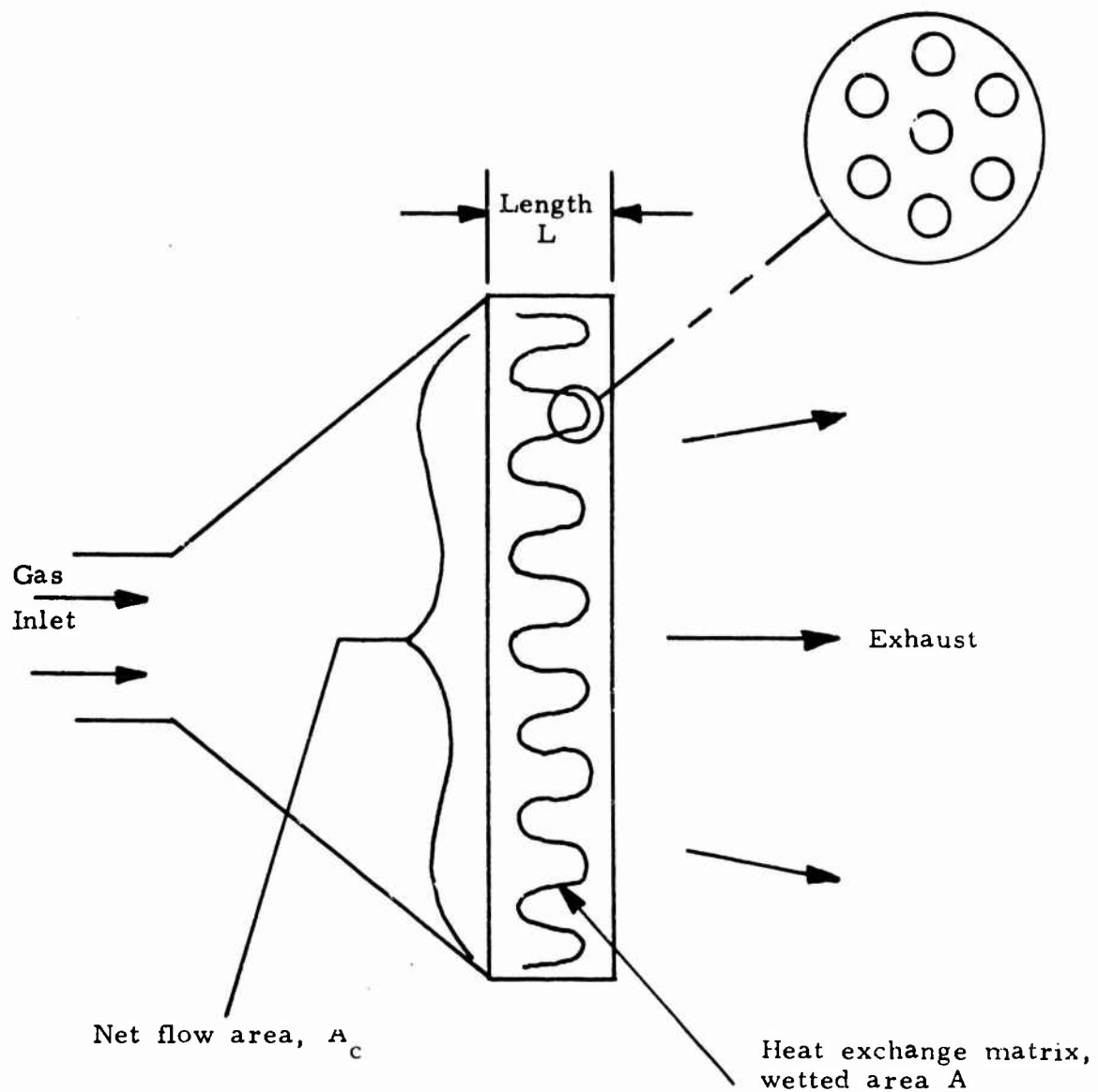


Figure C-5 Nomenclature for the Convective Heat
Exchanger for a Radiant Burner

$$\Delta p \approx \left(\frac{G^2}{2\rho g} \right) (NTU) (f/N_{st}) / \eta_s \quad (C-12)$$

Here ρ is the average value, proportional mainly to absolute gas temperature. Also η_s is the surface or "fin" effectiveness, involving local temperature gradients in the fin material or matrix. It is usually near unity for compact heat exchangers and to avoid hot spots in the structure. It occurs that for practically all compact heat exchange surfaces, and over a wide range of flow conditions (i. e. $100 < N_{Re} < 10,000$) the ratio f/N_{st} varies only over a narrow range. Considering the previous relation between Δp and NTU, and the gas parameters that are constant, the only remaining variable is G , inversely proportional to A_c . In short, there is no way to meet the heat transfer and pressure loss requirements except by limiting the throughflow velocity, using sufficient flow area. Due to this fact, the configuration of the radiant surface often directly dictates whether the heat exchanger can be of the flow-past type or must have the gases flow through the radiant surface.

After the flow velocity is determined, the data for a particular type of heat exchange surface or matrix can be used to determine the film coefficient and surface area, h and A . Then if a characteristic dimension, D , of the passages, fins, or screens is selected, the flow length or depth and total volume of the heat exchanger can be determined. Total volume involves a geometric solidity, σ , or packing density, β , such that

$$\text{Volume} = L A_c / \sigma = A \beta$$

Note that β is dimensional. The packing density increases in direct proportion as the characteristic dimension decreases for geometrically similar structures. In other words, the volume of the heat exchanger

can be reduced by using smaller elements such as tubes or wires. Heat transfer and pressure drop are not much affected, due to the near constancy of the factor f/N_{st} .

2.4 Radiant Heat Transfer

Radiant transfer is described by simple relations, but the constants involved are poorly known and the equations are difficult to manipulate with other heat transfer analysis. The approximate relation suitable for radiant burner design is

$$e_s = \epsilon \sigma (T_r/1000)^4$$

Symbols:

e_s = emissive power, BTU/hr-ft²

ϵ = total emissivity, dimensionless function of surface temperature and material condition

σ = Stephan Boltzmann constant, 1730 BTU/hr ft²-(°R/1000)⁴

T_r = Radiant surface absolute temperature, °R

To obtain the total heat flux from a surface, this equation must be integrated over the entire radiant surface. Considering the uncertainty of emissivity and the uncertain or approximate nature of the other estimates for the radiant burner, it is usually satisfactory to use area average values for emissivity and temperature, at least for initial estimates, e.g.

$$Q_r = A_r \epsilon \sigma (T_r/1000)^4$$

A_r = total radiant surface area, ft^2

Q_r = Radiant flux, BTU/hr

An error in this analysis can occur if the reflector system used with the radiant burner is shaped so that some of the emitted flux is returned to the hot surface, such as with a spherical back-reflector for a relatively large spherical source. Rough estimates of the local reduction in emissive power can be made, although accurate analysis is quite complex. (See Appendices A and B for a general discussion of source-reflector action.)

3. Design Synthesis

As stated in the beginning of Section 2 parametric design of a radiant burner must consider the flow rate-pressure characteristic of convective heat exchange and radiant heat release. The simplifying conclusions reached for practical design purposes are:

- (1) maximum pressure upstream of the heat exchanger is almost constant;
- (2) pressure limitations lead to an approximate upper limit on through-flow velocity, depending on desired fuel efficiency;
- (3) radiant area and convective area can be different, but the two heat fluxes must match and the gas flow area must suit the radiant configuration;

- (4) there are many surfaces or matrices that can be used for compact heat exchange.

A general conclusion from the study on reflector effectiveness, Section 4, is that if the minimum target heat flux is specified over a transverse span and axial range that is large compared to reflector envelope dimensions, and if the source shape (i.e. plane, cylinder, sphere) is specified, then the reflector can be optimized and the required source flux can be estimated fairly well. Then, for a given radiant flux, the variation of design parameters can be presented.

Perhaps the primary variable for a simple radiant burner is nominal fuel heat rate, proportional to fuel-air flow. Using this as the independent variable, the other parameters can be presented as in Figure C-6, correlating areas and temperatures. Then if several possible types of heat exchange surface are investigated, the amount or volume of the heat exchange material can be presented as a function of a characteristic dimension of the matrix, as shown in Figure C-7. This should assist in selecting a matrix type of configuration.

The next section describes the design synthesis of the Foster-Miller Hemispherical Radiant Burner. The design development takes into consideration the parametric variation of the previous sections.

4. Design Synthesis of the Foster-Miller Hemispherical Radiant Burner

Most available radiant burners use screens or a matrix as the radiant surface and flame holder, with low throughflow velocity. This results in a large, low-intensity radiant surface, but it only requires a very slight pressure rise in the jet pump. As an example of the opposite end of the design spectrum, a radiant burner was designed to

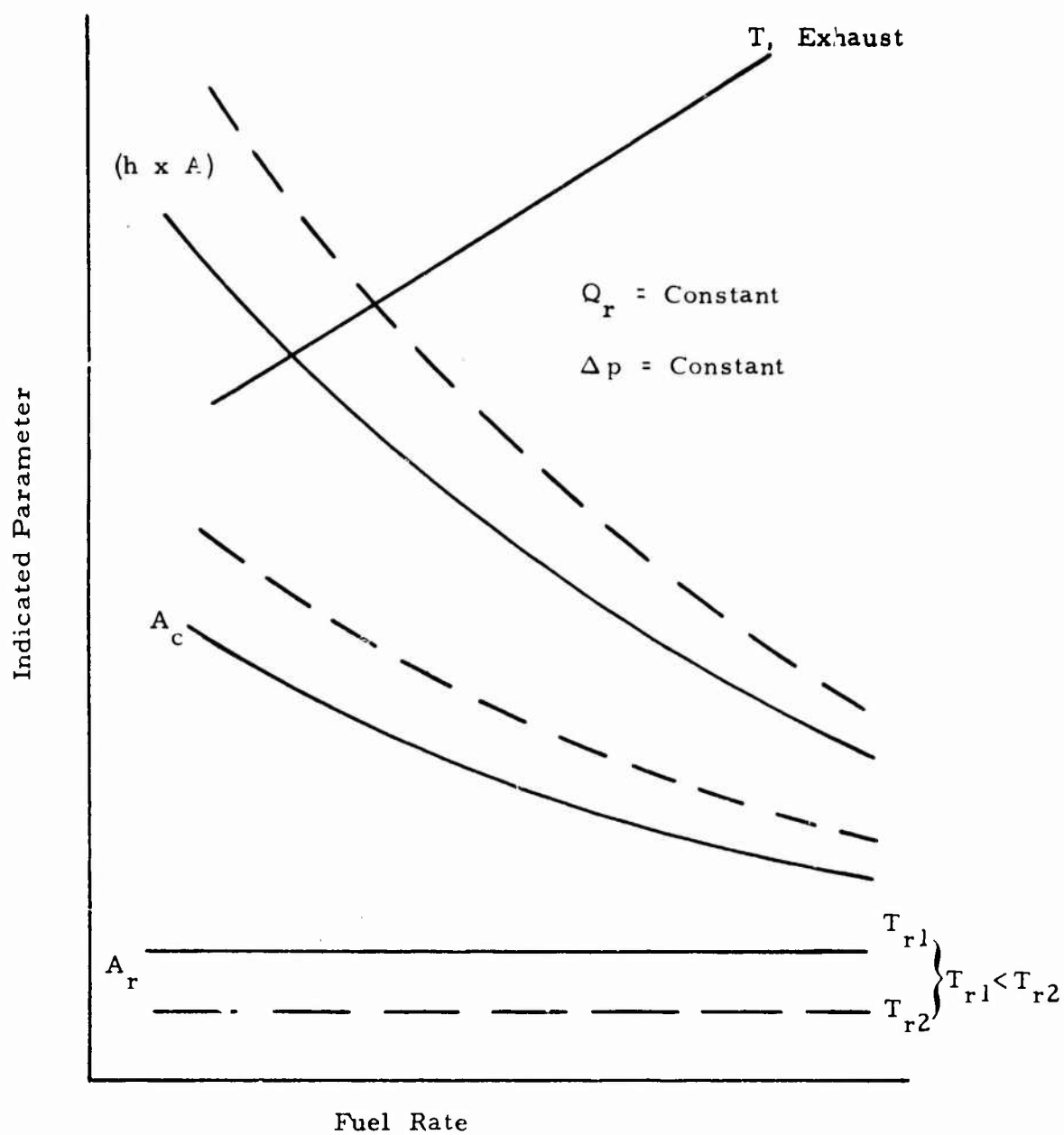


Figure C-6 Typical Variation of Radiant Burner Parameters

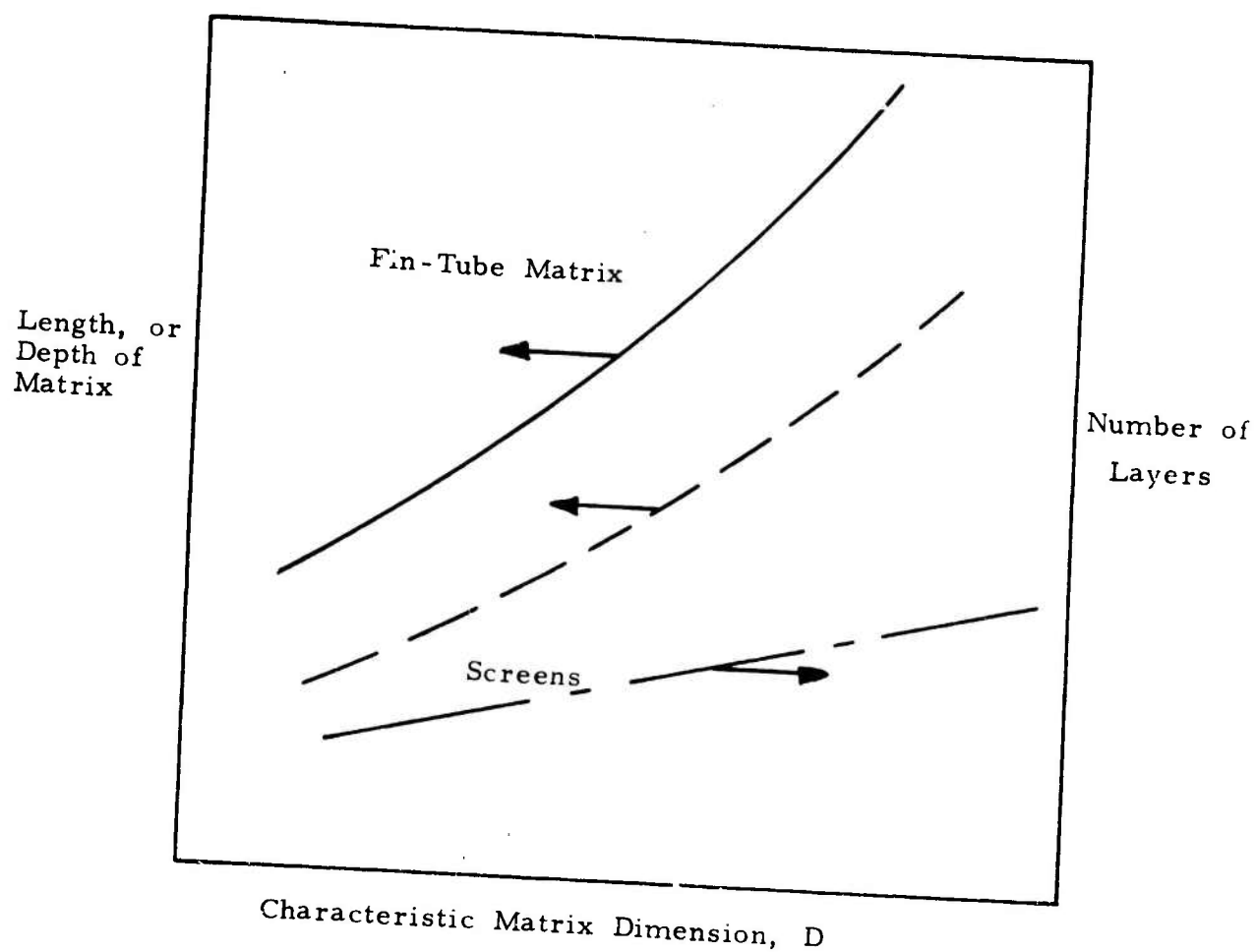


Figure C-7 Schematic Comparison of Different Heat Exchange Matrices versus Matrix Size

utilize a high-pressure jet pump and a convective heat exchange surface that is contiguous with but not the same as the radiant surface. The design is not claimed to be "optimum" for any fixed criteria, but rather, it is an attempt to illustrate a compact burner-heat-exchanger that is suitable for a roughly spherical source-reflector system. A description of the design and underlying assumptions follows.

4.1 Burner Design

The burner chosen is a propane burning torch, manufactured by Wingaersheek Corp., Lynn, Mass. This burner is compact for its nominal heat rate of 30,000 BTU, and has a relatively high pressure jet pump in order to obtain the highest flame velocity for the maximum local surface heating rate. This velocity is diffused in our design in order to recover the static pressure required to force the gases through the heat exchange matrix. Figure C-8 shows a schematic of the burner.

A burner designed specially for this application would be larger and would use a jet pump "trimmed" to develop maximum static pressure at the burner exit. This would minimize the inefficiency resulting from acceleration and diffusion of the burner flow.

The burner output is described as follows, using physical constants from Marks⁴ and Kays and London:³

- (1) fuel flow = 1.4 lb propane/hr
- (2) combustion products flow = 23 lb/hr
- (3) flame temperature = 3540°F or 4000°R

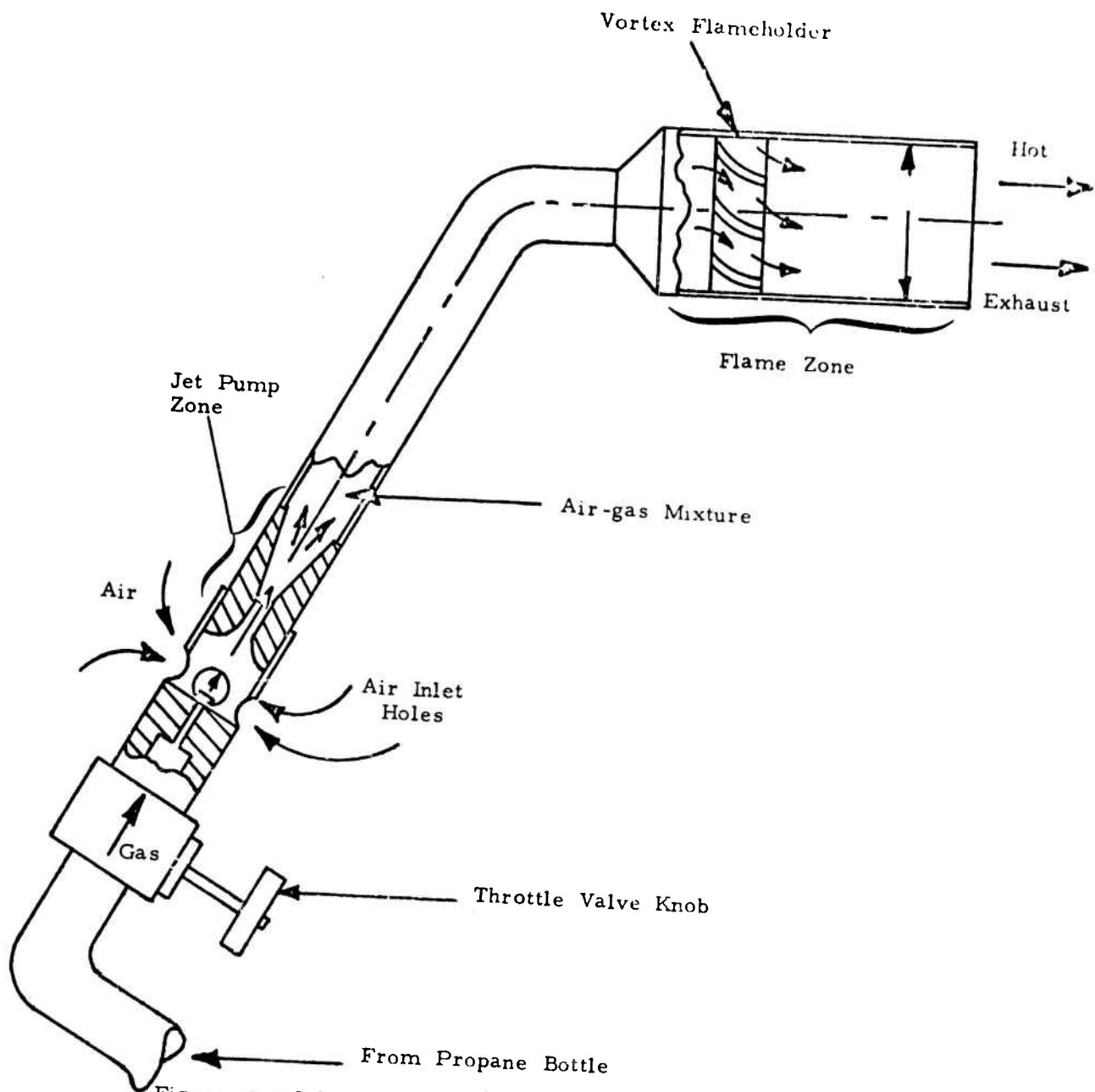


Figure C-8 Schematic of Wingaersheek Turbo Torch Burner

- (4) combustion products specific heat = approx.
0.3 BTU/lb°F
- (5) combustion products density = air at comparable temperature.

Based on the burner flame tube of one inch in diameter, the flow parameters for the burner exhaust are computed to be:

- (1) area, $A_c = 5.46 (10)^{-3} \text{ ft}^2$
- (2) specific volume, $= 100 \text{ ft}^3/\text{lb}$
 $\approx (\text{standard air}) \frac{{}^{\circ}\text{R} (\text{flame})}{{}^{\circ}\text{R} (\text{standard air})}$
- (3) weight flow per unit area, $G = 4200 \text{ lb/hr ft}^2$
- (4) dynamic pressure, $G^2/2 \rho g = 2.12 \text{ lb/ft}^2$
 $2.12 \text{ lb/ft}^2 = 0.41 \text{ inches water gage}$
- (5) Reynolds' number, $R_e = GD/\mu = 2200$

On the assumption that a diffuser cone attached to the exhaust of the burner can recover as static pressure about 70 percent of the flame dynamic pressure, the maximum pressure drop, Δp allowable in the heat exchanger is estimated to be approximately 1.5 lbs/ft^2 , at nominal flow rate. (With greater restriction and pressure drop, the burner jet-pump would yield less airflow for the same fuel flow, so the burner would run rich with reduced heat rate.)

4.2 Heat Exchanger Design

An effective heat exchanger for this particular application and for the burner design developed can be parametrically specified as one having a mean radiant temperature of 1540° F and an exchanger effectiveness of 63 percent. Then using the equations of Sections 2.3 and 2.4, the following design values were obtained:

- (1) convective and radiant heat rate,

$$Q = \eta_h w C_p (T_g - T_r) \approx 9 \text{ k BTU}$$

- (2) required radiant area, ($\epsilon \approx 0.9$)

$$A_r = Q / \epsilon \sigma (T_r / 1000)^4 = 0.36 \text{ ft}^2 = 52 \text{ in}^2$$

- (3) nominal over-all heat efficiency, radiant heat rate/nominal fuel heat rate 30 percent

These values represent a fairly compact radiant burner with a fair fuel efficiency.

A convective heat exchange surface that "fits inside" the radiating surface area and also achieves the desired effectiveness is required. An effectiveness of 63 percent corresponds to a NTU = 1.0. Then, using the generalized equation for pressure drop, the maximum allowable specific flow rate for any exchanger matrix is calculated to be,

$$\Delta p = (G^2 / 2 \rho g) (NTU) (f / N_{St}) / \eta_s$$

$$\Delta p \leq 1.5 \text{ lb/ft}^2, \quad G \leq 2000 \text{ lbs/hr ft}^2$$

assuming that η_s will be about 0.9 and (f/N_{St}) about 3 or 4 for pin-fin matrices.

This value of G dictates that the minimum through-flow area of the heat exchanger must be more than twice the burner exhaust area, or 1.65 in^2 .

The heat exchanger design is based on the maximum permissible velocity to provide the most compact design. The required minimum surface area can be computed for any specific matrix design (such as pin size and spacing) using empirical data and the relationships described in Section 2.3. For this design we chose to use small pins spaced one or two diameters apart, staggered and roughly normal to the gas flow and the radiant surface. Simple geometric calculations indicated that in this case the flow hydraulic radius is about the same magnitude as $D/4$, such that

$$N_{Re} = G D / \mu = \frac{2000 D \text{ (ft)}}{0.15} \approx 100$$

for pins ranging in diameter from $1/8$ to $1/16$ inch, a practical range for prototype construction. Then the average heat transfer coefficient is calculated from the following correlations to be

$$h/G C_p = N_{St} = N_{Pr}^{-2/3} C_h N_{Re}^{-0.4} \approx 22/10^3$$

Since h is seen to be a weak function of N_{Re} , the pin diameter is not critical.

Knowing h , the required area A can be computed from the relationship

$$NTU \approx h A \eta_s / G A_c C_p = N_{St} \eta_s A / A_c$$

or

$$A = NTU A_c / N_{St} \eta_s = 1 \times \frac{1.15}{100} \times \frac{10^3}{22} \times \frac{1}{0.9}$$

$$A \approx 0.58 \text{ ft}^2 = 83 \text{ in}^2$$

Thus the required convective transfer area is about 1.5 times the radiant area of 52 in^2 . This is not hard to achieve with short pins protruding from the back of the radiant surface.

The heat exchanger was designed, fabricated and tested during this program (see Section 6.4 of the report for test results) to approximate these preliminary design specifications. A schematic section is shown in Figure C-9. The approximate radius of the outer hemisphere is three inches and the pins are about 0.06 inch diameter, protruding 0.16 inches and spaced 45 per square inch. The geometry orders the following parameters:

$$(1) \quad A_r = 56.5 \text{ in}^2$$

$$(2) \quad A = 124 \text{ in}^2$$

$$(3) \quad A_c \sim 2 \text{ in}^2, \text{ adjustable}$$

The test model has more heat exchange area and flow area than the idealized design specification. The center piece is adjustable axially to trim the burner-heat-exchanger for maximum output.

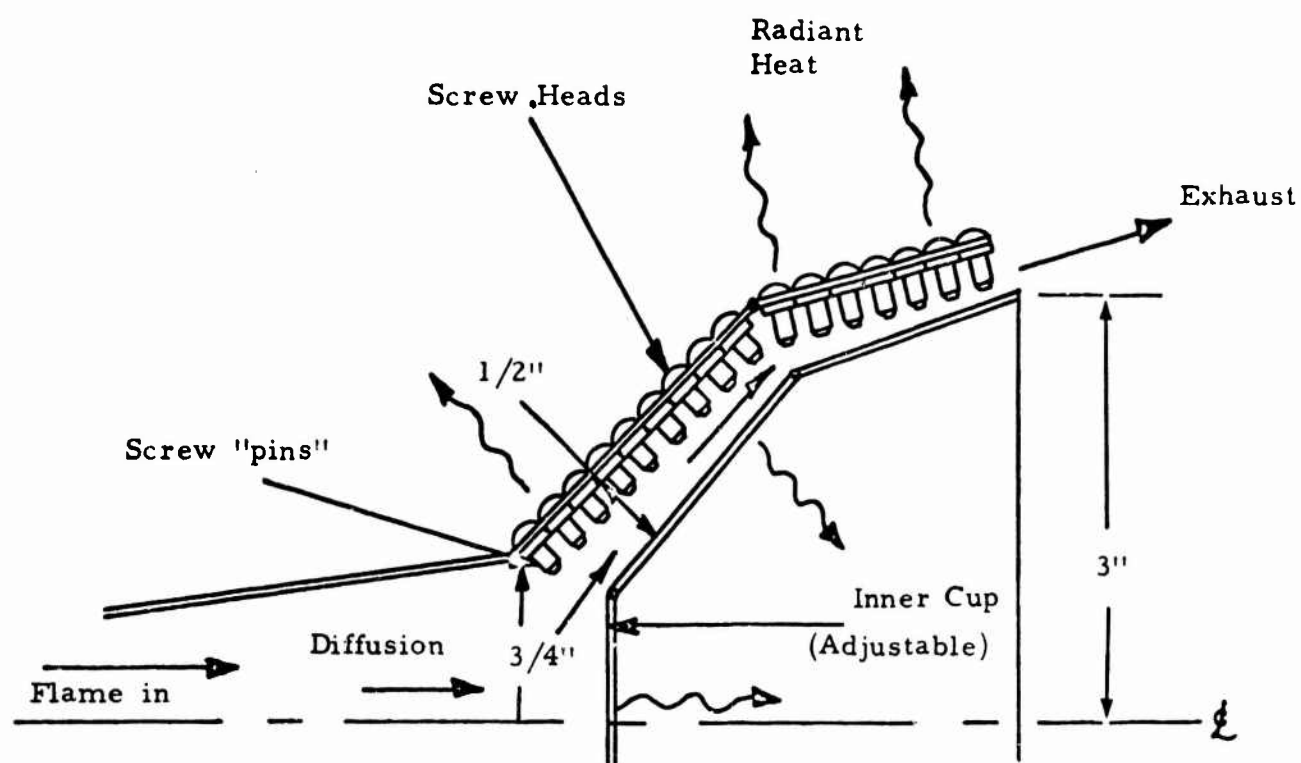


Figure C-9 Schematic Section of Experimental Hemispherical
Heat Exchanger

APPENDIX C

LITERATURE CITED

1. Perry, J. H., (Editor), "Chemical Engineers' Handbook," Fourth Edition, McGraw-Hill Book Co., New York.
2. Wingaersheek Turbine Co., Lynn, Massachusetts, Personal Communication.
3. Kays, W. M., and London, A. L., "Compact Heat Exchangers," Second Edition, McGraw-Hill Book Co., New York, 1964.
4. "Marks' Mechanical Engineers' Handbook," Sixth Edition, McGraw-Hill Book Co., New York, 1958.